DAMAGED TEXT IN ORIGINAL

An Investigation of the Deep Drawing Process with the Application of Ultrasonic Oscillations.

by

Alan Wilfred Smith, B.Sc.

Submitted in part fulfilment of the requirements for the degree of Doctor of Philosophy.

The University of Aston in Birmingham.

January 1977.

SYNOPSIS.

This research programme has investigated the application of vibrations to the three tools that constitute the deep-drawing process namely the punch, blank-holder and die. The deep-drawing process was simulated by using a modified form of the wedge drawing test. In this analogue a 'double' ended wedge shaped specimen was drawn through wedge shaped dies the wedge angle simulating the effect of circumferential compression upon the blank.

On applying axial punch vibrations at a frequency of 13 kHz to the deep-drawing process the mean punch load was reduced by up to 30 per cent. The peak load was believed to remain unchanged however since no increase in the limiting draw-ratio was observed.

'Radial' blank-holder vibrations were simulated by subjecting the wedge blank-holders to in-phase axial vibrations in a plane perpendicular to the axis of the punch.

Over the range of oscillatory amplitudes tested the punch load was reduced by up to 30 per cent and the limiting draw-ratio increased by 12 per cent. This second effect is attributed principally to the friction vector reversal mechanism whilst the first effect was caused by a combination of both the friction vector and the stress-superposition mechanism.

In the draw ironing process 'radial' die vibrations were simulated in a similar manner and at the highest reduction successfully undertaken, 25 per cent, the maximum punch load reduction was 20 per cent. The limiting draw-ratio was increased by 10 per cent which corresponded to an increase in the height of the ironed wall of 33 per cent. These maximum effects obtained from the apparatus were not considered to be at the limit of improvement because the effectiveness of the vibrations was still increasing at the maximum oscillatory amplitude that could be obtained from the wedge test analogue. Development of the axisymmetric equivalent is recommended to take advantage of the improvement that increased

oscillatory power can produce combined with the removal of the edge friction present in the wedge drawing apparatus.

The use of ultrasonic blank-holder vibrations parallel to the punch axis was not practical in this apparatus. A low frequency, 200 c.p.s., pulsating oil pressure was applied to the blank-holder hydraulic pressure supply. A marginal improvement of 3 per cent was obtained in the limiting draw-ratio.

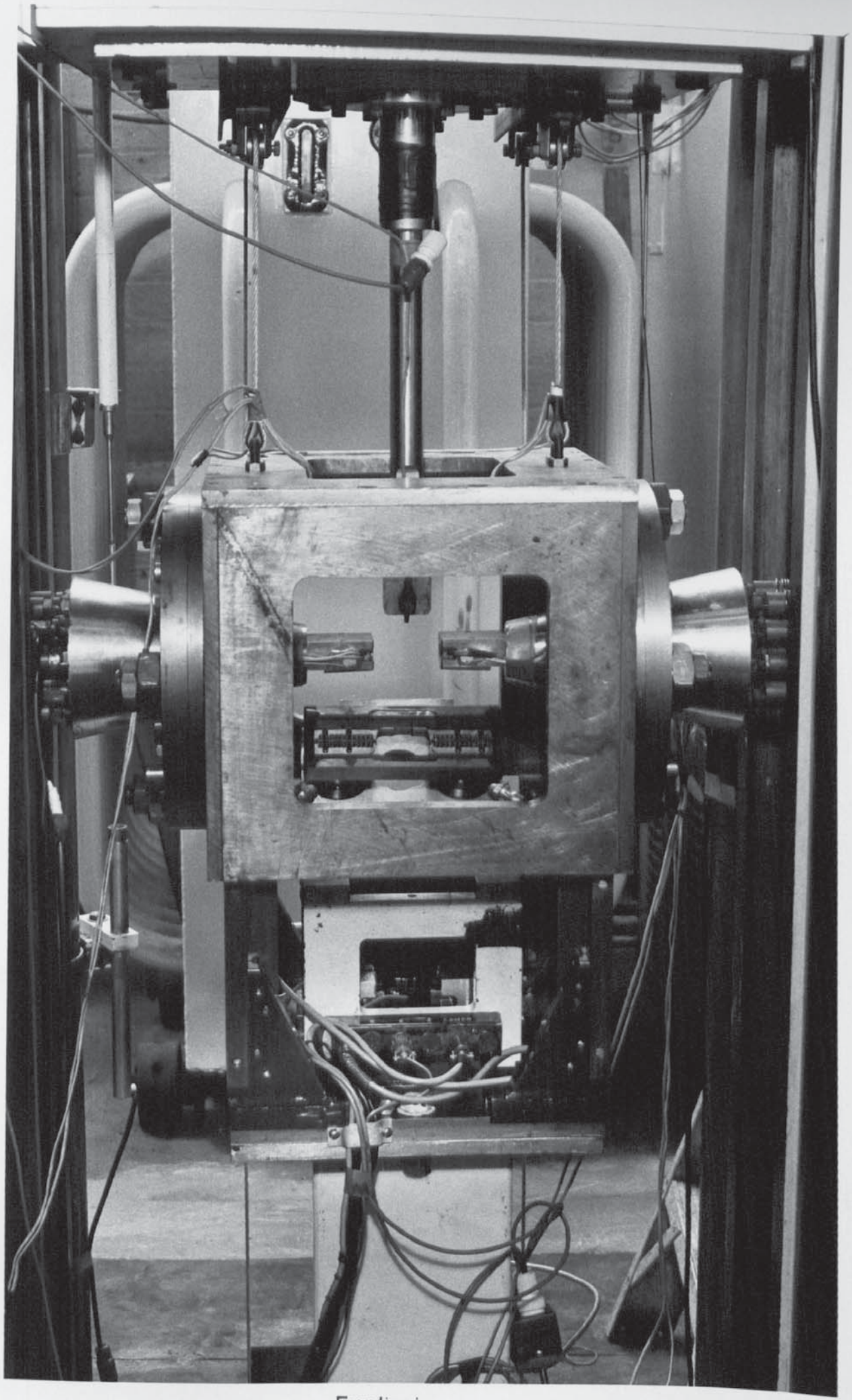

Frontispiece

LIST OF CONTENTS.

DAMAGED TEXT IN ORIGINAL

1. INTRODUCTION.

The deep-drawing process is a sheet metalworking operation characterised by the use of a punch and die, the punch being used to push the sheet through the die and in doing so the work material is bent over and wrapped around the punch nose to produce a cup shaped object.

The flange of the blank which is gradually drawn over the die radius is in a state of radial tension, caused by the drawing stress, and hoop compression resulting from the progressive reduction in the circumference of the periphery of the blank. As the material in the flange is rearranged into the sidewall this circumferential compressive stress causes instability within the flange which develops as wrinkling if there is some lack of uniformity in the movement or the resistance to movement in the cross-section of the metal. This tendency to wrinkle is suppressed by the use of a blank-holder which holds the flange of the material to the surface of the die. A blank-holder force sufficient to resist or compensate for the non-uniform movement will prevent wrinkling. Once a wrinkle starts the blank-holder is raised from the surface of the material so that others can form easily. Blank-holding can be either a constant clearance or constant pressure type, the latter allowing the blank-holder to rise and fall with the changes in the blank thickness during the drawing operation. The blank-holder force required varies according to the material thickness, thin materials require relatively large loads because the material itself has little resistance to the buckling which appears as wrinkling. With thicker materials the blank-holder load required decreases and for thick blanks is practically zero.

In its simplest form the deep-drawing operation produces a circular cup but other complex shapes can be produced with suitably shaped tools but these shapes are often a combination of deep-drawing and stretch forming. The difference between the two processes is

that in deep-drawing the blank-holder pressure whilst being sufficient to prevent wrinkling does allow the material from the flange to be drawn into the die whilst in stretch forming the blank is clamped around its periphery and the final shape is produced by thinning the material already in the die.

As the flange is drawn in, the compressive stress causes the material to thicken which leads to a non-uniform cup wall thickness, the cup wall being thickest at the top. This thickening can be controlled by ironing the cup wall which involves drawing the material through a die, the clearance between the die and punch being less than the metal thickness. This reduces the metal thickness and increases the height of the cup. This operation is often combined with the deep-drawing process if it is desired to control the thickening during the drawing rather than thin the cup wall. This distinction is necessary since in the drawing process the material in the cup wall is thinned as a consequence of bending and unbending under tension over the die radius. This thinning is masked by the thickening of the blank which occurs in the flange because of radial drawing in. Generally at a point approximately two thirds the way up the cup wall, the thinning and thickening effects combine to bring the cup wall thickness back to nominal starting gauge. Ironing beyond this point up the cup wall is employed to prevent the wall becoming excessively thick at the top of the cup. This operation can be accomplished quite successfully since the load necessary for this ironing is required at the end of the drawing stroke, which is remote from the maximum drawing load which occurs soon after the start of the draw, when the maximum amount of material is undergoing radial compression in the flange.

The limitation to the deep-drawing process occurs when the blank diameter is so large that the combined components of the draw load are greater than the partly drawn cup wall can withstand, the result being a tensile failure low down in the cup wall, which is

the thinnest part of the cup wall. Failure can occur for other reasons but this type of tensile failure is the most widespread. The draw-ratio, which is the ratio of blank to punch diameter, at which there is a transition from successful draws to failure is called the limiting draw-ratio. This as the name applies is the maximum size of blank which can be drawn under a given set of conditions and for a wide variety of materials of a deep-drawing quality the limiting draw ratio for a single stage draw seldom exceeds a value of 2.2 which gives a cup height to diameter ratio of approximately unity.

Having introduced the deep-drawing and associated processes and described some very general limitations of the process it can be appreciated that the proportions of a first stage cup will be insufficient for many applications. Consideration will therefore be given to ways of increasing the depth of the drawn cup. The normal way of producing deeper cups is to re-draw the cups to a smaller diameter either by the direct method or by reverse re-drawing which turns the cup inside out. This is the only way of producing long slender cups but it involves additional tooling to perform the re-draw and interstage annealing may be necessary. For many operations, however, re-drawing would not be necessary if the limiting draw-ratio could be improved slightly to enable the first stage cup to be fabricated to the right proportions.

The variables in the process are the material, lubrication and tooling, any or all of which can be changed to improve the drawing operation. The materials used for deep-drawing up to the highest limiting draw-ratios will have been manufactured with the metallurgical properties carefully controlled to a specification suitable for deep-drawing and therefore the improvements which can be made to such a material are often quite limited and also the desirable deep-drawing properties often have to be compromised with the properties required in the drawn article.

When the metals are in sliding contact under pressure during deep-drawing galling of the tools and work material can occur which increases the draw load and can cause the workpiece to fracture. When trying to increase the drawability of a material limited success can be obtained by using a better drawing lubricant to reduce the forming load. The cost and ease of removal of lubricant films are factors which sometimes detract from the use of better drawing compounds. One of the more recent developments in lubrication is the use of polymer films to act as the lubricant. Such films can be applied beforehand to impart mechanical and corrosion protection to the material whilst their removal after forming can be relatively simple. These films do, however, suffer from the disadvantages of being expensive and provide a uniform lubrication all over the blank when, for high draw-ratios, differential lubrication may be more appropriate.

Variations in tooling can also be used to reduce the forming load, such as improving the surface finish and increasing the drawing die radius. This latter operation does make the drawing operation less severe but the maximum die radius possible is limited by the onset of wrinkling over the draw radius which is out of the control of the blank holder.

In addition to these simple measures which can be used to improve critical drawing operations, there are different processes which can be used to enable useful increases in the depth of draw to be obtained.

One of the more successful developments is that of applying high pressure lubrication to the tooling. This can take a variety of forms, one of these being the filling of the closed die cavity with lubricant which is pressurised as the punch descends, the lubricant being forced out between blank and die thus reducing the friction at this interface to negligible proportions. Large increases in the limiting draw-ratio can be achieved by this method but the punch

loads required are much larger than those required conventionally, because of the self-pressurisation the punch must be of a solid shape similar to the required cup shape. This can be taken a stage further and the drawing die be eliminated, using a flexible membrane to separate the oil from the blank which is wrapped around the punch during the forming operation by the hydraulic pressure.

The natural thickening of the blank at its periphery once the draw has started can be used as a means of improving the lubrication. Lubricant entrapment can occur between the flange and die radius which results in a small amount of lubricant being forced over the die radius as the blank periphery contracts with the draw. When using constant blank-holder pressure this is more successful with thick lubricants since they are viscous enough to be retained during the initial application of blank-holder pressure before drawing commences.

One final method of pressurised lubrication is to use an external pressure supply to apply high pressure lubrication to the drawing operation through suitably located orifices, the pressure being sufficient to overcome contact pressure of the blank on the die. Such a system has the advantage of allowing the lubrication to be applied to a specific area of the tooling to compensate for the additional complication of an external pressure supply and the provision of suitable orifices in the tooling.

Another process from which reduced friction effects can result is that of oscillatory metal deformation. Claims have been made that the application of vibrations to the tooling can reduce the forces required to deform the metal, improve the surface finish and improve the metallurgical properties of the workpiece. One of the limitations to this process is that the effects are reduced at the higher drawing speeds and can disappear altogether if the drawing velocity exceeds the oscillatory velocity. The process of deep-drawing is one of the slower drawing processes and in addition there is a large frictional component within the total drawing load.

Therefore, for these two reasons this process could benefit significantly from the application of oscillatory metalworking techniques.

An earlier investigation had developed a modified form of the Wedge Test for the application of 'radial' vibrations to the drawing die. A wedge shaped specimen was drawn through wedge shaped dies over a die profile radius by a rectangular punch. This system closely simulated the conditions acting in the axi-symmetric case apart from the region over the punch nose.

This research project, which uses the same analogue, will examine the effects of vibrating the other two components that comprise the deep-drawing process, namely, the drawing punch and blank-holder. In addition, the effect of die vibrations on the draw ironing process where the material is drawn and simultaneously ironed will be examined along with the process of axially vibrating the die or blank-holder which will squeeze the flange of the deforming blank. These two latter processes will enable the effect to be realised of applying additional work to the process without increasing the tensile stress in the drawn product.

2. THE REVIEW.

2.1. General Introduction to Ultrasonic Metal Deformation.

The examination of the effect of ultrasonic vibrations upon the plastic deformation of metals can be said to have started in 1955 when some of the effects of subjecting single zinc crystals to ultrasonic vibrations were reported by Blaha and Langenecker[1]. Prior to this work the 'beneficial' effect of superimposed vibrations had been recognised [2], [3] but it was the implications of the later work that ultrasonic vibrations could affect the deformation properties of the metal itself which established the interest in the application of vibrational energy to commercial metal-working processes. This interest was undoubtedly assisted by the emergence in commercial quantities of the new materials necessary for the aero-space and nuclear energy industries which were proving difficult to work by conventional techniques.

From these beginnings the subject has been widely investigated to discover the fundamental mechanisms as well as the practical application of the phenomena to metal forming processes. Claims of reduced process stress, different metallurgical properties and improved surface finish are expressed as the benefits which can accrue from the use of vibratory metal forming techniques.

Vibratory energy applied to metal deformation processes has been considered to manifest itself in two ways which can be described as the Volume and Surface Effects. The Volume Effect refers to the inter-action of the vibratory stresses on the internal structure of the bulk material during plastic deformation, whilst the Surface Effect deals with the workpiece tool interface and is thus concerned with the various aspects of friction between workpiece and tooling. This separation of the effects in ultrasonic metal working can therefore be seen to resemble the traditional method of dividing process work into two components, one to execute the bulk plastic deformation the other being used to overcome friction within the process.

2.2. Mechanisms Describing Ultrasonic Metal Working.

2.2.1. The Volume Effect.

The first model describing the Volume Effect was proposed by Blaha and Langenecker[1]. It was postulated that vibratory energy was preferentially absorbed at dislocation sites within the crystal structure of the material being formed. This preferential absorption somehow eased the dislocations past obstacles in the crystal lattice structure which presented a barrier to the normal static stresses. Whilst this first model was accepted by some workers at that time, it lacked evidence on the manner in which this absorption of energy took place. It was during studies of this absorption problem that Nevil and Brotzen[4] were able to describe another model to account for the observed effects. This model became known as the 'superposition effect' since they found that the observed reduction in the yield stress could be the result of superposing the cyclic alternating stress upon the normal stress. Thus the reduction in the yield stress was equal to the periodic stress amplitude and therefore the peak stress during each cycle still equalled the current normal yield stress of the material.

This superposition mechanism as described gained almost universal acceptance since by careful measurements of the periodic stress amplitude the validity of the mechanism could be demonstrated.

The superposition effect, however, does not explain all the observations made during ultrasonic vibration. It does not explain the gross reductions in yield stress observed when materials are subject to high densities of ultrasonic oscillation, neither are changes in physical properties explained, which can occur during vibration.

It is believed by some workers that such changes are caused by heating of the specimen as the ultrasonic energy is dissipated within the specimen in a manner similar to conventional thermal effects.

One mechanism which was not anticipated, not understood and

therefore was not employed in the early days was that which is now termed the 'swaging effect'. This is well known as a conventional metal working process in which compressive stresses are applied transverse to the direction of flow. It has emerged as an important mechanism in oscillatory metal working, since by changing the stress state of a particular element by transverse compression, yield can be accomplished by the application of a smaller tensile stress than is normally required. The tensile stress in a drawn product can therefore be reduced thus lessening the risk of failure resulting from the lack of strength in the drawn product which is the major cause of failure in the metal drawing processes. Another reason for the late emergence of this mechanism is that it has only been possible recently to radially vibrate a die needed to apply these radial stresses rather than the transverse and longitudinal vibrations employed in the early investigations.

2.2.2. The Surface Effect.

The Surface Effect as applied to the frictional conditions which exist between tool and workpiece is more complex than the Volume Effect. The very early work using ultrasonic vibrations was concerned with the tensile test in which, of course, there is no sliding contact between tool and workpiece and thus the forces required to strain the specimen are not augmented by frictional effects.

Possibly because of the absence of friction from these early tests along with the subsequent disagreement over the true nature of the Volume Effect, the understanding of surface friction has emerged more slowly.

Fundamental investigations have shown several mechanisms which could be used to explain the effects of friction. Within this grouping, a further division could be made to separate the effects which rely on a change in the coefficient of friction from those which give a reduction in the friction force without a change in the

coefficient of friction.

The most commonly described effect is that of a periodic separation of the surfaces. The contact time and hence friction force is reduced. This does not always affect the process since deformation can only occur when the surfaces are in contact.

Fridman and Levesque[5] explained the improvement as a result of periodic breaking of the weldments whilst the re-distribution of the lubricant during separation was suggested by Lee et al[6].

A much later mechanism to be described was that of friction-vector reversal. This is concerned with oscillatory movement within the plane of sliding. A theoretical analysis by Mitskevich[7] indicated the friction force was reversed due to the motion. The mean force in the direction of sliding was therefore reduced even if the coefficient of friction remained unchanged. This model agreed with the work of Polhman and Lefeldt[8] and Lenkiewicz[9]. The first application of this mechanism was by Nosal and Rymsha[10] who applied it to the tube drawing process.

Improvements in the ultrasonic metalworking processes have also been attributed to a change in the coefficient of friction. Improvements in surface finish in tube drawing because of frictional conditions altering have been reported by Jones[11].

It is also believed that the oscillatory motion between tool and workpiece can improve the lubrication and a variety of models describing how the lubricant is pumped have been proposed but these mechanisms are not well understood.

One final method of improving the effectiveness of lubrication is the use of vibratory energy to 'activate' the lubricant. This is believed to be particularly useful when reactive lubricants are used. The effectiveness of such chemicals is improved by either heating, an effect often experienced, or by having the metal surfaces effectively cleaned by the ultrasonic excitation. The clean surface allows the lubricant to react with a higher proportion of the workpiece surface

and thus improve the lubrication properties.

This review has so far described the ways in which the early work on the effects of vibratory energy on the metal working processes developed. The papers referred to are by no means an exhaustive account of the work but are included because they are considered representative of the particular developments which were occurring at the time of publication.

A fuller account of this earlier work can be found in the exhaustive review of oscillatory metal working at both high and low frequencies by Dawson et al[12].

Having introduced the early work and the mechanisms believed to be operating in oscillatory metal working processes, the more recent papers published on the application of ultrasonic vibrations to the metal deformation processes will be reviewed with an emphasis being placed on the underlying mechanisms within these processes rather than the processes themselves.

2.3. Ultrasonic Metal Working Processes.

2.3.1. Compression Processes.

2.3.1.1. Forging.

In order to compare the effects of heating with ultrasonic vibrations an investigation was carried out by Severdenko and Petrenko[13]. This was a continuation of earlier work in which a temperature rise when using ultrasonic energy in free upsetting was noted. On comparing the effects of upsetting under conventional, heated and ultrasonically excited conditions reductions in the resistance to deformation of 45 per cent and 75 per cent, respectively, were found. This improvement was used to support the theory that energy was absorbed preferentially at lattice defects.

This conclusion, however, must be questioned since the temperature during the application of ultrasonic energy would be extremely difficult to monitor accurately. Additionally, however, a more important factor is the method of assessing the effectiveness of the process. This was based upon load measurements which would be subject to force superposition in the ultrasonic case. Thus the ultrasonically deformed sample could be deforming at the same stress level as the conventional sample, but a lower forming load would be recorded. Surface friction conditions are likely to differ between the heated and vibrated samples with the resultant difference in the yield situations. These three factors must be accounted for before any meaningful conclusions pertaining to the preferential energy absorption theory can be drawn.

In a later paper referring to the same process, Severdenko et al[14], the effects of ultrasonic vibration on the specific pressure and hardening curves as a function of the degree of deformation were examined. A decrease in external friction was stated as the reason for the reduction in specific pressure but, once again, few details of the load recording instruments were given resulting in the reader being unable to separate stress-superposition effects from the data

supplied. The hardening during a deformation with ultrasonic vibration was less than that obtained in conventional processing. This was attributed to a decrease in surface friction by the authors. No further information was given but it is reasonable to attribute the improvements in the process to less redundant deformation resulting from a lower coefficient of friction which may have been caused by the periodic separation of the surfaces.

On considering a similar process at a low frequency of 12.5 Hz (15) lower forces and greater uniformity were noted. The high amplitudes characteristic of low frequency oscillations ensured surface separation leading to lower friction because of the breaking of weldments and the redistribution of lubrication obtained during each cycle.

In an investigation of the effectiveness of various lubricants in the closed-upsetting process Severdenko and Petrenko(16) suggested that the axial ultrasonic vibrations developed micro-cracks in the surface which were able to pump the lubricant whilst chemical reactions between surface and lubricant were also accelerated. No evidence, however, was presented to support these conclusions and the observed effects could equally well have been attributed to stress-superposition along with lubricant redistribution during surface separation. From the details given in the paper the loads recorded appeared to be mean value rather than peak value, thus enhancing the apparent effectiveness of the ultrasonic oscillatory effect. Similarly, the decreasing effectiveness as the degree of deformation increased could have been caused by a reduction in ultrasonic amplitude as the system became more heavily loaded. The effectiveness ratio quoted in the paper appears incorrect since any improvements in lubrication caused by the vibration tend to decrease this ratio, rather than increase it.

The effects of axial vibration in the forging processes which have emerged from these papers can be summarised, therefore, as stress-

superposition with some effect upon the coefficient of friction acting in the forging process. This reduction in the coefficient of friction can be considered to have been caused by the separating surfaces breaking the weldments, thus permitting a redistribution of lubricant and enabling a more homogeneous deformation to occur.

2.3.1.2. Extrusion.

The reduction in friction obtained with the application of ultrasonic vibrations has been found to be useful also in the extrusion process.

The effectiveness of various methods of applying ultrasonic oscillations were investigated by Petukhov[17]. The effectiveness was judged by the magnitude of the force reduction and the degree of non-uniformity of the metal flow. With all the methods of applying the ultrasonic oscillations a reduction of the extrusion force and a decrease in the non-uniformity of the extrusion was obtained.

These findings are consistent with an effective reduction in friction between the workpiece and tooling. The load reductions recorded were not peak loads so an element of superposition effect was included in this recorded reduction. The more uniform deformation coupled with a decreasing effect as the extrusion speed rose, however, indicate a friction-vector reversal mechanism occurring between the container walls and the deforming material.

In a later paper [18] considering direct extrusion through a radially oscillated die Petukhov again reported reductions in the applied force and in the degree of non-uniformity. A decrease in friction between blank and die was reported as responsible for these effects. In addition to this friction reduction which would be of a reduced coefficient type except across the flat face of the die where friction-vector reversal could occur, the swaging effect is likely to have a significant effect on the loading necessary to

bring about a yielding situation.

A change in the micro-hardness of the extruded material was also reported and attributed to an "increase in plasticity". This statement was not expanded upon but a possible explanation would be of a heating effect, which would also account for some of the load reduction recorded. Without the ultrasonic power levels used, however, it cannot be confirmed. Another explanation would be that the reduced hardness was caused by the reduction in the redundant deformation, a factor which was quantified. This would reduce the amount of work hardening which was indicated by the lower micro-hardness on the surface of the extrusion.

In this paper the longitudinal oscillation arising from the radial oscillation was calculated using the simple relationship connecting longitudinal and lateral strains with the single applied stress. This use of Poisson's ratio appears to make an elementary error since no account was taken of the lateral stresses.

2.3.2. Drawing Processes.

2.3.2.1. Wire Drawing.

In the drawing processes the tensile strength of the drawn product limits the amount of deformation which can be achieved in any single stage. Thus any modification to improve the drawing process must reduce the tensile stress within the drawn product thus enabling greater reductions per pass to be achieved.

Wire drawing tests using longitudinal oscillations of the die were conducted by Vatrushin[19]. Liquid lubricants were considered ineffective because they were ejected from the die throat by the ultrasonic action. No changes in the frictional conditions were reported but a reduction in the deformation resistance within the die was confirmed by the fact that the strength of the drawn wire was lower. An increase in temperature was said to account for this observation. Transverse oscillations of the die were reported as

having negligible effects on the reductions obtained. All these results were based on the measured draw load which did not allow for the stress-superposition effects to be observed; consequently, the instantaneous stress within the wire cannot be determined.

Comparing these results with hydrodynamic drawing using low die angles the hydrodynamic method compares favourably with the ultrasonic systems. This observation is borne out in practice by the lack of commercial exploitation of ultrasonic wire drawing equipment. This is not unexpected since wire drawing through a single die with longitudinal oscillations applied does not maximise the advantages of ultrasonic metalworking. More conventional techniques for improving lubrication such as hydrodynamic drawing are better suited to the high speeds used in wire drawing than ultrasonic methods.

Transverse oscillations of the die which Vatrushin found to be of little value were described in a recent patent[20]. In this patent the use of the swaging effect, where ultrasonic stresses replace part of the drawing stress, was stated to be not particularly beneficial, when difficult to deform materials were being drawn, because of the high stresses involved. The use of a transverse oscillation of the die at a velocity antinode was preferred because of the frictional reduction effect it would have on the wire-die interface. It was claimed that this friction reduction allowed much higher processing speeds and enabled some materials to be drawn, which could not be drawn by conventional means.

These claims can be contrasted with the work of Severdenko[21] on drawing titanium alloy wires using transverse oscillations of the die. In this process the oscillatory die was maintained in resonance by drawing the wire through two further dies located at equal distances on either side of the main die. A sharp reduction in the draw force was recorded and when the ultrasonic vibration was switched off there was a lag before the draw load returned to its original level Fig. 2.3.2.1. This reduction in force was attributed to a drop

in the flow stress within the system bounded by the two additional dies although slight changes of wire diameter from the main die could have been a factor.

Fig. 2.3.2.1.

(Severdenko et al).[21]

The relative methods were discussed of bulk heating or a preferential absorption of energy at the dislocation sites to account for the ultrasonic energy input. Severdenko favoured a preferential absorption effect. Unfortunately, there seems little evidence to base this judgment on and no attempts were made to distinguish which factors predominated. Superposition of bending stresses brought about by transverse oscillations of the die must have been responsible for a large part of the apparent force reduction. Contact friction effects may be reduced by a redistribution of lubricant and therefore any real reduction in the drawing stress is likely to be confined to the reduction in the yield stress caused by the heating effect. This method of applying the ultrasonic energy to the die was compared with the location of the die at a stress antinode in an earlier paper by the same author[22]. In this paper oscillations of the die at a stress antinode were reported as being more effective in reducing the drawing load than when the die was situated at a displacement antinode which could result from a swaging effect.

High frequency bending stresses were developed when using longitudinal oscillations of the die provided the diameter of the wire was small enough. Sämann[23] found that despite the reduction in the externally applied force obtained when using such a system

there was still tensile failure in the drawn wire if too large an area reduction was attempted. This limitation was removed by the addition of a second die positioned downstream of the first. When drawing through this two die system the oscillatory first die produced the alternating flexural stresses which superposed on the mean drawing stress so as to equal the non-vibrated drawing stress. This drawing stress acted as the back tension for the second die. The oscillatory flexural stress was not transmitted through to the second die with the resulting lower stress in the drawn product. The lowering of the final tension in the drawn wire enabled the maximum reduction-of-area possible in the non-vibrated case to be increased to take advantage of the lower drawing stress without rupturing the wire.

In an earlier publication the use of multi-die systems to enable stress-superposition mechanisms to produce a genuine reduction of the peak stress within the wire have been described by Winsper and Sansome[24]. Before their multi-die investigations, results were obtained with a single longitudinally oscillated die in which the acoustic stress in the drawn product was monitored. In this process they demonstrated that the apparent drop in drawing stress was equal to the acoustic stress amplitude showing the process to be one of stress-superposition. This had been observed both at ultrasonic frequencies [25] and previously at low frequencies [26]. Referring again to their multi-die system, it was found that if the back tension applied to the die had an alternating component, only its mean value was effective in raising the front tension. This explanation showed good agreement with the observed mean and alternating stress levels as did the earlier work on a single die system.

Pohlman[27] compared two methods of wire drawing along with the concept of using a mode of vibration which imparted the least ultrasonic energy to the wire. This was in order to obtain the greatest benefit from friction reduction.

Using longitudinal die oscillations in a two die system, reductions of up to 50 per cent in the drawing force were obtained. Some of this reduction was, however, believed to be caused by stress-superposition which was only an apparent effect. The other method, using longitudinal die vibrations to generate high frequency bending stresses in the wire is very similar to that reported by Sāmann[23] and could well be the same piece of work. The limitation to this process was said to be the slow speed of drawing. Provided low drawing speeds were used reductions in the drawing force of 10 per cent were possible.

The usefulness of these multiple die systems for drawing wire can be contrasted with the single die system used by Langenecker and Jones[28]. High energy inputs resulted in large reductions-of-area being possible even at high drawing speeds whilst other authors report a definite decrease in the effectiveness of ultrasonic oscillations as the processing speed increases. The effect responsible for these observations has been named the "Blaha Effect" by Langenecker and is described as the softening of a material under ultrasonic vibration in the absence of a temperature rise.

The high energy inputs used by Langenecker are likely to result in over-heating with the consequent thermal softening of the material being drawn. The use of high drawing speeds could also result in the establishment of drawing under hydrodynamic conditions of lubrication which would further reduce the loading necessary to deform the wire. These two phenomena can be used to explain the results obtained by Langenecker without reference to the preferential absorption of energy model.

Longitudinal die vibrations have also been applied to the process of section drawing. Severdenko[29] obtained load reductions of 50 per cent, although much of this would be apparent resulting from stress-superposition. A reduction in the number of passes to produce a given section was recorded whilst the drawn material was

softer. In addition, micro-hardness readings, across the specimen, revealed a more uniformly deformed product when using ultrasonic oscillations. The drawn product also exhibited surface disruption when the vibrations were applied. Such a combination of effects could be attributed to improvements in lubrication arising as a result of the intermittent drawing and relative movement of the section within the die. This improvement in frictional conditions would be responsible for the increased metal deformation possible per pass and give a real contribution to the load reduction recorded.

Various methods of draw load reduction were demonstrated in ultrasonic strip drawing by Severdenko et al[30]. Dies of a cylindrical form were used, the direction of oscillation being $\pm$ 45 degrees to the drawing direction. Fig. 2.3.2.2.

Fig. 2.3.2.2.

(Severdenko et al).[30]

When the oscillations were phased so that the dies were moving towards each other this was equivalent to a longitudinal oscillation combined with a swaging action. An increase in the maximum possible reduction was obtained attributable to the swaging and possible improvements in lubrication. With oscillations phased so that the dies were moving in opposite directions a vector analysis of the motion reveals the system to be a fixed die angularly oscillating about an axis parallel to the surface of the strip and at right angles to it. Thus the strip was being deformed by a bending and

shearing action under tension with the additional influence of a friction-vector reversal on one surface of the strip. This frictional reduction depends on there being relative movement between strip and die, a condition which does not occur with normal strip drawing, or wire drawing, because when die and strip velocity are in the same direction the strip is elastically unloaded so that there is no opportunity for this friction-vector reversal effect to materialise. This second system of die oscillation does allow separation and relative movement to occur which enabled the maximum reduction of area to be increased from 58 to 88 per cent compared with a figure of 64 per cent for the first system of oscillation. Thus in this instance the system of introducing bending stresses combined with a friction reduction gives a greater effect than the application of a swaging action. The swaging action should be capable of doing all of the process work, however, and in certain circumstances, the draw load can be reduced dramatically [31]. This anomaly could therefore result from the increased loading within the second system causing a reduction of oscillatory amplitude with subsequent smaller effects upon the draw load and reduction of area obtainable.

2.3.2.2. Tube Drawing.

The process of tube sinking resembles wire and section drawing and the mechanisms which apply to the wire drawing can be likewise applied to the process of tube sinking. Severdenko[32] examined axial and transverse die vibrations in order to obtain a comparison of effectiveness. Periodic variations in the draw force were obtained when the dies were situated at displacement antinodes. The usefulness of such a reduction is, however, questionable since from the instrumentation described it was obvious that the loads recorded were not peak loads and information on the reduction of area was absent. Thus for the results of tube sinking with the die at a

longitudinal displacement antinode the only real effect can be a possible improvement in the lubrication resulting from intermittent drawing and possible surface separation. Dies placed at stress antinodes were subject to compressive stresses. The die positioned axially was oscillated radially by the Poisson effect whilst the die positioned transversely was distorted elliptically. With dies positioned at the stress antinode, the drawing stress was genuinely lower since the swaging imparted to the tube by the die, resulted in a modification of the state of stress and resulted in yield occurring at a lower drawing stress than under non-oscillatory conditions.

The problem of periodic variation in the draw force when using a single die system was avoided by Severdenko and Stepanko[33]. The tube was insulated from the die by a lubricant film so that the system operated continually in resonance. The usefulness of this process must, however, be questioned. Hydrodynamic lubrication is known to be speed dependent and in the paper it was shown that as the speed increased the degree of deformation possible, still maintaining hydrodynamic lubrication, also increased. Ultrasonic vibrations were actually detrimental to the establishment of hydrodynamic lubrication because this effect was only observed at higher drawing speeds and lower area reductions compared with the conventional drawing process. Ultrasonic vibrations have been shown to be more effective at lower drawing speeds, e.g. Winsper et al[25] and therefore their application seems counter-productive unless it was to improve drawing conditions at the start of the drawing process before the drawing speed was sufficient for hydrodynamic lubrication to be established. Periodic variation of the draw force, was also commented upon by Severdenko[34], when drawing aluminium alloy tubes using longitudinal vibrations of the die. With a single die the greatest effect was obtained when drawing annealed tubes. This demonstrated the predominance of stress-superposition upon the reduction of the draw load. The effect of a given cyclic stress

would be greatest upon the annealed tube since this deforms at a lower overall stress than an initially harder material.

The addition of a second die downstream of the first die, stabilised the drawing and also enabled the reduction to be increased c.f. Sämann[23].

The use of a third die upstream situated within the ultrasonic concentrator enabled a further reduction in the drawing load to be obtained. This third die, situated at the stress antinode of the concentrator was caused to oscillate radially by the Poisson effect, thus swaging the tube.

Reductions in the draw load and increases in the area reduction in the tube-sinking process have been obtained with axial or radial die oscillations and improvements in the frictional coefficient. Ultrasonic tube drawing over a fixed plug is, however, characterised by longitudinal vibrations being applied to the plug bar. Kolpashnikov et al[35] observed the effect of mandrel vibrations as causing a reduction in the drawing force and controlling the properties of aluminium alloy tubes. Substantial reductions in the draw load were recorded which, although periodic, can be attributed to friction-vector reversal between tube and plug interface. In addition, the material properties were sometimes affected by a rise in temperature of the aluminium within the deformation zone. These benefits increased with an increase in the oscillatory amplitude but at the higher amplitudes tested, the temperature rose rapidly causing the tube to adhere to the tooling. This over-heating of the material adversely affected the quality of the drawn tube.

The finished tubes produced with the ultrasonic oscillation were of lower strength and more ductile, indicative of the reduced frictional forces together with the modification of the work-hardness caused by the temperature rise. This variation of properties was not maintained after heat treatment of the drawn tube when the properties had become independent of the production route.

Dragan and Segal[36] reported an increase in the attainable reduction of up to twice those normally possible. The authors attributed this to a change in the material plastic properties. This is, however, clearly a case of friction vector reversal in addition to any effects upon material properties recorded. In a more recent paper [37] these increases in plasticity were described as a reduction in tensile strength, a decrease in hardness and an increase in ductility , which are clear indications of a more uniform drawn product. This may have been the result of a heating mechanism or just the friction reduction depending upon the energy input. Dragan and Segal reported that their results depended on a reduction in the friction vector.

These findings were in agreement with those of Winsper and Sansome[38]. They reported reductions in drawing load and plug bar load when drawing thin walled stainless steel tubes with axial vibrations applied to the plug bar. Improved surface finish and a reduction in slip-stick of the plug were noted. These changes did not affect the material properties and friction vector reversal was reported as the mechanism responsible for these beneficial effects.

Sugahara et al[39] clearly stated that friction vector effects were responsible for the 90 per cent reduction in plug bar load during experiements in tube drawing although the loading on the plug bar was light and consisted of approximately 15 per cent of the total draw load. When tube drawing with heavier reductions of area the reduction in plug and die forces was less as were the dimensional changes after drawing. This was attributed to the repeated impacting nature of the process but surface separation was not likely to occur. Lower die stresses with the corresponding reduction in die expansion would assist as would the reduction in residual stresses because of the friction reduction. Larger than normal reductions of area were possible and in this context a reduction in deformation resistance was mentioned but not substantiated. Plug 'chatter' was

prevented thus allowing poorer lubricants to be used. This effect upon chatter was speed dependent giving further support to the friction vector reversal mechanism.

Improvements in the dimensions of the finished tubes when using plug and die vibrations has also been reported by Waterhouse[40].

The process of tube drawing with a floating plug has been examined by Dawson[41]. Radial oscillations of the die were used because axial vibrations of the die in both wire and tube drawing have made only small improvements to the process when using a single die. Using radial vibrations, reductions of 18 per cent in the draw force were recorded. No axial cyclic stress was recorded in the drawn tube indicating that this reduction was real and not the mean value of an alternating drawing stress. On drawing, the 'chattering' of the floating plug was diminished or almost eliminated by the oscillatory power. This enabled poorer lubricants to be used successfully when the vibrations were applied to the die. The improvement in the maximum possible reduction was obtained in the absence of any heating of the tube being drawn and the surface finish was not adversely affected. Reductions in draw load were increased by greater die amplitudes but diminished at the higher drawing speeds.

Fig. 2.3.2.3.

(Dawson) [41]

The mechanism responsible for this action was the establishment of a neutral plane within the deformation zone. The reversal of metal flow in part of the die also reversed the frictional force. The back-tension upstream of the neutral plane was reduced thus decreasing the total drawing force. The reversal of the frictional force on part of the plug caused it to float further back in the die thus alleviating the problem of 'chatter' caused by the die intermittently 'swallowing' the plug.Fig.2.3.2.3.

The analysis of the process demonstrates how the swaging action of the radial die vibrations results in a real reduction of the draw force, with the possibility of further reductions if the die amplitude is large enough and the angle of friction larger than the die angle.

2.3.3. Processes examining basic mechanisms.

2.3.3.1. Friction.

From the preceding sections reviewing some of the recent work on the application of oscillatory energy to metal working processes, one recurring feature has been that of friction reduction by the application of ultrasonic vibrations.

The effect of longitudinal vibrations on the frictional force necessary to move a body was investigated by Mikhenl'man and Mashchinov[42]. The forces necessary to cause movement of one body were recorded both with and without ultrasonic oscillations and an effective coefficient of friction was determined. No lubrication was used which therefore eliminated possible lubricant effects, such as surface activation and hydrodynamic lubrication. The mode of friction reduction was therefore friction vector reversal since although a possible heating effect was mentioned there was no experimental evidence to support this statement.

The desirability of employing vibrations parallel to the frictional force was made clear by Konovalov[43]. In high speed

applications, however, this type of friction reduction is of little use because when the sliding velocity equals oscillatory velocity the effect disappears. This problem instigated the examination of the use of vibrations at right-angles to the friction force and the effect obtained was found to be independent of sliding speed. This reduction in friction was caused by cyclic surface separation which permitted the lubricant to redistribute itself during the operation. This was shown to be a useful method of reducing friction in metal working operations, although this work of Konovalov was performed under elastic conditions which resulted in better surface separation than under conditions of plastic deformation.

Further information on friction is contained in the friction section of a book by Severdenko[44]. A friction vector effect was described when ultrasonic vibrations were introduced parallel to the surface and perpendicular to the force of friction. The periodic swinging of the friction vector about its mean position resulted in a decrease in the friction in the drawing direction when summed over a cycle. This is because over part of this cycle it cannot increase beyond that which occurs in non-oscillatory deformation and over the remainder of the cycle it is equal to or less than that occurring in non-oscillatory deformation.

With vibrations normal to the surface a distinction was drawn between separation and non-separation. Even with non-separation a friction reduction was still said to occur due to relative movement of the contact surfaces but this was not supported by any direct experimental evidence.

Finally, concentrating on the effect of ultrasonic vibrations on the lubricants themselves, it was stated that their use resulted in an increase in the adhesion and absorption capacity of a metal. The vibrations were also said to aid the growth of microcracks into which lubricants penetrate. Rapid reciprocation of one surface relative to another raises the temperature; consequently, chemical reactions

were accelerated resulting in a reduction of the coefficient friction, although in some cases adverse effects caused a reduction in the effectiveness of the lubricant. These statements made by Severdenko that microcracks are a feature of oscillatory deformation have not been supported by direct experimental data in the metal deformation field but he suggests such mechanisms can occur in these processes.

The effectiveness of vibrations in the absence of lubrication was studied by Severdenko and Stephenko[45]. When in vacuum and using high metalworking temperatures galling of the tool-workpiece surface was severe. On applying vibrations the forming loads were reduced and the galling was eliminated. This improvement was attributed to periodic breaking of weldments as the tools were vibrated.

2.3.3.2. Material Properties.

Friction reduction due to both the periodic swinging of the friction-vector from its normal line of action and the variation in the coefficient friction is reasonably well understood in its application to oscillatory metalworking. The effect of such vibrations on the material properties of the workpiece is not so well understood and there is not the unanimity of opinion on the way in which ultrasonic vibrations are absorbed by the workpiece material. The majority of researchers consider ultrasonic vibrations to behave according to stress-superposition principles and at the higher energy input levels, treat ultrasonic energy as thermal energy apart from the usual methods of applying conventional thermal energy. The other group considers ultrasonic energy to be absorbed in an unique manner and thus have advantages over and above those which would normally accrue from a thermal energy input. This section reviews recent papers which reported the effect of vibratory energy in various processes.

A temperature rise in free upsetting during ultrasonic oscillation of the tooling was reported by Severdenko and Petrenko[46].

This temperature rise was used to account for the softening of the workpiece. The softening was a real process and not just an apparent reduction caused by stress-superposition because the hardness of the material was also reduced. The explanation of the observed softening was reported as caused by a reduction in the yield stress because of the oscillations releasing dislocations. This reduction in hardness could also be as a result of a more homogeneous deformation caused by improved lubrication whilst the yield stress could be reduced by the temperature rise. In the presence of this temperature rise it is not possible to distinguish between the various possible causes of the softening of the material. In a later paper [13] this shortcoming was recognised and further tests were devised to obtain more information. A comparison was effected between ultrasonically vibrated deformation and electrically heated samples deformed conventionally, the temperatures used in the latter case being the temperatures recorded during the deformation with vibrated tooling. The resistance to deformation was reported as being lower with ultrasonic energy than that when using electrically heated samples. The authors concluded that ultrasonic energy was absorbed at crystal lattice defects whilst thermal energy was absorbed uniformly throughout the volume of material. The experimental evidence presented in the paper, however, does not confirm which mechanism most closely describes the actual situation. Measurement of temperature during sonification is not a simple procedure but no information on the system used was given. The details of the load measuring system indicated that only the steady, non-oscillatory load was recorded and not the instantaneous load. Thus samples deformed with oscillations of the die would appear softer than the conventionally deformed samples because of stress-superposition rather than a change in material properties.

The variation in the residual stresses between conventional and vibratory free upsetting was determined by Severdenko and Petrenko[47].

In all cases the use of ultrasonic vibrations resulted in lower residual stresses which the authors attributed to a reduction in the non-uniformity of deformation. This would occur as a result of the reduced external frictional constraint between tool and workpiece. When using axial vibrations of the tooling, surface separation enabling a redistribution of the lubricant to occur would give this improvement. A second reason for the residual stress reduction was given as an increase of temperature at the crystal lattice defects, thus increasing atom mobility. No evidence was presented, however, to support this statement, no reference to temperature measurements or the mechanical properties either before or after deformation other than the reduction in residual stress which would also occur as a result of a bulk temperature rise were given.

Another paper concerned with residual stresses by the same authors [48] involved rolling with axially vibrated rolls, that is along the axis of the roll not the direction of rolling.

Lower residual stresses were reported as caused by increased shear stresses at the interface of the roll and work material. The yield point of the material was reduced because of heating and absorption of ultrasonic energy at lattice defects. Once again no attempts were reported of tests to determine the true nature of the problem, only speculation covering every mechanism such that the correct explanation would be included somewhere.

A means of estimating the resistance to deformation under ultrasonic deformation conditions was proposed by Mizuno and Kuno [49]. They found that dynamic hardness using the mean load was less than the static hardness, which in turn was less than the hardness calculated from the peak value of the loading force. The first finding can be attributed to stress-superposition whilst the latter is presumably an expression of strain-rate effects and the behaviour of the material as a viscous mass, being able to sustain high loads for short periods without suffering the deformation normally associated

with static loading. In the case of a hardness test this would appear as a smaller indentation with the subsequent 'harder' material designation. The validity of such a test to determine the formability of materials during ultrasonic working is questionable since any compression process will contain some frictional effects in addition to the pure mechanical properties and, in fact, it has been indicated by Kleesattel[50] that the tests of Mizuno and Kuno do not enable the formability to be established.

The effects of ultrasonic vibrations on the structure of aluminium were reported by Severdenko[51] and Gindin et al[52]. The former studied deformation bands on the surface of a vibrated sample. Slip planes were only formed after a specific number of ultrasonic cycles. Once these slip planes were formed the topography of the surface increased with an increasing number of oscillatory cycles, until fracture occurred. This behaviour was compared with the effects obtained when the samples were subject to conventional fatigue testing.

The second paper applied ultrasonic vibrations to statically loaded aluminium samples. Heating effects caused by the absorption of oscillatory energy were discounted because the vibrations were applied in short bursts with long time intervals between each burst. On examination of the effect of these vibrations on the structure a dependence of the dislocation movement and consequently the strain mechanism on the number of ultrasonic pulses was found. These effects described can be explained on a microscopic scale by referring to the stress-strain curve of aluminium. It was reported that with higher static loading the elongation of each ultrasonic pulse was greater. This can be explained by the diminishing slope of the stress-strain curve as the material work hardened as shown in Fig.2.3.3.1.

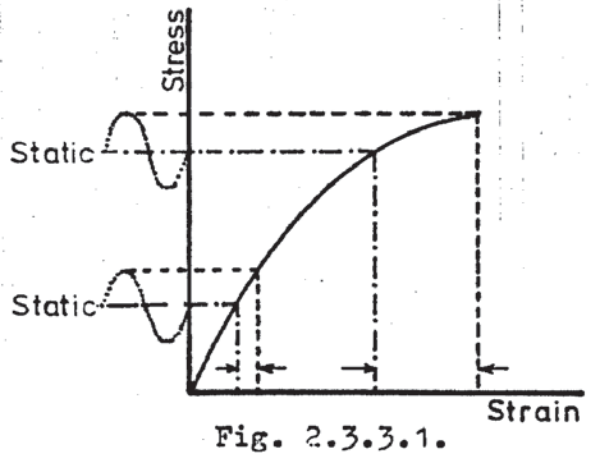

Fig. 2.3.3.1.

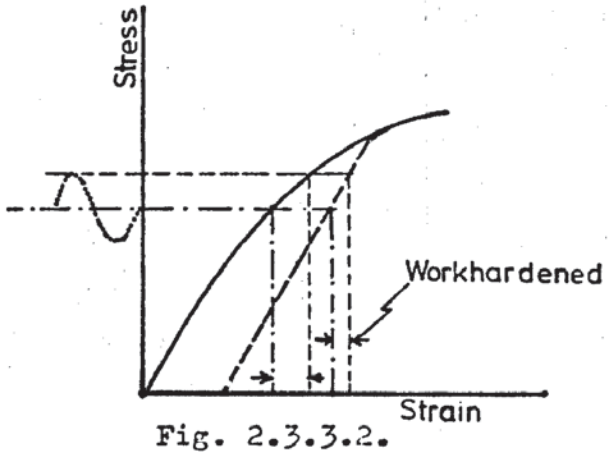

Fig. 2.3.3.2.

Preliminary hardening of the material made it more resistant to elongation, which is a consequence of work hardening, Fig. 2.3.3.2. From these observations the authors conclude that the softening (stress-superposition effect) depends upon the initial condition of the aluminium.

The effects of the ultrasonic vibrations on the mechanical properties of mild steel were reported by Puskar[53]. Tensile test pieces were subjected to longitudinal vibrations and tested afterwards in an Instron tensile testing machine. The effects of the ultrasonic vibrations, applied for various times, on the mechanical properties, were recorded. The temperature reached by the vibrated sample was a function of sonification time and stress level. Higher temperatures were recorded with cold-worked as against annealed samples, which can be interpreted as caused by the greater energy input necessary to cyclicly stress a cold-worked material on account of its stronger mechanical properties. The proof and ultimate tensile stresses of vibrated samples were increased whilst the elongation was reduced once the oscillatory amplitude became great enough to stress the material into the plastic state. As the material was cold-worked the effect of ultrasonic oscillations on the properties became more acute, with the change in properties beginning at lower cyclic stress levels. The effect of a long sonification time was to increase the strength and lower the extension of the material, when the applied stress level was within

the elastic range and the stress exceeded some threshold value, which can be attributed to the effects of fatigue upon the samples.

This can be compared with the paper by Dragan and Segal[54] on the effect of ultrasonic vibrations on carbon steel. A reduction in the yield and ultimate tensile stresses was recorded as the ultrasonic stress level increased. The method employed to record these stresses was not described and stress-superposition effects could cause an apparent softening. Heating was more likely, however, because of the residual effects on the mechanical properties, a reduction in hardness and an increase in elongation being consistent with an annealing process. On cold-working the previously vibrated material the mechanical properties, modified by the oscillatory process, were recovered, demonstrating the absence of any lasting effects attributable to the application of ultrasonic vibrations.

Several hypothesis to account for the observed effects of ultrasonic vibrations were presented by Langenecker et al[55]. Ultrasonic softening was accounted for by preferential absorption at the dislocation sites enabling dislocations to surmount the potential barriers between equilibrium positions. This model was described in more detail in [56] in which refinements were made to the model to account for permanent changes in dislocation structures observed during plastic deformation such as hardening.

Microscopic studies of plastic deformation with ultrasonic vibrations applied were compared with plastic deformation at elevated temperatures and high deformation rates. The end results were very similar supporting the consideration of ultrasonic metalworking being an extension of conventional metalworking which perhaps is contradictory to the preferential absorption models proposed by the same author. Curves showing shear stress extension for various levels of excitation were illustrated demonstrating the initial hardening effect followed by the softening effect Fig. 2.3.3.3.

Fig. 2.3.3.3.

(Langenecker et al).[55]

No mention was made of the superposition of stresses during ultrasonic oscillations; also some of the curves (b,c) shown have the same appearance as would be obtained if the specimens were over-heated. Acoustic heating was postulated as different from external heating.

A reduction in Young's modulus, on the application of ultrasonic oscillations, was also reported but from the evidence presented this could be caused by temperature rather than ultrasonic effects. The paper presents many ideas to explain the effects of ultrasonic vibrations but it is difficult to assess these because of the lack of evidence supplied.

The preferential absorption concepts were again re-presented in a later paper [57] with an emphasis on efficient application of the ultrasonics during conditions of varying load. Only processes within the crystal lattice which could be completed in the time equal to that of a half-cycle of an ultrasonic oscillation were said to be possible. This time limit was said to account for the difference in Wöhler curves obtained during conventional and ultrasonically vibrated fatigue tests.

The model was again repeated in [58] as an explanation for observations of plastic flow using ultrasonic oscillations in which

flow occurred at stresses lower than the yield stress at room temperature of the material. This phenomenon has only been observed by Langenecker and his co-workers. Other authors attribute such observations either to stress-superposition or heating. The former gives an apparent softening of the material whilst the latter effect leads to a reduction in the current yield stress, the heating resulting from the absorption of acoustic energy being akin to that produced by conventional thermal energy.

Over-heating of the samples being tested is one of the major problems encountered when using ultrasonic vibrations. If this problem is solved by proper cooling with attention paid to a cooling medium which does not corrode (stress corrosion) the sample, Bajons et al[59] have reported that the frequency effect between the frequencies examined of 200Hz - 20kHz is insignificant. Thus the reason of poor experimental method in controlling sample temperatures could be responsible for the frequency factor rather than the processes within the crystal lattice described by Langenecker.

2.4. Deep-Drawing and Draw Ironing with Ultrasonic Vibrations.

The application of oscillatory energy to the process of deep-drawing was first reported in 1963 by McKaig[60]. Ultrasonic vibrations were applied to the die and an increase in the depth of draw of 37 per cent was recorded compared with the non-vibrated process for a given loading.

In both conventional and ultrasonic drawing the load recorded by the press was 1000 lbf. The instantaneous load when using the ultrasonic vibrations would have been higher than that recorded because of stress-superposition effects of the oscillatory load. This would not be particularly useful when the limiting draw ratio was reached since the material would respond to the peak stress and therefore fail at the same stress as would the non-oscillatory draw. The increases in depth of draw reported were obtained with partial draws, rather than increases caused by raising the limiting draw-ratio.

When drawing with a form using ultrasonic vibrations the part conformed to the die whilst for the same press load when drawing conventionally the definition was poor and the workpiece did not go to the bottom of the die, again demonstrating the stress-superposition effect of the vibrations. No details of the ultrasonic system were given except that the vibrations were applied to the die, making it difficult to ascertain the effects of the vibrations. In addition to stress-superposition there could have been frictional changes which would contribute to the greater depths of draw obtained.

The dimpling of aluminium and titanium sheet using axial vibrations of the punch or die was examined by Peacock[61] who reported greater degrees of deformation for a given loading compared with the non-oscillatory process. The strain increases were attributed to the impacting of the tools producing high forces of short duration, that is, stress-superposition, whilst the reduced contact time caused by the oscillating nature of the load brought about a reduction in friction.

This friction reduction could be considered a real effect contributing to a genuine reduction in the forming load, providing there was surface separation which may have occurred in the compression of thin strip material.

Langenecker et al[62] used longitudinal vibrations of the die when deep drawing. No further details of the deep drawing were given but when using a similar method of applying the vibrations to the ironing process a reduction in the load of 65 per cent when ironing copper cups was reported. In addition to the load reduction a greater reduction of area per pass was claimed. These advantages were said to be caused by a reduction in the yield stress of the material at the high levels of oscillatory energy used. The load recording system used was that of the testing machine which would only record the mean load. Some of this load reduction can therefore be attributed to stress-superposition. The reduction in the number of passes to achieve a given reduction of area could also have been produced by swaging within the ironing die. The die entry was situated at the strain antinode which would preclude any swaging but further into the die, which from the diagram appears to be rather long, the increasing cyclic stress amplitude would cause the die to oscillate radially because of the Poisson effect.

The importance of dynamic force measurement was emphasised by Kristoffy[63] in the application of axial oscillations to the punch and radial oscillations to the die in the deep drawing and ironing of aluminium and steel. The measurement of the dynamic force enabled Kristoffy to conclude that the punch load reduction observed when oscillating the punch axially was due entirely to stress-superposition, the peak force in the drawn product being unchanged.

When the die was vibrated, however, a true reduction in the punch load was obtained. With the low frequency 20 Hz oscillations, the die was arranged to move circumferentially to the punch. The reduction in friction which was obtained was attributed to the change in

the direction of friction from axial to axial-tangential at the die-throat. This periodic 'swinging' of the line of action of the friction force about the axial direction resulted in a reduction in the mean value of friction force in the axial direction. Friction reduction by this method has been demonstrated by Rothman and Sansome[64] who rotated the drawing die when rod drawing.

At the ultrasonic frequency of 20 kHz the die was vibrated by two diametrically opposed transducers, which although giving a 'radial' vibration would be unlikely to produce a uniform motion around the entire circumference, producing instead an elliptical motion of the die. With this 'radial' vibration changes of friction at the die-throat were not possible because of the die being vibrated perpendicularly to the punch motion. It was anticipated that the state of stress could be changed at both frequencies giving a tangential shear at low frequency and additional radial compression at the high frequency which Kristoffy correctly concluded would result in a forming force reduction. The energy requirements of the system were said to be unchanged, energy saved on the forming equipment being supplied by the vibrator.

The omission by Kristoffy to appreciate the contribution to the total draw load of the frictional force acting between specimen and die and blank-holder surfaces was recognised by Young[65] who by the use of a modified form of the Wedge Drawing Test was able to monitor directly the effect of 'radial' die vibrations on this frictional force. The use of the Wedge Drawing Test in a tensile testing machine as an alternative to cup-drawing tests when assessing the drawability of materials was investigated by Loxley and Swift[66].

Using 'radial' vibrations in a 'cupping' operation Young recorded increases in the limiting draw-ratio of up to 20 per cent. This improvement was attributed mainly to the reduction in friction between the specimen/blank-holder interface with an additional contribution being made by a reduction in the frictional force acting over

the die radius.

This work was extended to the complete cup-drawing operation by Biddell and Sansome[67], who concentrated on the design of efficient radial resonators. Using a radially vibrated die they reported increases in the maximum depth of the drawn cup of up to 20 per cent. In addition to the friction reduction over the die and die radius surface some contribution to the ironing operation was expected from the swaging effect at the die throat. Young had specifically avoided this latter process by the use of generous clearance tools to prevent it complicating his work on the friction effects. This work has been extended by the present author to examine the effects of axial punch vibrations[68], axial and 'radial' blank-holder vibrations[69] and 'radial' die vibrations in the draw ironing process.

Summarising the development of ultrasonic metalworking it can be said that the confusion of ideas has arisen because the effects and number of them were unknown and it was not appreciated that several factors could occur simultaneously and in various proportions in different processes. This resulted in concentrated examination of the effects ultrasonic vibrations have on the yield stress almost to the exclusion of everything else. The discussion of friction reduction either by changes in the coefficient of friction or friction-vector has also suffered. The importance of stress-superposition was recognised by few workers as was the significance of swaging. An example of this is the work of Kristoffy; he correctly stated the importance of stress-superposition yet failed to distinguish between the beneficial effect of swaging in ironing and its virtual non-existence in deep drawing. The friction reduction at the die throat when using circumferential vibrations was also recognised and yet the friction reduction between specimen and blank-holder in deep drawing subsequently demonstrated by Young was not appreciated.

Further discussion on the effects of the application of ultra-

sonic vibrations to metal deformation processes and the mechanisms now believed to be responsible for these effects, can be found in the review paper by Eaves et al[70].

3. THEORETICAL CONSIDERATIONS.

3.1. The Theory of Cup Drawing.

3.1.1. Introduction.

The analysis carried out by Chung and Swift [71] considers the instantaneous distribution of drawing stress and the strain undergone by any particular element in the flange during drawing.

From a series of stress distribution plots representing various stages in drawing the progress of any particular element through the complete process can be traced, leading in its most comprehensive form to a plot of punch load v punch travel.

The analysis is developed by considering several different stages of drawing and in turn deriving expressions for the principal drawing stresses. The radial stress, which is of most interest in relation to the punch load is considered to be made up of five components defined as follows:-

(I) The component of radial stress due to drawing in of the flange. See Fig. 3.1.1. stresses acting during deep-drawing.

(II) A contribution to the above stress attributed to the blank-holding load acting at the periphery of the blank.

(III) Plastic bending under tension at the start of the die radius.

(IV) Friction and radial stress components related to the motion of the blank over the die profile radius.

(V) Unbending under tension at exit from the die radius.

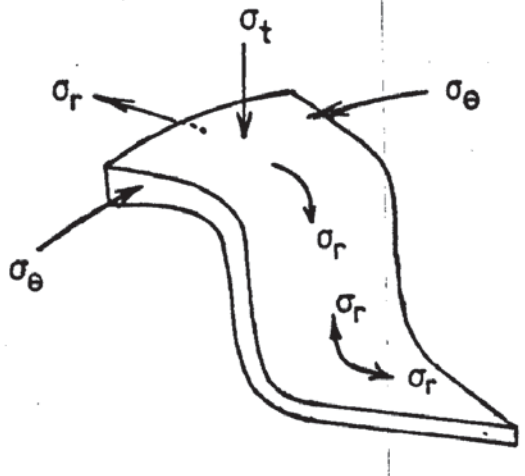

Fig. 3.1.1. Stresses acting on a radial segment during deep-drawing.

Fig. 3.1.2. Radial Stress Distribution in Deep Drawing

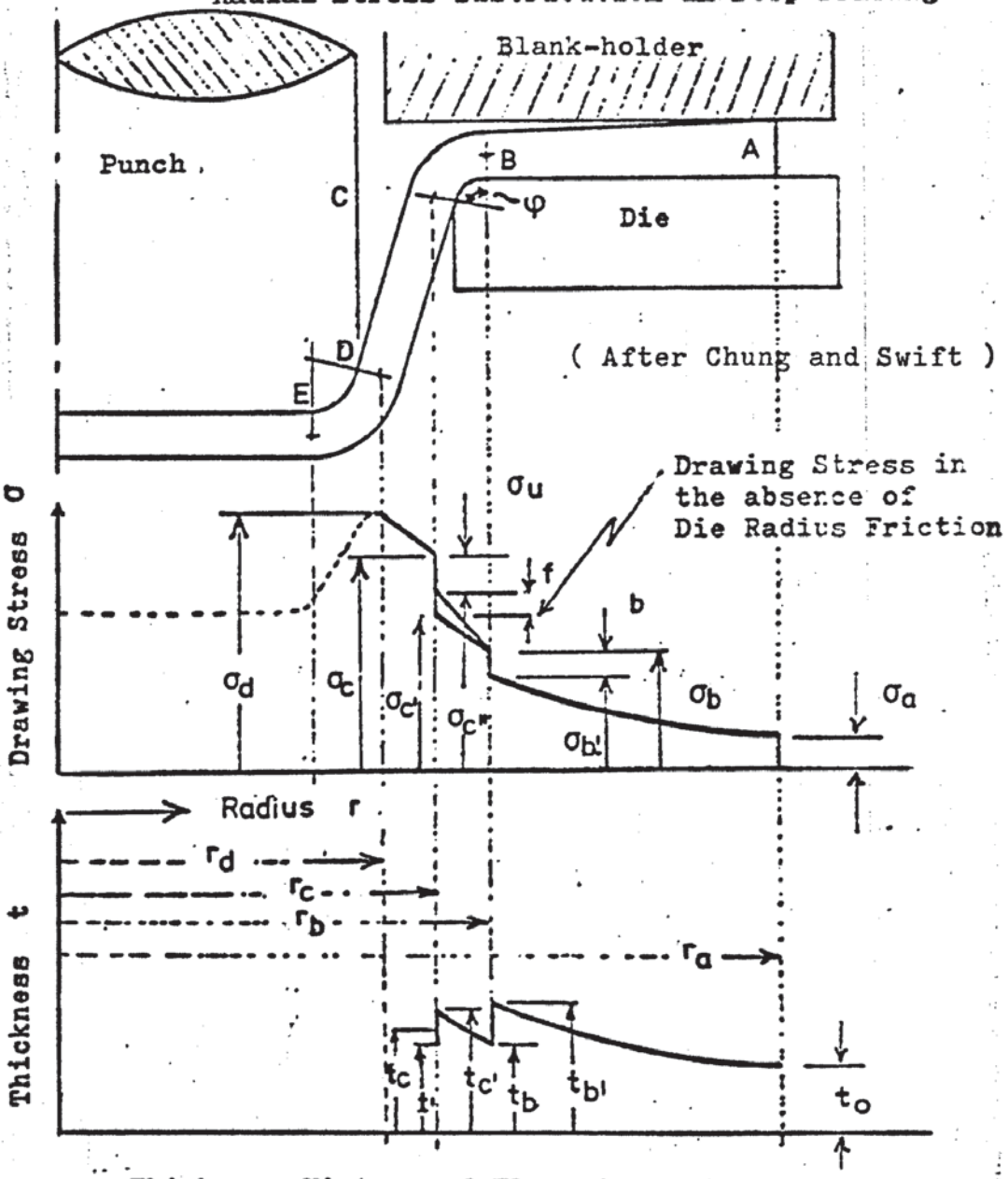

Thickness History of Element

Fig. 3.1.3.

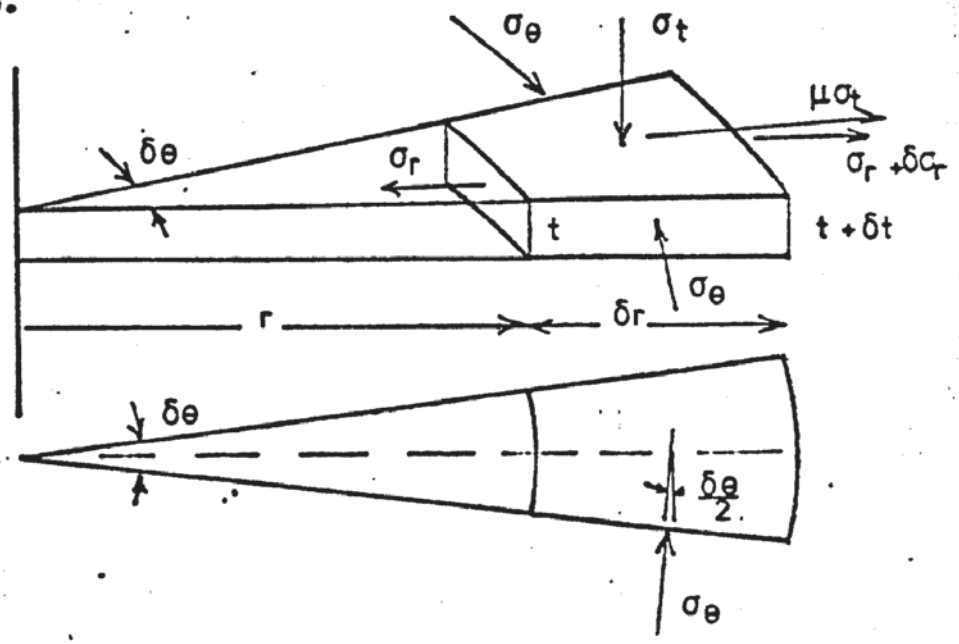

Stresses acting on an Elementary Ring in Radial Drawing

The stress increments due to each of the above stages of drawing are considered to be simply additive and the punch load is derived directly from the cup wall stress, which is the sum of the above stress increments. See Fig. 3.1.2.

3.1.2. Stresses Acting in Radial Drawing.

The equilibrium equation describing the instantaneous force system in the flange during drawing may be determined as follows: Resolve forces horizontally. Fig. 3.1.3.

$$\sigma_r r\delta\theta t-(\sigma_r+\delta\sigma_r)\ (r+\delta r)\ (t+\delta t)\delta\theta-2\sigma_\theta\left(\frac{2t+\delta t}{2}\right)\delta r\sin\frac{\delta\theta}{2}$$

$$-2\mu\sigma_t\pi(2r+\delta r)\delta r\frac{\delta\theta}{2\pi}=0 \qquad \text{--------3.1.1.}$$

Assume $\sin\delta\theta=\delta\theta$ then, ignoring products of increments and dividing through by $\delta\theta$ gives:

$$-\delta\sigma_r rt-\sigma_r t\delta r-\sigma_r\delta t r-\sigma_\theta t\delta r-2\mu\sigma_t r\delta r=0$$

and dividing by rt:

$$\delta\sigma_r=-\sigma\frac{\delta t}{rt}-(\sigma_r+\sigma_\theta)\frac{\delta r}{r}-2\mu\sigma_t\frac{\delta r}{t} \qquad \text{----------3.1.2.}$$

Yield criterion

Von Mises: $(\sigma_1-\sigma_2)^2+(\sigma_2-\sigma_3)^2+(\sigma_1-\sigma_3)^2=2Y^2$ ----3.1.3. (relating principal stresses to yield strength in uniaxial tension, Y).

Assume σ_t (blank-holder pressure) acts at periphery and is zero over the remainder of the flange, then $\sigma_t=\sigma_2=0$ and equation 3.1.3. becomes:

$$\sigma_1^2-\sigma_1\sigma_3+\sigma_3^2=Y^2$$

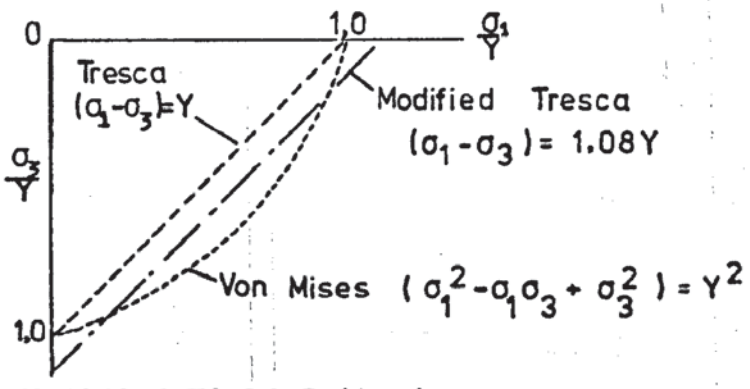

Fig.3.1.4. Modified Yield Criterion.

This is a cumbersome expression to incorporate into equation 3.1.2. The Tresca yield criterion defining the condition of maximum shear stress is more convenient although less accurate.

$$\sigma_1 - \sigma_3 = 2k = Y \qquad \text{----------3.1.4.}$$

The Tresca equation can be made a close approximation to the Von Mises criterion by a suitable multiplying factor, m., defined in Fig. 3.1.4.

From equation 3.1.4. we can write:

$$\sigma_r - (-\sigma_\theta) = 1.08Y$$

If we assume no change in wall thickness, which is a reasonable approximation at any instant, and $\sigma_t = 0$, except at the blank periphery, then equation 3.1.2. becomes:

$$\delta\sigma_r = -m.Y\frac{\delta r}{r} \qquad \text{----------3.1.5.}$$

In the limit we may write:

$d\sigma_r = -mY\frac{\delta r}{r}$ which on integrating between the limits, $\sigma_r = \sigma_{r_a}$ $r = r_a$ at the current rim radius and $\sigma_r = \sigma_{rb}$, $r = r_b$ at the onset of bending gives: $\sigma_{rb} = m.Y. \ln \frac{r_a}{r_b} + \sigma_{r_a}$ where σ_{r_a} is the radial stress due to the blank-holding force, H acting at the periphery.

3.1.3. Component of Radial Stress due to Blank-holder Pressure

(Blank-holder force = H)

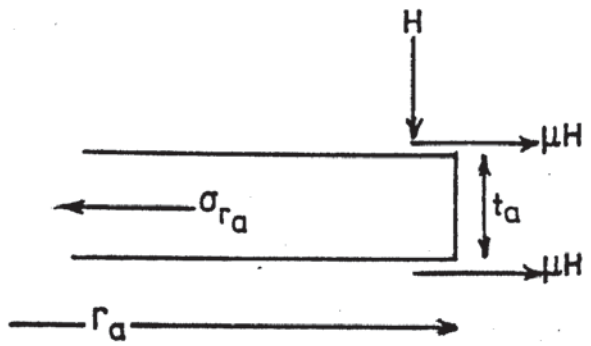

$$\sigma_{r_a}\, 2\pi r_a t_a = 2H\mu$$

$$\sigma_{r_a} = \frac{H\mu}{\pi r_a t_a}$$

Fig. 3.1.5.

The instantaneous radial stress, σ_r is given by:

$$\sigma_{r_b} = m\bar{Y} \ln \frac{r_a}{r_b} + \frac{H\mu}{\pi r_a t_a} \qquad \text{----------3.1.6.}$$

assuming a constant yield stress (reasonable for cold rolled sheet).

It is, however, necessary to determine t, the blank thickness appropriate to each value of r_a chosen, (indicating the stage of drawing).

This may be determined by numerical integration of the following expression:

$$\frac{dt}{t} = -\left[2 + \frac{3}{\frac{H\mu}{\pi r_a t_a} m\bar{Y} + \ln \frac{r_a}{r} - 2}\right]\frac{dr}{r} \qquad \text{----------3.1.6a.}$$

once again, for a non-work hardening material, $\bar{Y}$ = mean yield stress.

Work Hardening

Assumptions:-

(1) Assume a uniform strain rate during drawing

(2) That effective stress, given by:

$$\bar{\sigma} = \frac{1}{\sqrt{2}}\left[(\sigma_1 - \sigma_2)^2 + (\sigma_2 - \sigma_3)^2 + (\sigma_1 - \sigma_3)^2\right]^{\frac{1}{2}}$$

is entirely dependent upon the effective strain:

$$\bar{\varepsilon} = \left[\frac{2}{3}\left((\varepsilon_1 - \varepsilon_2)^2 + (\varepsilon_2 - \varepsilon_3)^2 + (\varepsilon_1 - \varepsilon_3)^2 \right)\right]^{\frac{1}{2}}$$

Hill [72] has shown that the effective strain in any element during radial drawing, for draw ratios less than 2 never differ from the absolute magnitude of the circumferential strain $\varepsilon_\theta = \ln \frac{R}{r}$ by more than 3 per cent, i.e. the current yield stress of any element corresponds to the circumferential strain received.

We may, therefore, take some empirical stress/strain function appropriate to the material being considered and substitute this into the equilibrium equation for radial drawing 3.1.5.

e.g. $\bar{\sigma} = \sigma_0 + B\bar{\varepsilon}^n$

Note. The differential equation 3.1.5. gives the distribution of stress at any instant during drawing whereas the stress strain function above considers the continous radial displacement of a circumferential element. It is therefore necessary to determine the initial radius R of the element appropriate to any instantaneous radius r.

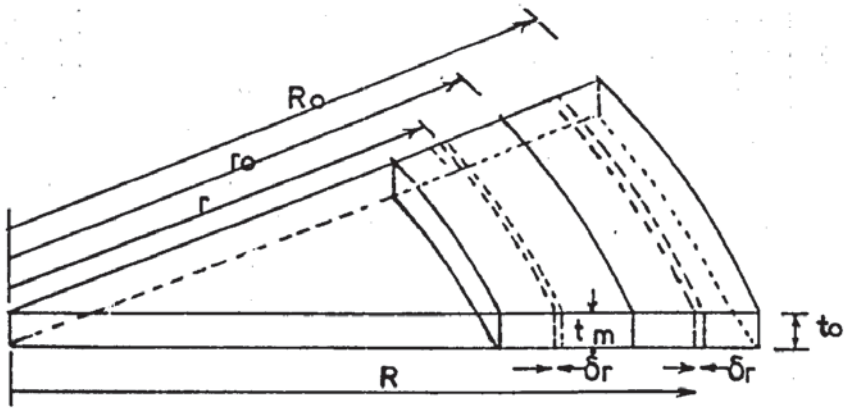

Fig. 3.1.6.

Consider a circumferential element dr at radius R and initial periphery R_0. The effective strain on moving to r with periphery r_0 is then $\ln \frac{R}{r}$, therefore

$$\bar{\sigma} = Y = \sigma_\theta + B(\ln\tfrac{R}{r})^n \qquad \text{----------3.1.7.}$$

In order to relate this to the instantaneous situation it is necessary however to define $\frac{R}{r}$ in terms of R_0, r_0 and r. This may be done by applying the conditions of constancy of volume to an element dr as it moves from R→r. Thus

$$\pi t_0 (R_0^2 - R^2) = \pi t_m (r_0^2 - r^2)$$

where t_m is the current mean thickness and t_0 the initial thickness. then:-

$$R_0^2 t_0 - R^2 t_0 = r_0^2 t_m - r^2 t_m$$

$$R^2 = R_0^2 - \frac{t_m}{t_0} r_0^2 + \frac{t_m}{t_0} r^2; \qquad (\frac{R}{r})^2 = (\frac{R_0}{r})^2 - \frac{t_m}{t_0} (\frac{r_0}{r})^2 + \frac{t_m}{t_0}$$

$$(\frac{R}{r})^2 \frac{t_0}{t_m} = (\frac{R_0}{r})^2 \frac{t_0}{t_m} - (\frac{r_0}{r})^2 + 1; \qquad (\frac{R}{r})^2 \frac{t_0}{t_m} - 1 = \frac{1}{r^2} (R_0^2 \frac{(t_0)}{(t_m)} - r_0^2)$$

$$\frac{R}{r} = \left[\frac{t_m}{t_0}\left(\frac{1}{r^2}\left(R_0^2\,\frac{t_0}{t_m} - r_0^2\right) + 1\right)\right]^{\frac{1}{2}}$$

and 3.1.7. becomes:

$$Y = \bar{\sigma}_\theta + B\,\frac{1}{2}\left[\ln\left(\frac{t_m}{t_0}\left(\frac{C}{r^2} + 1\right)\right)\right]^n \qquad \text{----------3.1.8.}$$

where:

$$\frac{C}{r^2} = \frac{1}{r^2}\left(R_0^2\left(\frac{t_0}{t_m}\right) - r_0^2\right.$$

substituting 3.1.8. into the equilibrium equation 3.1.5. and integrating we have:

$$\sigma_{rb} = m\bar{\sigma}_\theta \ln\frac{r_a}{r_b} + mB\int_{r_b}^{r_a}\left(\frac{1}{2}\ln\left[\frac{t_m}{t_0}\left(\frac{C}{r^2} + 1\right)\right]\right)\frac{dr}{r} + \sigma_{r_a} \qquad \text{---3.1.9.}$$

The second term on the right hand side must be solved by numerical integration substituting values of t_m determined from equation 3.1.6a.

3.1.4. Plastic Bending under Tension.

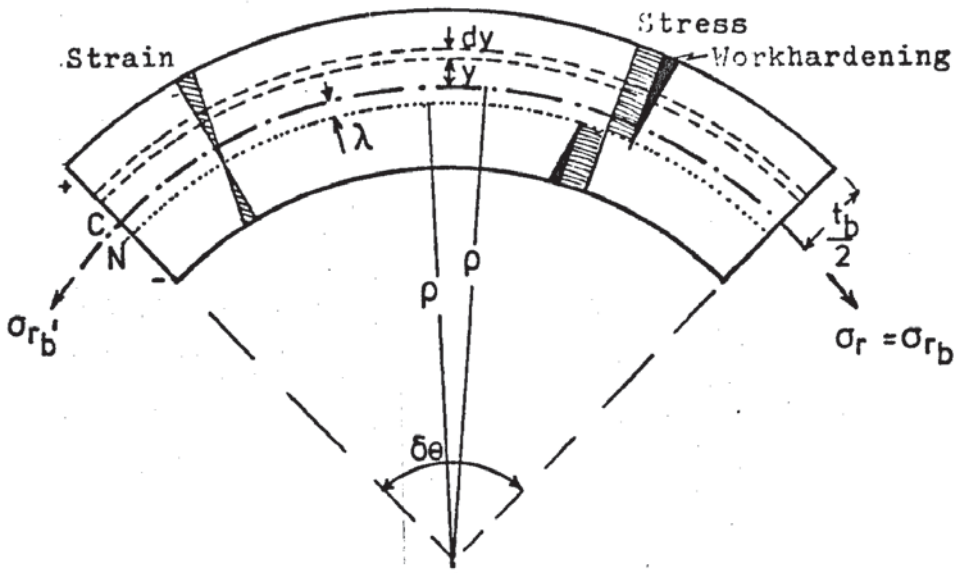

Fig. 3.1.7. Bending stress and strain in an element of the blank δθ, undergoing instantaneous bending at radius r_b.

Assumptions:

(i) Constant yield stress $\bar{Y}$

(ii) Plane strain conditions - if bending is assumed to be

instantaneous then circumferential strain $\varepsilon_\theta = 0$ and hence yielding occurs when $\sigma_r = \frac{2}{\sqrt{3}}\bar{\sigma}$ where $\bar{\sigma}$ is the effective stress.

(iii) Elastic strains may be neglected.

(iv) Plane sections normal to the neutral axis remain plane after bending, i.e. no shear occurs.

(v) The normal stress perpendicular to the die radius is relatively small; hence $\sigma_2 \simeq 0$.

Plastic bending under tension results in a displacement of the neutral axis, which is related to the excess of resultant tensile over compressive stress across the section. The imbalance of stress is due to the application of a tensile back stress σ_r, which induces a radial stress.

The displacement of the neutral axis from the central axis can be found by equating the applied force $\left[\sigma^1 = \sigma_{r_b}\right]$ with the 'out of balance' force induced in the sheet by the displacement of the neutral axis.

$$\sigma^1 t_b = \int_{\frac{t_b}{2} - \lambda}^{\frac{t_b}{2} + \lambda} \frac{2}{\sqrt{3}} \bar{Y}.dy$$

$$\sigma^1 t_b = \frac{2}{\sqrt{3}} \bar{Y}.2\lambda$$

Thus $$\lambda = \frac{\sqrt{3}\,\sigma_{r_b}.t_b}{4\bar{Y}} \qquad \text{----------3.1.10.}$$

To determine the increase in drawing stress, σ_b due to bending, equate the work done in bending to the work done by the drawing stress.

The work done in bending, per unit width is given by the product (stress x elementary strain x elementary volume).

i.e. $\delta w = \bar{\sigma}\,\delta\varepsilon\,(\rho N + y)\,\delta\theta\,\delta y$

$$\frac{w}{\delta\theta} = \int_0^{\frac{t_b}{2}+\lambda} (\rho N + y) \int_0^{\ln(1+\frac{y}{\rho N})} \frac{2}{\sqrt{3}} \bar{Y}\, d\bar{\varepsilon}\, dy + \int_0^{\frac{t_b}{2}-\lambda} (\rho N - y) \int_0^{\ln(1+\frac{y}{\rho N})} \frac{2}{\sqrt{3}} \bar{Y}\, d\bar{\varepsilon}\, dy$$

Elementary strain is given by $\ln\left(\frac{\rho N + y}{\rho N}\right)$ and effective strain is

thus $\bar{\varepsilon} = \frac{2}{\sqrt{3}} \ln\left(\frac{\rho N + y}{\rho N}\right) \simeq \frac{2}{\sqrt{3}} \frac{y}{\rho N}$

We may therefore rewrite the above expression:-

$$\frac{w}{\delta\theta} = \int_0^{\frac{t_b}{2}+\lambda} (\rho N + y) \int_0^{\frac{y}{\rho N}} \frac{4}{3} \bar{Y} d\bar{\varepsilon}\, dy + \int_0^{\frac{t_b}{2}-\lambda} (\rho N - y) \int_0^{\frac{y}{\rho N}} \frac{4}{3} \bar{Y}.d\bar{\varepsilon} dy$$

$$= \frac{4}{3}\bar{Y} \left(\int_0^{\frac{t_b}{2}+\lambda} (\rho N + y) \frac{y}{\rho N}.dy + \int_0^{\frac{t_b}{2}-\lambda} (\rho N - y) \frac{y}{\rho N} dy \right)$$

$$= \frac{4}{3}\bar{Y} \left[\frac{y^2}{2} + \frac{y^3}{3\rho N} \right]_0^{\frac{t_b}{2}+\lambda} + \frac{4}{3}\bar{Y} \left[\frac{y^2}{2} - \frac{y^3}{3\rho N} \right]_0^{\frac{t_b}{2}-\lambda}$$

$\frac{w}{\delta\theta} = \frac{4}{3}\bar{Y}\left[\frac{t_b^2}{4}(1 + \frac{2\lambda}{\rho N}) + \lambda^2\right]$ neglecting $\frac{\lambda^3}{\rho N}$ since it is much smaller than t_b

The portion of drawing stress required to provide bending strain work σ_b, is given by $w = \sigma_b t_b$ x mean distance

$$\therefore\ w = \sigma_b\, t_b\, \rho_c\, \delta\theta$$

and $\frac{w}{\delta o} = \sigma_b\, t_b\, \rho_c = \frac{4}{3}\bar{Y}\left[\frac{t_b^2}{4}(1 + 2\frac{\lambda}{\rho N}) + \lambda^2\right]$

$$\therefore\ \sigma_b = \frac{4Y}{3t_b\rho_c}\left[\frac{t_b^2}{4}(1 + \frac{2\lambda}{\rho N}) + \lambda^2\right] \quad \text{----------3.1.11.}$$

Note Stress, σ_u for unbending is an analogous process and may be determined from an expression similar to 3.1.11. but writing λ^1 for λ, where $\lambda^1 = \frac{3}{4} \frac{\sigma_{rc}^1 t_c}{Y}$ and σ_{rc}^1 is the radial drawing stress at the point of unbending $r = r_c$

3.1.5. Stress due to Friction and Radial Drawing over the Die Radius.

The radial stress due to the motion of the blank over the die radius is derived by considering an elementary ring of surface length $s = \rho_c \delta\theta$ at a radius r from the cup axis - Fig. 3.1.8.

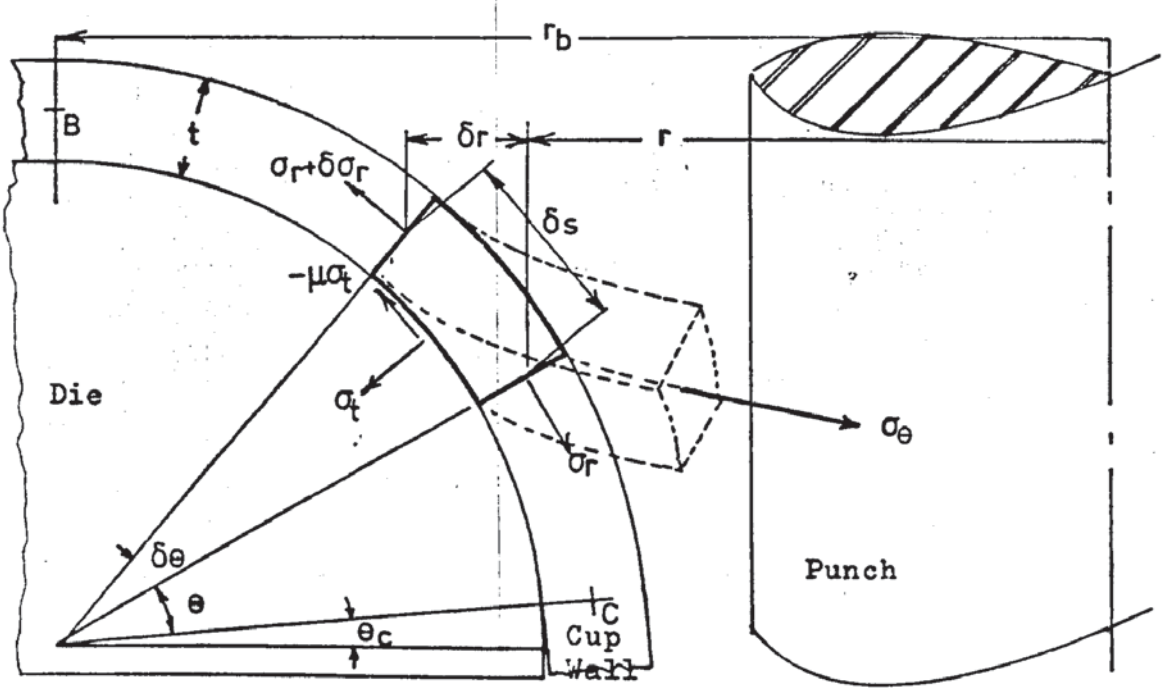

Fig. 3.1.8.

(i) Assume constant thickness over die radius.

(ii) Assume constant yield stress.

(iii) $\delta s = \frac{\delta r}{\sin\theta}$

(iv) $\cos(\theta+\delta\theta) \simeq \cos\theta$; $\sin(\theta+\delta\theta) \simeq \sin\theta$

Resolving forces vertically

$$(\sigma_r + \delta\sigma_r)\, t\, 2\pi(r+\delta r)\cos(\theta+\delta\theta) - \mu\sigma_t . 2\pi r \frac{\delta r}{\sin\theta}\cos\theta$$

$$= 2\pi(r+\delta r)\sigma_t . \frac{\delta r}{\sin\theta}\sin\theta + \sigma_r t . \cos\theta . 2\pi r \qquad \text{----3.1.12.}$$

(Each resultant force has been integrated with respect to the angle subtended by an arc of the elementary ring at the cup axis).

e.g. resolving $\sigma_r + \delta\sigma_r$ gives:-

$$\int_0^{2\pi} (\sigma_r + \delta\sigma_r)\, t \cos(\theta+\delta\theta)\ (r + \delta r).d\alpha$$

$$= (\sigma_r + \delta\sigma_r)t.\ \cos(\theta+\delta\theta)\ (r + \delta r)\ 2\pi$$

On simplifying 3.1.12. by ignoring the products of small increments, we have:-

$$\sigma_r rt\cos\theta - \sigma_r rt \sin\theta\delta\theta + \delta\sigma_r t\, r\cos\theta + \sigma_r \delta r t\cos\theta$$

$$- \mu\sigma_t\, r\delta r \cot\theta = \sigma_t\, r\delta r + \sigma_r.t\, r\cos\theta$$

The 2nd, 3rd and 4th terms may be considered collectively as the product differential $t\frac{d}{dr}(\sigma_r r\cos\theta)$

Thus equation 3.1.12. becomes:

$$t\frac{d}{dr}(\sigma_r r\cos\theta) - \sigma_t r(1 + \mu\cot\theta) = 0. \qquad \text{--------3.1.13.}$$

Resolving forces horizontally and considering one half of the elementary ring

(note, the projected area is taken, not the circular area).

$$2\sigma_\theta \frac{\delta r}{\sin\theta}\, t + \sigma_r t \sin\theta\ 2r = -\ \mu\sigma\frac{\delta r}{t\sin\theta}\ \sin\theta 2r$$

$$+\ \sigma\frac{\delta r}{t\sin\theta}\ \cos\theta.2r + (\sigma_r + \delta\sigma_r)\, t\ (r + \delta r)2.\sin(\theta+\delta\theta)$$

$$\sigma_\theta\frac{\delta r}{\sin\theta}\, t + \sigma_r trsin\theta - \mu\sigma_t\delta r\ r = \sigma_t\delta r\ r\cot\theta + \sigma_r tr\sin\theta$$

$$+ \sigma_r tr\cos\theta\delta\theta + \sigma_r t\delta r\sin\theta + \delta\sigma_r\ trsin\theta$$

Thus $t\frac{d}{dr}(\sigma_r r.\sin\theta) + r\sigma_t(\cot\theta - \mu) = \frac{\sigma_\theta t}{\sin\theta}$ -------3.1.14.

eliminate σ_θ between equations 3.1.13 and 3.1.14.

from 3.1.13.

$$\sigma_t = \frac{t\frac{d}{dr}(\sigma_r r\cos\theta)}{r(1 + \mu\cot\theta)}$$

Thus $t\frac{d}{dr}(\sigma_r r.\sin\theta) + \frac{r(\cot\theta - \mu)}{r(1 + \mu\cot\theta)}\ t\frac{d}{dr}(\sigma_r r\cos\theta) = \frac{\sigma_\theta t}{\sin\theta}$

$$\sigma_\theta . t - \sin\theta . t \frac{d}{dr}(\sigma_r r . \sin\theta) - \cos \frac{(1-\mu\tan\theta)}{(1+\mu\cot\theta)} . t \frac{d}{dr}(\sigma_r r \cos\theta) = 0 \quad \text{-3.1.15.}$$

Since $\frac{d}{dr}(\sigma_r r . \sin\theta) = \sigma_r r \cos\theta \frac{d\theta}{dr} + \sigma_r \sin\theta + \frac{d\sigma_r}{dr} . r \sin\theta$

expanding equation 3.1.15. gives: $\sigma_\theta - \sin\theta(\sigma_r r \cos\theta \frac{d\theta}{dr} + \sigma_r \sin\theta + r\sin\theta \frac{d\sigma_r}{dr})$

$$- \cos\theta \left(\frac{1-\mu\tan\theta}{1+\mu\cot\theta}\right) \sigma_r \cos\theta + r\cos \frac{d\sigma_r}{dr} - \sigma_r r \sin\theta \frac{d\theta}{dr}) = 0 \quad \text{-------3.1.16.}$$

Multiply through by $(1+\mu\cot\theta)$ and collect the differential terms $\sigma_r . r \frac{d\theta}{dr}$ $(\sin^2\theta\cot\theta)(1+\mu\cot\theta) - \cos^2\theta\tan\theta(1-\mu\tan\theta)$

$$= \sigma_r r \mu \frac{d\theta}{dr}$$

since $(\sin\theta\cos\theta + \cos^2\theta\mu - \cos\theta\sin\theta + \sin^2\theta\mu) = \mu$

$$r \frac{d\sigma_r}{dr} \left[\sin^2\theta(1+\mu\cot\theta) + \cos^2\theta(1-\mu\tan\theta)\right] = r \frac{d\sigma_r}{dr}$$

$$\sigma_r \left[\sin^2\theta(1+\mu\cot\theta) + \cos^2\theta\ (1-\mu\tan\theta)\right] = \sigma_r$$

Thus equation 3.1.16. becomes:

$$\sigma_\theta(1+\mu\cot\theta) - \mu\sigma_r r \frac{d\theta}{dr} - \frac{d}{dr}(r\sigma_r) = 0 \quad \text{----------3.1.17.}$$

Using the modified Tresca Yield criterion:

$\sigma_1 - \sigma_3 = m\bar{Y}$ gives $\sigma_\theta = \sigma_r - m\bar{Y}$

Thus $(\sigma_r - m\bar{Y})(1 + \mu\cot\theta) - \mu\sigma_r r \frac{d\theta}{dr} - r \frac{d\sigma_r}{dr} - \sigma_r = 0$

Multiply by $\frac{dr}{r}$

$$d\sigma_r = -m\bar{Y} \frac{dr}{r} - \frac{\mu d\theta \rho_c}{r} \left[m\bar{Y}\cos\theta - \sigma_r(\cos\theta - \frac{r}{\rho_c})\right]$$

$$\text{Thus } \sigma_r = -\int_{r_c}^{r_b} m\bar{Y} \frac{dr}{r} - \int_{\frac{\pi}{2}} \frac{\mu\rho_c}{r} \left[m\bar{Y}\cos\theta - \sigma_r(\cos\theta - \frac{r}{\rho_c})\right] d\theta \quad \text{----3.1.18.}$$

The first term is the component of stress due to radial drawing and the 2nd is due to friction over the die radius. which we

may write as:- $df = \mu\left[\frac{\rho_c}{r}(m\bar{Y}\cos\theta - \sigma_r\cos\theta) + \sigma_r\right] d\theta$

Since $r_b - r = \rho_c\cos\theta$

$$r = r_b - \rho_c\cos\theta$$

Thus $df = \mu\left[\frac{(m\bar{Y}-\sigma_r)\cos\theta}{\frac{r_b}{\rho_c} - \cos\theta} + \sigma_r\right] d\theta$ which is solved by numerical integration

Since σ_r and r vary with O 'f' may be obtained from a simplified approach analogous to friction over a pulley.

i.e. when $\sigma_\theta \to 0$ and $r \to \infty$

equation 3.1.15. becomes:

$$-\frac{d\sigma_r}{\sigma_r} = \mu d\theta$$

where σ_r is the radial tension.

Integrating between the limits $\sigma_r = \sigma_{rf}$ and $\theta = \theta_c$ $\sigma_r = \sigma_{r_b'}$ at $\theta = \frac{\pi}{2}$

$$\therefore \ln\frac{\sigma_{rf}}{\sigma_{r_b'}} = -\mu(\theta_c - \frac{\pi}{2})$$

$$\sigma_{rf} = \sigma_{r_b'} + f$$

$$\therefore f = \sigma_{r_b'}\left[e^{\mu(\pi/2 - \theta_c)} - 1\right] \quad \text{putting } \varphi = \frac{\pi}{2} - \theta_c$$

$$f = \sigma_{r_b'}\left[e^{\mu\theta} - 1\right]$$

3.1.6. Punch Load and Punch Travel.

Punch load L is given by:

$$L = 2\pi r_c\, t_c\, \sigma_c \sin\varphi$$

r_c = mean radius of cup wall where it leaves die.

t_c = mean thickness.

φ = angle of embrace of the die profile.

The value of σ_c taken includes:

(a) Radial drawing stress.

(b) Stress to bend and unbend the cup on the die.

(c) Stress arising from the frictional drag over the die profile.

(d) The change in the radial stress in drawing over the die radius.

(e) The stress changes caused by the two stages of thinning in bending and unbending.

The punch travel can be obtained by considering the area of sheet that has passed the radius r_c.

This becomes:

$$A = r_c^2 + 2\pi\, t_o \int_{r_c}^{R} \frac{R}{t}\, dR$$

3.2. Wedge Drawing.

3.2.1. The Wedge Drawing Test.

The wedge drawing test was originally proposed by Sachs[73] as a simple means of determining the suitability of a material for a deep-drawing process. A detailed examination of this test was made by Loxley and Swift[66] and their conclusions included a comparison of the wedge drawing test with the cup-drawing operation which indicated some important differences between the two processes. The punch load increments caused by plastic bending and unbending, radial drawing in and friction over the die radius in the cupping operation are absent in the wedge drawing test because it is unidirectional. The main disadvantage of the wedge drawing test is, however, friction acting along the edges of the wedge specimen as shown in Fig. 3.2.1. from which a simple estimate of the effect of this friction can be obtained.

Resolving forces vertically

$$T = 2P_f \sin(\alpha + \varphi)$$

if $$Q = P_f \cos(\alpha + \varphi)$$

thus $$T = 2Q \tan(\alpha + \varphi)$$

where Q = horizontal force required to produce plastic flow. Assuming Q to be unaffected by the edge friction force P_0 then, in the absence of friction

$$T_0 = 2Q (\tan \alpha)$$

giving the ratio $$\frac{T}{T_0} = \frac{\tan(\alpha + \varphi)}{\tan \alpha}$$

For small angles this can be expanded and simplified

$$\frac{T}{T_0} = 1 + \frac{\tan \varphi}{\tan \alpha}$$

Also, $\tan \varphi = \mu$, the coefficient of friction.

Thus the drawing force can be seen to be dependant upon the ratio $\frac{\mu}{\tan \alpha}$ which for the die angles associated with the wedge test cannot be neglected.

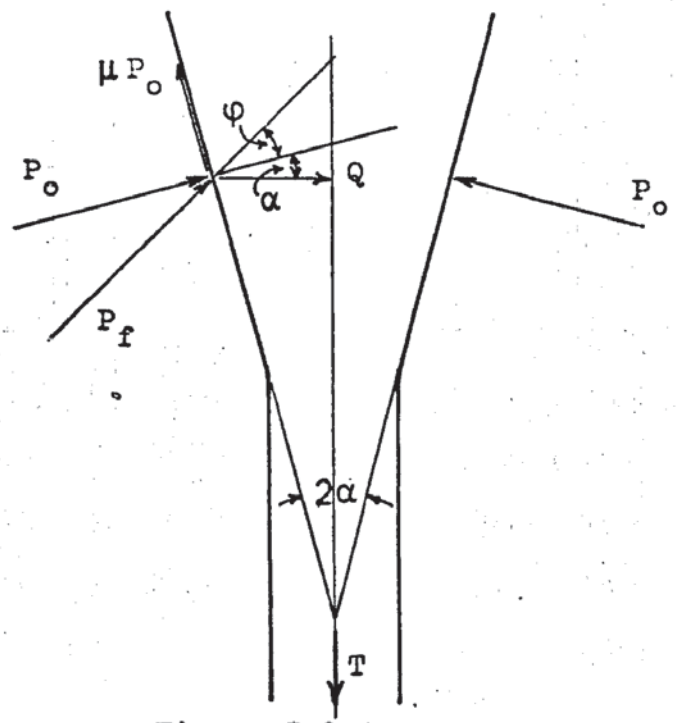

Figure 3.2.1.

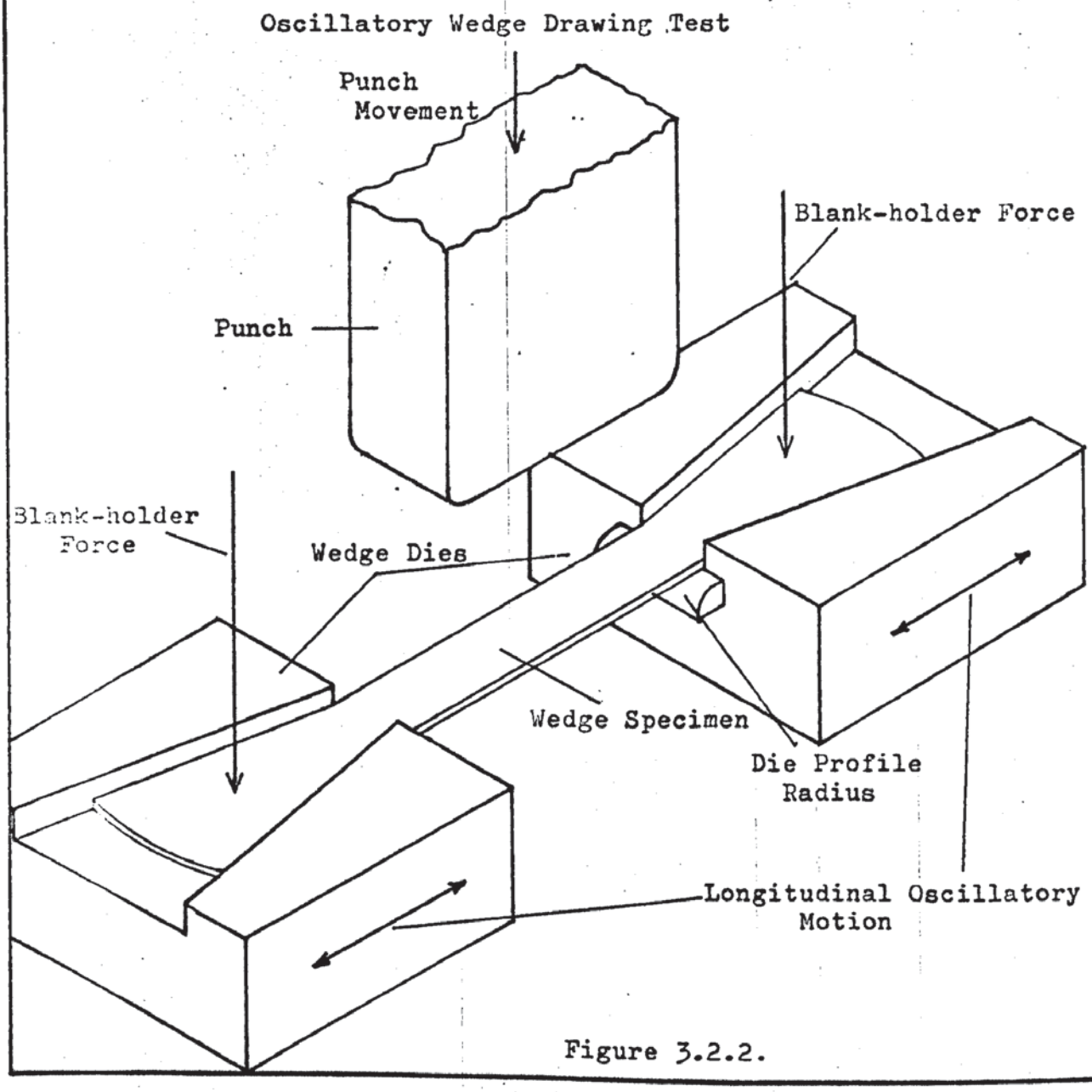

Figure 3.2.2.

The effect of edge friction in increasing the drawing load was demonstrated by the much lower limiting draw-ratio obtained when using the wedge drawing test compared with the cupping test.

3.2.2. The Oscillatory Wedge Drawing Test.

The oscillatory wedge test was developed by Young[65] in order that the characteristics of oscillatory deep-drawing with radially vibrated tooling could be simulated using longitudinal vibrations.

A 'double' ended wedge specimen was used, which represented two segments of the corresponding circular blank in the cupping test. The specimen shape is shown in Appendix A2, drawing A.2.1. In use the wedge dies were 'diametrically' opposed and the specimen was drawn through the dies and over the die radius by a punch moving perpendicular to the plane of the wedge specimen, as shown in Fig. 3.2.2.

With the addition of drawing over the die radius this test only differed from the cupping test in two ways. The first was the lack of any radial drawing in, over the die radius, and the second was the presence of edge friction. Of these differences the first was not considered very significant whilst edge friction was shown to be unchanged between oscillatory and non-oscillatory tests. Thus it was considered that observations made about the oscillatory wedge drawing could also be applied to oscillatory cup-drawing.

3.3. Punch Vibration.

The effect of applying axial punch vibrations to the deep-drawing process will be considered in two parts. The first is the action of punch vibrations on a system in which the punch is the only component vibrating. The second case will consider the effects when the wedge dies are forced to vibrate by the oscillating punch.

In the first case with only the punch vibrating the conditions within the wedge dies will be considered to be the same as during non-oscillatory drawing since the only variation possible is in drawn strip tension and drawing speed.

A representation of the oscillatory and drawing velocities along with the corresponding displacements is shown in Fig. 3.3.1. Referring to the velocity-time diagram, if the oscillatory and drawing velocities are summed it can be seen that for part of the cycle the oscillatory velocity becomes greater than and opposite to the drawing velocity. At the point where the punch oscillatory velocity upwards equals the drawing velocity downwards drawing ceases. Beyond this point the strain in the drawn wall is reduced and the surfaces may separate if the oscillatory amplitude is large enough. When the oscillatory velocity, having passed its maximum, again equals the drawing velocity the punch begins to re-apply the drawing stress. Meanwhile, the drawing velocity has advanced the mean position of the punch in the drawing direction with the result that another strain cycle will occur. This cyclic off-loading will cause the material to deform incrementally at the peak stress level and in so doing will give a mean punch load less than the non-oscillatory punch load because of stress-superposition. The peak stress level may be slightly higher than the non-oscillatory stress because of the transition from static to dynamic friction.

In the second case to be considered, it is assumed that the oscillatory punch will cause the wedge dies to resonate at the same frequency as the punch, this being caused by variations in drawn

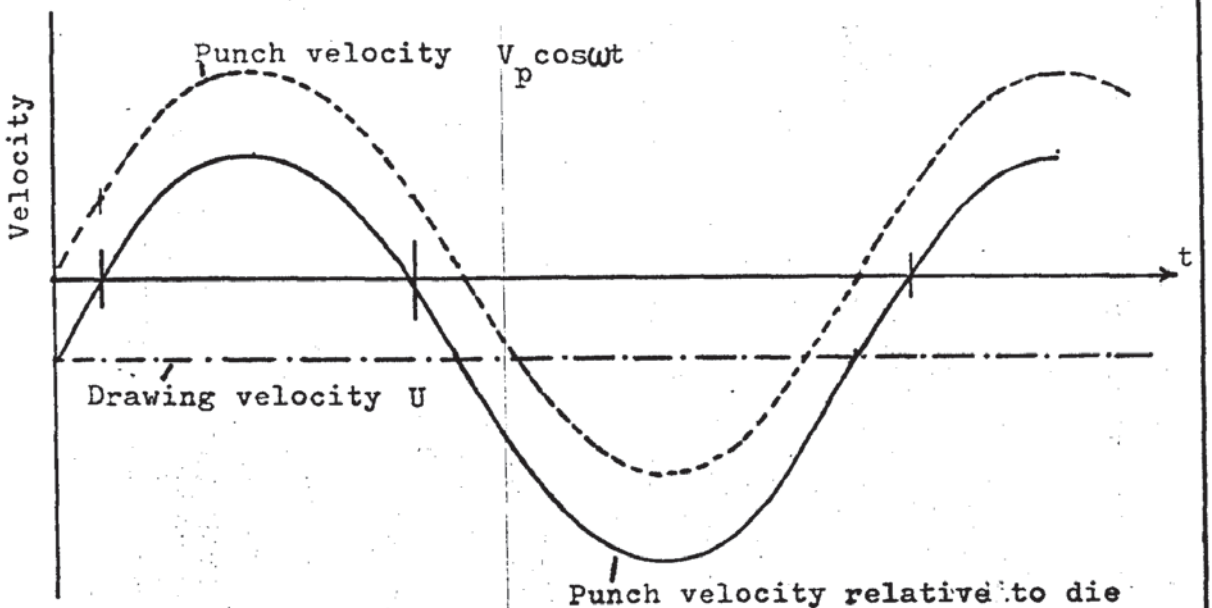

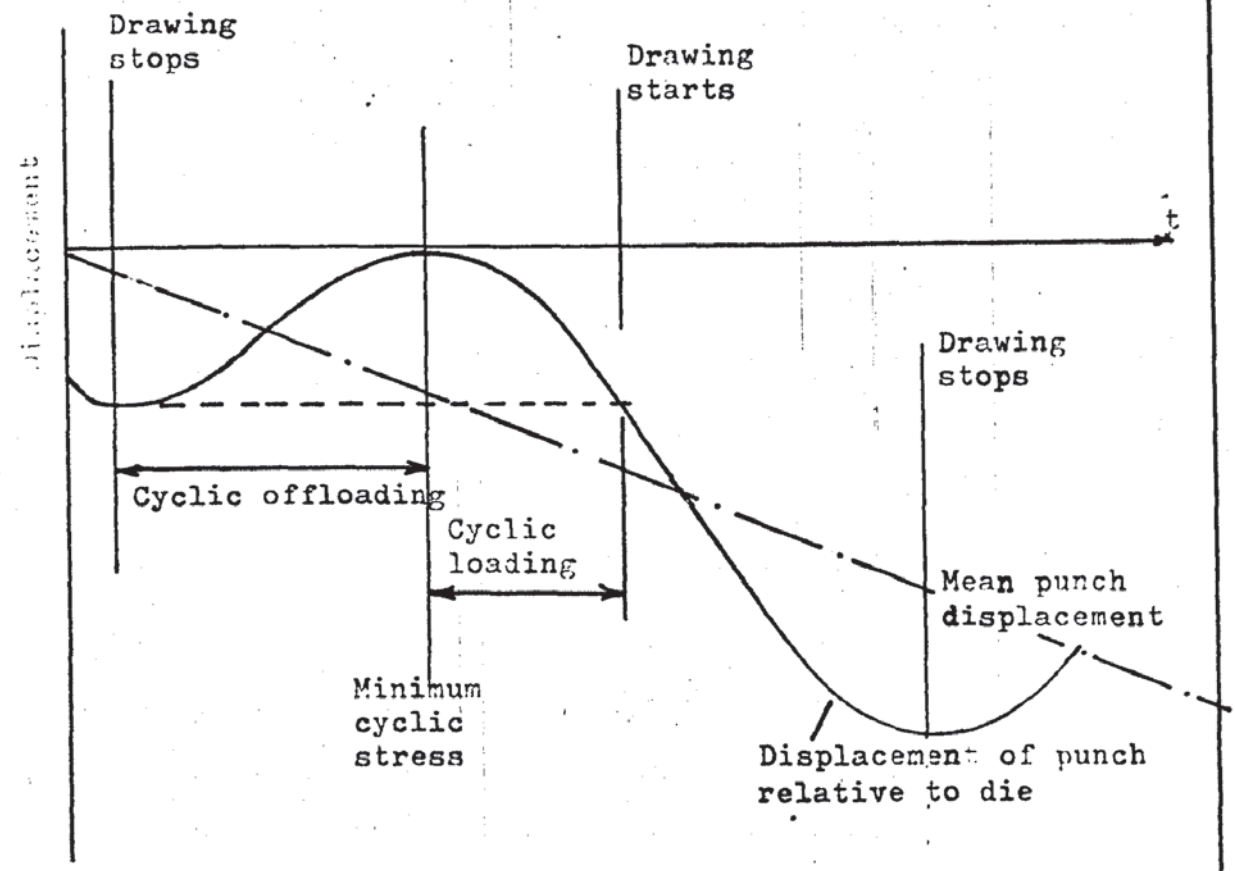

Figure 3.3.1.

Velocity and Displacement of Oscillatory Punch

strip tension. In addition to the situation previously described, the effect of the oscillations on the section of the specimen between the die and blank-holder will be examined.

Considering Fig. 3.3.2 which represents a partly drawn specimen into which cyclic stresses are induced by the oscillating punch, when the punch is moving in the drawing direction the specimen is drawn through the dies. If when the punch direction reverses the oscillatory velocity is greater than the drawing velocity, as it generally is, drawing stops and elastic strain within the specimen is released. On reversal of the oscillatory motion drawing recommences once again. Thus there is a drawing stress applied periodically to the specimen. As this drawing stress is transmitted through the drawn section to the wedge dies these, too, are subject to an oscillatory force. If this force oscillates at the resonant frequency of the dies, the dies will vibrate provided the input power is sufficient to overcome the losses within the system.

When the punch oscillatory movement is in the drawing direction the dies will be moving together with something less than the amplitude of the punch. This will cause relative movement of the blank in the dies which will be additional to that caused by the non-oscillatory drawing velocity; drawing will therefore be possible. During this period the top surface of the blank in contact with the blank-holder will be moving over this surface towards the punch and therefore the frictional force associated with this interface will be opposing the motion. As the punch oscillatory movement reverses the relative motion between punch and die is only that of the drawing velocity and the conditions are momentarily as in a normal non-vibrated drawing operation. As the punch oscillatory velocity in the opposite direction begins to increase the drawing velocity is effectively reduced by this velocity until the two velocities are equal and opposite at which point drawing stops. In the period between these two extremes the die is also moving its direction now

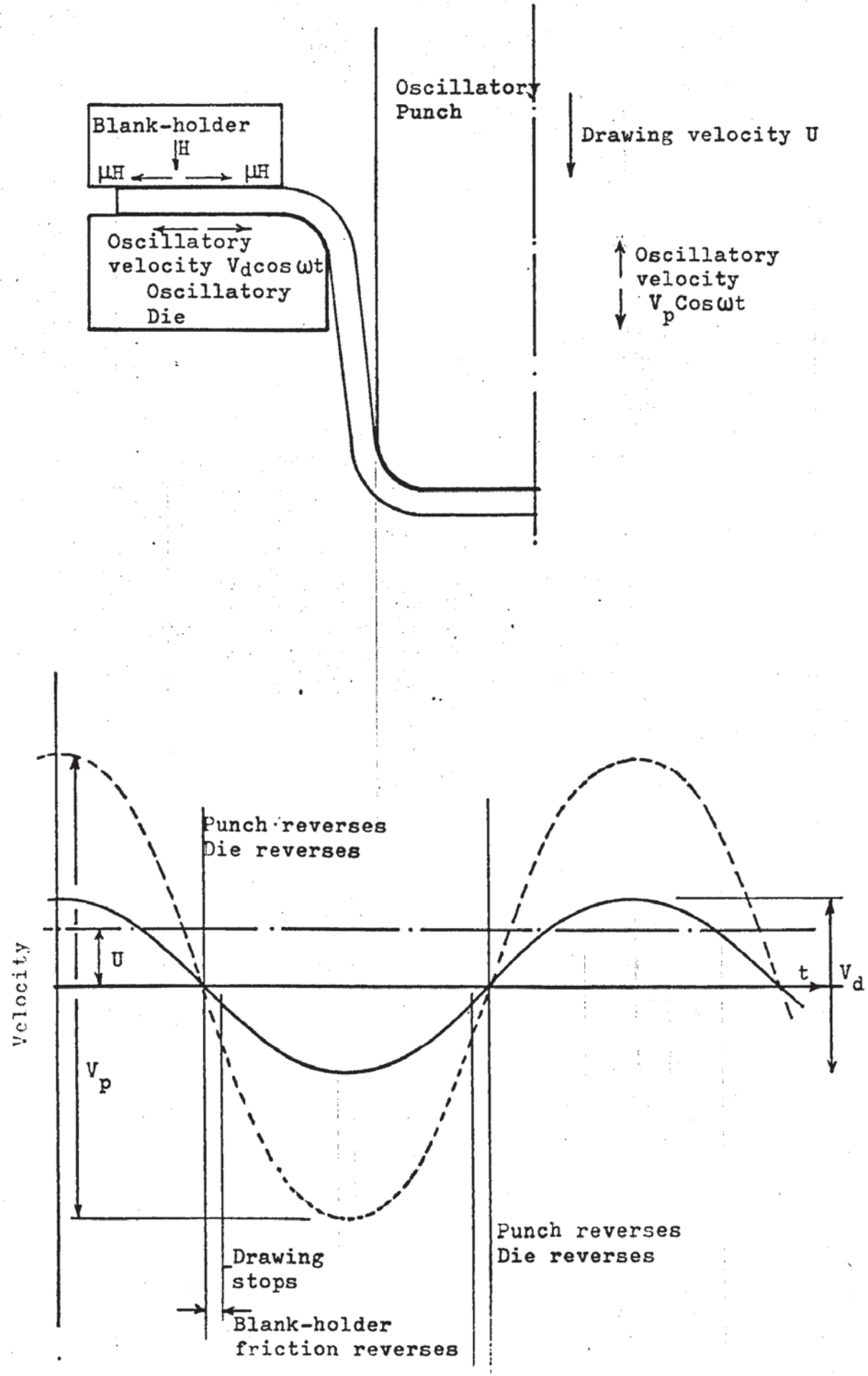

Figure 3.3.2.

Velocity of Oscillatory Die

being away from the punch. Considering the interface of the blank-holder and specimen, the movement of the specimen is now in a direction away from the punch axis. This results in the friction force between blank-holder and specimen acting towards the punch axis provided the die oscillatory velocity exceeds the drawing velocity of the material through the die. This drawing velocity within the die varies from its maximum value at the die throat to its minimum value at the periphery of the blank. The blank-holder friction force is therefore now tending to force the specimen through the wedge dies, thus reducing the drawing stress by an amount equal to that normally required to overcome the frictional constraint between the blank-holder and specimen. Once the punch oscillatory velocity equals the non-oscillatory drawing velocity drawing stops until the punch velocity passes its maximum and again equals the non-oscillatory drawing velocity. Beyond this the non-oscillatory drawing velocity which is now greater than the oscillatory velocity re-applies the stress and drawing re-starts. This second period in which the friction force assists the drawing will be shorter than the first period and it may not exist at all if the oscillatory motion of the die reverses before drawing recommences. Thus, as described above, there is a period in each cycle when the frictional force acting between the specimen and blank-holder is acting in the drawing direction assisting the drawing process. This friction-vector reversal should result in an improvement in the drawing process efficiency as indicated by an increase in the limiting draw-ratio although the magnitude of this assistance may not be very significant because of the small fraction of the cycle over which it acts.

In addition the effects of the punch oscillatory motion described previously will apply with an apparent punch load reduction resulting from stress-superposition effects.

3.4. Blank-holder Vibration.

The purpose of applying blank-holder vibrations to the deep-drawing process is to obtain a reduction in the friction force thereby reducing the drawing load and enabling an increase in the limiting draw-ratio to be obtained. The schematic of the process for applying 'radial' blank-holder vibrations to the wedge test analogue is shown in Fig. 3.4.1. The blank-holders are assumed to vibrate in phase and with simple harmonic motion, the specimen being drawn through the dies at a constant velocity by the advancing punch.

Under non-oscillatory conditions the total drawing load contains components to overcome the frictional constraint acting on both faces of the deforming blank within the wedge dies. When the blank-holders are vibrated and the punch is stationary, that is zero drawing velocity, the blank-holders move over the top surface of the specimen towards the punch for a half-cycle and away from the punch for the other half-cycle. When the blank-holders are moving towards the punch the frictional force opposes the motion thus tending to push the specimen through the wedge dies. As the blank-holder reverses in direction the frictional force on the top surface now acts in the conventional direction.

This process still occurs when the specimen is being drawn except that the fraction of the oscillatory cycle over which the friction reversal occurs decreases with an increase in drawing velocity as shown in Figs. 3.4.2 and 3.4.3. The friction reversal ceases altogether when the drawing velocity exceeds the maximum oscillatory velocity because at this point the blank-holder is never moving towards the punch relative to the strip. Thus the effective frictional force acting on the top surface of the deforming specimen when summed over a complete oscillatory cycle varies from zero when the drawing velocity is zero to its non-oscillatory value when the drawing velocity exceeds the maximum oscillatory velocity.

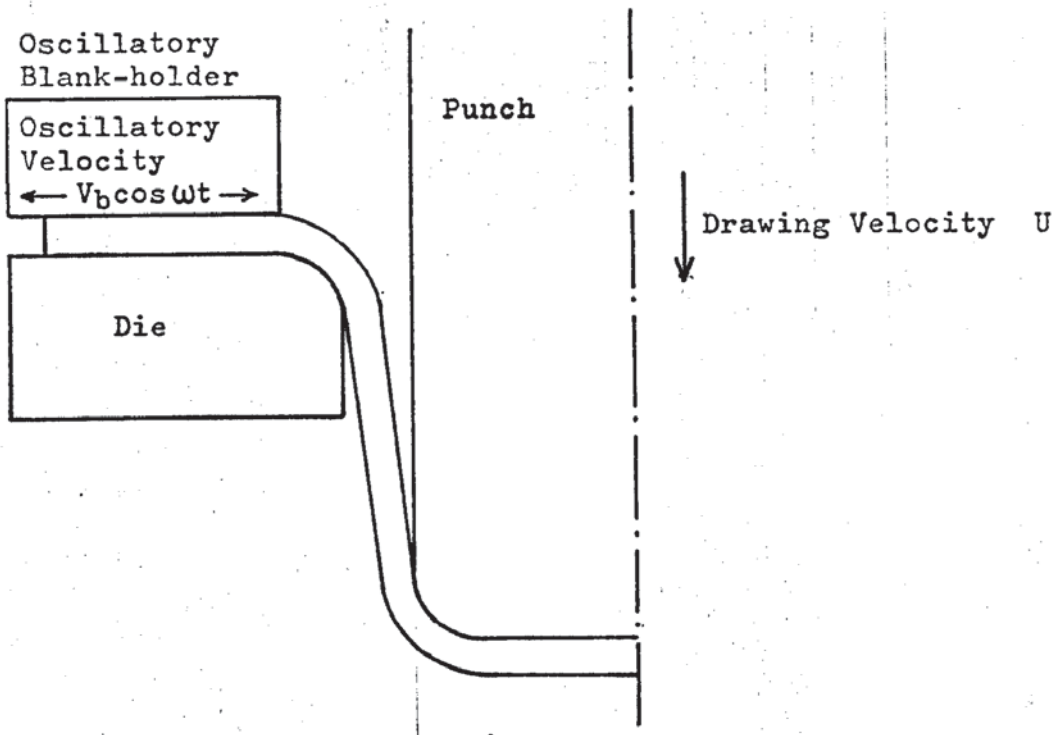

Figure 3.4.1.

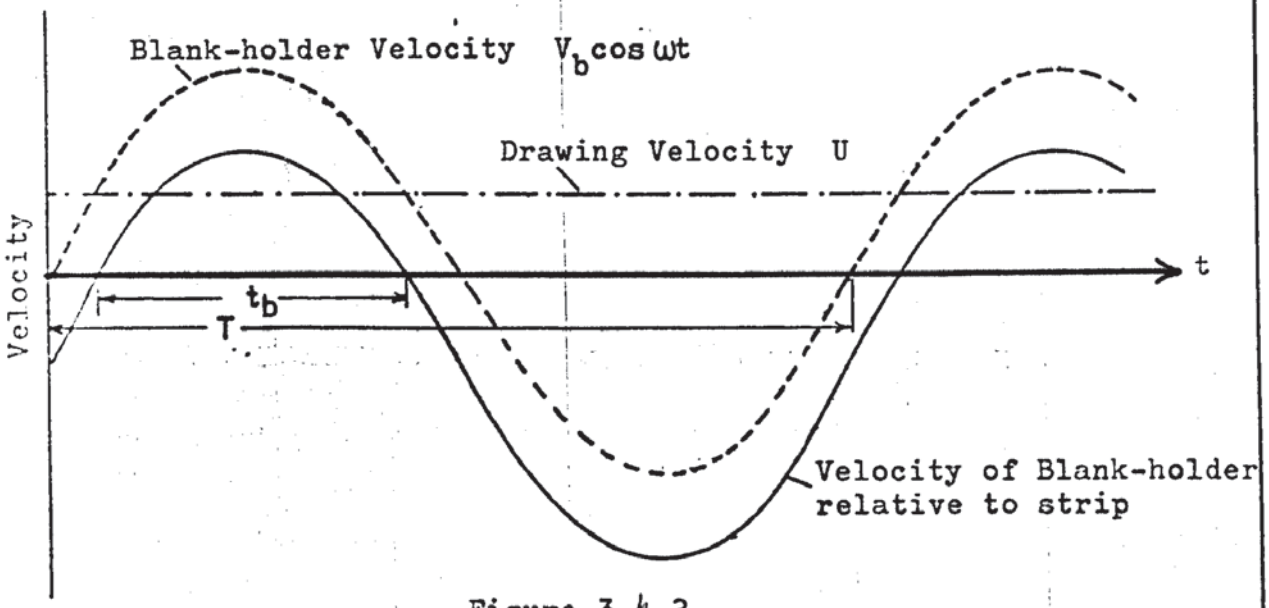

Figure 3.4.2.

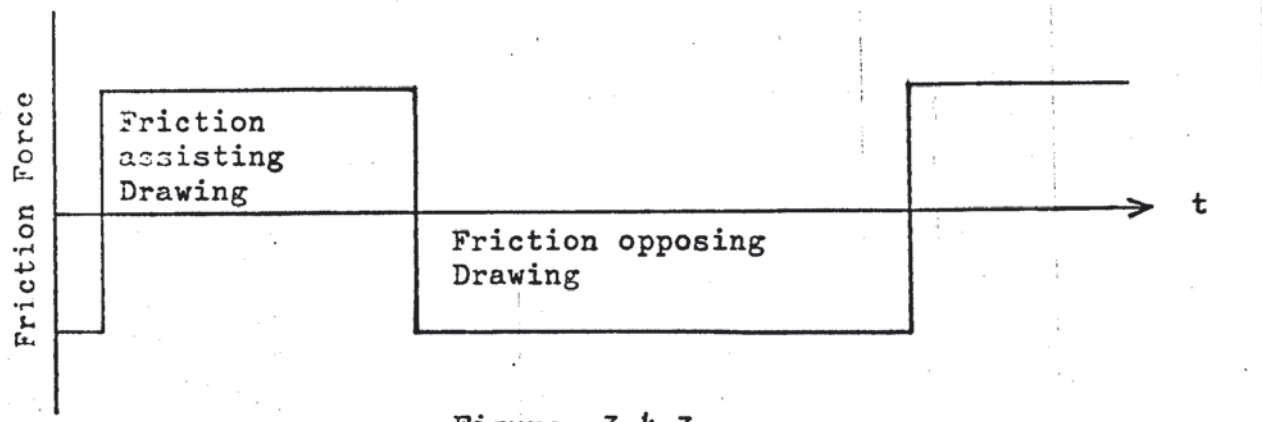

Figure 3.4.3.

Referring to Figs. 3.4.2 and 3.4.3.

Blank-holder oscillatory velocity = $V_b \cos\omega t$

Drawing velocity = U

Friction force F assisting drawing process when

$$V_b \cos\omega t > U$$

i.e. over time period t_b

Friction force F acting in normal direction when

$$V_b \cos\omega t < U$$

i.e. over time period $(T-t_b)$

work done again friction on the top surface of the blank becomes

$$F \left[(T-t_b) - t_b\right]$$

$$= F(T-2t_b)$$

and the reduction in the work done against friction is therefore

$$\frac{F(T) - F(T-2t_b)}{F(T)}$$

$$= \left(\frac{2t_b}{T}\right) \times 100 \quad \text{per cent}$$

The effective reduction in friction is therefore dependent upon the ratio $\frac{2t_b}{T}$

T is fixed by the oscillatory frequency, $f = \frac{1}{T}$ and thus the friction reduction will vary with changes in t_b.

It is therefore dependent upon the velocity ratio

$$\frac{V_b \cos\omega t}{U}$$

For a constant oscillatory frequency and drawing velocity the friction reduction is dependent upon the oscillatory amplitude. The effect of velocity ratio on the reduction in friction on the top surface of the specimen is shown in Graph 3.4.1.

Graph No. 3.4.1.

Reduction in Friction v Blank-holder Velocity Ratio on Top Surface of Specimen

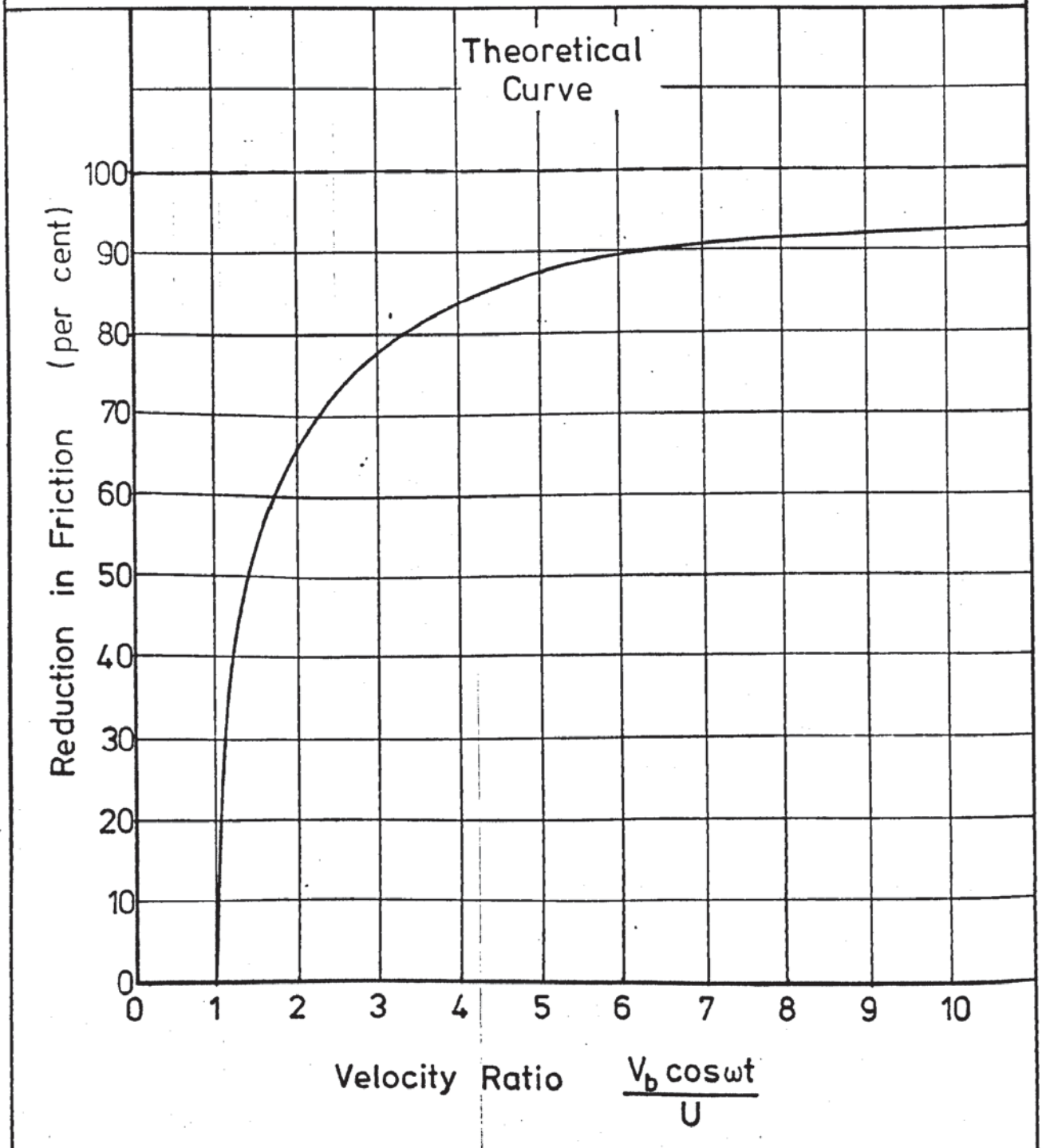

3.5. Draw Ironing Die Vibration.

3.5.1. The Drawing Operation.

The schematic of the application of 'radial' vibrations to the drawing ~~part of the draw-ironing~~ process is shown in Fig. ~~3.5.1.~~ The specimen within the ~~wedge~~ die is assumed to remain in contact with the die and is therefore subject to the same oscillatory motion as the dies.

The effect of the oscillatory velocity on the process is shown in Fig. ~~3.5.2.~~ Considering the wedge dies to be moving towards the punch from their position of maximum separation, the oscillatory velocity increases from zero until it equals the drawing velocity. At this point drawing stops and as the oscillatory velocity increases further the strain in the drawn product is reduced. Over this portion of the oscillatory cycle the specimen within the wedge dies always moves towards the punch and thus the friction force acting on the top surface of the blank acts in the direction opposing the drawing, that is, away from the punch as shown in Fig. ~~3.5.3.~~ Once the oscillatory velocity has passed its maximum value and decreased until it is less than the drawing velocity, deformation restarts. Drawing continues as the oscillatory velocity reverses and the dies begin to move away from the punch. When the oscillatory velocity becomes equal and opposite to the drawing velocity the velocity of the deforming strip relative to the blank-holder becomes zero. Further increase in the oscillatory velocity causes the material in the ~~wedge~~ dies to move over the blank-holder surface away from the punch. The friction force acting on the top surface now acts towards the punch, thus assisting the drawing process and reducing the stress within the drawn specimen.

Decreases in the drawing velocity or increases in the die oscillatory amplitude extend the periods during each oscillatory cycle when there is no drawing and when the blank-holder friction is reversed. These changes increase the effectiveness of the process

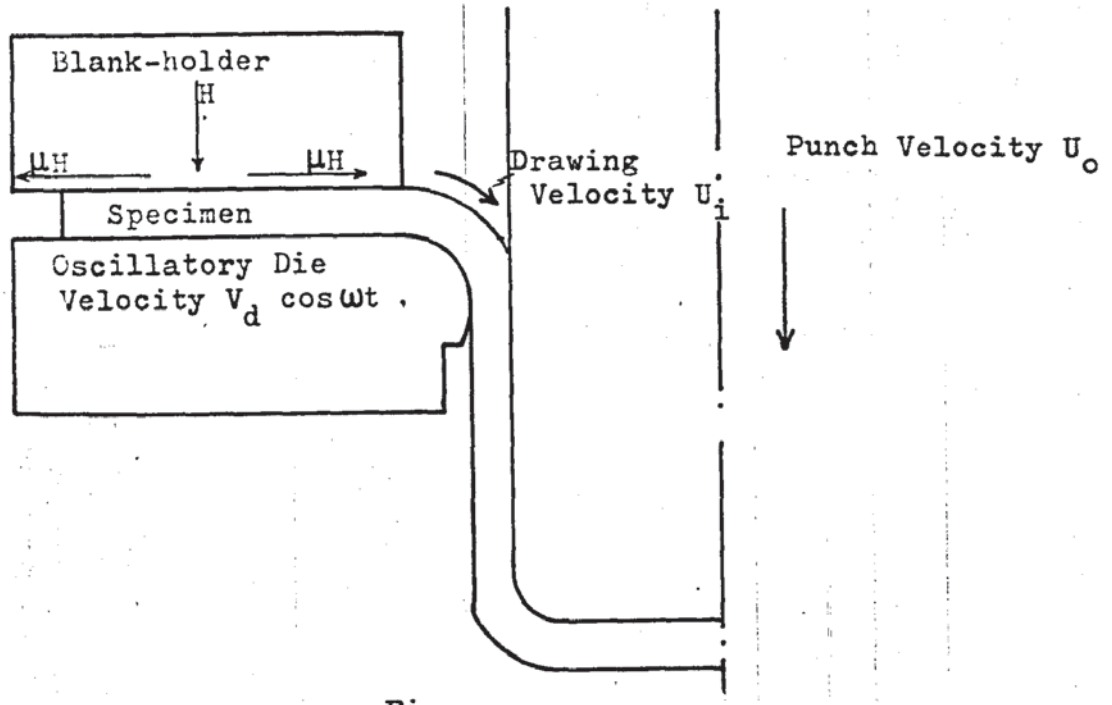

Figure

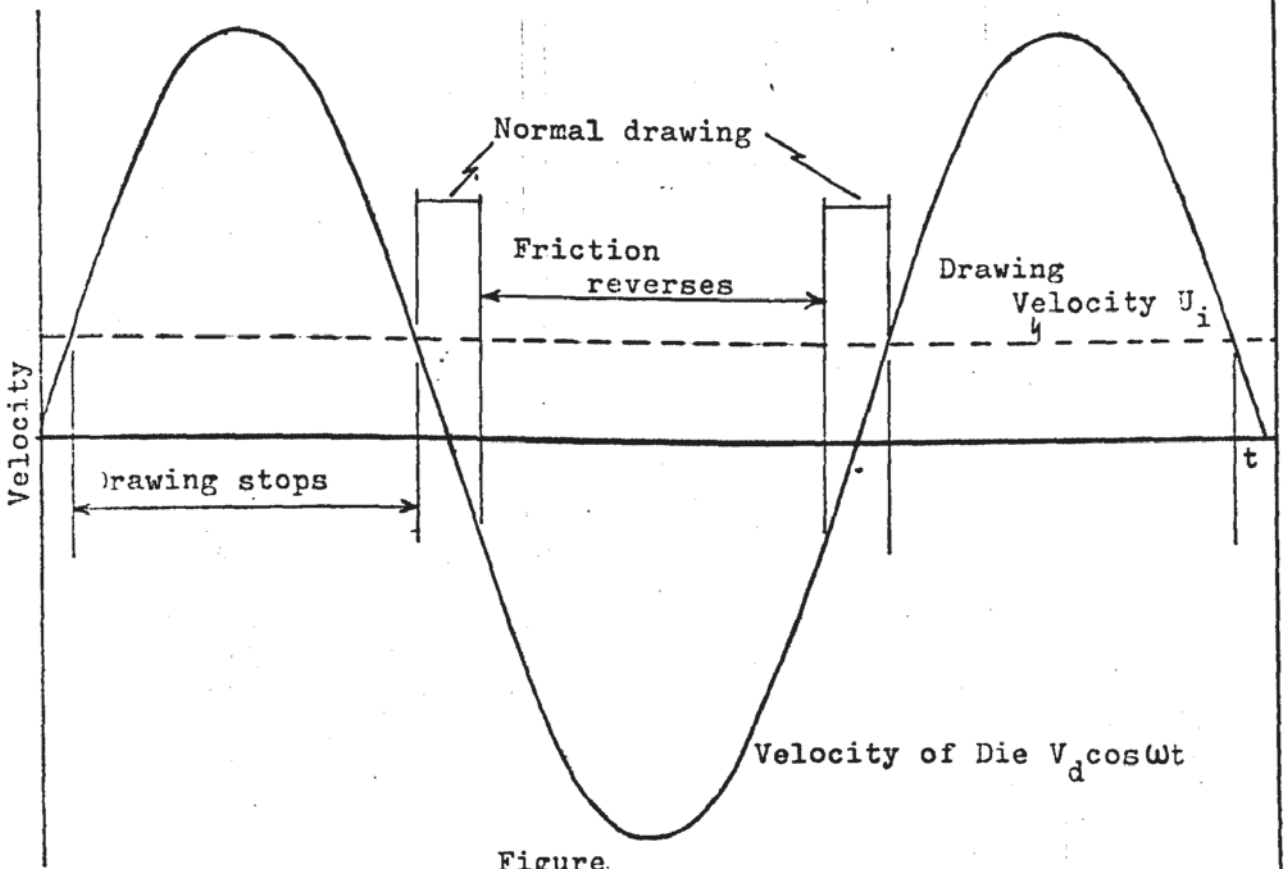

Figure

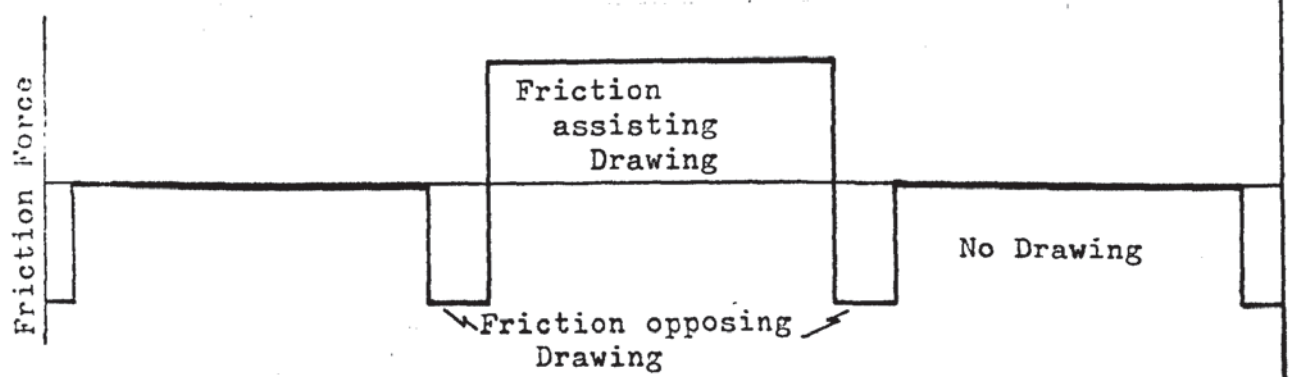

Figure

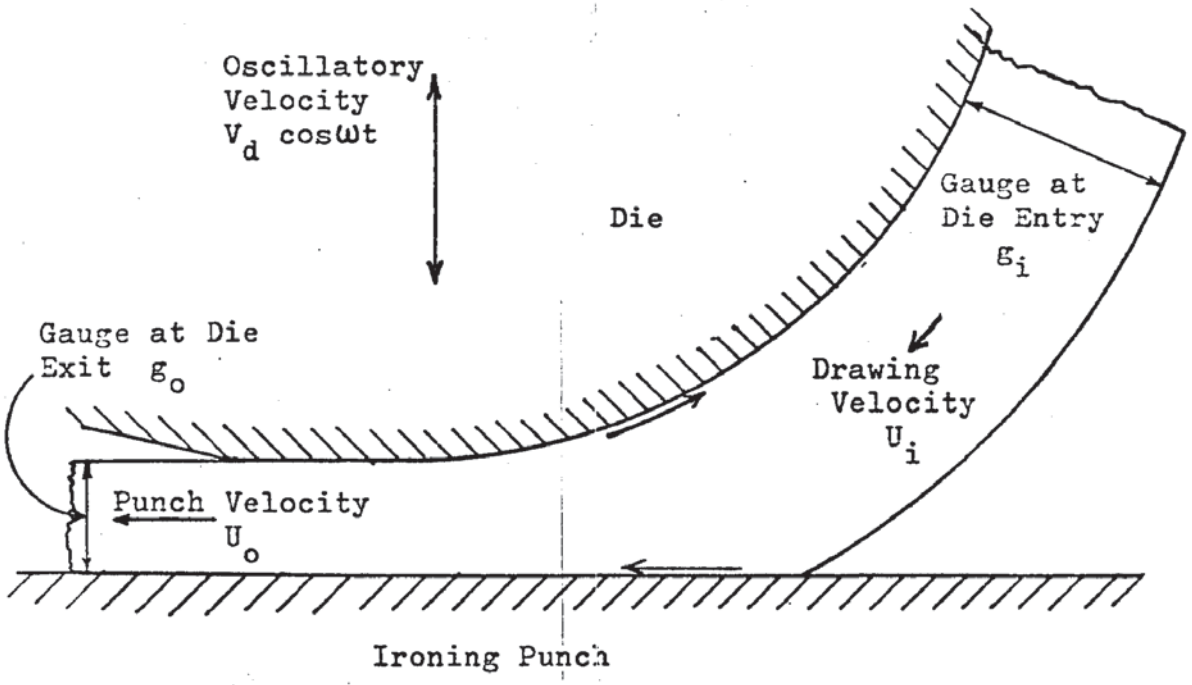

Figure 3.5.4.

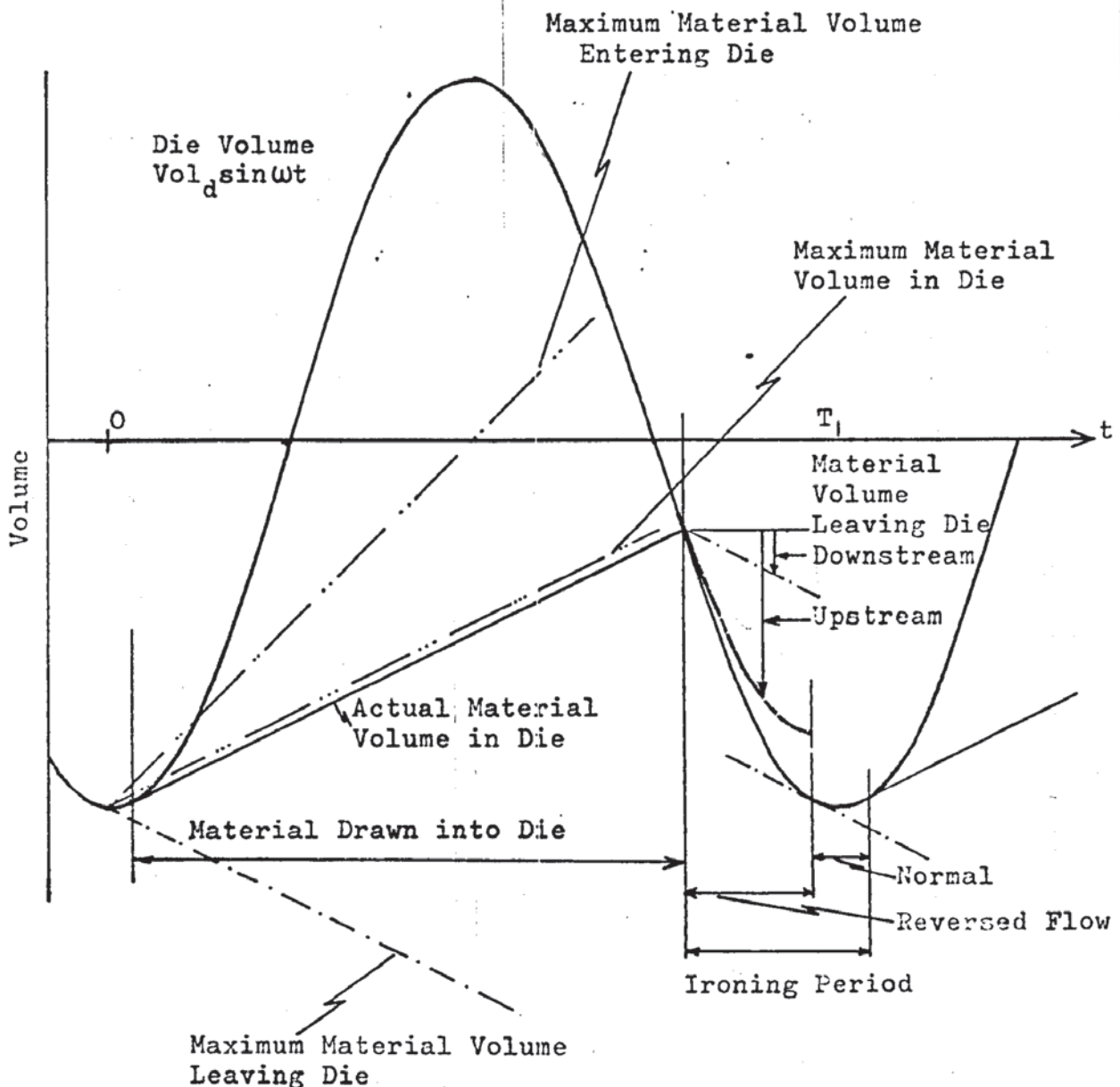

Figure 3.5.5.

since the portion of each cycle when the conditions are as in the non-vibrated drawing case is reduced. Limitations of the process are when the drawing velocity either approaches zero or exceeds the peak oscillatory velocity. In the first case drawing only occurs during the half-cycle that blank-holder friction assists the drawing process whilst in the latter case this friction reduction effect disappears altogether. (The theoretical relationship between friction reduction and velocity ratio for this process is similar to that shown in Graph 3.4.1.)

3.5.2. The Ironing Operation.

The schematic of the ironing part of the draw ironing process is shown in Fig. 3.5.4. Initially, considering non-oscillatory ironing, the ironing reduction and velocity are related by a constancy of volume of material in the die.

Thus, for non-oscillatory ironing

Volume flow into die = Volume flow out of die

For plane strain deformation, (strip width always greater than 5 times the length of the arc of contact on the die.), the continuity equation becomes

$$U_o g_o - U_i g_i = 0$$

$$\text{also area reduction} = \frac{g_i - g_o}{g_i}$$

Assuming no elastic recovery of material in the deformation zone this volume flow equality is disturbed by the application of oscillatory motion to the dies because this produces a periodic variation in the volume of the ironing die.

The effect of oscillating the die can be seen in Fig. 3.5.5. in which the material flow in and out of the die over one oscillatory cycle is considered.

The variation in the die volume is given by $\text{Vol}_d \sin \omega t$

The flow of material into the die after time $t = (U_i g_i)t$

similarly the flow out of the die = $(U_o g_o)t$

When the die is at its minimum volume position the ironing process is momentarily similar to the non-oscillatory case. As the die volume begins to increase an additional amount of material is drawn into the die to fill the extra volume created. This increased flow rate is achieved by increasing the inlet velocity of material into the die. Once the die volume is increasing at a rate greater than the maximum rate of increase of material in the die the ironing process stops. At this point the inlet velocity U_i equals the outlet velocity U_o and this velocity is merely indexing the undeformed material into the die.

i.e. change of volume of material in die

$$= U_o(g_i - g_o)t$$

and Volume of die = $\text{Vol}_d \sin \omega t$

Ironing stops when $\frac{d}{dt}\left[\text{Vol}_d \sin \omega t\right] = \frac{d}{dt}\left[U_o(g_i - g_o)t\right]$

or, $\text{Vol}_d \, \omega \cos \omega t = U_o(g_i - g_o)$

As the die volume further increases the surfaces of the die and deforming specimen separate until the die volume, having passed its maximum position, begins to decrease and the point is reached where the die volume is again equal to the volume of material in the die.

i.e. $\text{Vol}_d \sin \omega t = U_o(g_i - g_o)t$

Beyond this point the rate of decrease of the die volume is now greater than the rate at which the volume of material in the die can be reduced by flow through the die throat exit.

i.e. $\left|\text{Vol}_d \, \omega \cos \omega t\right| > U_o g_o$

The volume of material in the die must however equal the die volume and the only way this can occur, for an incompressible material, is if some of the material already in the die is ejected back out through the die inlet. Thus whilst this inequality holds there is a reversal of flow within the die. Material is still being drawn from the die outlet in the downstream direction however and there

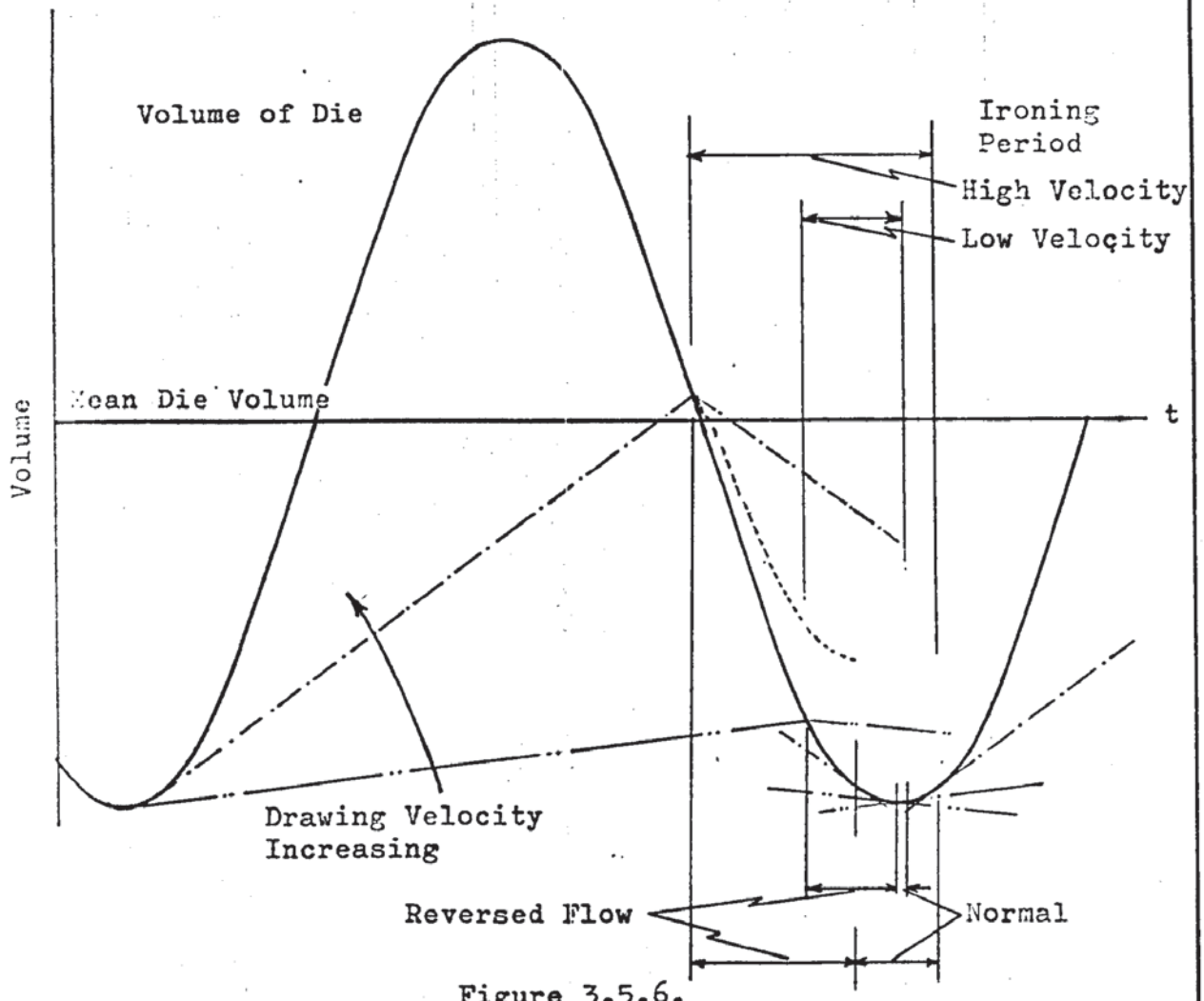

Figure 3.5.6.

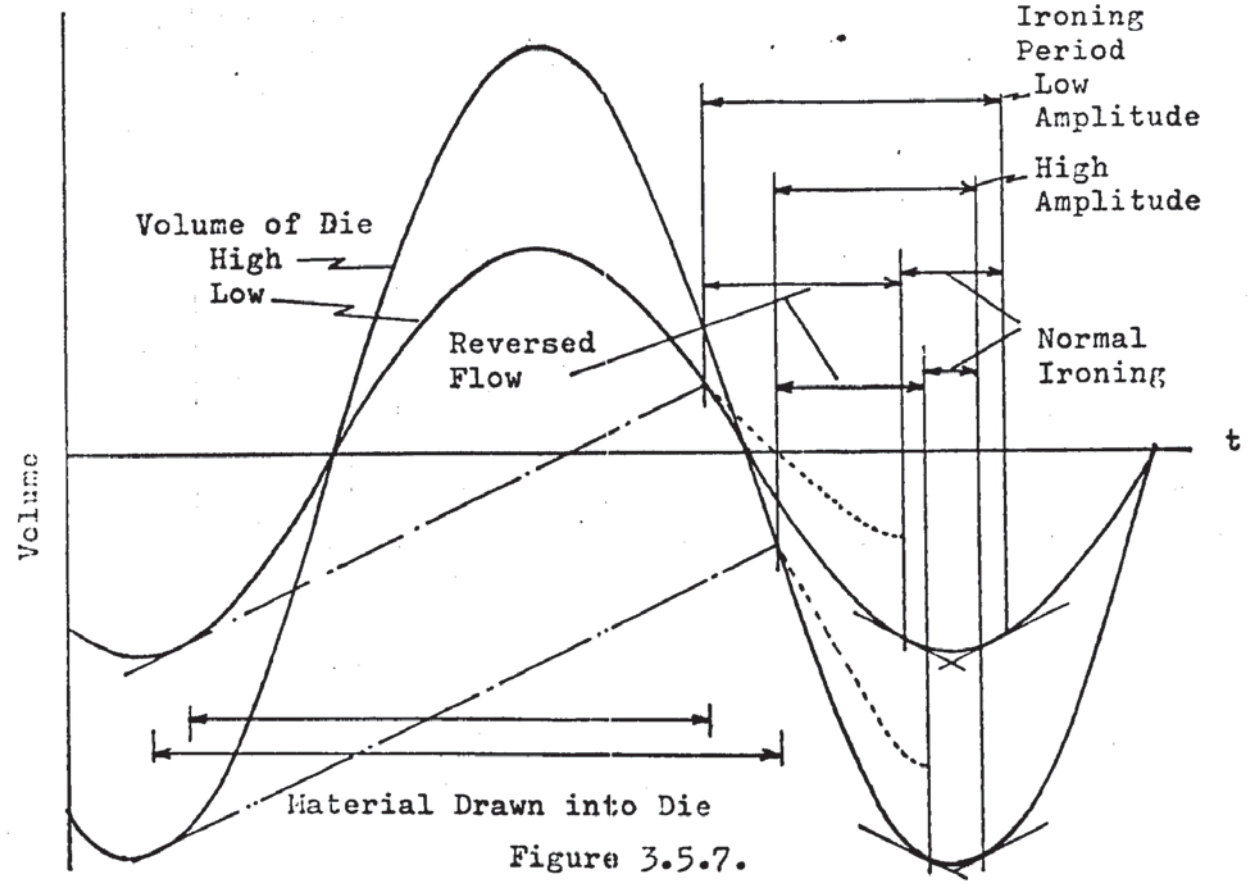

Figure 3.5.7.

must, therefore, be a neutral plane established within the die at the point of flow reversal. The position of the neutral plane is dependent upon the drawing velocity and the rate of change of die volume.

As the die volume approaches its minimum value at the end of the oscillatory cycle the rate of decrease of volume becomes equal to the flow rate of material from the die outlet (downstream)

i.e. $Vol_d \omega \cos \omega t = U_o g_o$

The flow reversal in the die stops, $U_i = 0$ and the draw ironing process continues in a conventional manner through the minimum die volume position until the die volume is again increasing at a greater rate than the maximum flow of material into the die. Ironing stops at this point and the cycle described above is repeated. The rate of progress of the material through the die is determined by the fraction of each oscillatory cycle during which ironing, whether normal or reverse flow, takes place.

The effect of increasing the punch velocity is shown in Fig. 3.5.6. The portion of each oscillatory cycle during which the material is ironed, is increased at the higher punch velocities. The assistance given to the process by the reverse flow ironing is reduced, however, because the proportion of normal to reverse flow ironing increases. In addition, the rate of ejection of material from the die inlet is reduced with the increased punch velocity despite the greater volume of material in the die at the start of the reversed flow period. This reduction in the reverse flow rate is caused by the higher rate of removal from the die outlet and, therefore, the neutral plane within the die moves towards the die inlet. This reduces the region of reversed flow within the die and, therefore, the frictional assistance to the process is similarly reduced.

The effect of decreasing the oscillatory amplitude is shown in Fig. 3.5.7. The ironing portion of each oscillatory cycle is extended and the proportion of normal to reverse flow ironing is

reduced, moving the neutral plane towards the die inlet. Thus the effects of increased punch velocity or decreased oscillatory amplitude can be seen to be similar in reducing the effectiveness of die oscillations in the ironing process. Die vibrations assist this process by reducing the frictional force within the die thereby reducing the tensile load in the drawn product.

The oscillatory amplitude necessary for the flow reversal effect to occur for a typical ironing reduction and drawing velocity is shown below.

Referring to Fig. 3.5.4.

U_o = 0.35 in sec^{-1}

g_o = 0.028

f = 13 kHz

For a circular die form the change in volume Vol_d is given by arc length x oscillatory amplitude.

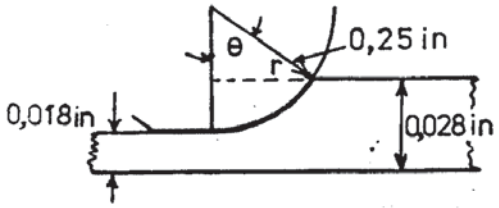

Figure 3.5.8.

From Fig. 3.5.8. $\cos\theta = \frac{0.240}{0.250} = 0.96$

θ = 15 deg.

arc length $\simeq r\theta$

$r\theta$ = 0.25 x 0.26 = 0.065 in

therefore Vol_d = 0.065 x Oscillatory Amplitude

For reversed flow

$$Vol_d > \frac{U_o g_o}{\omega \cos \omega t}$$

$$\text{Osc. Amp.} = \frac{U_o g_o}{2\pi \times 0.065} = \frac{0.35 \times 0.028}{2 \times 3.142 \times 13.000} \simeq 2 \times 10^{-6} \text{ in}$$

3.6. Blank-holder Swaging.

The schematic of the process of applying blank-holder vibrations normal to the plane of the deforming blank is shown in Fig. 3.6.1. When the blank-holder is vibrated with simple harmonic motion the clearance that exists between blank-holder and die over one periodic cycle is shown in Fig. 3.6.2.

The motion of an elemental section (annular ring) of the material in the blank having a thickness equal to the minimum clearance between oscillating blank-holder and die will be considered. As the blank-holder moves away from the material, separation of the surfaces occurs and the frictional constraint that acted on both the die and blank-holder surfaces of the blank is eliminated thus reducing the radial drawing-in component within the total drawing load. As the blank-holder oscillatory motion reverses and the blank-holder moves towards the position of minimum clearance the blank-holder again comes into contact with the blank. This point does not correspond to the minimum clearance position because in the period during which the blank-holder was not in contact with the blank, circumferential compression due to radial drawing in has increased the thickness of the elemental ring. In the following period until the blank-holder reaches the minimum clearance position and reverses in direction the elemental ring would continue to move towards the punch with the consequential further thickening as shown. This thickening cannot occur however and the actual thickness follows the movement of the blank-holder. This reduction in the thickness can only be achieved by elongating the ring in the radial direction and the material is therefore extruded both in and opposite to the drawing direction. If the rate at which this ring is elongated exceeds the instantaneous drawing velocity there will be a reversal in the direction of friction in the region over which material is extruded away from the punch.

The increase in the normal pressure as the blank-holder contacts

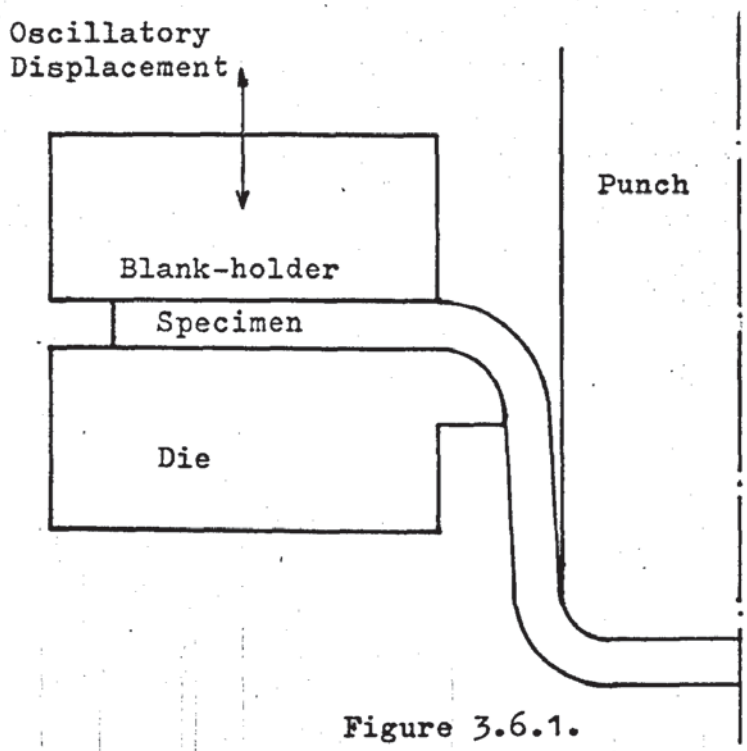

Figure 3.6.1.

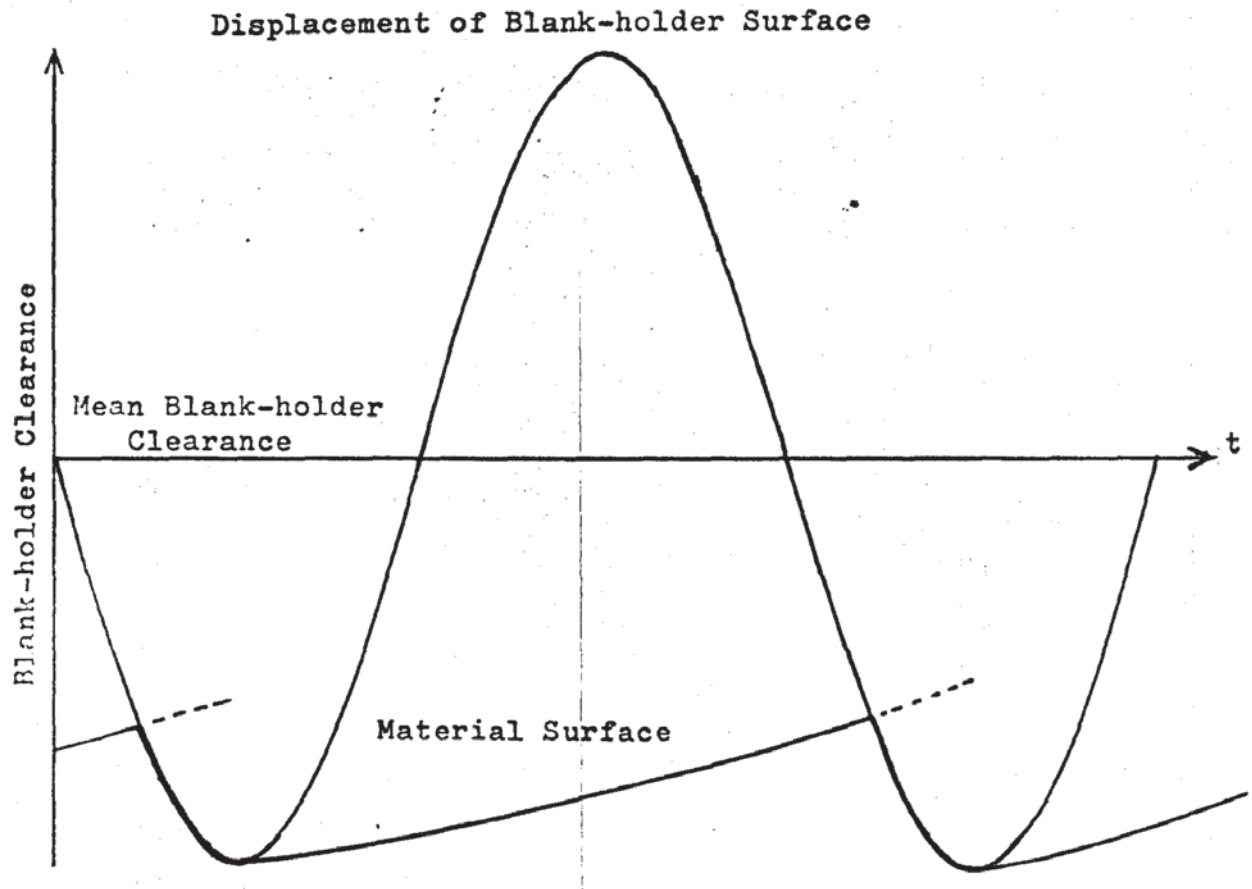

Figure 3.6.2.

the blank reduces the tensile drawing stress because the yielding situation is altered by the application of this stress which extrudes the material through the die. This system is therefore similar to that described in section 3.5.2. for the ironing process, except that the die angle is zero. The resultant of the friction and blank-holder pressure forces therefore always acts in the drawing direction in the reversed flow region.

The relationship for the thickening of the blank during radial drawing in developed by Chung and Swift (equation 3.1.6a.) assumed that blank-holder pressure is confined to the outer periphery of the blank once the drawing-in process starts. This relationship can be applied to the oscillatory process since once the blank-holder has passed its minimum clearance position there is no blank-holder stress applied to the specimen until the blank-holder again contacts the specimen surface after an increment of drawing. On determining this position of contact the proportion of the cycle over which the blank-holder forces the material through the die and the rate at which this occurs can be found.

The radial drawing in process is a non-steady state however and therefore the total effect varies as the blank is drawn over the die. The thickening of the elemental ring depends upon the reduction in its circumference that occurs during the period when a clearance exists between the two surfaces. This in turn is dependent upon the instantaneous velocity of the element which increases radially inwards, approaching the punch velocity at the die throat.

It is therefore possible to reduce the drawing stress over both portions of the oscillatory cycle. This application of vibrations should therefore result in a reduction in the punch load and an increase in the limiting draw-ratio.

4. EQUIPMENT.

4.1. Punch Vibration Equipment.

4.1.1. General Description.

The basis of the experimental equipment necessary for the application of punch vibrations was in existence from the previous work, on die vibrations, by Young. A detailed description is given in Young's thesis[65] but briefly this equipment comprised the sub-press consisting of the wedge dies, blank-holders and hydraulic blank-holder pressure supply. The wedge dies were attached to the end of conical concentrators which were used to apply the ultrasonic vibrations to the dies. These two concentrators were mounted on thin flanges positioned at the nodal point on the conical concentrator. The dies were supported on linear roller-bearings so that they would vibrate and not deflect during the drawing operation. The blank-holders which located in the wedge dies were separated by a load-cell which was used to record the compressive stress produced by the frictional force acting between the top surface of the specimen and the surface of the blank-holder as the drawing operation took place.

The blank-holder pressure was applied to the top surface of the blank-holders by two hydraulic pistons mounted in the blank-holder cover plate. Linear roller-bearings were positioned in between these components to prevent any constraint on the movement of the blank-holders which would affect the loads recorded on the friction load cell.

The only major item requiring manufacture was a punch system to which vibratory energy could be applied. The major limiting condition on the design was that the punch system, when completed, should resonate at the same frequency as the die system used in the previous research project. Thus the design of the oscillatory punch system is described in greater detail.

4.1.2. Design of the Oscillatory Punch System.

In order to obtain design information some preliminary testing was performed with the apparatus set up for die vibrations. The drawing of specimens at a number of draw-ratios was examined and the frequency at which the system resonated was noted in each case. Over the range of specimen sizes tested, resonance did occur within the design range but the precise resonant frequency was dependent, to some extent, upon the size of blank used. A frequency in the middle of the range applicable to the various specimen sizes was selected and the design frequency for the oscillatory punch was set at this figure.

The amplitude of vibration used in ultrasonic metalworking is considered to be a critical variable in the effectiveness of the process. The theoretical maximum amplitude obtainable from the magneto-strictive effect at the ends of the nickel transducers which were to be used to convert the electrical power into mechanical oscillations was considered to be too small for the envisaged duty. Some form of amplitude amplification was therefore desirable. A conical concentrator was finally preferred on account of its better transformation characteristic than the simpler stepped concentrator whilst it did not have the manufacturing difficulty associated with an exponential form which has the most effective profile for amplitude conversion.

The space available for the punch system was quite adequate and so it was possible to incorporate an active mounting device in the oscillatory system. The advantage of such a system is its ability to maintain resonance at the design frequency, whatever the loading conditions. The principle of such a mount, is a mount which in addition to the central loaded section has another section which is free to vibrate in the unloaded condition. As the loading conditions vary within the loaded section of the mount the resonant

condition is maintained by the unloaded section. This section vibrating in free air is subject to constant loading and hence the resonant frequency of the system is maintained at the desired value, whatever the loading on the remainder of the system.

With the type of mount selected it was designed by combining the known requirements and the theory of vibrating systems to arrive at the required dimensions of the system. In order to predict the exact length of the system some consideration had to be given to the loading conditions expected at the punch end of the system. The conditions could range from a free end to a completely fixed one, with most practical systems coming somewhere between these limits. It was expected that the conditions in practice would not be very far removed from that of a free-end system and for the purpose of design calculations this free-end condition was assumed. In addition, the free-end system was longer than the fixed-end system so that even if during drawing the conditions differed from a free-end, as they must, the punch would be too long, rather than too short. It would, therefore, be possible to rectify this by shortening the punch during the manual tuning after initial manufacture. The calculations were performed in order that a better understanding of the limitations of the theory would be obtained should a more accurate specification of the finished article be required in future. The design calculations are shown in Appendix A.1.

The complete punch oscillatory system is shown in Fig. 4.1.1. The $\frac{1}{2}$-wave length laminated nickel transducers were screwed into the larger diameter (low amplitude) end of the conical concentrator. At the other (high amplitude) end of the conical concentrator was attached a $\frac{1}{2}$-wave length parallel section over which the active mounting sleeve would be fixed. Beyond this section was another $\frac{1}{2}$-wave length section transforming the circular cross-section into the rectangular cross-section necessary for the drawing punch itself,

Figure No. 4.1.1.

Detail of Oscillatory Punch Assembly

with Ultrasonic Stress and Displacement Distribution

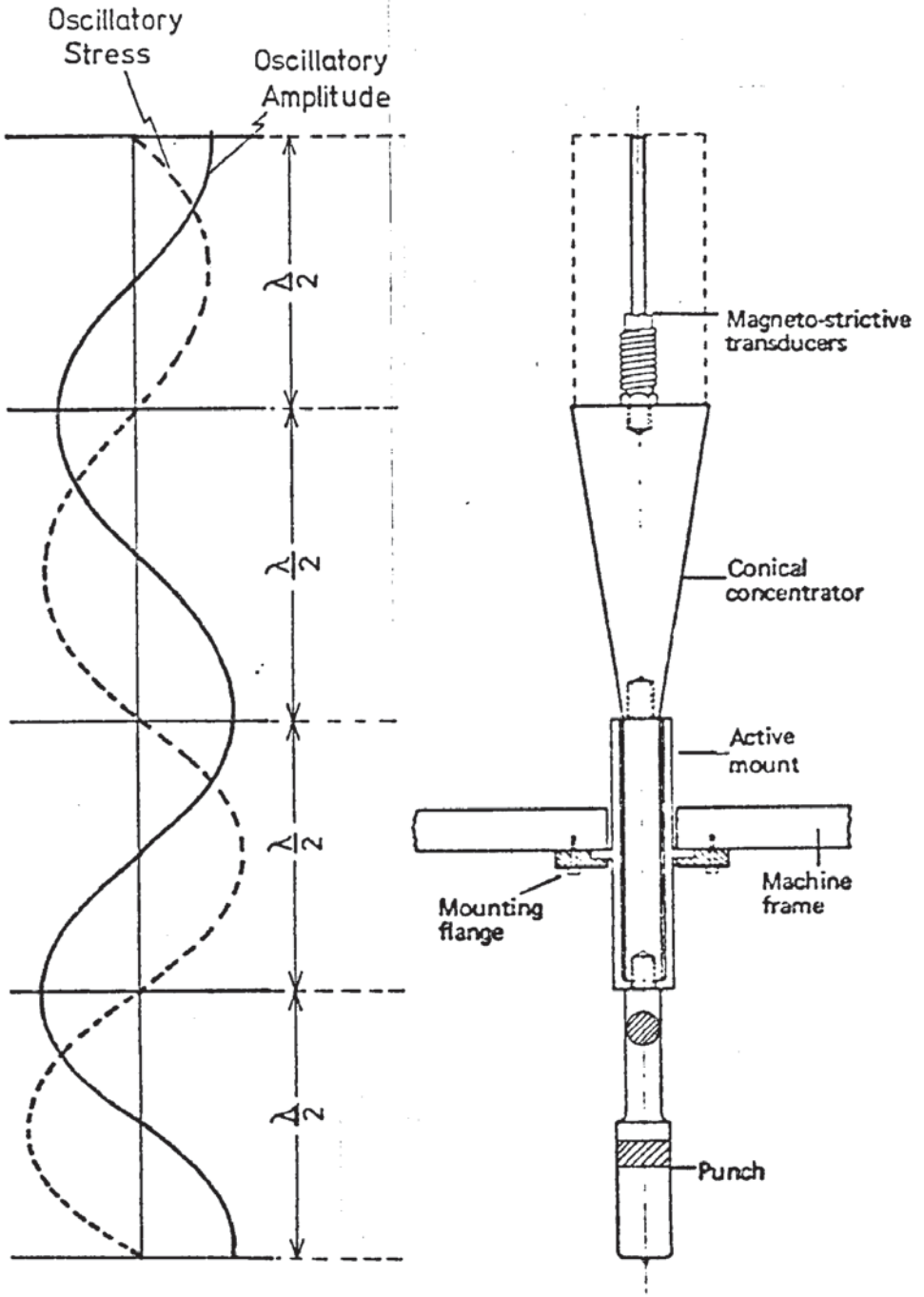

which was to be an integral part of the ultrasonic system.

The choice of material for the punch was based upon a number of criteria. A material to withstand the fatigue conditions created by the ultrasonic systems; a material that was readily available and had the necessary strength to withstand both oscillatory and metal deformation working stresses; a material that could be worked with normal workshop machinery was essential.

All of these requirements were met to a greater or lesser extent by the same nickel die-steel which had been used for the manufacture of the die system. This material was therefore selected since there was the additional advantage that both of the ultrasonic systems were constructed of the same material. The joints in the punch system necessary for manufacturing purposes were designed having consideration for fatigue and stress concentration effects so that problems arising at the joints could be minimised. Screw-thread attachments were the only practical possibility for the construction of the punch system because of the necessity to dismantle the system for tuning purposes.

After considerable delays caused initially by the delivery time on the raw material, followed by a lack of workshop facilities, the system was finally maufactured; the grinding of the punch profile radii being contracted out because of a lack of proper equipment within the workshop.

4.1.3. Tuning of the Oscillatory Punch System.

The tuning of the punch system to alter its post-manufacture resonant frequency to that originally specified was a complicated procedure. At first the conical concentrator was separated from the punch system so that its resonant frequency could be determined. The magneto-strictive transducers were screwed into the large diameter end, and the coils of the transducers were wired into the ultrasonic generator. The frequency of the ultrasonic vibrations was varied until the resonant frequency of the conical concentrator was determined. This determination could be monitored in a number of ways. Resonance within the R-C network of the ultrasonic generator was indicated by a drop in the voltage across the coils on the magneto-strictive transducers. Therefore, the monitoring of the applied voltage by a suitable voltmeter was used to detect resonance within the electrical circuits. The corresponding mechanical resonance was detected by the use of a piezo-ceramic crystal attached to the end of the concentrator. The signal from this was observed on an oscilloscope, the maximum amplitude being obtained at resonance.

Other more subjective means of determining resonance could be used; these included the sound the vibratory system made at resonance which was distinctly different from the off-resonant sound. Another, more accurate, method was one of touch; the systems were lightly stroked whilst the oscillatory frequency was varied. The normal metallic feeling completely disappeared at resonance, the highest amplitude giving rise to a 'glassy' feeling as if there was a cushion of air between finger and concentrator. This technique was useful once a determination of the correct mode of vibrations had been observed using a piezo-ceramic crystal and oscilloscope.

This latter test was necessary since frequency was determined and displayed by a counter/timer connected to the oscillator within the ultrasonic generator. Thus it was necessary to confirm that the system was operating in the fundamental mode. Once this had been

established the progression of the coarse tuning could be monitored by touch since the procedure was less time consuming than observation with an oscilloscope.

Prior to tuning, the resonant frequency of the conical concentrator was too low because it had been manufactured with its length greater than the designed size. For the coarse tuning, material was removed from the large end of the cone because for a given change in length a greater change in resonant frequency was obtained by removing material from the large diameter end rather than the narrow end. After removal of the material, which was done by turning in a lathe (with purpose built adaptors to mount the conical section), the transducers were replaced and tightened down to an essentially constant torque, the coils were replaced, and the unit connected to the ultrasonic generator and the new resonant frequency noted. A graph was plotted of material removed against natural (resonant) frequency to indicate progress in tuning. After monitoring the resonant frequency the concentrator was again dismantled, remounted in the lathe and more material removed. The procedure was repeated as the tuning process continued. The final tuning adjustments were made to the narrow end because the resonant frequency was less sensitive to length changes. Having tuned the conical concentrator the other components comprising the complete system ideally would be tuned individually until each part was resonating at the design frequency. This procedure could not be adopted, however, because of the lack of any driving ultrasonic system on the component parts other than the conical concentrator. The rest of the system had to be tuned, therefore, as a complete assembly. This was not too difficult since the ultrasonic system after the concentrator was of a uniform section apart from the last $\frac{1}{4}$ wave-length which was rectangular; this meant that there was little discrepancy between theory and practice.

The main tuning problem arose with the active mounting system;

this was attached to the punch system at the end of the mount which was clamped between the two sections of the assembly. Another flange located a $\frac{1}{4}$ of a wave-length along the mount was for attachment to the frame of the testing machine. The problem was to determine the effect of the thickness of each of these flanges upon the resonant length of the mount since ideally these flanges should be very thin; a minimum thickness was necessary, however, for strength considerations. The procedure adopted was to assemble the completed system and to note the frequency at which the mount system vibrated. This information was used to determine how the flange thickness affected the resonant length of the mount. The result of this was that it was possible to predict the required length with a good degree of accuracy, when the effect of the flange was known. Having established this, the mount was machined until its resonant frequency coincided with that of the conical concentrator.

A spacer washer of thickness equal to that of the flange at the end of the mount was manufactured and substituted into the assembled punch system in place of the mount. This gave a length to the system equal to that when the mount was in place so that the remainder of the punch could be tuned without the added complication of the active mount. Once again a tuning curve was plotted to monitor the progress and material was successively removed from the cylindrical rod, which normally fitted inside the mount, until the resonant frequency of the assembly was equal to that of the conical concentrator alone. The tuning was finally checked with the mount assembled into its correct position before installation into the testing machine.

Before the punch could be installed into the existing press the normal punch, which had been used for the die vibrations work, was removed along with the mounting plate of the cross-slide. This mounting plate required modification to allow the active mount to pass through prior to it being secured by a clamping ring which fitted

over the flange of the mount. This flange was clamped at the outer perimeter to prevent any undue restriction on the flange movement. Having completed the machining modifications to the plate it was replaced upon the cross-slide of the hydraulic testing machine. In order to accommodate the longer punch this cross-slide had to be moved upwards by one position on the machine frame. Consequently, the punch system was ready to be positioned in the press and therefore the conical section was removed to enable the lower section to be threaded upwards through the newly machined hole in the mounting plate and clamped firmly in position.

The conical concentrator was replaced, tightened into position and the magneto-strictive trasnducers and coils were fitted. During the tuning process it had been noted that the behaviour of the system was affected by the tightness of the joints in the system and also the tightness of the individual nickel transducers. In order to obtain a uniform set of conditions which were reproducible during the tuning and assembly processes all the screwed joints were tightened to a pre-determined torque. This was accomplished by means of a spring-balance and various lengths of tubing to serve as torque arms, the lack of access prevented a conventional torque wrench from being used.

This re-assembly of the punch system within the press should therefore not have affected any of the previous tuning procedures. All the joints in the punch system were tightened down on very thin soft copper washers, so that any imperfections in the mating surfaces were filled-in by soft copper to improve the surface contact and the transfer of acoustic energy.

4.1.4. The Subpress.

The subpress, consisting of dies and blank-holders, as used by Young was largely complete apart from some of the instrumentation which had ceased to function correctly. After stripping down the subpress to effect these repairs the opportunity was taken to repolish the dies and blank-holders.

The female shape of the wedge dies precluded any mechanical polishing and so this had to be done by hand. The surfaces were first trued by the use of specially made lapping plates and carborundum paste. Once a uniform matt surface had been obtained the polishing operation proper was started using new lapping plates and finer abrasive powder. This process was continued through the various grades of powder until finally a polishing compound was used. At this stage, recourse was made to a small polishing mop attached to a 'Diprofil' polishing machine which produced a small reciprocating movement of the mop and speeded up the polishing process.

The blank-holder surfaces were easier to treat because of the male form which enabled hand polishing to proceed much more rapidly than with the dies.

Having re-conditioned the dies they were attached to the end of the concentrators using new soft copper washers and these were replaced in the subpress. Correct angular alignment of the concentrator mounting flange, so that the die surfaces were parallel to the base of the subpress, was checked with a dial-gauge mounted upon the base plate.

The general arrangement of the component parts of the subpress for punch vibrations is shown in Fig. 4.1.2.

Figure No. 4.1.2.

General Arrangement of Oscillatory Punch Apparatus

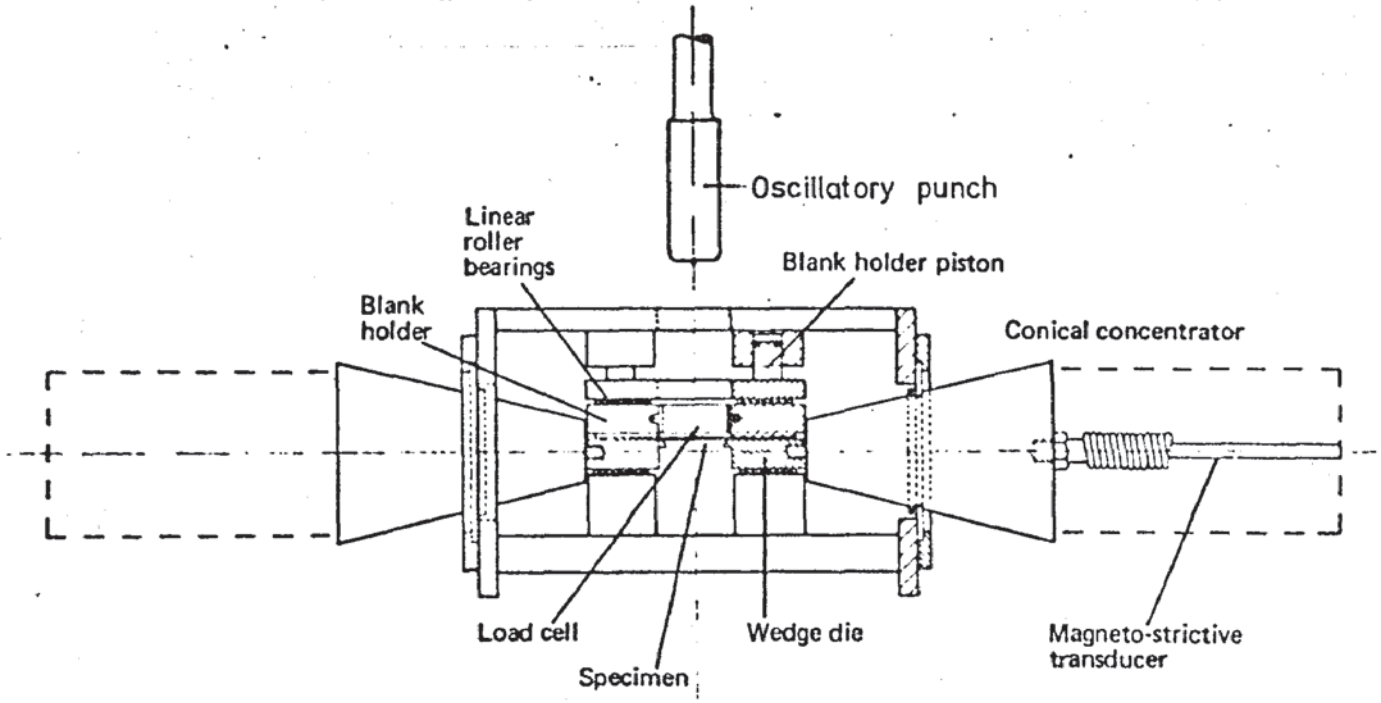

4.1.5. Punch Alignment.

After assembly the punch had to be positioned correctly relative to the subpress. Angular positioning of the punch was achieved by swivelling the assembly in its clamping ring until the side faces of the punch were parallel to the central axis through the wedge dies.

The angular alignment was checked by clamping parallel strips to the subpress sides to form a slide for a dial-gauge mounting block. The dial-gauge could then be moved along the punch side surface and give an indication of the out-of-parallel of the punch to the subpress. Once the angular position of the punch was correct it had to be centralised within the dies.

Strips were made and ground to size such that their thickness equalled the clearance between the die and punch. The clamping ring was mounted on a plate with slotted holes such that it could only be moved in one direction, and so this adjustment was made to equalise the clearance between punch and die. The final and least critical of the alignments was that in the direction at right angles to the previous one. A specimen was placed in the wedge dies and the punch brought immediately above this. The spigot in the punch base was observed through the locating hole in the specimen with a mirror and it was necessary to centralise the spigot by moving the clamping ring and plate as a unit attached to a second plate which was slotted to the cross head of the press such that it could only be moved in the required direction. These adjustments ensured that the punch was aligned correctly with the wedge dies in the subpress. In addition, the hydraulic ram of the testing machine was, within reasonable limits, self-aligning. The careful alignment as described above, however, was considered necessary because of the large mass of the ram. It was considered that the deflection of the ram from its normal position, even when floating, would impose an unrepresentative strain on the specimen.

4.2. Blank-holder Vibration Equipment.

4.2.1. General Description.

When the subpress was designed by Young, provision was made for the blank-holders to be vibrated and therefore the blank-holders were machined in the same manner as the wedge dies, so that they would fit on the ends of the conical concentrators. They were also of a similar physical size with the result that the resonant frequency of the blank-holder system ought to be approximately the same as the system used when vibrating the dies. At the outset the problems defined were how to vibrate the blank-holders whilst at the same time having control over the blank-holder pressure applied and also the ease of locating specimens in the apparatus. The solution chosen was to construct a rigid box structure which would locate the concentrators in the correct position whilst at the same time allowing the concentrators to move in a vertical direction to allow both the hydraulic blank-holder system to operate and also allow specimens to be inserted into the wedge dies. Unfortunately, apart from the wedge blank-holders and the conical concentrators, no other parts of the existing apparatus could be used.

4.2.2. Design of Blank-holder Equipment.

A five-sided box structure was designed with an open base and large rectangular holes in the top, front and back plates. The two side plates were to be used to mount the concentrators in. The space limitation within the hydraulic testing machine meant that the nodal flange support system for the conical concentrators had to be used again. Each flange was clamped around its periphery by an annular clamping ring, attached to a heavier section annular ring which was mounted to the box structure by four adjustable sleeves, it being located on a further four dowel pins. The adjustment was necessary to enable the blank-holders to be positioned correctly when the equipment was being assembled.

Figure No. 4.2.1.

Wedge Die for Blank-holder Vibrations

Material:- En 30B 2 Off
Heat Treatment:- Heat 810-830°C,
Oil quench, Temper at 200°C

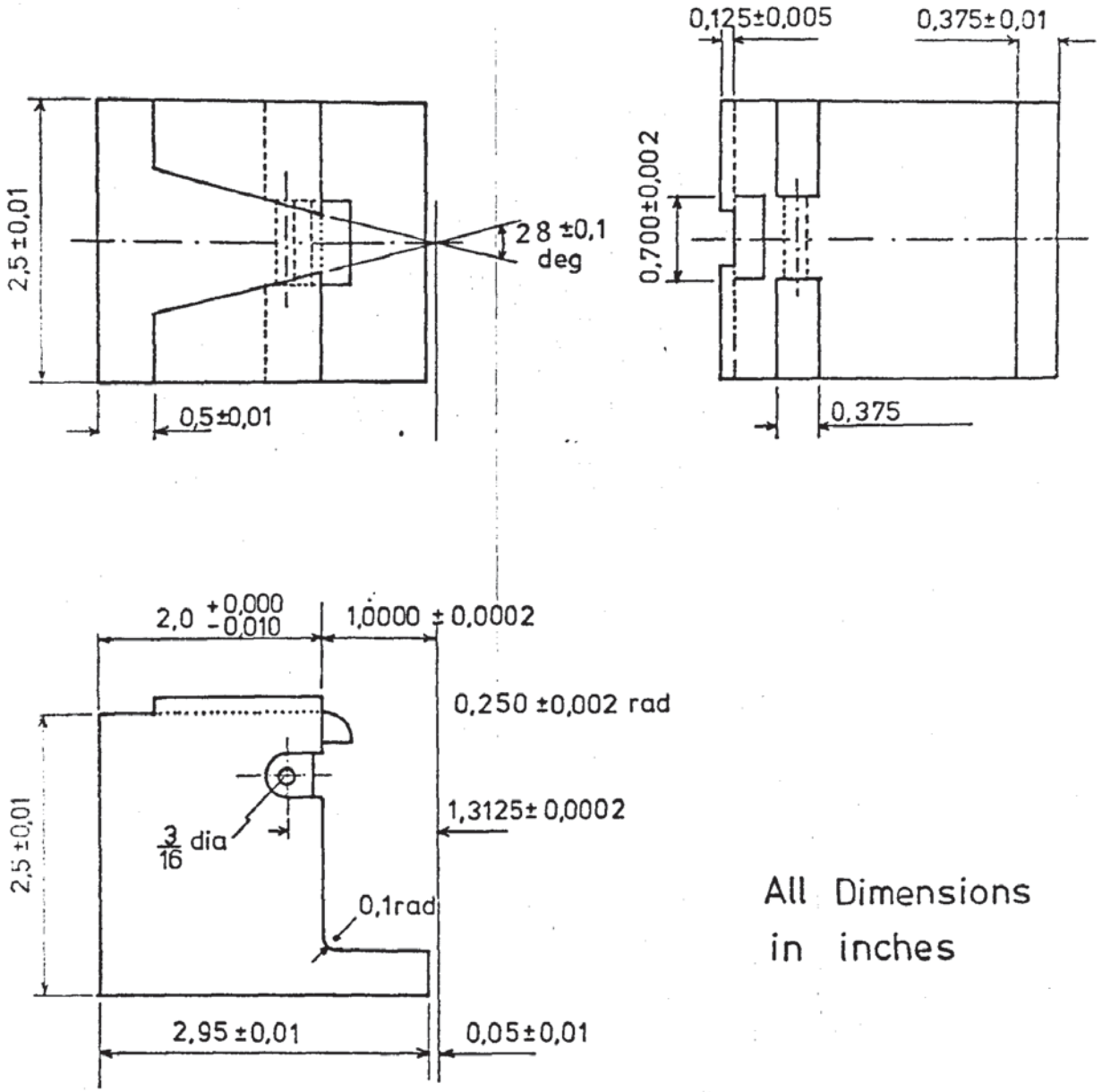

All Dimensions in inches

3rd Angle Projection

In order to guide the box structure during removal and replacement of the specimens four guides were required on the base of the subpress, these being adjustable so that during the first assembly there was some means of controlling the amount of sideplay within the box. The existing subpress was too large for the box to fit over and so provision was made for this to be reduced in size when the subpress was stripped down.

During the drawing process the subpress assembly would move upwards towards a stationary punch. Thus the system used to support the weight of the box also had to maintain its support whilst the box was moving during the drawing operation and for this reason it was decided to suspend it on steel cables and counter balance with large weights which were to be located below floor level in the pit of the hydraulic testing machine.

The wedge dies already in existence were not suitable since they were liable to tilt during the drawing process so new ones were designed, the base of which extended beyond the die radius so that the line of action of the drawing force would be inside the die and thus there would be no tendency to tilt. These dies would be made of En 30B high-nickel die steel, as shown in Fig. 4.2.1. Provision was also made for a load cell to pin the two wedge dies together, so as to measure the die separating force during drawing. To minimise frictional constraint the wedge dies were separated from the base of the subpress by linear roller bearings.

4.2.3. Assembly of Blank-holder System.

The box section and annular clamping rings were manufactured from pre-ground mild steel plate to assist with the careful alignment necessary to position the blank-holders correctly. Both sides of the box section, along with the annular rings, were jig bored so that the conical concentrators would be located on the same axis.

The box section was assembled and aligned using a mandrel

positioned through the holes in the side plates, into which the conical concentrators would normally fit, before being locked into this position by dowel pins inserted along the edges of the assembled unit.

The subpress was completely dismantled and the subpress base was machined to reduce its size so that the box section could fit over. The guides were attached to the base plate and they were brought to final size by high speed milling taking a very light cut so that they were perpendicular to the base plate. The base plate was fitted into the box and the movable shims of the guides adjusted so that there was a light sliding fit between the box section and the base plate. These guides were smeared with carborundum paste and the box was reciprocated over these guides, the paste cutting away any high spots that remained. This lapping operation was continued until the box section moved smoothly upon the guides with neither tight spots nor slackness within the region that the base plate would normally occupy during the drawing operation.

The wedge blank-holders were lapped and repolished to remove the scuff marks from previous operations and they were attached to the conical concentrators by means of tool steel studs, a thin soft copper washer was included between the mating surfaces of the concentrator and the blank-holder with the intention of improving acoustic contact.

The mounting flange of the concentrator was sandwiched between the two annular clamping plates and these in turn were located on the dowel pegs in the sides of the box section. The blank-holder was aligned by rotating the nodal flange in its annular ring until the working surface of the blank-holder was parallel to the base of the box section. The flange was clamped firmly in this position by a series of small set pins located within the annular rings. This was repeated for the other concentrator so that both the blank-holders were in the correct plane. It was also necessary to adjust the posi-

tion on the blank-holders within this plane. A test block was ground so that its length corresponded to the separation required of the blank-holders and the adjustable columns, onto which the annular rings were mounted, were rotated until the blank-holders were in the required position when the lock nuts were tightened to fix these positions permanently.

The box section, complete with concentrators, was weighed in order to ascertain the weight required to counter-balance it. The box section was attached to the suspension cables, which ran vertically up to the fixed head of the hydraulic testing machine, turned through two 90 degree bends over pulleys with the other end of the cables hanging clear of the rear of the machine enabling weight hangers to be attached which extended the cables to below floor level into the machine pit. There was some frictional constraint present in this system and so it was not desirable to counter-balance the system perfectly since in this situation a further force would be necessary to overcome friction when the box was being moved. It was decided to bias the counter-balancing, such that when the box was moving vertically upwards as it would do during the drawing operation, it was free to move, once given an initial impulse to overcome static friction, neither accelerating or retarding. This condition was obtained by adding small weights to each hanger in turn in addition to the weights necessary from calculations of the mass of the box section and tooling.

The subpress base plate and stand were moved into position under the suspended box section and the stand was bolted down in the centre of the bed of the testing machine. The box section was lowered towards the guides until it was just clear of the top of the guides. The positions of the pulleys directly above the box section were adjusted, slotted holes being provided for this facility, until the box was positioned correctly over the guides before the pulleys were locked in position. The general arrangement of this apparatus is

Figure No. 4.2.2.

General Arrangement of Subpress for Blank-holder Vibrations

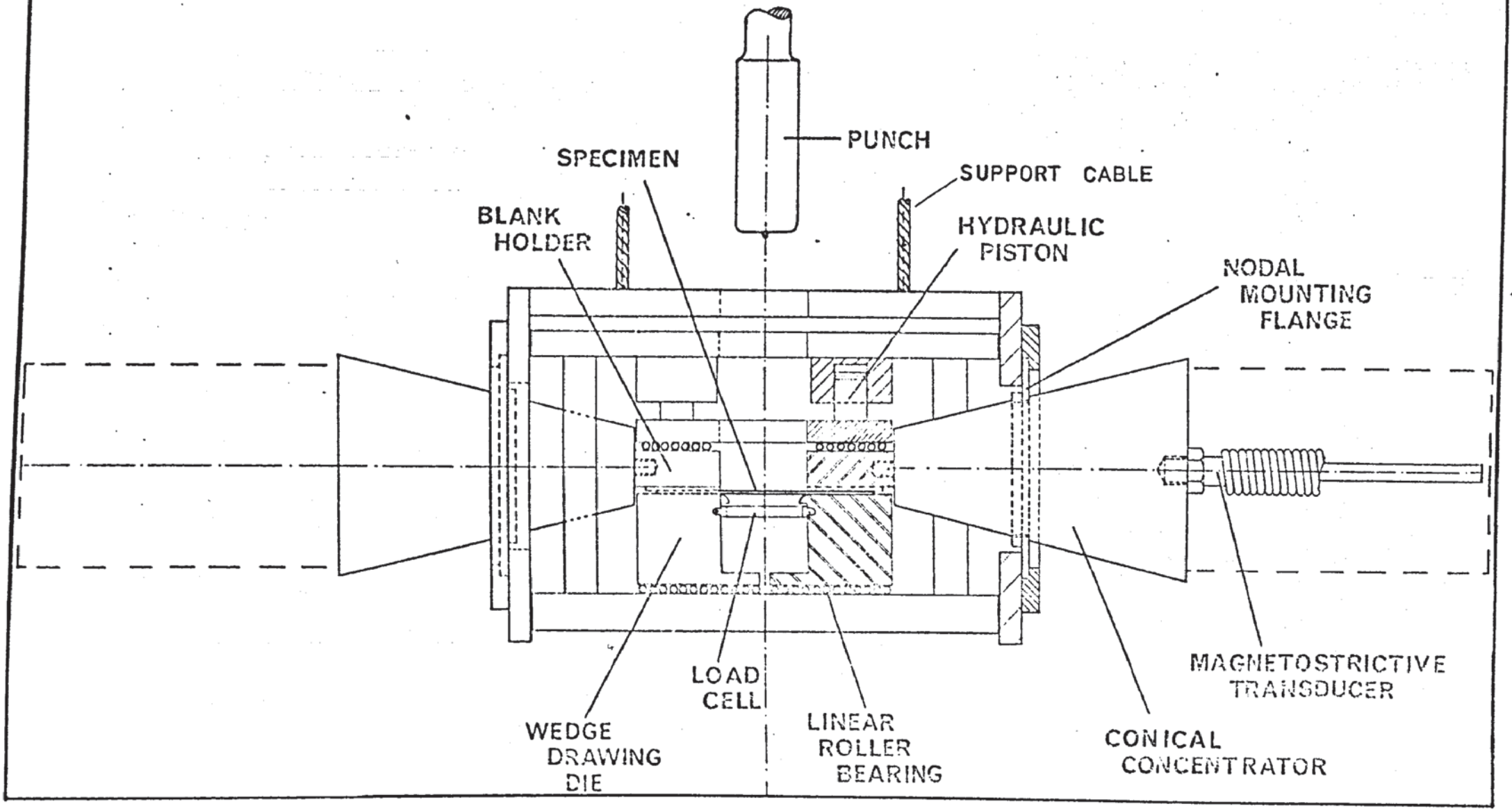

shown in Fig. 4.2.2.

The punch load cell positioned on the active mount originally used in the punch vibration work was also suitable for this application but it was necessary to manufacture a longer punch because the box section prevented the subpress being raised to its original position. A longer punch of the same thickness and radii as the tuned oscillatory punch was manufactured and fitted. The press was advanced until the punch passed between the blank-holders and the position of the punch clamping rings was altered until the punch and box section were coaxial and also positioned correctly angularly; feeler gauges, dial gauges and specially manufactured spacer pieces being used in these operations, which were similar to those described in Section 4.1.5. This completed the final assembly alignment and the only remaining items were the reconnection of the blank-holder pressure plate hydraulic system with subsequent bleeding and the placement in position of the two wedge dies pinned together with the load cell. These were free to move up on the linear roller-bearings and when in use the initial alignment was given by the male form of the blank-holders mating with the corresponding wedge shape on the top surface of the dies.

On attempting to position the blank-holder pressure plate on top of the blank-holders it was discovered that because the conical concentrators were positioned at a high level in the subpress they interfered with the pressure plate. The blank-holder pressure plate had to be ground down to enable it to fit properly, grinding being necessary because of the hardened condition of the pressure plate.

The complete assembly of the apparatus for blank-holder vibrations is shown in the frontispiece, whilst Figs. 4.2.3 and 4.2.4 show the wedge blank-holders and linear roller-bearings in more detail.

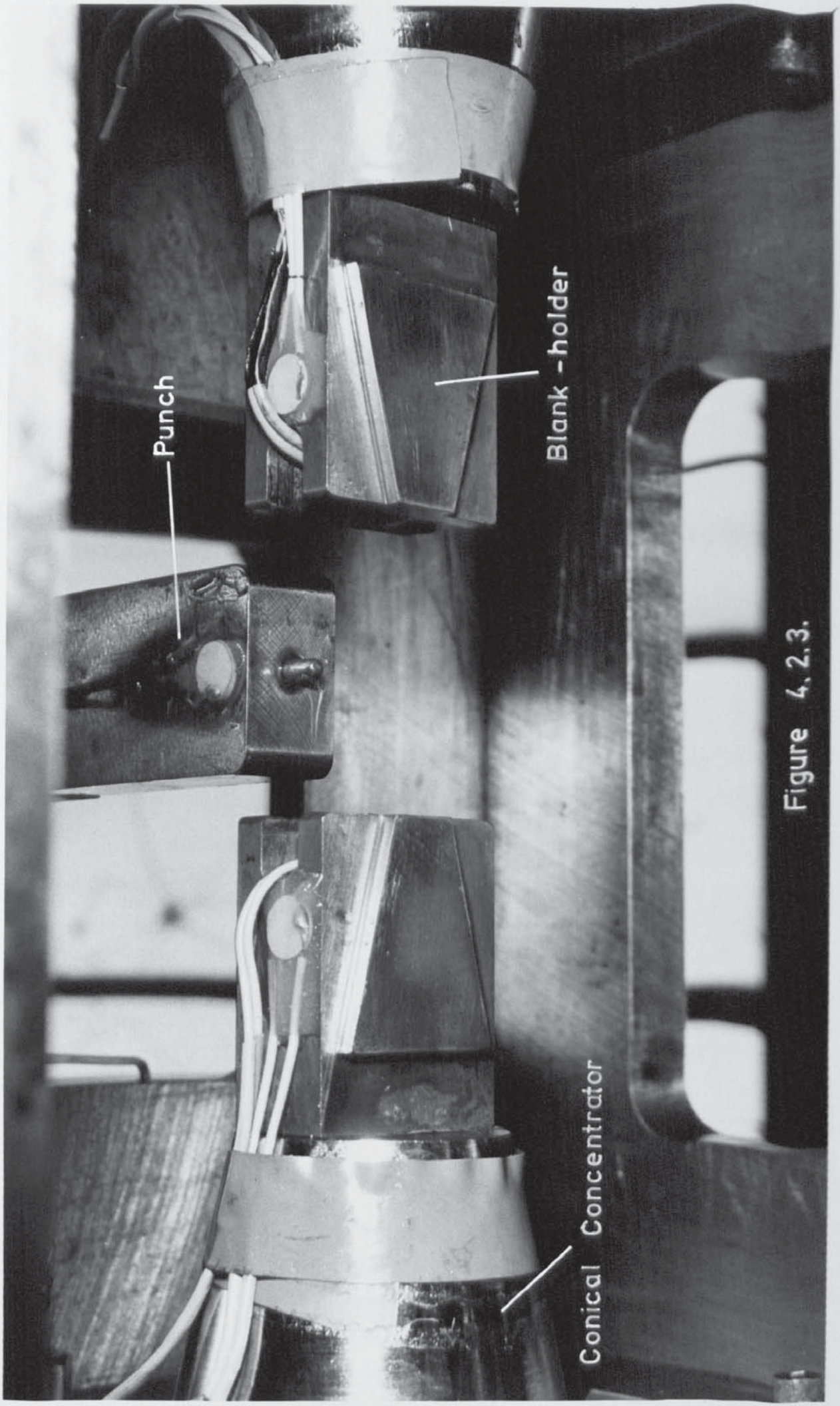

Figure 4.2.3.

Figure 4.2.4.

4.3. Draw Ironing Die Vibration Equipment.

4.3.1. General Description.

The subpress had originally been designed for the examination of die vibrations and therefore it was basically suitable for applying axial vibrations to wedge draw ironing die thus simulating the draw ironing process with radial vibrations applied to the die.

In order to obtain a range of ironing reductions it was necessary to vary the clearance between the punch and wedge dies. This could be achieved by either varying the die size or the punch size. Various die sizes could be effectively reproduced by adjusting the distance apart of the wedge dies, these being attached to the subpress base by slotted fillet plates. This system had the disadvantage that each die position would require a different size of wedge shaped specimens. The same size of wedge specimens could be used if the ironing reduction was varied by the use of different sized punches but this suffered from the disadvantage that these punches would not have the same characteristics.

To overcome these difficulties it was decided to construct an expanding punch so that various ironing reductions could be obtained using the same punch whilst at the same time having the advantage that the punch nose profile and surface finish were unchanged thereby eliminating a possible variable from the process.

The die profile of wedge dies that had been used previously was a simple 90 degree arc. This profile had been suitable for deep drawing with a positive clearance between punch and die because the drawn strip left the die radius before reaching the edge of the profile. Under conditions of draw ironing, however, contact would be all around the profile and this edge would be subject to wear. It was decided, therefore, to manufacture wedge dies with a different die profile.

Figure No. 4.3.1.

Detail of Expanding Draw-Ironing Punch

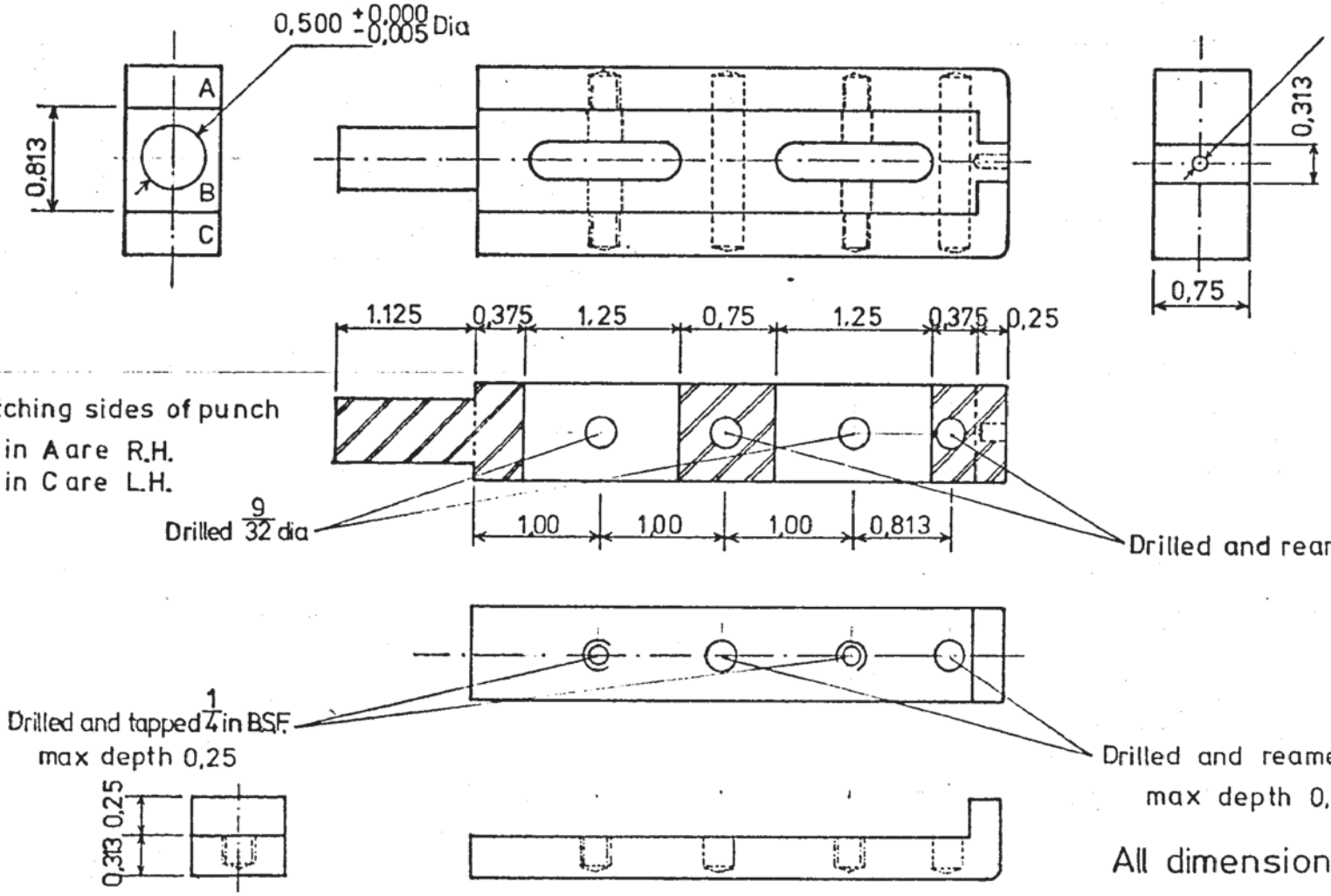

Note:-
A, C Matching sides of punch
Threads in A are R.H.
Threads in C are L.H.

Material:- En 30B

Heat Treatment:-
Heat 810-830°C,
Oil quench,
Temper at 200°C.

All dimensions in inches.

Tolerances ± 0,01 unless stated.

3rd Angle Projection.

4.3.2. Draw Ironing Punch.

The expanding punch was designed so that the width of the punch was easily adjusted and also there was no discontinuity of the punch surface that contacted the drawn part of the specimen.

The design chosen is shown in Fig. 4.3.1. The punch consisted of a central core with two side pieces which contained the punch nose profile and the working surface. The three pieces were held together by threaded tie rods, the guidance of the three parts being accomplished with dowel pins. The thickness of the punch was varied by the use of shims placed between the central core and side piece, both sides of the punch were shimmed in order to maintain the symmetry of the punch. One of the punch side pieces and the corresponding end of the threaded tie rods had left hand threads so that when the tie rods were rotated, by means of a central capstan wheel positioned in the central core, the two side pieces were pulled together onto the shims inserted between the central core and the side piece. These tie rods were only necessary to pinch the pieces together because during drawing the punch was held together by compressive stresses generated in the ironing of the specimen. The tensile stress in the drawn wall was transferred to the central core by means of the 'L' shape of the side piece adjacent to the punch nose.

The punch was manufactured from En 30B, its ability to harden without a severe quenching operation being a prime consideration because of the intricate nature of the sections being hardened. After manufacture it was found impossible to assemble the punch because the shallow holes in the side pieces had not been tapped perpendicular to the surface with the consequence that the threaded rods used to pull the side pieces together began to bind before the shims were clamped into position. Rather than remake the side pieces it was decided to ease the threads on the tapped rods from the 'full' thread which was originally intended to minimise any

Figure No 4.3.2

Draw Ironing Punch Loadcell Mounting Flange

Material:- En 24

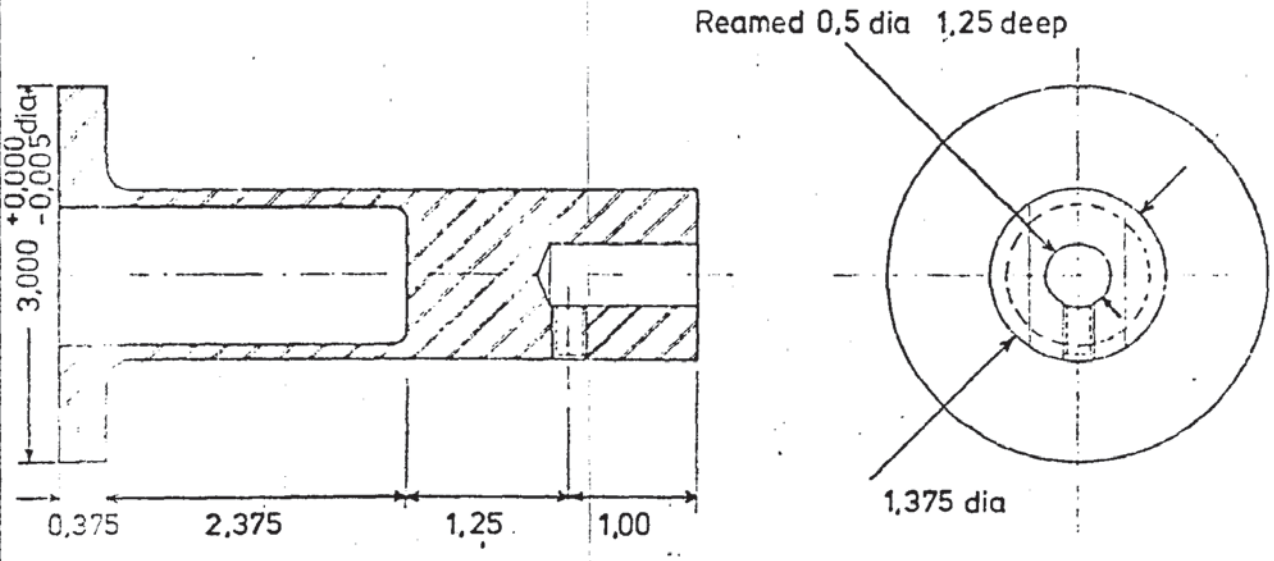

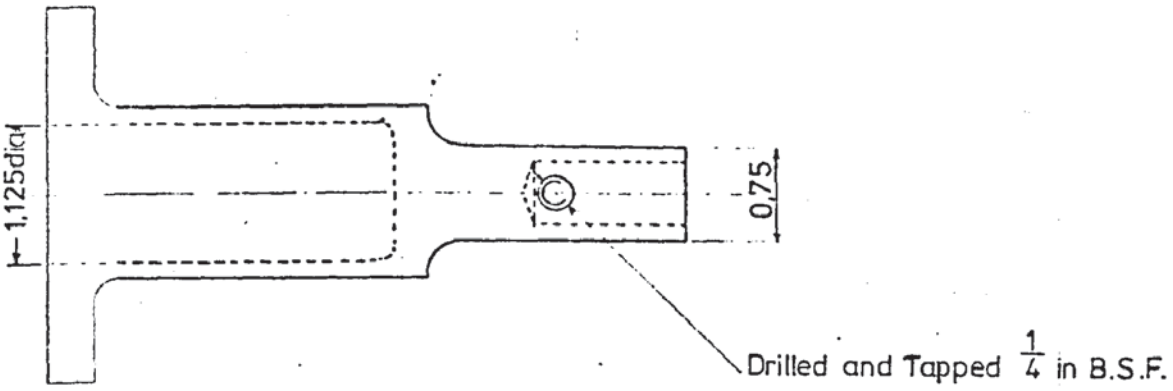

Blend radii 0,125

3rd Angle Projection

All Dimensions in inches

Tolerances ± 0,010 unless stated

Figure No. 4.3.3.

Wedge Die for Draw Ironing Die Vibrations

Material:- En 30B 2 Off
Heat Treatment:- Heat 810 - 830 °C,
Oil quench, Temper at 200 °C

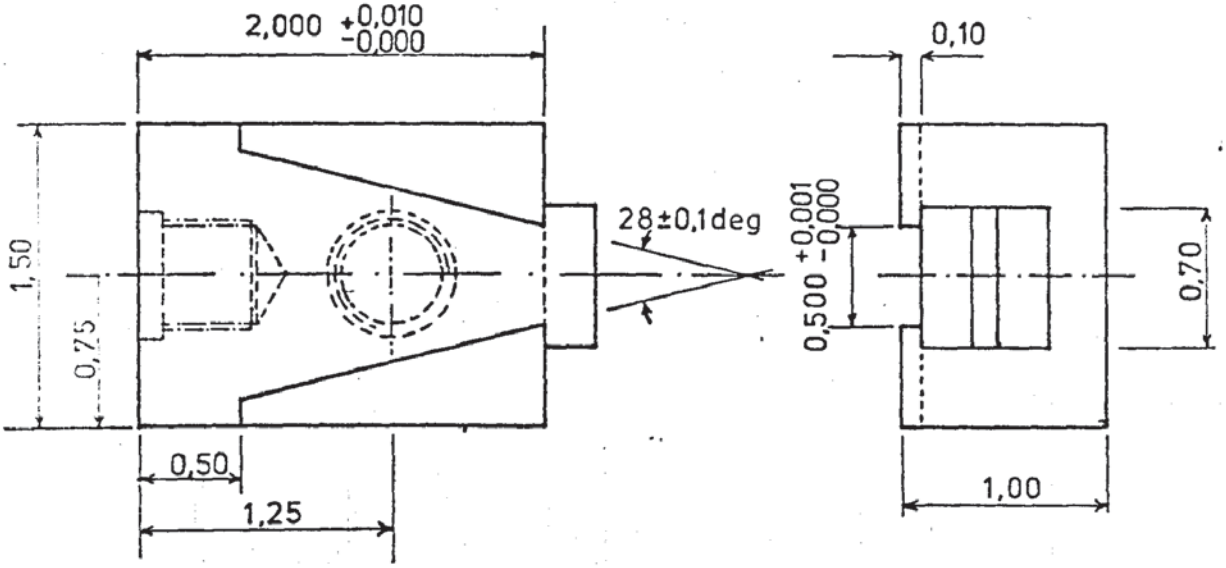

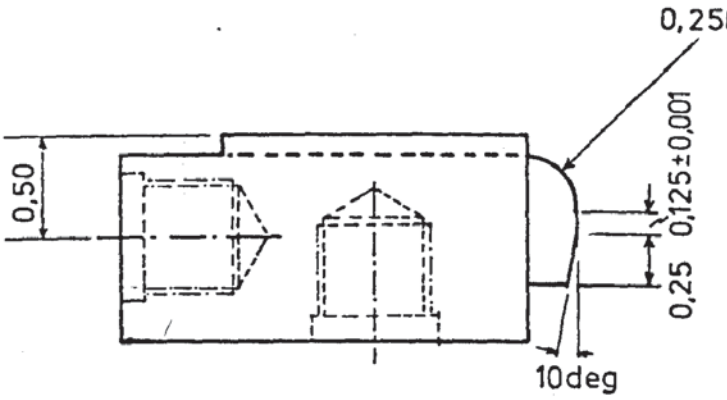

All Dimensions in inches

Tolerances ±0,010 unless stated

2 Holes drilled and tapped
$\frac{1}{2}$ in. B.S.F. × $\frac{9}{16}$ deep
counterbored $\frac{5}{8}$ × $\frac{1}{8}$ deep

3rd Angle Projection

slackening due to the vibration. This cutting of undersize threads was undertaken with some caution since it was desired only to remove sufficient material to enable the punch to be assembled.

After the punch had been assembled and the mating of the load bearing surfaces checked for contact the complete assembly was ground to size and the punch nose radii formed. Finally the working surfaces were given a light polish to remove the grinding marks.

A set of shims to enable various punch widths to be obtained was manufactured by constructing a simple jig to hold the shim stock rigid whilst it was drilled and milled to the correct shape to fit the punch.

The small cross section of the central core of the expanding punch prevented the use of a shank of the same type as the oscillatory punch. It was therefore necessary to design a load cell mounting flange for the punch. This mount which contained a thin tubular section to increase the strain for the strain-gauge load cell is shown in Fig. 4.3.2. The flange was manufactured from En 24, the end faces being ground after hardening to ensure that on assembly the punch would be perpendicular to the cross head of the testing machine.

4.3.3. Draw Ironing Dies.

New wedge dies were manufactured in accordance with Fig. 4.3.3. These dies were similar to those used previously, except that the die radius was extended to incorporate a parallel land suitable for the ironing process; the backing off of this land was gradual to prevent the appearance of transverse marks on the ironed strip.

In addition, tapped holes were provided on the underside of these dies in order that the concentrators could be attached at these points to vibrate the dies in a direction parallel to that of the punch travel for possible future applications.

The dies were manufactured of En 30B on account of its wear and fatigue resistance and were hand polished as previously described.

Figure No. 4.3.4.

General Arrangement of Subpress for Draw Ironing Die Vibrations

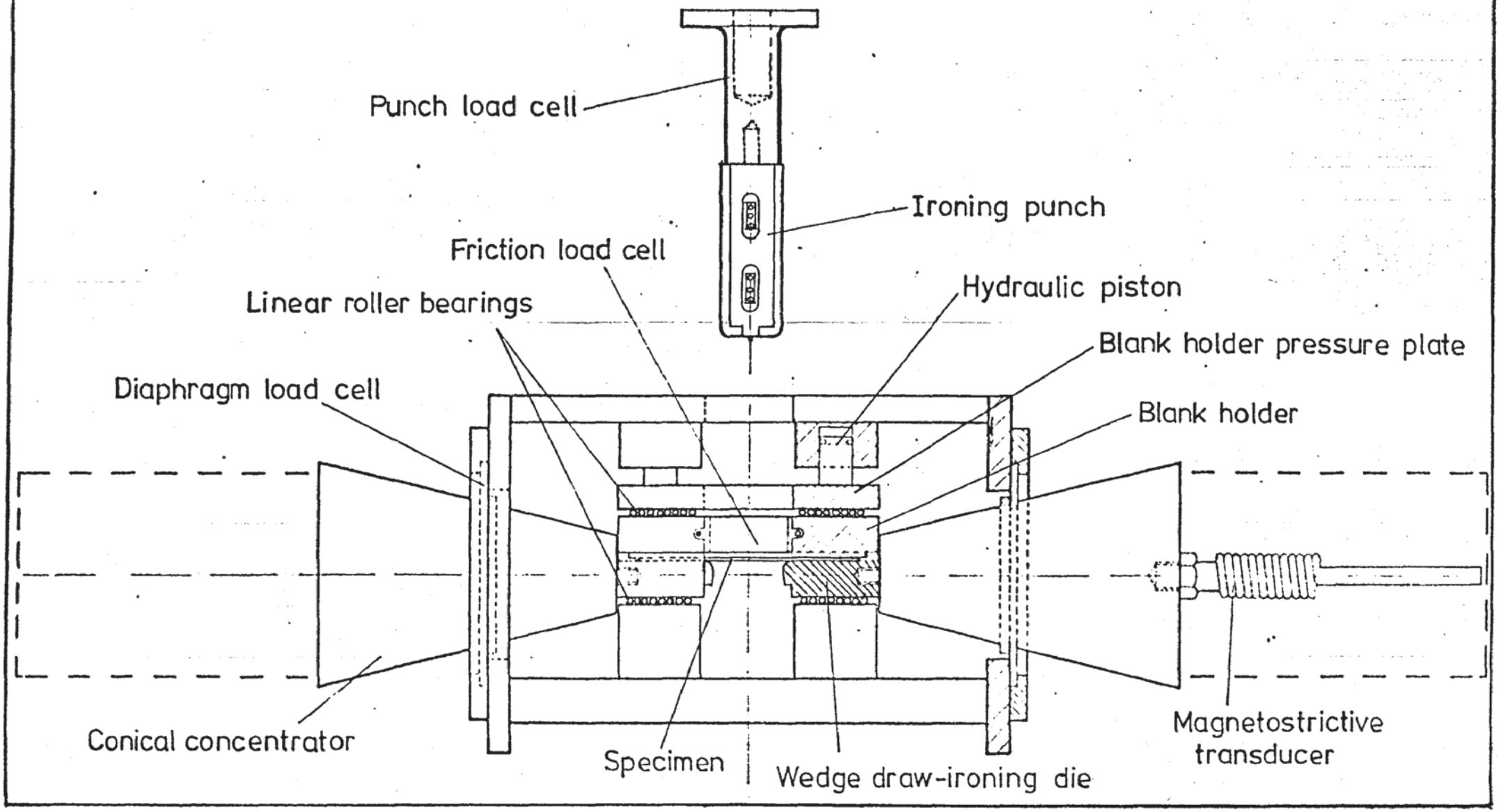

4.3.4. Assembly of Draw Ironing Equipment.

The wedge blank-holders were removed from the conical concentrators and repolished, these being replaced by the wedge draw ironing dies. The nodal flanges which had been removed for instrumentation were remounted on to the conical concentrators, care being taken to protect the instrumentation from damage. The flanges were fixed to the side plates of the subpress with the annular clamping rings and the completed sub-assemblies were positioned on the fillet plates attached to the subpress base.

The concentrators were rotated to align the wedge dies in the horizontal plane and the gap between the underside of the die and the top of the linear roller bearings was measured with feeler gauges. This gap was eliminated by packing the bearing support with shim steel. Previously this slight clearance was not important as the dies deflected under load until the linear bearings contacted the undersurface of the dies and prevented further deflection. This deflection distorted the nodal flange and because of the use of these flanges as load cells it was desired to eliminate this bending of the flange so that only the die separating force was recorded by the diaphragm load cell.

The new punch load cell mount was attached to the fixed crosshead of the hydraulic testing machine by means of a concentric clamping ring and the ironing punch was held in this mount by a grub screw bearing on the punch spigot. The general arrangement of this apparatus is shown in Fig. 4.3.4.

The alignment of this punch and the wedge dies was performed in an identical manner to that described in the punch vibrations section, Sections 4.1.4 and 4.1.5.

4.4. Blank-holder Swaging Equipment.

4.4.1. General Description.

Originally it was hoped that this work could have been carried out with vibrations of an ultrasonic frequency and for this purpose the wedge draw ironing dies, Section 4.3.3, were manufactured with threaded holes on their undersides to enable these dies to be attached to the conical concentrators. The distance between these attachment points when the dies were positioned correctly was, however, insufficient to allow the conical concentrators to be positioned below the subpress. This problem could be overcome by two methods. The first was to include a $\frac{1}{2}$-wave length section between the die and concentrator, this wave guide being curved to allow the dies to be positioned correctly without the concentrators touching each other.

The second method was to position the concentrators vertically and increase the length of the central section of the wedge specimen so that the dies could be placed farther apart.

The first method involved considerable manufacturing difficulties associated with the wave guides and the angled mounting for the nodal flanges, whilst the second method required a long subpress and a modified shape to the wedge specimen. Thus either of these options involved virtually rebuilding the apparatus completely and because of the time and cost involved it was not considered desirable to extend the wedge test analogue in this manner, at this time or during this project.

An alternative to this process which could be accomplished quite readily was the application of a low frequency oscillatory hydraulic pressure to the blank-holder hydraulic system, thereby obtaining an oscillatory force to the surface of the deforming specimen within the wedge dies.

Figure No 4.4.1.

Schematic of Low Frequency Blank-holder Swaging Equipment

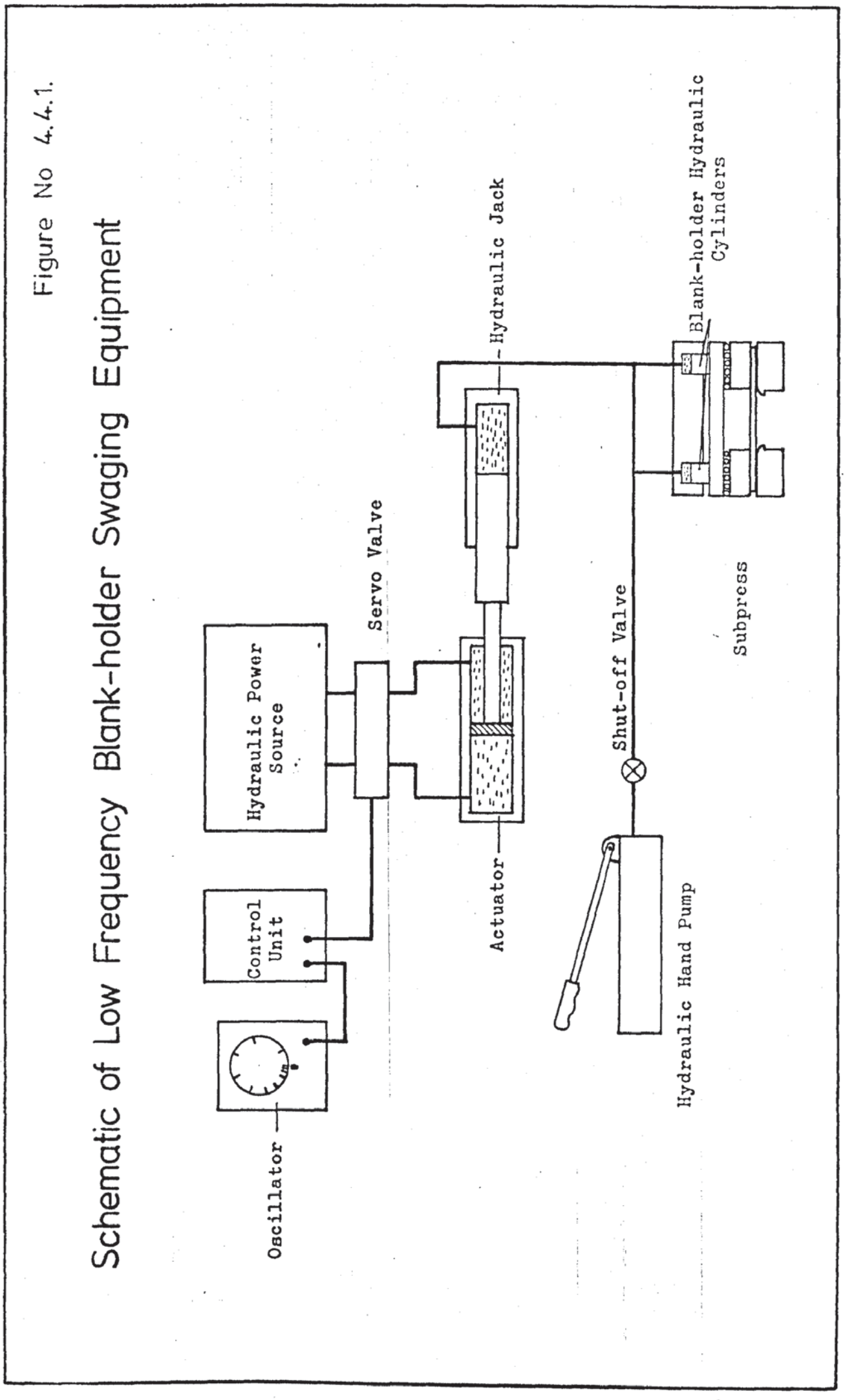

4.4.2. Hydraulic Oscillator Unit.

The hydraulic power supply, actuator and associated control system were available from a previous project examining low frequency vibrations. These components enabled the piston of the actuator, which was a double acting hydraulic cylinder, to be oscillated mechanically at any desired frequency within the range of the unit. The specification of these components can be found in Appendix A.6.

4.4.3. Blank-holder Hydraulic Circuit.

The mechanical oscillations produced by the actuator were converted to pressure variations by using the actuator piston rod to drive the ram of a hydraulic jack, thus producing an oscillatory hydraulic pressure.

The actuator piston rod and the hydraulic jack ram were linked mechanically and the bodies of these components were aligned and mounted on a base plate. A flexible hydraulic pipe was used to connect the jack to the hydraulic circuit of the subpress blank-holder. The blank-holder hydraulic circuit was disconnected from the variable pressure supply which had been used previously because this hydraulic pump maintained a constant pressure and therefore it would tend to smooth out any oscillatory pressure variation within the system.

An hydraulic hand pump was provided in the place of the motorised unit in order that an initial hydraulic pressure could be provided, onto which the oscillatory pressure could be superposed

A shut-off valve was also provided to enable the hand pump to be isolated from the system to prevent leakage of blank-holder pressure.

A schematic of the equipment used is shown in Figure 4.4.1.

5. INSTRUMENTATION AND CALIBRATION.

5.1. Punch Vibration Instrumentation and Calibration.

5.1.1. Punch Amplitude Measurement.

Oscillatory amplitude was to be measured by monitoring the output from a piezo-ceramic crystal. The piezo-ceramic crystal had fine wires soldered to its silvered faces and this assembly was insulated with a layer of epoxy resin. After curing, the crystal was bonded to the side of the punch located as close to the end as possible. In this position the alternating stress within the material resulting from the ultrasonic oscillations was of a very small magnitude (since the end corresponded to a stress node in the standing wave régime). It was reasonable, therefore, to assume that the only stress within the crystal was that caused by the acceleration of its own mass. The oscillatory motion closely resembled simple harmonic motion and therefore the acceleration was assumed proportional to its amplitude. Thus it was considered acceptable to use this type of sensor for recording the amplitude. The output from the piezo-ceramic crystal was wired to a high input-impedance meter, an a.c. milli-voltmeter, so that the signal from the crystal would not be distorted by the recording instruments. Within this meter the signal was rectified, after amplification, for display on the integral meter. This provided a convenient means of recording the signal on the ultra-violet recorder.

The output from the amplifier was, after rectification, disconnected from the internal moving-coil meter and wired to a jack plug let into the meter casing. Thus it was possible to display the input on the internal meter or, when the jack plug was in position, to take this output and use it, after a suitable damping resistor network, to drive an ultra-violet galvanometer. This latter procedure gave a permanent record of the amplitude variation during the drawing process.

4.1.2. Punch Amplitude Calibration.

The electrical signal obtained from the vibrating crystal had to be related to oscillatory amplitude. The amplitudes normally associated with ultrasonic frequencies are quite small, typically 0.0005 in. Some means of measuring this amplitude had therefore to be devised, an additional complication being that the signal for the crystal was only obtained during vibration, it not being possible to obtain the limits of the oscillatory motion statically. At this time, two methods of calibration were available. The first method relied upon the change in capacitance of the variable air gap between the punch surface and the capacitance probe obtained when the system was vibrating. This system, however, was not very reliable because of the effects of stray capacitance which affected the readings given. A second method which was more reliable but less convenient was an optical one. This involved the observation of a line scribed at right angles to the direction of the motion. When observed during the application of the high-frequency oscillations the line was moving too rapidly for the eye to distinguish. This resulted in the line appearing as a blur, the distance between the limits of the blur corresponding to the amplitude of the oscillations. The amplitude of the system was too small to observe with the naked eye so a travelling microscope was used. The microscope was a conventional one which was modified by the fitting of a different base which could be clamped to the subpress with the optical system in the correct position for viewing the end of the punch.

The normal rotatable objective lens carriage was removed and an adaptor holding a single objective was fitted to enable the microscope to fit into the available space. The magnification obtained with the microscope was checked by measuring the distance apart of the lines scribed on a diffraction grating. This distance was compared with the known ruling of the grating and it was found that

the actual and quoted magnification of the microscope were not the same. It was therefore necessary to calibrate the microscope separately. Prior to this calibration it was decided to calibrate the punch amplitude and retain these microscope settings whilst performing the secondary calibration.

To facilitate the punch calibration a small section of stainless steel was lapped and polished on a diamond lap to produce a highly reflective, scratch free surface. This piece of material was bonded to the side of the punch as near to the end as possible on the opposite face to the piezo-ceramic crystal. A number of very light scribe marks were made on this surface parallel to the end of the punch with a new scalpel blade. The finely scribed lines were viewed through the microscope and the line which gave the most uniform image was selected as the datum line. On switching on the ultrasonic power this line became a blur. The various objective lenses were tried in turn in order to achieve a compromise of large enough band-width, determined by magnification, and an acceptable standard of edge definition of the scribed line, which deteriorated with increasing magnification. Having selected the magnification, the band-width was measured by means of a traversable cross-wire in the focal plane of the eye-piece lens. This was traversed from one edge of the band to the other by turning the micrometer thimble.

Punch amplitude was set at various levels by adjustment of the 'Variac' variable transformer which controlled the output of the ultrasonic generator. For each of these individual settings the amplitude was measured by the travelling microscope and the signal corresponding to this amplitude level was recorded on the ultra-violet recorder. Thus these primary measurements were in units of length as indicated by the micrometer on the microscope eye-piece. The secondary calibration was carried out to determine the microscope magnification. This was achieved by bringing the lines of a

diffraction grating into focus, keeping the objective and eye-piece lenses in the position that were used during the punch calibration. The cross-wires within the eye-piece were positioned over one of the lines and the micrometer readings noted. A suitable number of lines were traversed before the micrometer was re-read and knowing the ruling of the grating a magnification factor of the microscope was determined. This factor was used to convert the oscillatory amplitude readings previously obtained into standard units. Thus, the punch oscillatory amplitude was determined under conditions of no loading.

On plotting these results the relationship, over the amplitude levels tested, was linear. It was noticed, however, that after prolonged vibration the crystal did heat up slightly and the output from the crystal in this condition no longer behaved linearly. The intermittent nature of the testing during deep drawing and the rapid recovery of initial properties on switching off the power were considered to minimise any non-linearity problems during the actual testing.

5.1.3. Die Amplitude Measurement.

The die amplitude was to be monitored in the same way as the punch amplitude, that was with the signal from the piezo-ceramic crystals. Both of the crystals which remained from the previous research project were damaged and were replaced after the wedge-dies had been reconditioned. These crystals were located on the end faces of the dies, beside the protruding die radii where the signal would only be dependent upon the oscillatory velocity as explained in the section on punch amplitude.

5.1.4. Die Amplitude Calibration.

The calibration of the die oscillatory amplitude was performed in an identical manner to that of the punch vibration except that the secondary determination of the microscope magnification was omitted because the objective lens and microscope settings were not varied from the positions determined during the calibration of the punch vibrations.

5.1.5. Punch Load Cell.

The punch load during the drawing operation was to be measured by a strain-gauge bridge and recorded on a channel of the ultra-violet recorder.

One of the problems in attaching strain-gauges to the surface of components in the ultrasonic system was that of over-heating caused by the vibration. Non-metallic materials were particularly prone to this phenomenon and so although strain gauge elements are metallic they are set in an epoxy resin backing and bonded to the surface with another epoxy resin. Consequently, they became very hot unless carefully located at a stress node.

It was possible to build into strain-gauge bridges temperature compensation and although this was the normal procedure it was considered good practice to try and avoid heating effects, if possible, rather than compensate for them after they occurred. For this reason it was considered undesirable to attach any strain-gauge bridge to the punch system itself and in this instance the mount system was used. In addition, the bridge was located at a stress node so that the alternating stress, and hence hysteresis loss, were at a minimum. This was advantageous both for fatigue and heating minimisation. It was only planned to measure the mean stress within the test piece mainly because of the difficulty in attributing any measurement of alternating stress to the alternating stress within the test piece itself. Obviously the alternating stress could be

measured on the strain-gauge bridge since it was only a matter of using recording equipment with a sufficient response. This, however, would be very difficult to relate to the stresses within the test piece with confidence. Attempts to record the stress situation within the test piece could be approached by direct measurements, by means of strain gauges attached to the test piece. Any testing of this nature is both costly and time consuming because the gauges can be used for only one drawing.

Punch load measurement was therefore recorded by means of a full bridge with temperature and bending compensation all built on to the tubular active mounting system. Protection of this once it had been built and wired up presented a slight problem. The normal method of protecting with layers of insulating tape was not acceptable because of heating which developed with the ultrasonic oscillations. The solution adopted was to use a very thin layer of polyurethane lacquer to provide protection against atmospheric corrosion and rely upon the remote location of the bridge to protect it from mechanical damage. The galvanometer signal from the strain-gauge bridge was taken through a suitable amplifier because of the low strain within the punch system. After amplification the signal went through a suitable damping network compatible with the galvanometer used in the ultra-violet recorder.

This complete bridge was built on the active mount before final assembly of the punch system described previously.

5.1.6. Punch Load Cell Calibration.

The punch load cell which was built into the mounting system was calibrated in-situ using a hydraulic jack and hand pump to apply a compressive load to the apparatus. The compressive load applied was indicated by means of a proving ring which was positioned between the punch and the jack. Spherical seatings were used at both ends of the proving ring to achieve pure axiality of loading. The cali-

bration was made after cycling the load cell a few times to ensure good reproducibility. The loading was taken to a value of 400 lbf in increments of 50 lbf. Unloading was done by similar decrements, the load being indicated by the deflection of the proving ring and measured by a dial gauge integral with the ring. The hydraulic testing machine was not used for the calibration because of the low loads that were required in comparison with the capacity of the press. This meant that the machine was set on the lowest scale setting of 5 tonf and even then 400 lbf was only a small proportion of this. Therefore, it was considered more accurate to use a proving ring for this calibration which had the added advantage that the loading was regulated by a hand pump. This method was easier than holding a constant load on the testing machine.

5.1.7. Friction Load Cell.

The friction load cell which was interposed between the two blank-holder blocks was also defective in that the strain-gauge bridge did not function. This was caused by several of the gauges on both the load cell and the dummy block of steel being damaged and there were no replacements of that particular type of gauge available.

A similar bridge was built with a small gauge that was available but on testing the completed assembly there was a serious problem of electrical interference on the galvanometer trace. This problem was not helped by the fact that a small gauge was being used with a consequential small level of bridge excitation that could safely be used. In order to obtain a higher signal-to-noise ratio a gauge larger than the original one was next tried. This was too large to bond to the edges of the load cell and so had to be bonded to the side faces. A full bridge was used to eliminate any possibility of pick-up between the active gauges and dummy block located in the vicinity of the load cell which may have occurred previously. This

use of these larger gauges with the consequential higher voltage that could be safely applied to the bridge did have a slightly beneficial effect upon the pick-up, but it was still too severe to enable any meaningful results to be obtained from the friction load cell. In addition, the load cell was now very sensitive to stresses other than direct tension and compression. This was not unexpected because some of the gauges were close to the corners of the load cell where the stress system was complex. Also it was noticed that the temperature compensation was not particularly good even with all the gauges of the full bridge built onto the load cell.

This was attributed to the fact that the side sections of the load cell were thin and connected together by other thin sections. The thermal capacity of these sections were small and so it was considered possible to have a temperature differential across the load cell. This destroyed the advantage of having the complete bridge on the load cell and, therefore, because of the very limited space available it was decided to revert back to the dummy-block system for the passive gauges, as shown in Fig. 5.1.1.

Smaller gauges, slightly larger than the original ones, were now available. By carefully trimming these gauges it was possible to fit them on to the edges of the sections, well away from the corners. The dummy-block was made an equal mass and of similar thickness to the sections of the load cell so that its thermal behaviour would be similar to that of the load cell. This load cell with the higher signal-to-noise ratio was better than the first one and so attempts were made to reduce the amount of interference obtained on the bridge signal.

It was determined that some of the pick-up was generated before the signal from the load cell was amplified to an acceptable level. In addition, the amplifier itself added more noise since, when the input was shorted out, the output still contained some interference. Little could be done about the noise generated within the amplifier

Figure No. 5.1.1.

The Friction Load Cell

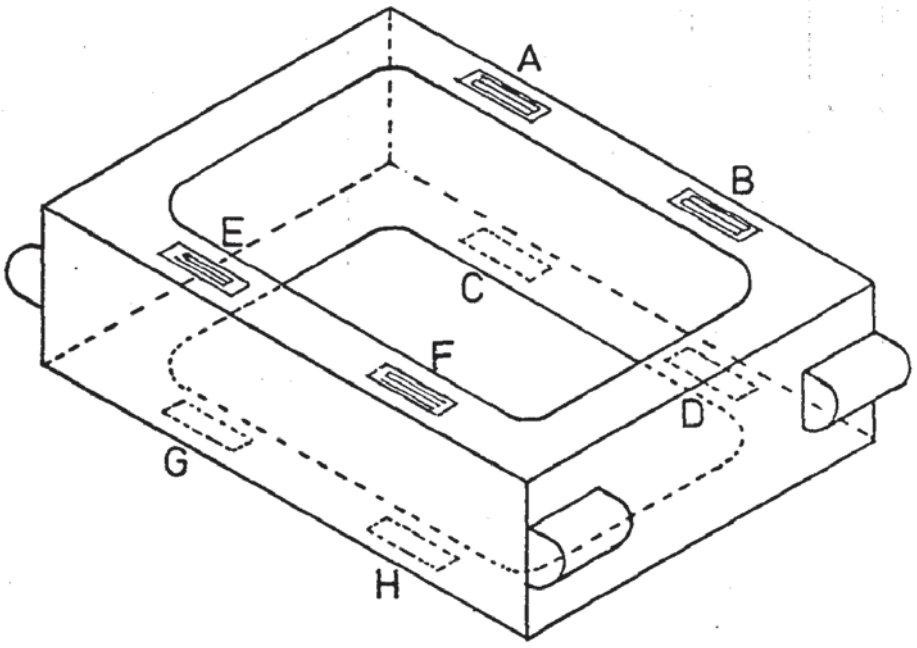

8 leads from loadcell

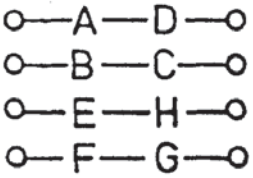

Gauge Arrangement

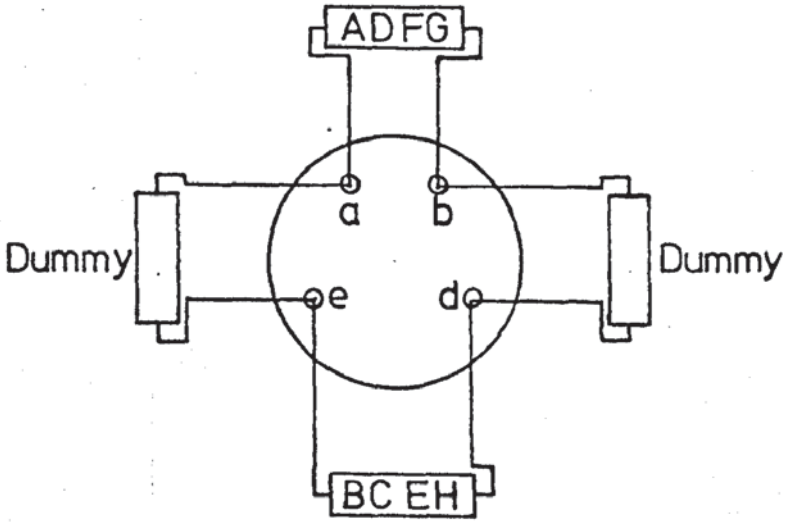

Bridge Connections

and so attempts to minimise the interference had to be directed towards minimising pick-up in the other elements of the system. All the leads from the load cell were screened, as were leads from the amplifier to the ultra-violet recorder. Various combinations of earthing the screens were used; sometimes all the leads, sometimes just the galvanometer signal. The facility was built into the wiring that all the screens could be brought to a common point of earthing. This was generally the amplifier although various earthing points were tried in practice. Sometimes earthing the screens made matters worse. This pick-up did seem to vary day-by-day and one of the most effective ways of dealing with this was to move the amplifier and control box around to an orientation that gave least interference. Obviously there were several sources of interference and several pick-up points but the elaborate precautions taken to prevent or eliminate the problem did not have much of an effect. From these series of tests undertaken the conclusion was reached that the fault lay mainly with a too small signal-to-noise ratio and some thought was given to the use of other devices for the load measurement, such as semi-conductor strain-gauges. These devices were considered but the disadvantages seemed to outweigh the advantages in this particular application.

The selection of galvanometer combined with the gain of the amplifier had some effect upon the magnitude of the recorded interference. A high-gain setting on the amplifier combined with a stiff galvanometer was preferable to a low-gain setting and a sensitive galvanometer. This was no doubt because the amplifier signal-to-noise ratio was at its best when the gain was set at its highest, since in this position the interference was proportionately less from the amplifier onwards. Obviously if the interference was on the signal before input to the amplifier the above reasoning would be no longer applicable.

A new amplifier, purpose built for strain-gauge amplification

was obtained, with better noise characteristics but this was found to give only a slight improvement. After this it was evident that measures to prevent this interference were only partially effective and recourse was made to filtering out the unwanted signal from the load cell signal. Previous tests had established that the frequency of the pick-up was approximately 100 Hz. A tunable filter was obtained and this was connected across the galvanometer terminals. The filter was adjusted until the optimum filtering of the interference was affected. The values of capacitance and resistance used at this setting were noted and a simple filter was constructed to this specification and substituted for the variable filter in the circuit. Obviously any sort of filter cannot distinguish between wanted and unwanted signals of the same frequency and so the use of a filter was only accepted after all other avenues had been exhausted. Fortunately the interference frequency, however, was well below the drawing frequency since measurements at the ultrasonic frequency could not be made using the ultra-violet recorder. The risk of filtering out useful information was therefore considered very unlikely.

These combined measures resulted in a signal from the friction load cell of an acceptable standard for the work envisaged.

3.1.8. Friction Load Cell Calibration.

Calibration was performed by applying a tensile load by means of a Denison dead-weight tester. The load cell was located within the jaws of this machine by specially made mild steel adaptors which enabled the wedge jaws to grip securely. Connection to the load cell was by means of polished dowel pins so that the loading was axial. After cycling a few times a calibration curve was plotted for both loading and unloading up to 60 lbf in increments of 5 lbf. Additionally, the load cell was fitted into the blank-holders and calibrated using the master load cell technique used by Young, in

which the master load cell was held down by the blank-holders in a similar manner to an actual specimen. The master load cell was shortened by means of a turnscrew such that the friction load cell was subject to a compressive force, applied in the same manner as the partly drawn specimens would load the blank-holders during the actual drawing process. The compressive force acting on the blank-holders was balanced by the tensile force on the master load cell. Thus by calibrating the master load cell in tension in the dead-weight tester it was possible to relate the compressive forces on the friction load cell to a reproducible standard. A comparison was made between the two methods of calibration and after making an allowance for friction between the blank-holders and the blank-holder pressure plate, the surfaces being separated by linear roller-bearings, there was no difference to the final result whichever method of calibration was used. The allowance for friction was made by recording the force required to move the blank-holder and die in the direction of drawing against the two sets of linear roller-bearings, one on the top surface of the blank-holder, the other on the bottom surface of the die (the die was separated from the conical concentrator). One half of this frictional force could then be attributed to each set of rollers and could be used to modify the friction load cell calibration curve.

This dual approach to calibration was to determine a reliable method other than the in-situ calibration used by Young. This was necessary because the other areas of investigation planned required a similar sort of calibration. The increased complexity of the apparatus would preclude any attempt to calibrate in-situ because of the lack of access to the subpress. On examination of these two methods the dead-weight tester calibration with an allowance for the friction introduced by the roller-bearings proved to be as reliable as the in-situ method. Having established the reliability of the calibration using the dead-weight tester this method was used

in recalibrations that were performed periodically.

5.1.9. Punch Velocity and Punch Displacement.

In order to obtain a relationship between oscillatory velocity and drawing velocity it was necessary to record the punch velocity. At this time, a direct velocity measuring device was not available. A displacement potentiometer which had been used by Young for displacement measurements was available and it was decided to use this for both displacement and velocity measurements, the velocity being deduced from the gradient of the displacement/time record which was produced upon the ultra-violet recorder. In order to make this conversion simply it became a requirement that the displacement transducer should give a linear output with displacement. The method used previously of applying a constant voltage to the potentiometer coil and applying the varying voltage obtained at the potentiometer slide to an ultra-violet recorder galvanometer did not give the potentiometer a linear output. This, after some consideration, was seen to be due to the fact that the galvanometer was taking a current to operate it and was thus disturbing the linearity of the potentiometer.

The requirement was for a very high input-impedance into which the signal from the potentiometer could be taken so that there would be no current flow to disturb the linearity. The signal was, therefore, connected to an oscilloscope, which had the required input-impedance and the signal to the ultra-violet galvanometer was taken from the output of the internal amplifier of the oscilloscope. In this way a linear displacement record was obtained on the ultra-violet recorder.

5.1.10. Displacement Transducer Calibration.

The displacement transducer was calibrated by constructing a simple clamp to hold the body of the transducer whilst the inner slider was indexed along by contact with a vernier height gauge so that the displacements given to the slider could be measured accurately. This calibration was continued over the complete length of travel of the slider because in the drawing operation the majority of this travel was going to be used.

5.1.11. Blank-holder Load Cell.

The blank-holder loads were measured by strain-gauge bridges built onto the pistons of the hydraulic cylinders which applied the blank-holder pressure. These had been used in the previous project but one of the strain-gauge bridges had been damaged. The lead wires had become detached and since the bridges were protected with a potting compound it was necessary to completely remove and rebuild the strain-gauge bridge using a full 4-gauge bridge configuration.

5.1.12. Blank-holder Load Cell Calibration.

The blank-holder cells were calibrated when they were removed from the subpress during the rebuilding. They were loaded in compression using a hydraulic jack and a proving ring to indicate the load on the blank-holder. The signal from the strain-gauge bridge was sufficient to drive an ultra-violet galvanometer directly without amplification and each blank-holder was calibrated by loading in 50 lbf increments up to a maximum load of 1000 lbf and unloading in similar decrements.

5.2. Blank-holder Vibration Instrumentation and Calibration.

5.2.1. Blank-holder Amplitude Measurement.

Blank-holder oscillatory amplitude was recorded by monitoring the signal from a piezo-ceramic crystal bonded to the end of each blank-holder. Two crystals were bonded to each blank-holder, one to the end face and one on the side, because, as a result of past experience it had been found that these crystals were susceptible to breakdown due to fatigue of the fine lead wires. This problem was alleviated, to some extent, by supporting the metal foil, which was connected to each face of the crystal, in close fitting P.V.C. sleeving and embedding this sleeving in epoxy resin. This method had the advantage that if the lead wires did fracture it was usually close to the point where the encapsulation finished so it was possible to carefully strip away the epoxy resin and remake the connection. The crystals at the end face of the blank-holders were subject to only the accelerative forces of the simple harmonic motion, whilst those on the side were subject to the additional oscillatory stress transmitted from the blank-holder but, since the latter were close to the end the effect was considered and, subsequently, shown to be negligible.

The output from each crystal during oscillation was an alternating charge. In order to record this signal it was necessary to amplify it with an instrument with a high input-impedance. Two valve-voltmeters were obtained, one for each blank-holder. The output from each instrument was displayed on a conventional moving-coil meter. The voltmeters were modified slightly by inserting a change-over circuit into the instrument. This circuit was to be operated remotely with a micro-switch controlled by the movement of the hydraulic press. This switch transferred the output from the internal meter to a suitable matching circuit for an ultra-violet galvanometer to enable a permanent record of the oscillatory amplitude during the draw to be made.

5.2.2. Blank-holder Amplitude Calibration.

The crystals gave an output proportional to amplitude and this was calibrated using a 'Distec' displacement sensor. This device was a non-contact sensor operating on the eddy-current loss principle, which gave a voltage signal, directly proportional to the displacement of the sensor from the end of the blank-holder. The sensor position from the end face of the blank-holder was adjusted until the reference voltage output was obtained. This ensured that the datum point was within the linear output range of the sensor. When switching on the ultrasonic generator an alternating voltage was obtained. An oscilloscope was used to display this signal and peak-to-peak measurements could be related to the actual displacement by means of a calibration curve plotted using static displacements of the sensor measured by the appropriate mechanical device for the range being considered.

In this application the static calibration of the 'Distec' sensor was obtained by attaching the sensor to the head of a vernier height gauge and measuring the voltage change as the sensor distance from a block of the die steel was varied.

5.2.3. Punch Load Cell.

The punch load was to be measured using the same load cell as had been used for the punch vibrations. After checking the load cell for damage it was recalibrated using the hydraulic jack and proving ring as previously described in section 5.1.6. A number of loading and unloading cycles were undertaken with the readings plotted graphically and compared with the earlier calibrations made when punch vibrations were being investigated. Good agreement was obtained, long term drift was insignificant and the hysteresis present in the system was also negligible, both these factors indicating the strain gauge installation to be in good condition.

5.2.4. Die Separating Force Load Cell.

The two wedge dies were pinned together by the die separation force load cell. This load cell was constructed from En 30B a high-nickel die steel and it was made very slender to increase the strains within the measuring arms. The strains were to be measured by means of a strain gauge bridge bonded to the two tension members of the load cell. A half-bridge with four gauges was used on the load cell which had bending compensation in a vertical plane built into it by wiring gauges attached to the top and bottom surfaces of the load cell in series in one arm of the bridge. Bending compensation in the horizontal plane was achieved by wiring gauges of opposite tension members of the load cell into the same arm of the bridge.

A considerable amount of trouble was experienced when the load cell was being built, due to faulty bonding of the gauges. The first adhesive, a polyester recommended for the gauges proved to be very brittle and the gauges lifted as the tape used to hold them in position during bonding was removed. A different adhesive was tried, an epoxy resin, but this failed to harden despite repeated attempts. It was finally concluded, however, that the mixing instructions supplied with the adhesive were in error after a number of test mixes were prepared, each with a different proportion of hardener and adhesive ranging from the 10 per cent hardener given in the instructions to a 50 per cent hardener. It was found that only the mixes containing almost equal amounts of adhesive and hardener cured under the recommended conditions, the other mixtures being much more difficult to cure, higher temperatures than specified being required. The mix containing the 'recommended' proportions never cured. The adhesive finally used was 'Araldite' epoxy resin which proved to be very reliable.

Temperature compensation was obtained by mounting the dummy gauges upon a block of similar thermal capacity as the load cell and locating this dummy block in the immediate vicinity of the load cell.

The conflicting requirements of thick sections for greatest bending resistance and thin sections for maximum strain resulted in the stress levels within the load cell being of quite small magnitude and hence the signal produced from the load cell needed amplification. Unfortunately, the use of an amplifier aggravated the problem of the electrical noise and interference on the signal coming from the bridge. This problem was recurrent throughout the test programme and was caused by the signal-to-noise ratio being small. This was fundamental to the strain gauge installation and the only improvement that could be made was by increasing the bridge supply voltage. There is a limit, however, to the amount by which it can be raised before detrimental effects are noticed; these usually appear as a general deterioration of the stability of the system rather than a catastrophic failure.

A combination of increased supply voltage, screening and positioning of the lead wires and finally small capacitors across the terminals of the ultra-violet galvanometer were used to obtain an acceptable signal from the load cell.

5.2.5. Die Separating Force Load Cell Calibration.

This load cell was calibrated in tension using a 'Denison' dead weight tester and two adaptors pivoted to the ends of the load cell and with parallel ends for gripping in the wedge jaws of the tester. Calibration consisted of cycling the load cell a few times and recording the galvanometer deflection for various loads both during the loading and unloading cycles. Two sets of calibrations were obtained initially by varying the amplifier gain to cover the range of loads anticipated. The calibration curves were retained in order to enable periodic checks to be made on the condition of the installation by comparison of the calibration curves.

5.2.6. Punch Displacement Transducer.

The punch displacement was determined by the same linear potentiometer which had been used previously. The longer punch entailed a lower drawing position and the adjustable stop was therefore repositioned. The transducer was recalibrated in accordance with section 5.1.10.

5.2.7. Punch Velocity Transducer.

Punch velocity measurement was obtained by using a linear differential transformer. The body was attached to the subpress mount and the magnetic core was attached to a long rod connected to the fixed cross-slide, the length being arranged so that in the mid-draw position the magnetic core was in the middle of the shielded coils.

The differential transformer produced a voltage proportional to the linear velocity of the core within the coils which was monitored using a valve-voltmeter with the meter circuit modified to obtain an output for an ultra-violet galvanometer. By selecting the appropriate range the output of the meter could be matched to the output of the transducer. In addition, when the press was lightly loaded and moving slowly there was a pulsating load caused by the hydraulic pump. This pulsating was detected by the transducer but when using the valve-voltmeter the pulsations were smoothed out, thus preventing the galvanometer trace from swamping the ultra-violet chart.

This transducer was calibrated indirectly by running the press at various drawing speeds whilst the output from the velocity transducer was recorded on the ultra-violet chart along with the punch displacement signal.

The punch velocity was determined from the punch displacement and the timing marks on the ultra-violet chart for each of the drawing speeds selected.

5.2.8. Blank-holder Load Cell.

The blank-holder load cells used previously for the punch vibration section were recalibrated before being re-assembled into the subpress. This recalibration was in accordance with the procedure described in section 5.1.12.

5.2.9. Press Operated Controls.

When the main ram of the press was raised to the position where drawing would normally commence a microswitch was closed which in turn operated the relay within the ultrasonic generator which applied the high voltage alternating current to the magneto-strictive transducer coils. Simultaneously, two more microswitches were operated to transfer the output of the left and right hand blank-holder piezo-ceramic crystals from the meters of the valve-voltmeters to the ultra-violet galvanometers. One of the contactors of the ultrasonic generator relay carried mains voltage which was used to energise another relay located remotely from the generator. This second relay operated the motor of the ultra-violet recorder so that the paper drive of the recorder was started. A second relay was used because it was considered undesirable to have the controlling leads of the recorder within the cabinet of the generator because of the possibility of pick-up which in turn could be transferred on to the galvanometer traces. Having switched on the ultrasonic generator and the ultra-violet recorder the microswitches were kept closed by the use of a spring loaded plunger which had sufficient travel to accommodate the movement of the ram during the drawing process. As an additional safeguard, as the press reached the end of the draw, the ultrasonic vibrations were switched off. This on-off switch was operated by the opposite end of the plunger of the spring loaded device. In addition, the lever arm of the switch was on a flexible coupling so that once it had been operated further travel of the plunger forced the lever out of the way thus preventing damage as the

press continued upwards to the end of its stroke. The length of this plunger was adjustable by means of a hollow sleeve to accommodate the shorter press travel required when drawing at the lower-ratios.

The hydraulic pump of the testing machine was arranged to stop by the fitting of an adjustable trip to operate the limit-switch on the press. This limit-switch was operated just before the punch came into contact with the base of the dies, a suitable clearance being allowed for the specimen interposed between the two. As the hydraulic ram returned and approached its lowest position cords attached to the lever arms of the switches became taut and reset the switches to the closed position just as the ram bottomed, in readiness for the next drawing cycle.

5.3. Draw Ironing Die Vibration Instrumentation and Calibration.

5.3.1. Draw Ironing Die Amplitude Measurement.

The draw ironing wedge dies were prepared for amplitude measurement before assembly onto the conical concentrators by bonding piezo-ceramic crystals to the surface of the dies. This was accomplished in a manner similar to that employed for the blank-holders as described in Section 5.2.1. Two crystals were again used and particular attention was paid to the bonding of the lead wires from the crystals.

5.3.2. Draw Ironing Die Amplitude Calibration.

The oscillatory amplitude of the dies was calibrated by the use of a 'Distec' displacement sensor as described in Section 5.2.2. The output from the piezo-ceramic crystals was proportional to the oscillatory amplitude at low levels of excitation but at the higher levels the output levelled off as described in Section 5.1.2. This was not considered to be a problem because the amplitude under drawing conditions would not reach the maximum amplitudes obtained when calibrating the unloaded dies.

5.3.3. Draw Ironing Punch Load Cell.

The punch load cell was built onto the mounting flange in the centre of the uniform tubular wall section. A conventional strain-gauge bridge was built using eight gauges positioned equally around the periphery. Diametrically opposed gauges were connected into the same arm of the bridge so as to give bending compensation, these two pairs of axially aligned gauges providing the majority of the resistance change, the four circumferentially aligned gauges compensating for temperature variations and also increasing the bridge sensitivity as a result of the Poisson effect.

The gauges were bonded with an epoxy resin adhesive and, after wiring, environmental protection for the gauges was provided with a

polyurethane lacquer.

Mechanical protection was afforded by wrapping the complete installation with P.V.C. adhesive tape.

5.3.4. Ironing Punch Load Cell Calibration.

The output from the punch load cell had to be amplified in order to obtain a suitable signal for the ultra-violet galvanometer. The load cell was calibrated when positioned on the cross head of the testing machine using the hydraulic jack and proving ring method described in Section 5.1.6.

5.3.5. Die Separating Force Diaphragm Load Cell.

In order to measure the die separating force on the oscillatory draw ironing dies it was decided to make use of the deflection of the diaphragm plates which, when assembled, formed the nodal flanges of the conical concentrators. In order to build a full strain-gauge bridge on each of the diaphragm plates it was necessary to attach strain-gauges to both sides of these plates. Four equi-spaced gauges were attached to each side, and these were aligned in a radial direction. Difficulty was experienced with the bonding of these strain-gauges to the diaphragm plates which was originally considered to be caused by the chromium plating on the surface but after removal of the chrome at the gauge positions there was still a poor bond between the gauge and flange. This problem had been experienced previously with the friction load cell, Section 5.1.7, when using polyester adhesives. The reasons for poor bonding were not ascertained since instructions regarding mixing and application were closely followed and different batches of adhesive and hardener were used on these occasions. These bonding failures necessitated the rebuilding of the bridge and finally an epoxy resin adhesive was used which proved successful.

The spacing of the gauges around the flange and on both sides of it involved the use of fairly long interconnecting wires. To avoid any temperature effects with these long wires they were all cut to the same length before wiring commenced. A groove was machined in the flange clamping ring to enable the wires to pass to the other side of the flange when this was clamped in position.

The strain-gauge bridge was protected from the atmosphere by coats of polyurethane lacquer but mechanical protection was mainly provided by the remote location since there was insufficient space for any protective layer to be applied to the gauges. This proved satisfactory since the major danger of damage occurred during the assembly of the equipment.

5.3.6. Diaphragm Load Cell Calibration.

The load cells were originally calibrated with the flanges clamped around their periphery by the mounting rings. The flange was loaded centrally through a stepped plug which was placed into the central hole in the flange. This plug was a close fit in the hole and its outer diameter was the same as that of the locking ring used when the concentrator was assembled onto the flange. Calibration was performed using the hydraulic jack and proving ring as described previously.

On comparing the deflections obtained with some preliminary test results it was realised that there was no edge constraint provided by the central plug and therefore the deflections obtained were larger than would be obtained were the flange assembled in the subpress.

This problem was overcome by calibrating the completed assembly in position on the subpress. By removing one complete concentrator assembly sufficient space was created to position the hydraulic jack and proving ring horizontally to apply the load to the end of the wedge die, using spherical seatings at each end of the proving ring.

In addition, the studs holding the diaphragm plate in position were tightened to a predetermined torque as was the locking ring on the conical concentrator in order to apply a uniform and reproducible pressure to the inner and outer edges of both diaphragm plates.

The load cell was calibrated by loading and unloading incrementally up to the maximum load and observing the galvanometer deflections. These diaphragm load cells did not give an output which was proportional to the deflection and in addition, on unloading, the values of strain were higher than the ones recorded on loading. It was considered that this hysterisis was introduced by the movement of the ends of the plates under the clamping pressure.

When the diaphragm was loaded its deflection was reduced from that of a 'free end' system by frictional constraint at each edge. On unloading the diaphragm retained its loaded position until the applied load had fallen sufficiently for the force differential to be great enough for the plate to move once more against the frictional constraint. Whilst this situation was not ideal it was considered reasonable to accept this load cell characteristic provided it was reproducible over many cycles and between recalibrations. The calibration was performed a number of times and the load cells were left for a few days and recalibrated. On comparing the calibrations, however, no changes were detected. These results were therefore accepted and two values of load for each galvanometer deflection were provided, the correct value to use being determined by the overall trend of the die separation force trace, a rising trace using a 'loading' value and vice versa.

5.3.7. Friction Load Cell.

The load cell which had been used for the recording of the blankholder frictional force in the punch vibrations series was available for further use once it had been recalibrated in accordance with Section 5.1.8.

5.4. Blank-holder Swaging Instrumentation and Calibration.

5.4.1. General Description.

The instrumentation required on the subpress was that used in the previous sections although with the absence of any ultrasonic vibrations the instrumentation problems were simplified. No attempt was made to monitor the blank-holder amplitude but the oscillatory force was recorded by the blank-holder load cells, the galvanometers used having sufficient frequency response to enable the oscillatory load to be displayed upon the ultra-violet trace.

The control unit for the hydraulic pressure supply was connected to the servo-valves which controlled the oil flow to the actuator. The oscillatory frequency for this unit was derived from an external oscillator. A small transistorised oscillator was available and this was used to set the oscillatory frequency, its output being checked with the frequency counter previously used on the ultrasonic generator.

6. TEST PROCEDURE.

6.1. Punch Vibration Test Procedure.

6.1.1. General Testing Procedure.

The testing procedure adopted was to examine a series of draw-ratios for the effect of punch oscillatory amplitude on the punch load and limiting draw-ratio.

A supply of specimens was prepared from one sheet of 0.028 in. thick, commercially pure aluminium, the longitudinal axis of each specimen being orientated in the rolling direction. The preparation of these specimens is described in Appendix A.2. The lubrication used throughout this series of tests was Shell 'Macoma 45', a high viscosity mineral oil with 'Extreme Pressure' additives.

This oil gave a uniform lubrication film when the specimens were immersed in it and when the excess oil had been allowed to drain away.

The draw-ratio under test was selected and the blank-holder pressure adjusted so as to give an initial compressive stress on the undeformed blank of 450 $lbf.in^{-2}$. Details of the selection of blank-holder pressure are to be found in Appendix A.4. The lubricated specimen was placed into the wedge dies and the wedge blank-holders, separated by the friction load cell, were placed on top of the specimen, the male form of the blank-holders locating in the female form of the dies. The blank-holder pressure plate was replaced on top of the blank-holders and locked into place by inserting the dowel pins through the corners of the subpress sides into the plate housing the blank-holder hydraulic pistons. The load range on the 'Avery' Hydraulic Testing Machine was set to its lowest scale of 5 tonf. maximum and the modified by-pass valve opened to bring the subpress up to the punch. On reaching this position the by-pass valve was closed. The load cells were re-zeroed and the oscillatory amplitude required was selected by setting the 'Variac' of the ultrasonic generator. The ultra-violet recorder was started followed by the

Figure No. 6.1.1.

Punch Vibrations U-V Trace

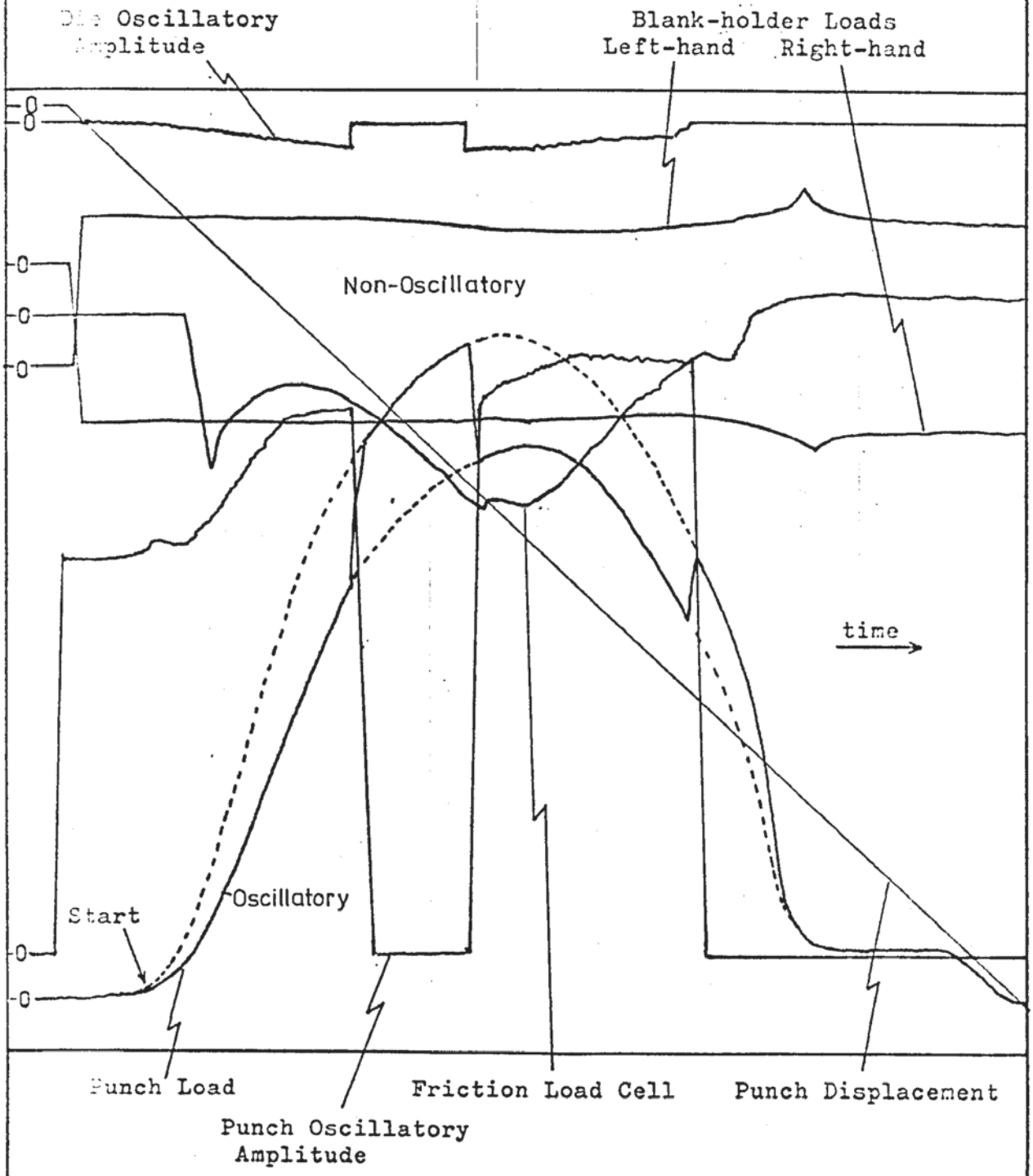

closing of the spool-valve to apply the hydraulic pressure to the blank-holders. Simultaneously the by-pass valve was opened to the desired draw velocity setting and the subpress moved towards the punch. Before drawing began the ultrasonic power to the punch was switched on. The ultrasonic system was tuned manually before the drawing process began, resonance of the punch system was detected by observing the output from the piezo-ceramic crystal displayed on an oscilloscope.

During the draw, all the data were recorded on the ultra-violet recorder with the exception of the oscillatory frequency, which was displayed on a digital counter. On completion of the draw the specimen was removed and a serial number was allotted to both the specimen and the ultra-violet trace so that both would be easily associated for future reference. A typical ultra-violet chart which shows the effect of the punch vibrations on the recorded parameters during the drawing operation is reproduced in Fig. 6.1.1.

The procedure for testing a particular draw-ratio involved tests at zero amplitude and at a number of different oscillatory amplitudes up to the maximum amplitude available, which was obtained when the 'Variac' was at its maximum setting.

The tooling was wiped to remove excess oil after each specimen had been drawn in order to maintain the consistency of lubrication which had been achieved by the controlled method of lubrication.

On completion of the testing of a particular draw-ratio the blank-holder oil pressure was re-adjusted to maintain the standard initial pressure on the undeformed blank. A periodic re-adjustment of the oil pressure during prolonged testing periods was required due to the drop in pressure within the system as the oil warmed up and as a consequence became thinner.

The above procedure was applied throughout the drawing of the complete range of draw-ratios and oscillatory amplitudes.

6.1.2. Low Velocity Tests.

The majority of the specimens were drawn at the maximum drawing speed available from the hydraulic press. A limited number of specimens were, however, drawn at low velocities in order that the ratio of oscillatory velocity to drawing velocity could be increased above that normally achievable. This increase in the velocity ratio enabled the effectiveness of high ultrasonic energy input to be examined.

6.2. Blank-holder Vibration Test Procedure.

6.2.1. General Testing Procedure.

Prior to an experimental programme commencing the blank-holder hydraulic unit and hydraulic testing machine were left with the motors running for at least 30 minutes to enable the hydraulic oil to attain its normal working temperature and viscosity.

The instrumentation was allowed a similar warm-up period, which was particularly beneficial to instruments using thermionic valves and the strain-gauge bridges. The ultrasonic generator low-tension circuit was switched on during this warm-up period but not the high-tension circuit because under conditions of imperfect matching larger currents flowed resulting in higher tempratures within the two main pentode valves.

The specimens which had been prepared beforehand as described in Appendix A.2 were lubricated with an Edgar Vaughan lubricant, 'Evodraw 4357', recommended for deep-drawing aluminium.

Preliminary tests were carried out which involved dipping samples of material of a known size into the oil and allowing to drain. The comparison of the mass of a lubricated sample with that of an unlubricated one enabled the oil coating per unit area of sample to be calculated. This mass was taken after various lengths of draining time. It was found that after draining for approximately one minute, the mass of lubricant remaining became virtually constant.

This procedure gave a reproducible lubricant film thickness on the specimen and the above procedure was adopted as standard; the specimens were lubricated in batches and suspended on wire through the centre hole to drain before testing.

After lubrication the specimen was placed in position in the wedge dies. These dies, pinned together by the die separation force load cell, were free to move on linear-roller bearings on the base of the subpress. The blank-holders attached to the counter-balanced box were brought down into contact with the dies and the position of

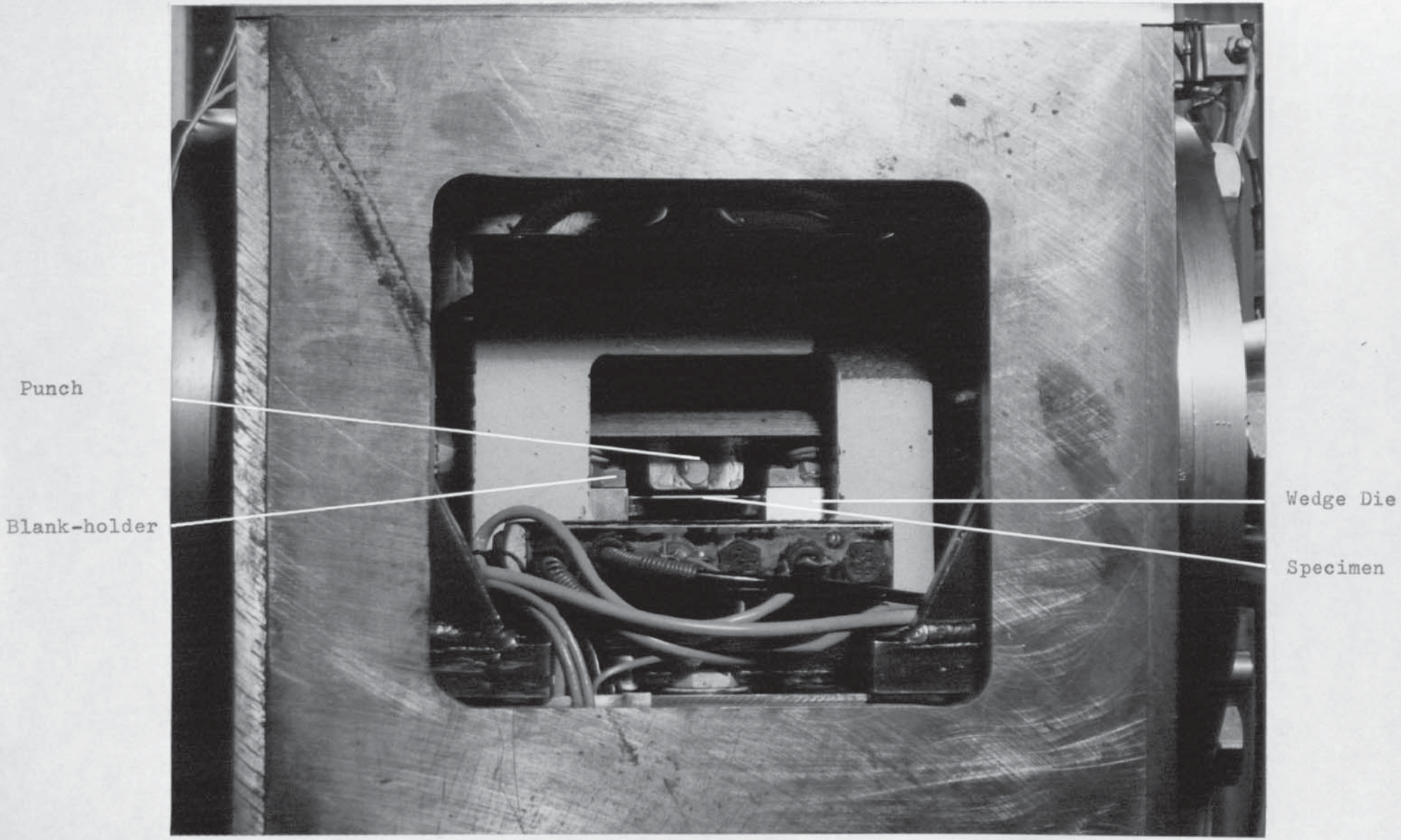

Figure 6.2.1.

the dies was adjusted until the male wedge shape of the blank-holders mated within the female shape of the wedge-dies. The blank-holder pressure plate was located on top of the blank-holders and was secured in this position by four dowel pins through the subpress vertical plates. The specimen is shown in position in Fig. 6.2.1.

When locked in this position the blank-holders were able to move with the application of hydraulic pressure but apart from this movement the complete subpress assembly, including the box section, now acted as one unit when the hydraulic testing machine was operated.

The testing machine was raised from its normal lowest position by operation of the manual by-pass valve. This modified by-pass was fitted with an indicator plate with various valve openings, any of which could be selected depending upon the press speed required. When the press was a few inches from the position at which drawing commenced the by-pass valve was closed to hold the press in this position. This delay was to enable all the instrumentation to be checked for correct functioning and the ultra-violet galvanometers were re-zeroed if necessary.

The ultrasonic generator was switched on manually and the blank-holder load applied by closing the slide-valve in the hydraulic system. In this loaded position with the blank-holders vibrating the oscillatory outputs were displayed upon the valve voltmeter scale which enabled the relative amplitude of both blank-holders to be checked readily and, if necessary, adjusted by a slight change in operating frequency. This tuning was carried out as rapidly as possible to prevent the specimen from welding to the blank-holder. Having completed this tuning operation the ultrasonic generator manual over-ride switch was put to the automatic position and the by-pass valve opened to the required position. As the specimen approached the dies the ultra-violet recorder paper drive was operated followed by the switching of oscillatory amplitude output from the display meters to the ultra-violet recorder and the switching on of the ultra-

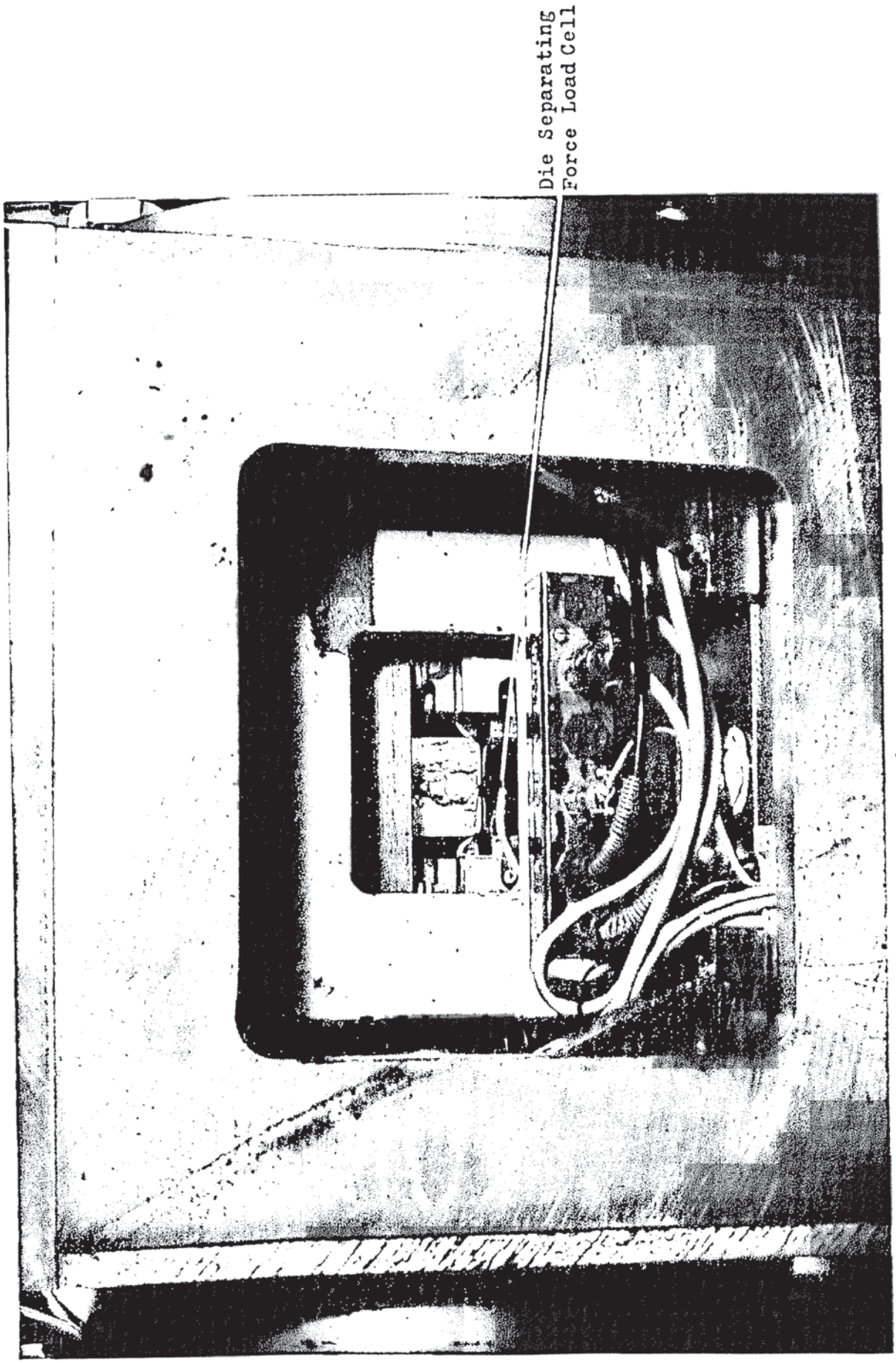

Figure 6.2.2.

sonic generator. The subpress continued to move upwards as the specimen proceeded to wrap itself around the punch as the draw continued as shown in Fig. 6.2.2. When the draw was complete, as indicated by the blank-holders moving into direct contact with the dies as the specimen disappeared over the die radius, the hydraulic pressure to each blank-holder piston was released by operating the slide valve. The vibrations were switched off as the press approached its limit of travel followed by the ultra-violet recorder and the hydraulic press motor. The draw was now complete, the by-pass valve was opened in the opposite direction to reverse the flow of oil and the subpress slowly returned to its starting position. The drawn specimen was easily removed from the front of the press through the holes in the box and subpress vertical member. In the event of a specimen failing the partly drawn wedges were easily removed once the dowel pin had been extracted and the box member containing the blank-holders raised taking the pressure plate with it.

After removal of the specimen the tools were wiped to remove the used lubricant thus preparing the press for another cycle.

When a specimen failed the test was stopped immediately, the ultrasonic vibrations were switched off manually in order to prevent the welding to the blank-holders of the broken portion of the specimen which was now stationary within the die.

For every draw-ratio several specimens were drawn without ultrasonic vibrations at the commencement and conclusion of each batch in order to act as a control on the consistency of the many press variables. The other specimens were drawn with various blank-holder amplitudes. These amplitudes were varied by operation of the 'Variac' variable transformer on the ultrasonic generator. For the main testing programme four amplitude settings were generally used. The oscillatory amplitude was not proportional to the voltage obtained from the 'Variac' transformer; therefore, the amplitude levels chosen were not simple ratios of the applied voltage.

Figure No. 6.2.3.

Blank-holder Vibrations U-V Trace

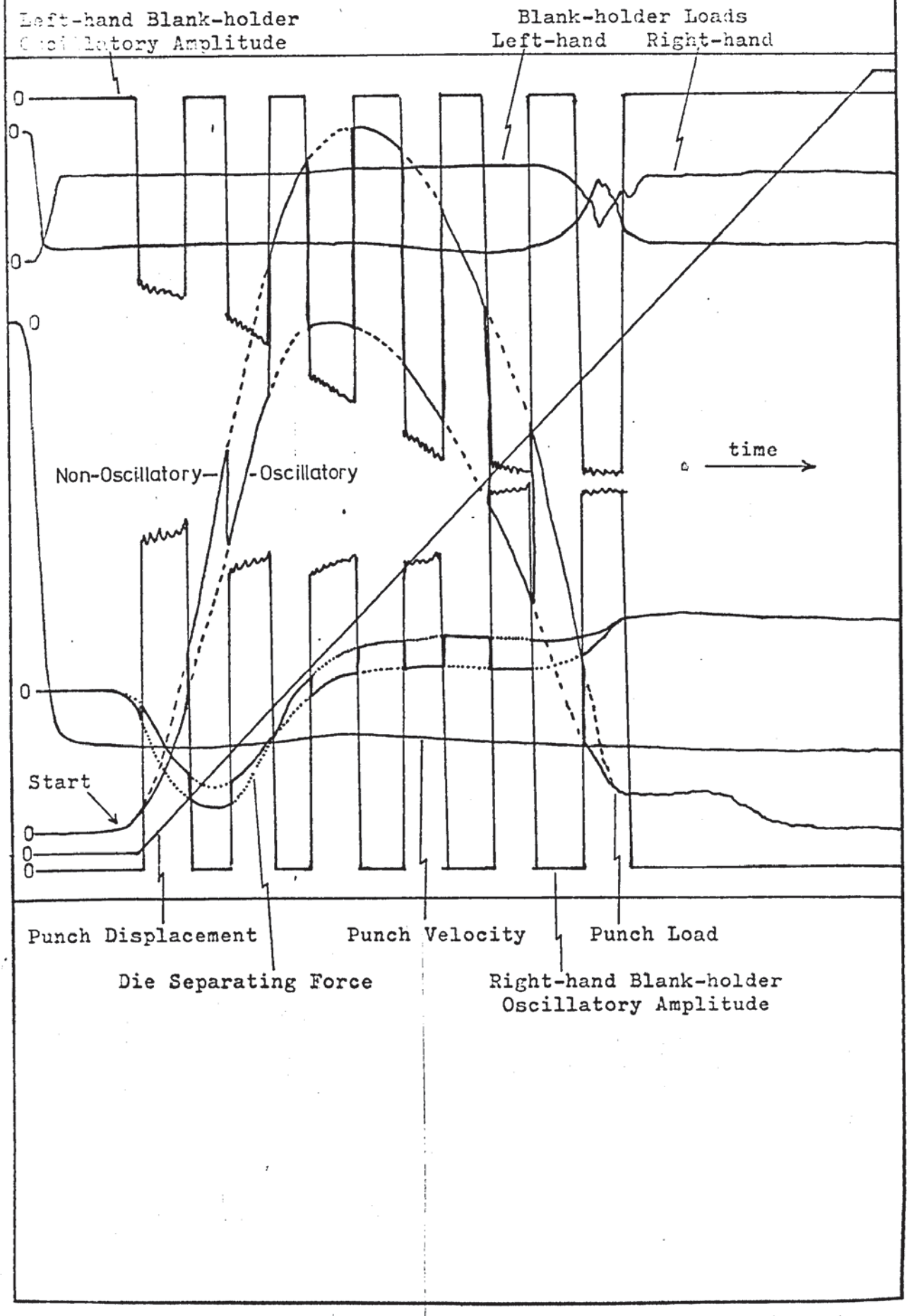

Generally, two specimens were drawn at each amplitude setting until there was a failure when a few more were drawn to establish a better idea of whether the conditions were closer to a draw situation or a fail situation. At the end of a particular draw-ratio the hydraulic blank-holder pressure was adjusted in accordance with Appendix A.4 for the next batch before testing could recommence. Each trace was allotted a serial number containing information on the process, draw-ratio and oscillatory amplitude. The frequency of the ultrasonic vibrations was also noted down. This serial number was repeated on the drawn specimen in order that the two could be associated easily. A typical ultra-violet chart is shown in Fig. 6.2.3.

6.2.2. Intermittent Testing.

Some testing was performed with the ultrasonic vibrations only applied intermittently. This switching of the generator was automatic with equal on and off periods. The device for this switching was a miniature sub-micro-switch complete with a roller lever. A suitable toothed profile was designed so that the on and off periods were equal. The necessary tooth shape was reproduced along a template of length in excess of the drawing stroke. A change-over switch incorporated enabled the on-off periods to be inter-changed so that the draw could commence with the vibrations either on or off. Two such templates were manufactured, one with a rapid switching sequence, the other with three changes during the drawing stroke.

6.2.3. Lubricant Testing.

The procedure adopted was to first select a critical draw-ratio as indicated by the general tests with the standard lubricant. This particular size of specimen was tested with various other lubricants in order that their effectiveness be ascertained. During this programme the tools were degreased with a chlorinated solvent after each individual lubricant had been used so that there was no contamination

of the various lubricants applied to the specimen. The lubricants tested were molybdenum disulphide in a variety of oils and in a volatile solvent, colloidal graphite in oil and volatile solvent, another mineral oil for drawing aluminium, lanoline and P.T.F.E. film.

6.2.4. Low Velocity Tests.

Low velocity tests were performed during which ultrasonic vibrations were applied to the normal amplitudes. The purpose of these was to effect an increase in the velocity ratio beyond the levels that could be achieved by increasing oscillatory amplitude alone. These tests were applied to one draw-ratio and they went from the normal (maximum) speed of testing down to the lowest speed that was consistent with a reasonably smooth velocity from the testing machine. Normally the velocity was quite smooth with a slight ripple due to the pulsation of the oil pump. As the speed was progressively decreased, however, the pulses increased in magnitude, especially at very low velocities. This pulsing was recorded on the velocity and load traces, therefore extremely low velocities were not tested for this reason. In addition, there was a very great tendency for the specimen to weld to the oscillatory tools, at these low drawing velocities, thus causing premature failure.

6.3. Draw Ironing Die Vibration Test Procedure.

6.3.1. General Testing Procedure.

The testing procedures used for the draw ironing die vibrations which combined drawing and ironing closely followed those described for the punch and blank-holder vibrations, Sections 6.1 and 6.2.

A batch of specimens was prepared as described in Appendix A.2 and after deburring were lubricated with 'Evodraw 4357'. The width of the expanding punch required for a particular ironing reduction was determined and both sides of the expanding punch were shimmed equally to obtain this width. The clamping of the punch side pieces into place concluded the initial setting up operations and the wedge specimens were located in the wedge dies in preparation for testing. Starting with the lowest draw-ratio, testing continued through increasing draw-ratios until failures were obtained at all the levels of oscillatory amplitude used. Having completed one series of tests the ironing punch was altered to change the ironing reduction and the testing procedure repeated. A typical ultra-violet chart showing the effect of draw ironing die vibrations is reproduced in Fig. 6.3.1.

6.3.2. Intermittent Testing.

For one draw ironing reduction a limited number of tests was performed in which the vibrations were applied intermittently to each sample. The method is described in Section 6.2.2.

6.3.3. Lubricant Testing.

A series of different drawing lubricants were examined for one particular draw ironing reduction in order to determine the effects of ultrasonic vibration on the lubricants and also to compare the effectiveness of lubricants with ultrasonic vibrations. Various lubricants were tested including P.T.F.E. film. The use of P.T.F.E. film required the wedge specimens to be modified slightly in order that the film could be used on all faces of the specimen.

Draw Ironing Die Vibration U-V Trace

Figure No. 6.3.1.

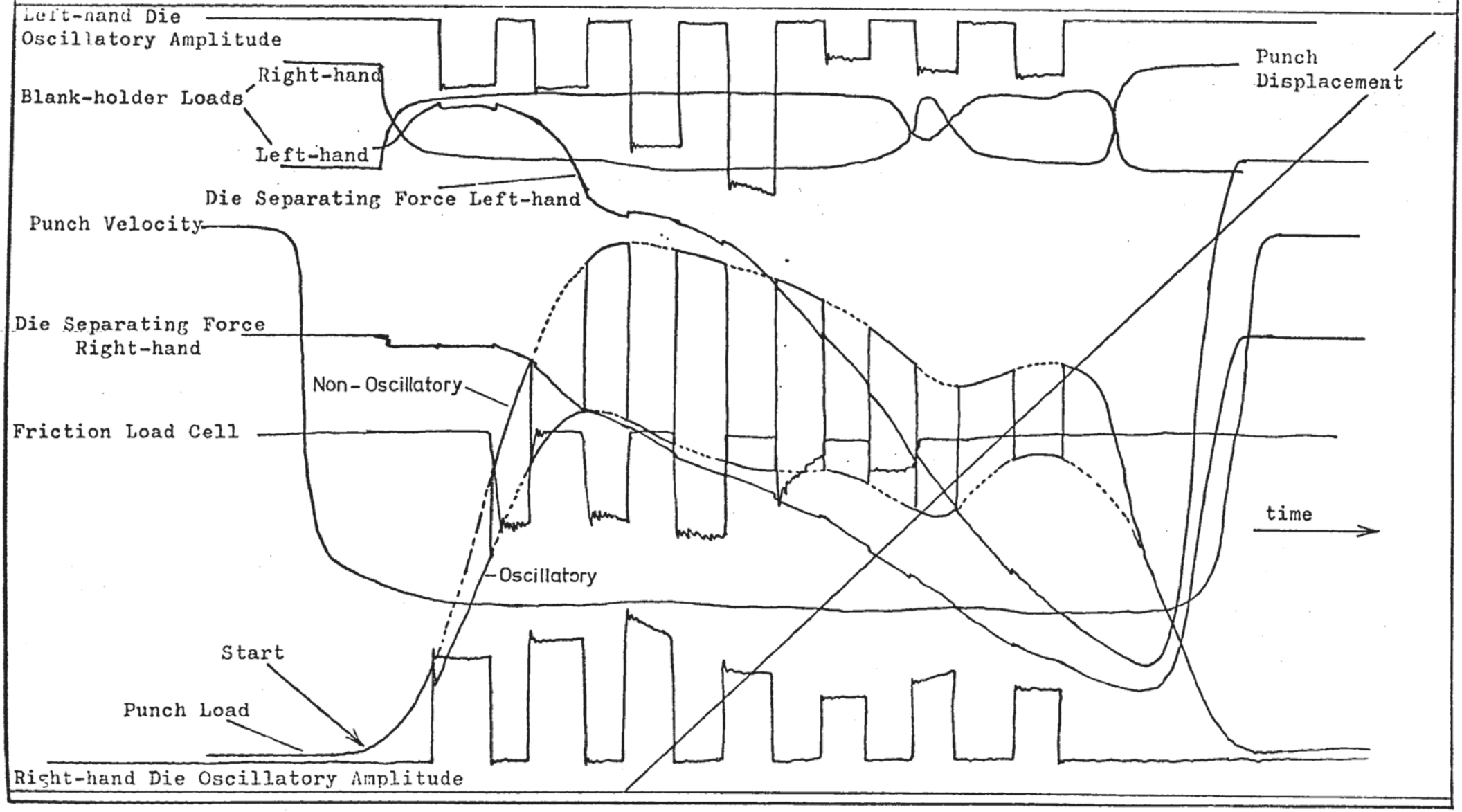

Normally specimens were a close fit in the wedge dies and therefore it was not possible to include a solid P.T.F.E. film along the edge of the wedge specimens. The solution to this problem was to elongate the central portion of the wedge specimen to enable the P.T.F.E. film to be inserted along the edge. The method chosen to achieve this local elongation without affecting the wedge sections of the specimens was to subject the central region to a light compression between flat platens. Using well lubricated platens it was possible to elongate the specimens by plane strain deformation, until they were long enough to allow the insertion of the P.T.F.E. sheet.

In use, wedge shaped pieces of P.T.F.E. sheet were cut from a sheet. The bottom piece was placed in the wedge die and the specimen placed on top so that the sheet wrapped around sides of the specimen. A second piece was used on top of the specimen so that all of the surface in contact with either the die or blank-holder was separated by the P.T.F.E. film.

6.3.4. Low Velocity Tests.

In order to attain a higher ratio of oscillatory velocity to drawing velocity a limited number of low velocity drawing tests were undertaken as described in Section 6.2.4. These followed the same pattern as the normal tests, the standard drawing lubricant was used throughout.

6.3.5. Tests Using Automatic Frequency Control.

The resonant frequency of the system was dependent upon the loading on the wedge dies and therefore the resonant frequency varied with the changes in load on the dies during the drawing operation. Normally the oscillatory frequency was set during the tuning operation immediately prior to the draw commencing this frequency being maintained throughout the draw.

In order to maintain the oscillator system resonant thereby maximising the oscillatory amplitude throughout the draw a series of tests were performed using an automatic frequency control on the ultrasonic generator. The a.f.c. unit was built onto a 'drive chassis' which was substituted for the existing chassis in the generator. The a.f.c. was controlled by a feedback signal from a sensor unit which monitored the oscillatory amplitude and varied the frequency to keep the system resonant. In use the frequency was set manually at the nominal resonant frequency and the drawing process was carried out as before, the feedback signal for the a.f.c. being derived from one of the piezo-ceramic crystals on the draw ironing dies.

6.4. Blank-Holder Swaging Test Procedure.

6.4.1. General Testing Procedure.

The general procedure for specimen preparation, lubrication and loading into the apparatus was similar to that used previously. The blank-holder pressure was applied to the specimen by the use of the hydraulic hand pump. This initial pressure required upon the undeformed blank was expressed as a blank-holder load and the system was pressurised until the required blank-holder load was obtained as indicated by the blank-holder load cells. Having applied the required pressure the hand pump was isolated from the hydraulic system by the shut-off valve.

The subpress was advanced to within a few inches of the drawing operation commencing and at this point the instrumentation was re-checked for correct functioning. The hydraulic power supply was started and the actuator piston which had been set at its mid-position for the initial blank-holder pressurisation was oscillated at the desired frequency by the operation of the control system.

The ultra-violet recorder and the press were started simultaneously and the draw commenced. On completion of the draw the oscillatory oil pressure was shut off and the static pressure released prior to removing the specimen in preparation for another cycle. The procedure was repeated for various oscillatory pressure levels throughout a range of specimen sizes. A typical ultra-violet chart showing the effect of blank-holder swaging is shown in Fig.6.4.1.

6.4.2. Low Velocity Tests.

The use of low frequency oscillations of the blank-holder pressure supply meant that there were considerably fewer cycles during the draw than when ultrasonic vibrations were used. For this reason several tests were performed using low drawing velocities to increase the number of cycles and therefore increase the effectiveness of the oscillatory blank-holder pressure.

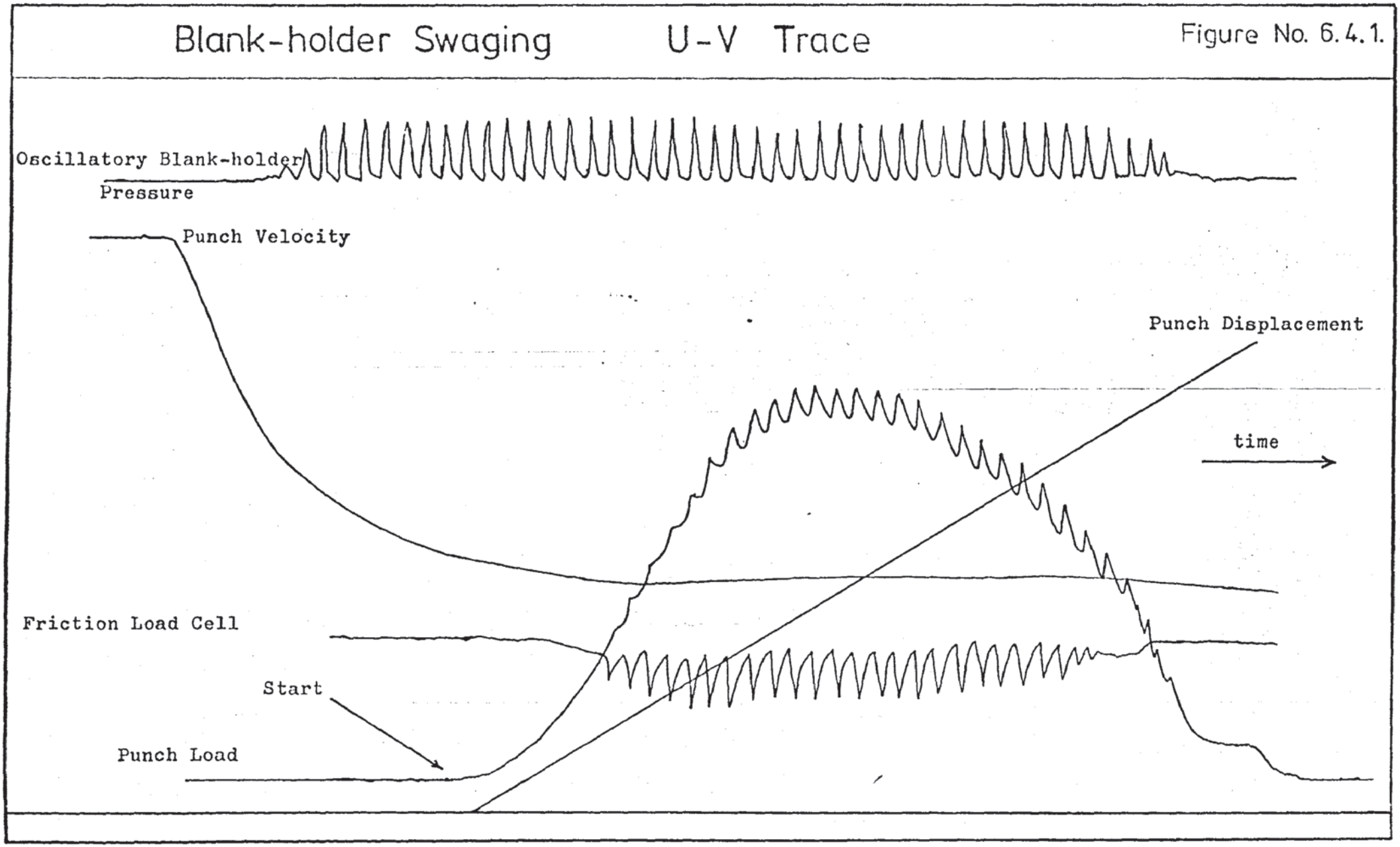
Blank-holder Swaging U-V Trace
Figure No. 6.4.1.
Oscillatory Blank-holder Pressure
Punch Velocity
Punch Displacement
time
Friction Load Cell
Start
Punch Load

Graph No. 7.1.1.

Maximum Punch Load v Punch Velocity Ratio for various Draw-ratios

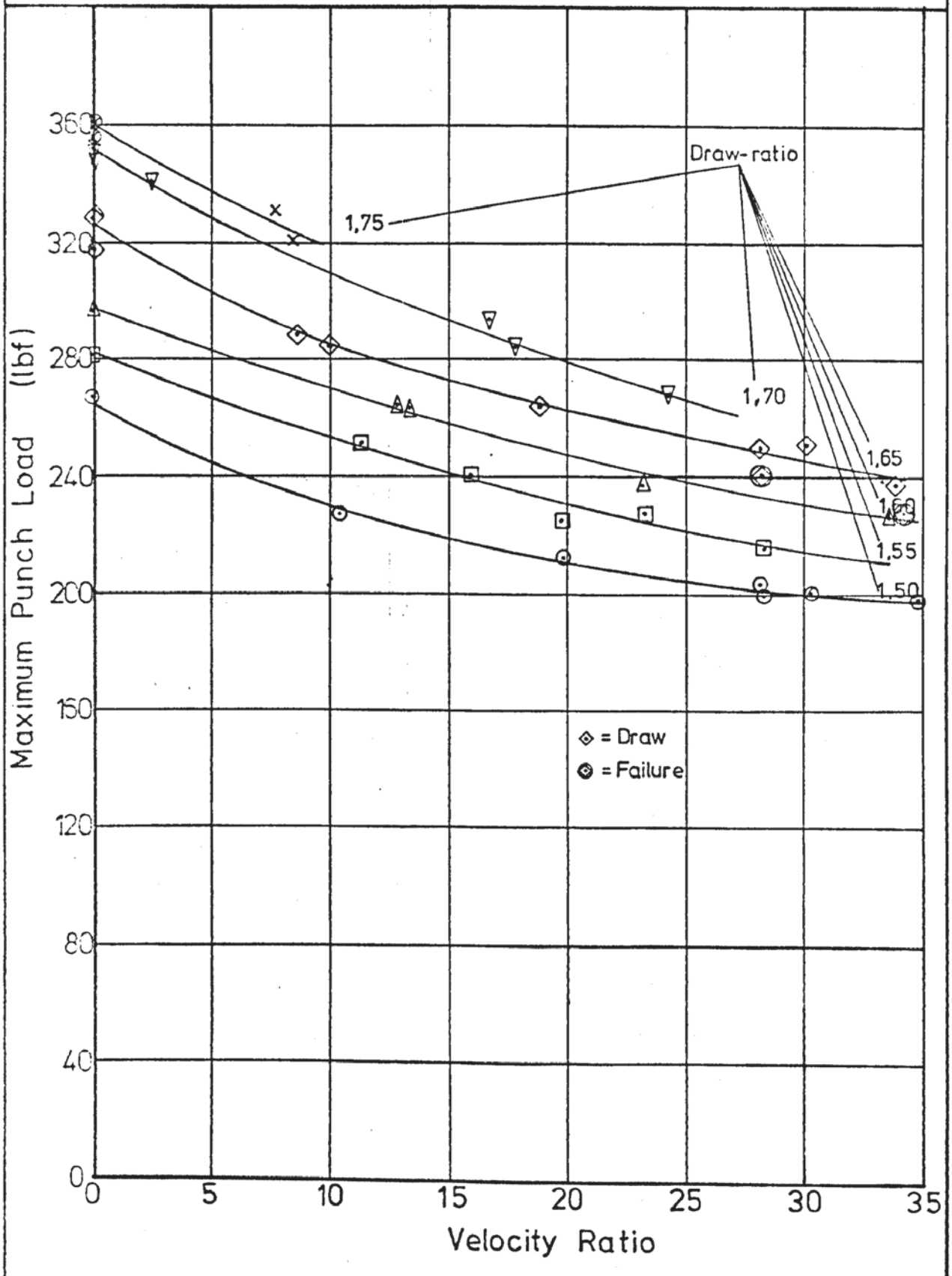

Graph No. 7.1.2.

Blank-holder Friction Force v Punch Oscillatory Amplitude at Minimum Friction Force for various Draw-ratios

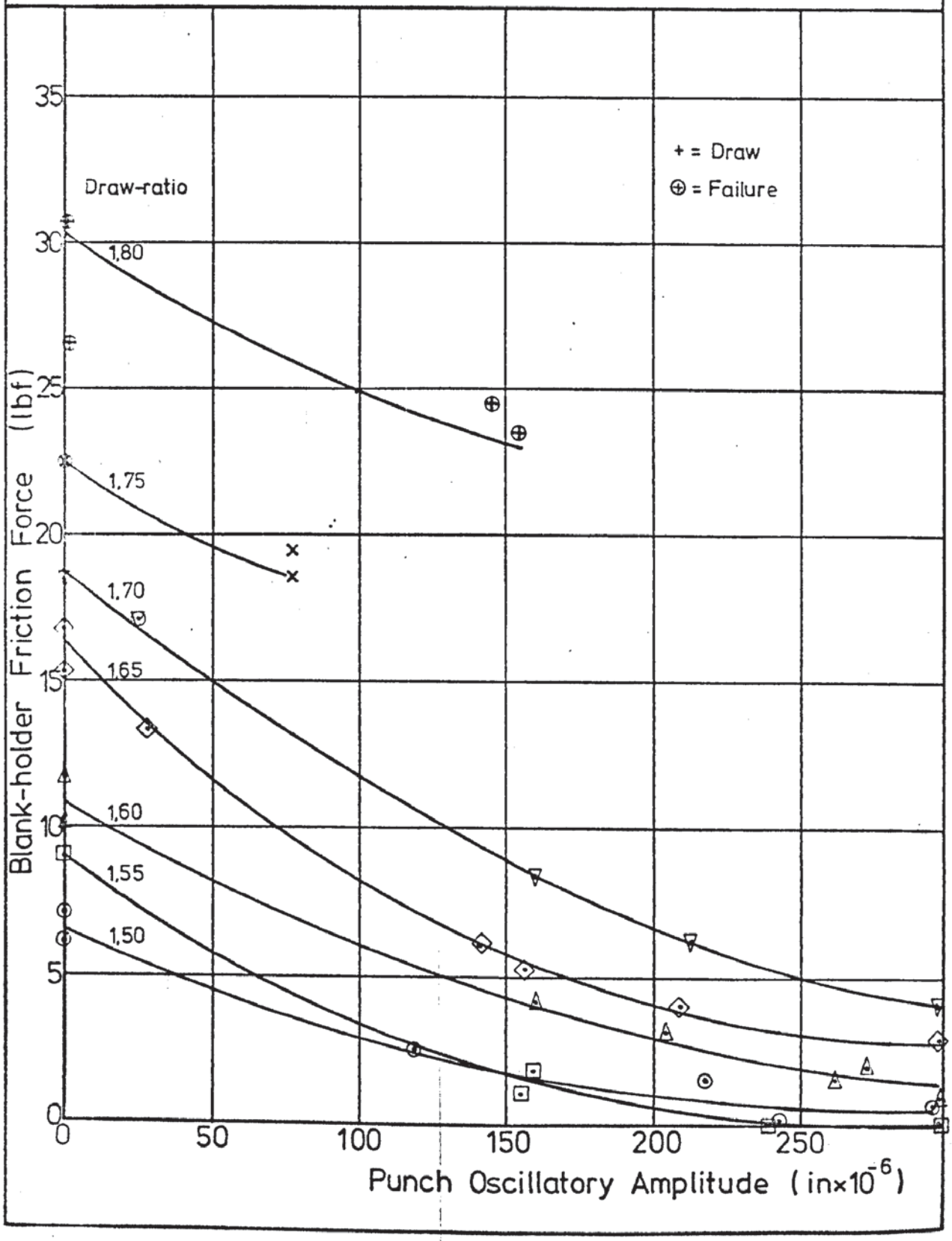

Graph No. 7.1.3.

Blank-holder Friction Force v Die Oscillatory Amplitude at Maximum Punch Load for various Draw-ratios

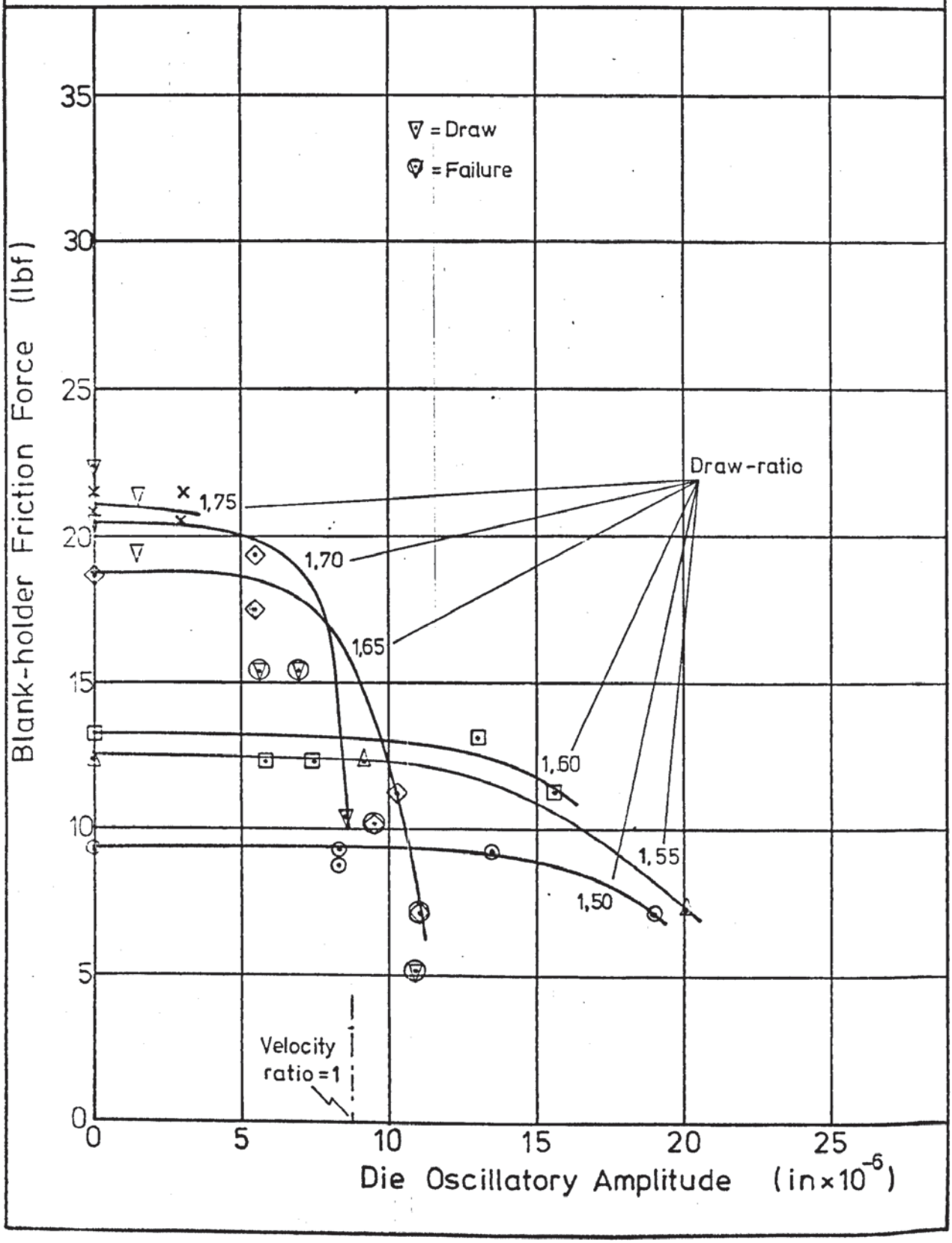

Graph No. 7.1.4.

Effect of Punch Oscillatory Amplitude on Maximum Punch Load for various Draw-ratios

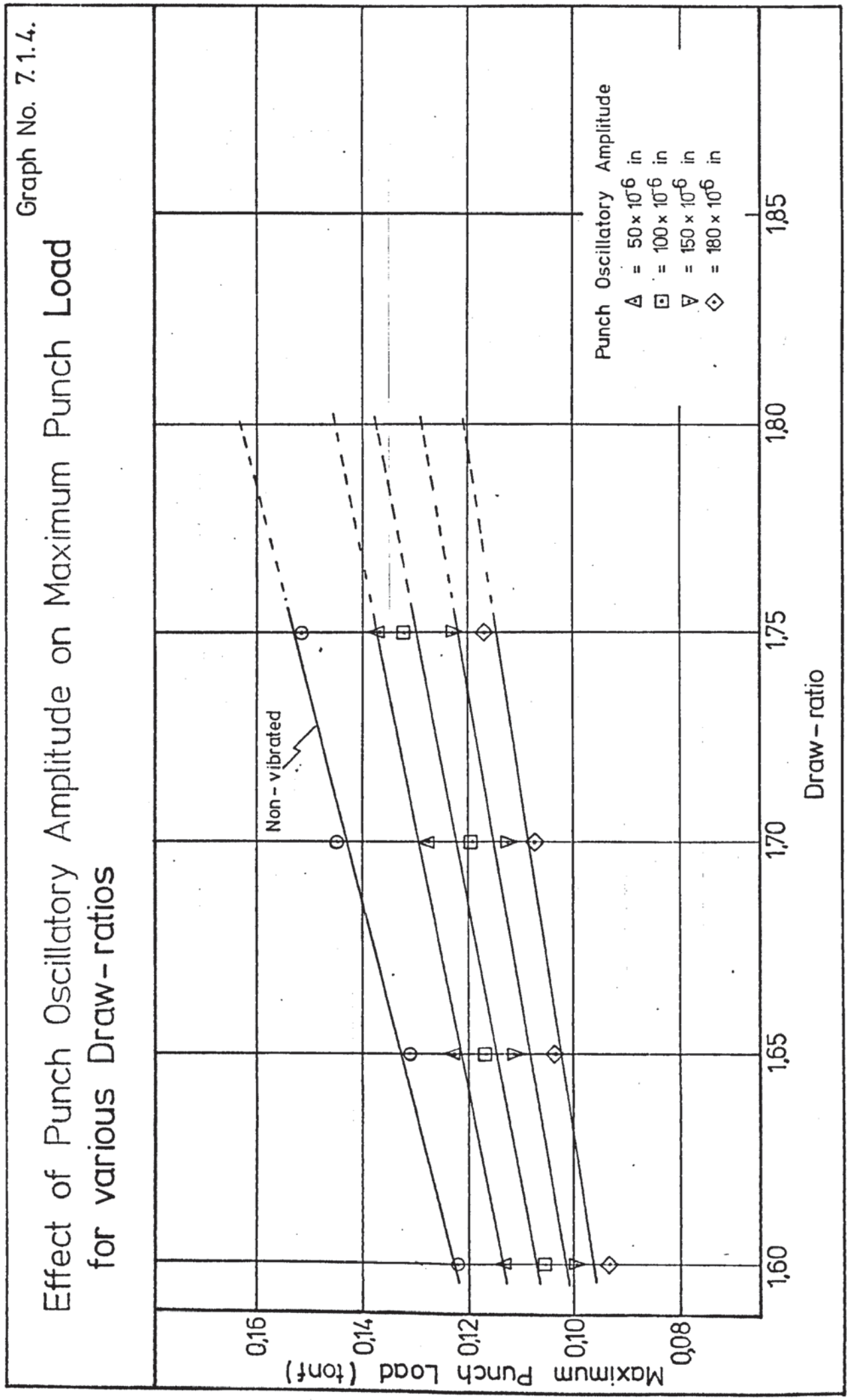

Graph No. 7.1.5.

Effect of Die Oscillatory Amplitude on Maximum Punch Load for various Draw-ratios

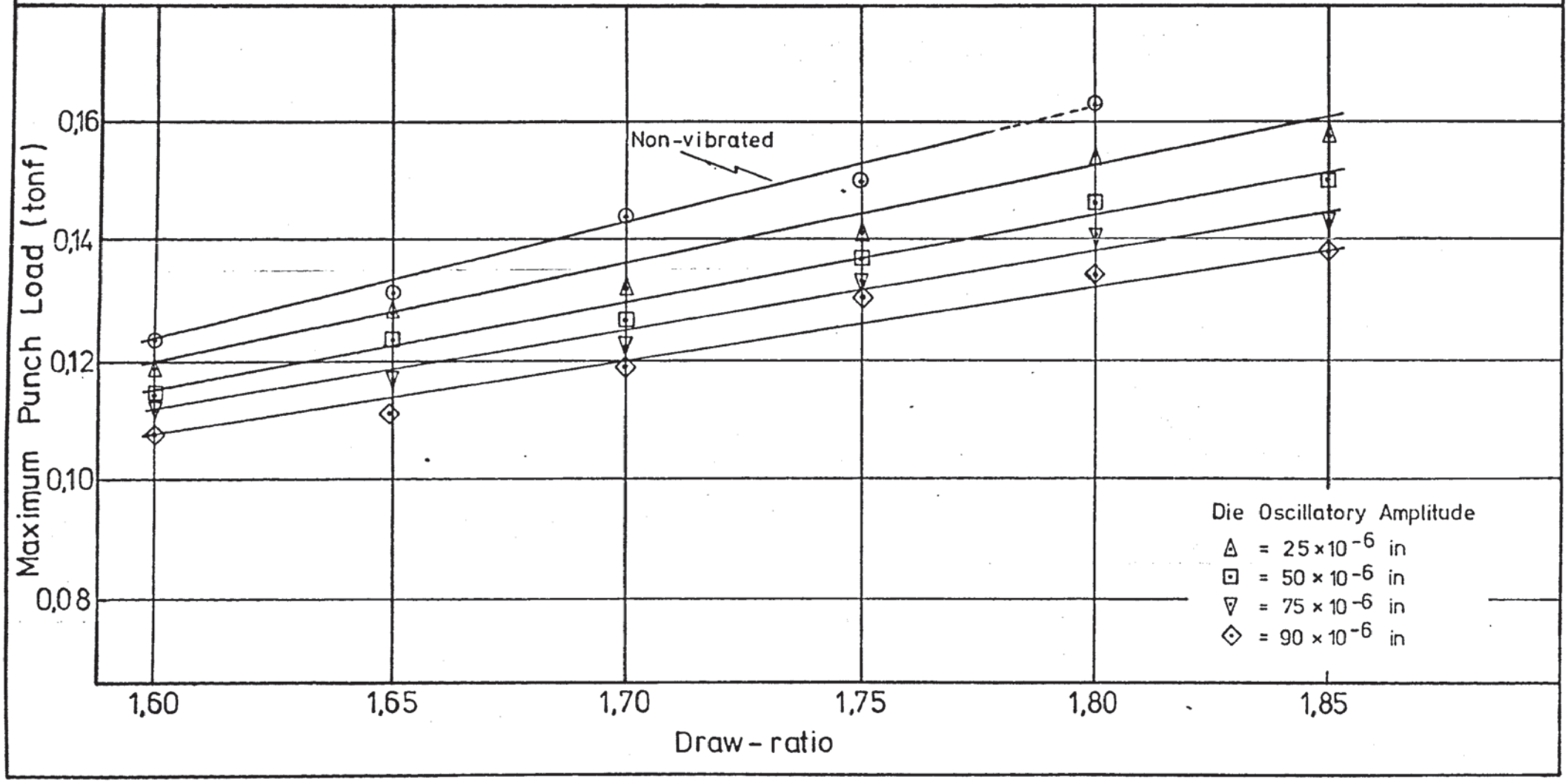

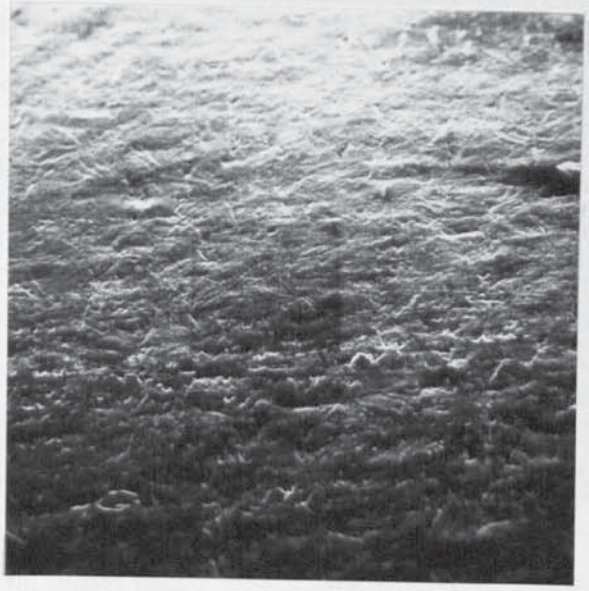

Fig. 7.1.1. P240 Top x 160

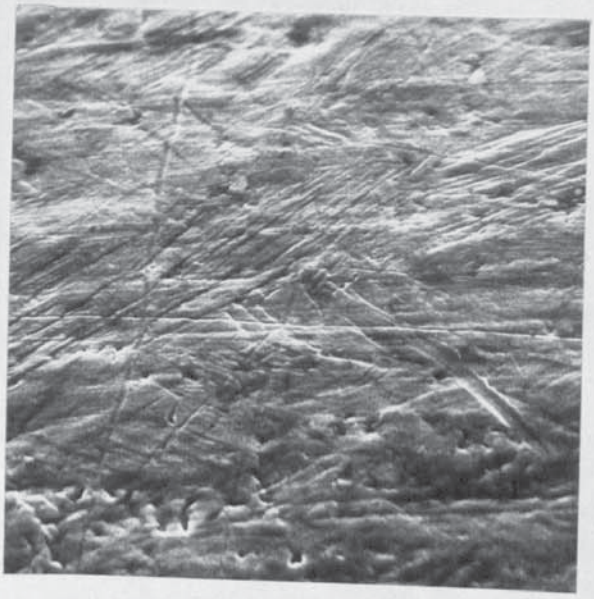

Fig. 7.1.2. P240 Top x 1.6k

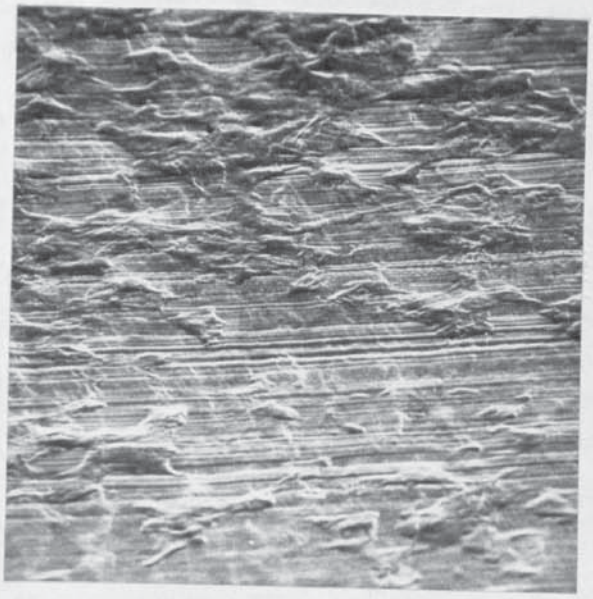

Fig. 7.1.3. P240 Bottom x 160

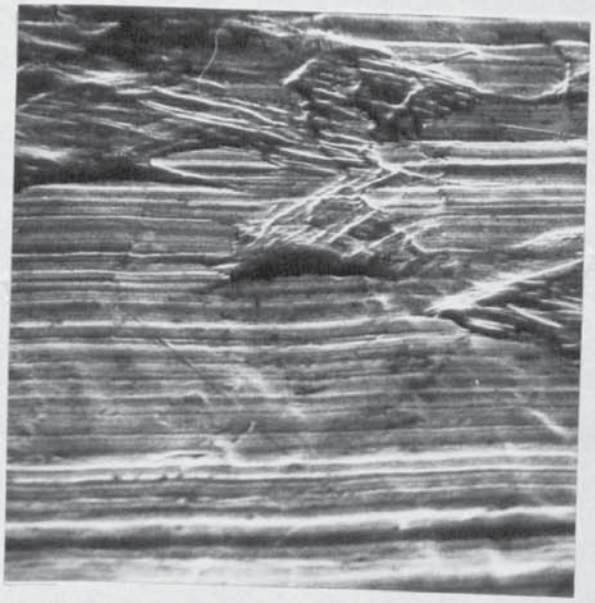

Fig. 7.1.4. P240 Bottom x 1.6k

Fig. 7.1.5. P240 Edge x 160

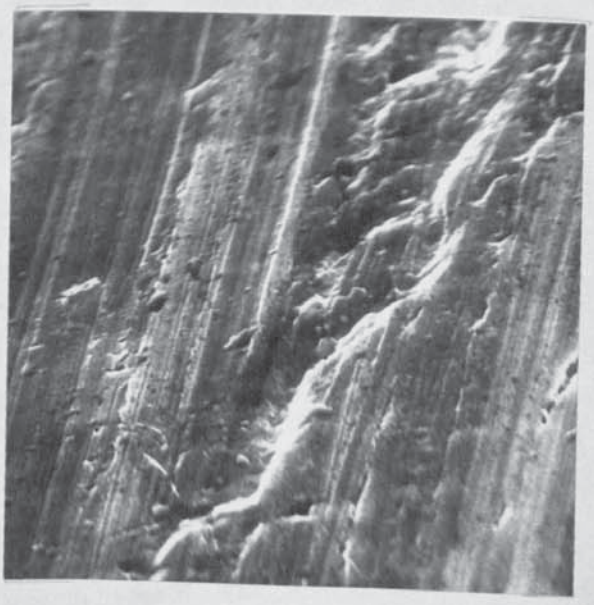

Fig. 7.1.6. P240 Edge x 1.6k

Graph No. 7.2.1.

Maximum Punch Load v Blank-holder Oscillatory Amplitude for various Draw-ratios

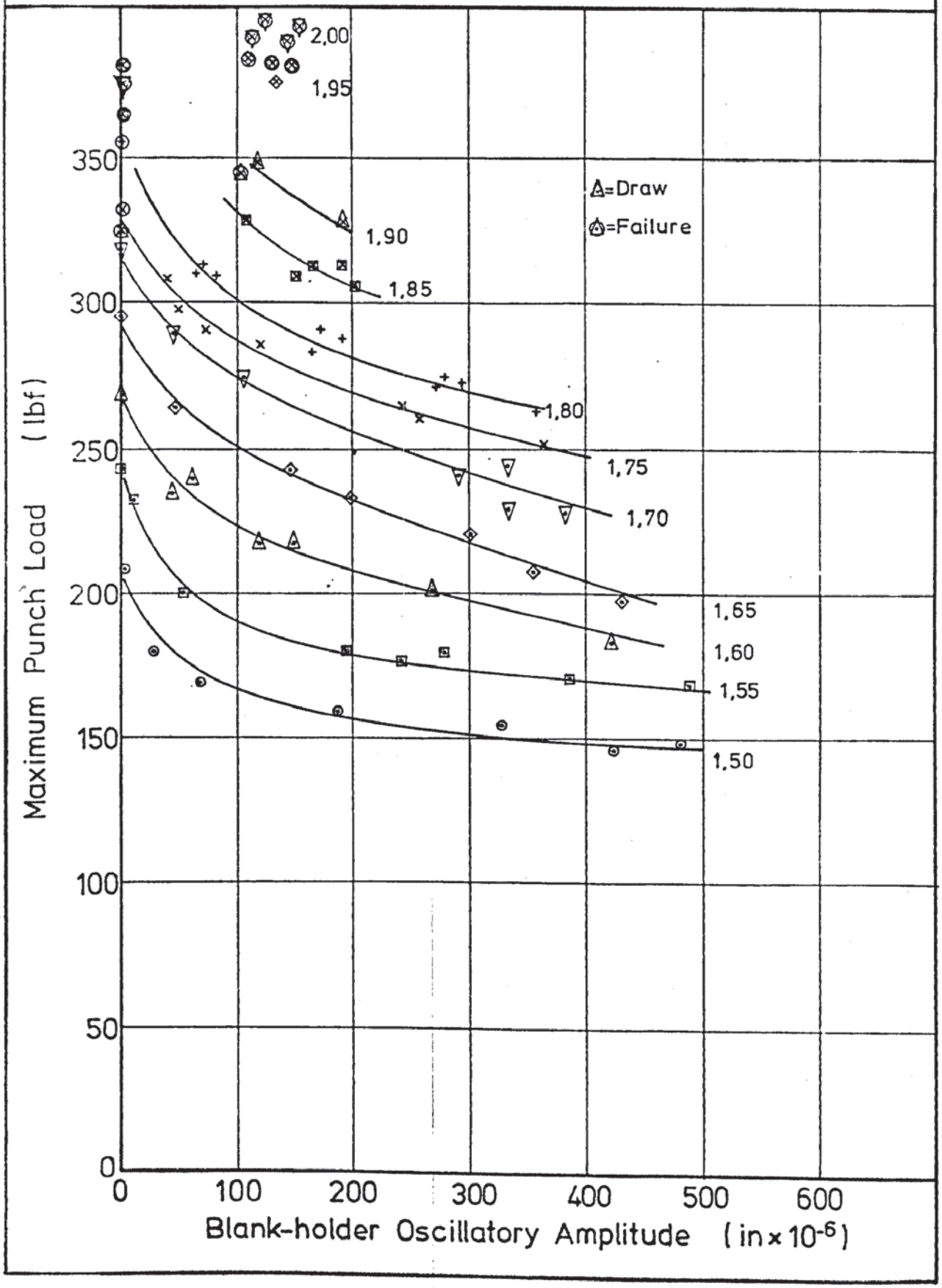

Graph No 7.2.2.

Effect of Blank-holder Oscillatory Amplitude on the Limiting Draw-ratio

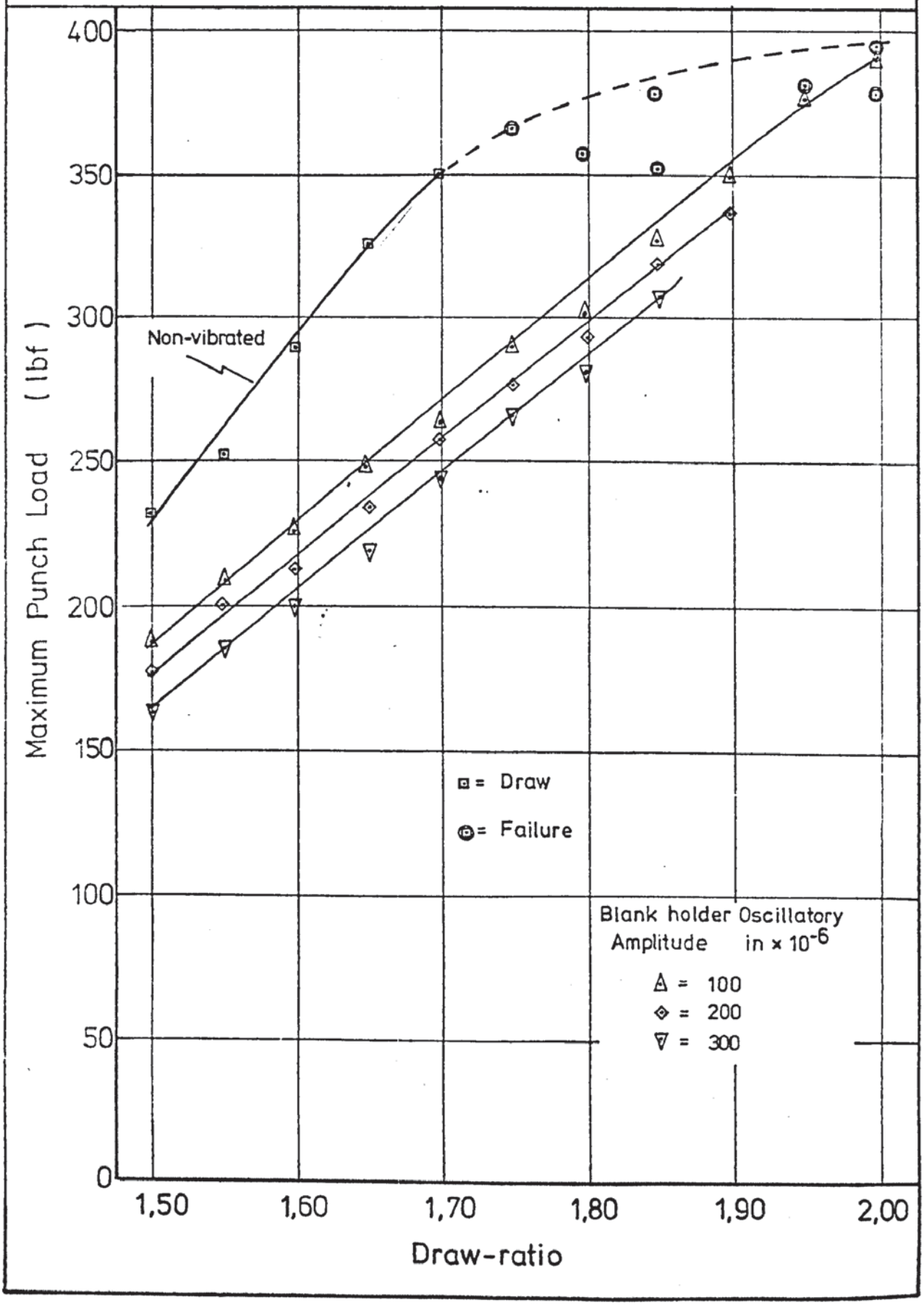

Graph No. 7.2.3.

Reduction in Die Separating Force v Blank-holder Oscillatory Amplitude at Maximum Compressive Force for various Draw-ratios

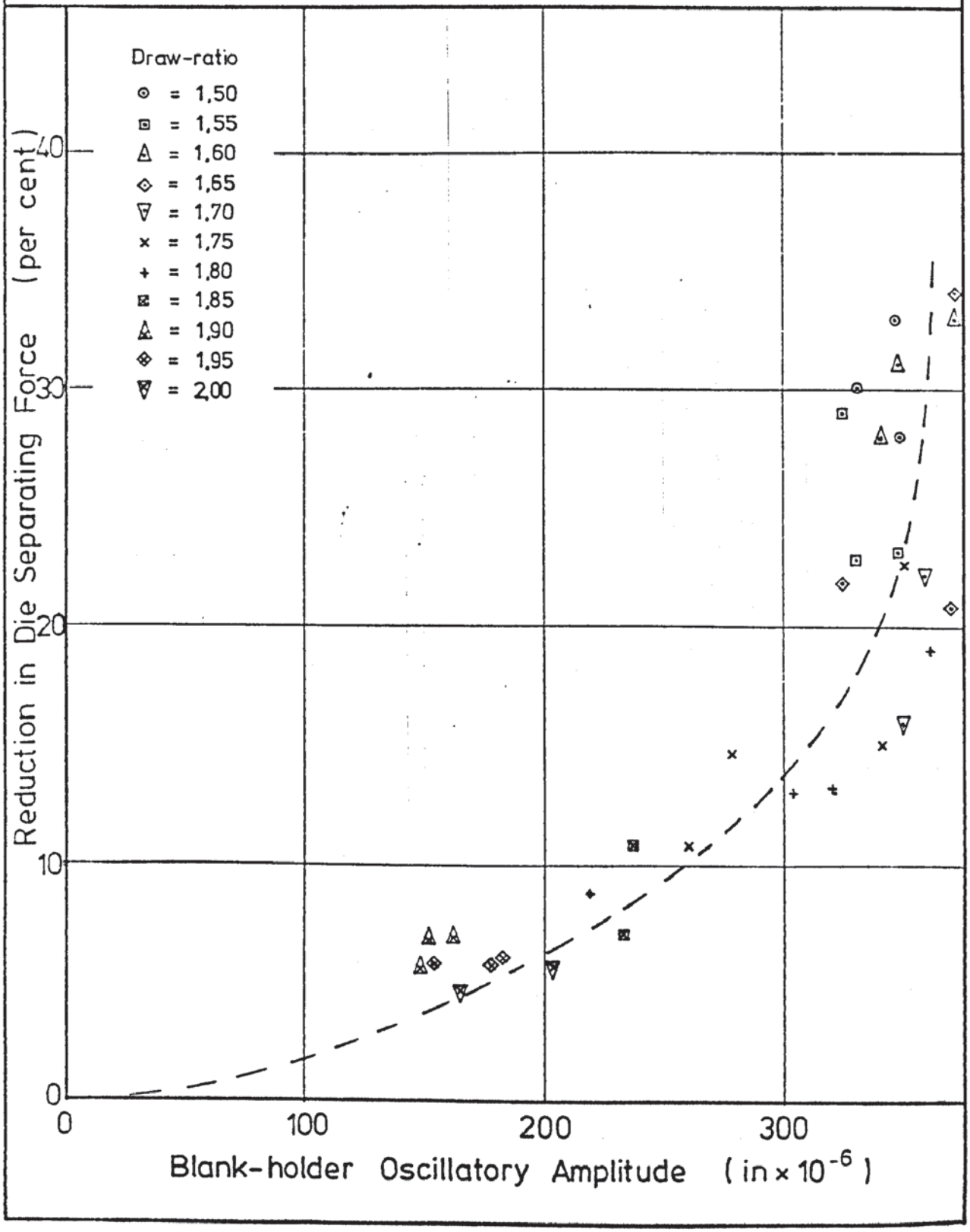

Intermittent Tests Results — Table No 7.2.1.

Test No.	Max Punch Load P lbf		Die Sep Force D lbf at P max		Die Sep Force D lbf at D max		B.H. Amplitude in x 10⁻⁴		
	Osc	Non Osc	Osc	Non Osc	Osc	Non Osc	L.H.	R.H.	Mean
BH-150-140I	168	235	2.0	0	27.3	39.1	223	438	331
BH-150-200I	179	240	3.9	2.0	35.2	48.8	264	433	349
BH-150-260I	163	237	5.9	2.0	35.2	52.7	264	428	346
BH-155-140I	184	269	3.9	3.9	37.1	46.9	328	318	323
BH-155-200I	211	291	3.9	2.0	39.1	50.8	328	363	346
BH-155-260I	189	269	9.8	5.9	39.1	50.8	275	383	329
BH-160-140I	219	312	0	7.8	35.2	48.8	352	328	340
BH-160-200I	213	301	0	3.9	35.2	50.8	293	403	348
BH-160-260I	208	301	3.9	3.9	37.1	52.7	352	464	408
BH-165-140I	251	339	5.9	17.6	33.2	43.0	311	333	322
BH-165-200I	224	328	0	9.8	48.8	62.5	293	454	374
BH-165-260I	224	342	0	11.7	37.1	56.6	293	454	374
BH-170-200I	245	352*	2.0	15.6	52.7	65.5	264	438	351
BH-170-260I	240	366*	2.0	15.6	48.8	62.5	264	454	359
BH-175-140I	275	368*	13.7	0	54.7	62.5	264	252	258
BH-175-200I	261	360*	13.7	3.9	46.9	52.7	293	252	273
BH-175-260I	283	379*	17.6	13.7	54.7	64.5	352	353	353
BH-175-260I	267	374*	17.6	9.8	44.9	58.6	293	388	341
BH-180-200I	291	379*	35.2	9.8	58.6	64.5	234	202	218
BH-180-200I	253	366	21.5	7.8	50.8	58.6	234	378	306
BH-180-260I	304	374*	9.8	2.0	43.0	54.7	381	353	367
BH-180-260I	293	374*	19.6	9.8	52.7	60.5	293	353	323
BH-185-200I	310	371*	19.6	2.0	54.7	58.6	264	202	233
BH-185-260I	318	374*	15.6	0	46.9	52.7	264	202	233
BH-190-200I	280	368*	25.4	23.4	53.5	58.6	205	126	166
BH-190-260I	256	360*	25.4	23.4	56.6	60.5	176	126	151
BH-190-260I	275	360*	21.5	19.6	52.7	56.6	176	126	151
BH-195-200I	293	401*			64.5	68.4	205	101	153
BH-195-260I	304	401*			68.4	72.3	234	126	180
BH-195-260I	301	398*			68.4	72.3	234	126	180
BH-200-200I	304	392*			68.4	72.3	205	126	166
BH-200-260I	307	392*			74.2	78.1	527	252	390
BH-200-260I	307	398*			68.4	74.2	234	176	205

* = Specimen Failed

Drawing Speed = 0.35 $in.s^{-1}$

Tests using Different Lubricants. Table No. 7.2.2.

Lubricant	Maximum Punch Load	
	Oscillatory	Non-Oscillatory
	Draw ratio = 1.80	
1. Colloidial Molybdenum Disulphide in Toluene	316	360*
2. Colloidial Graphite in oil	308	349*
3. Lanoline	288	347*
4. Alldraw No.8	290	350*
5. TD 45	292	358*
6. Cindolube 4573	294	355*
7. P.T.F.E. Sheet	284	295
	Draw ratio = 1.85	
P.T.F.E. Sheet		307
	Draw ratio = 1.90	
P.T.F.E. Sheet		338
	Draw ratio = 1.95	
P.T.F.E. Sheet		390*

* = Specimen Failed Drawing Velocity = 0.35 $in.s^{-1}$

Lubricant Suppliers

1,2 Acheson Colloids Company

4, Allcard & Company

5,6 Edgar Vaughan & Company

Low Velocity Tests Results. Table No. 7.2.3.						
Test No.	Drawing Speed $in.s^{-1}$	Max. Osc. Punch Load lbf	Max. Osc. Die Sep. Force lbf	B.H. Amplitude in $\times 10^{-6}$ L.H.	R.H.	Mean
Draw ratio: 1.90						
BH-190-260	0.35	344	45.0	176	101	139
BH-190-260V7	0.30	347	48.8	205	176	191
BH-190-260V5	0.23	344	50.8	234	101	168
BH-190-260V3	0.09	355	56.6	147	101	124
BH-190-260V3	0.09	350	52.7	205	51	128
BH-190-260V2	0.01	331	58.6	147	51	99
Draw ratio: 1.95						
BH-195-260	0.34	390	58.6	147	60	104
BH-195-260V5	0.24	390	62.5	147	60	104
BH-195-260V3	0.09	387	58.6	117	51	84
BH-195-260V2	0.01	368	64.5	70	20	45

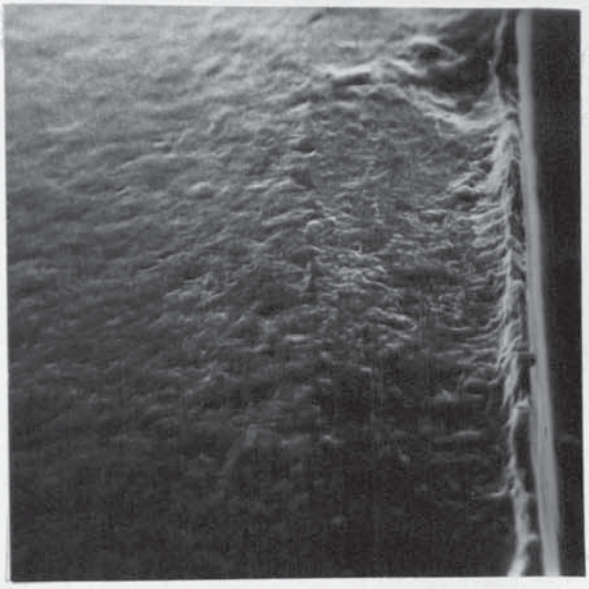

Fig. 7.2.1. BHO Top x 100

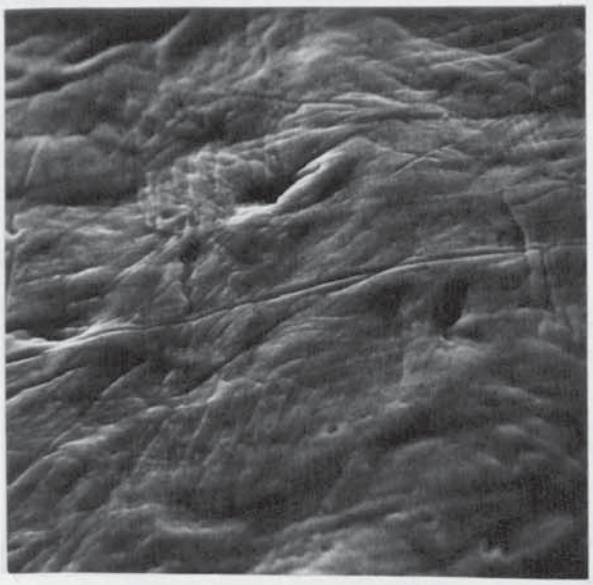

Fig. 7.2.2. BHO Top x 1k

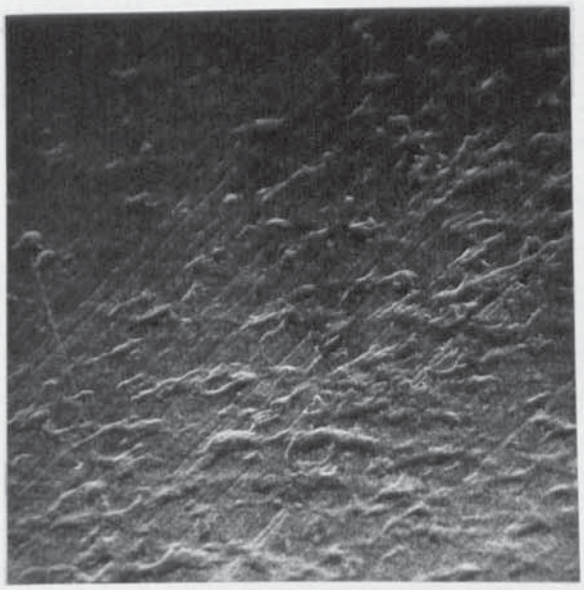

Fig. 7.2.3. BHO Bottom x 100

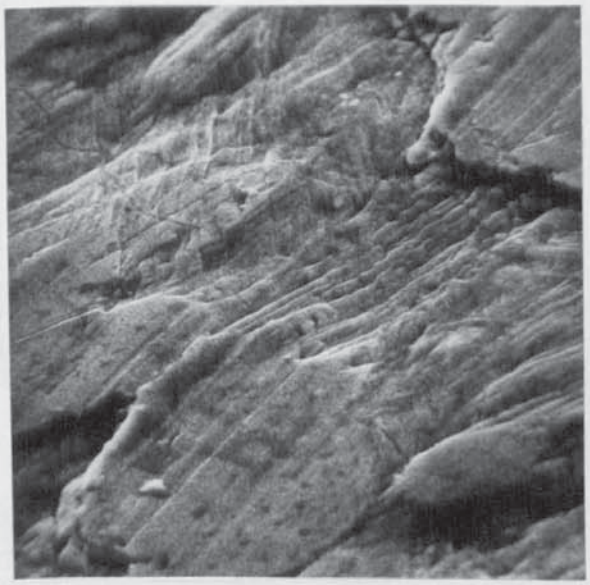

Fig. 7.2.4. BHO Bottom x 1k

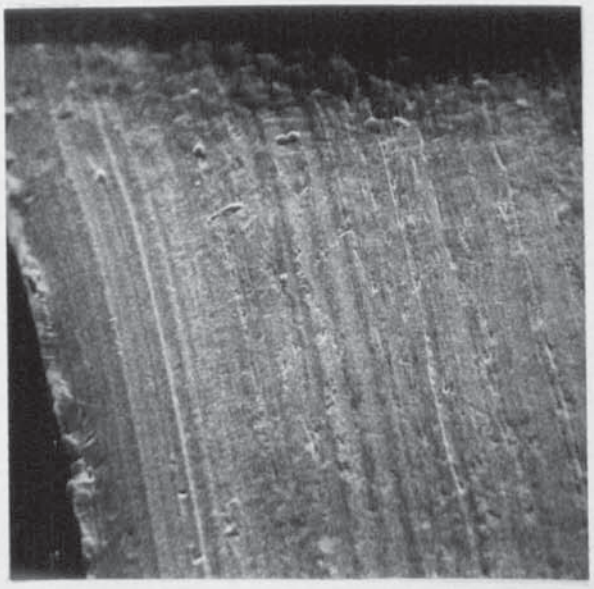

Fig. 7.2.5. BHO Edge x 100

Fig. 7.2.6. BHO Edge x 1k

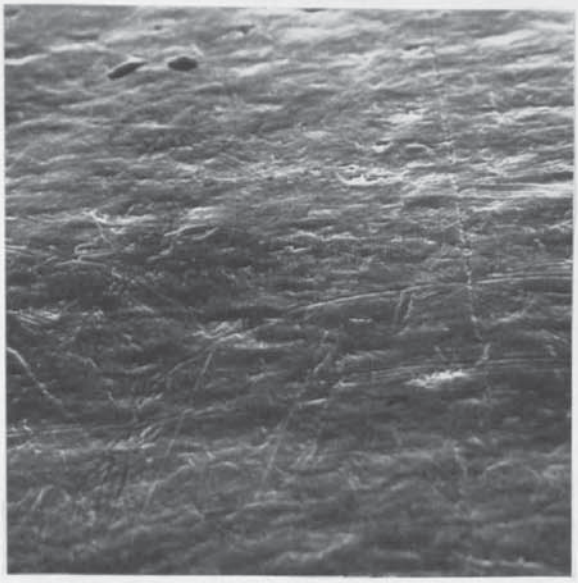

Fig. 7.2.7. BH260 Top x 160

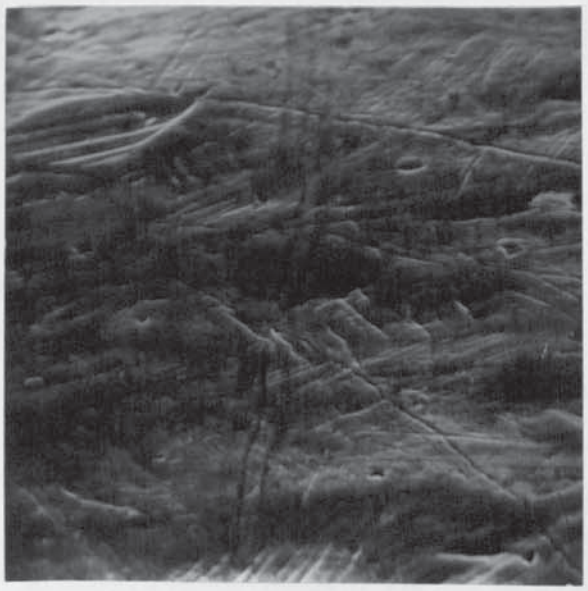

Fig. 7.2.8. BH260 Top x 1.6k

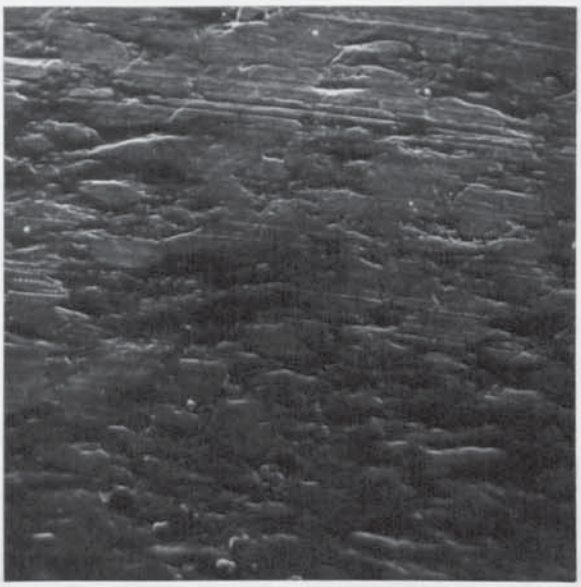

Fig. 7.2.9. BH260 Bottom x 160

Fig. 7.2.10. BH260 Bottom x 1.6k

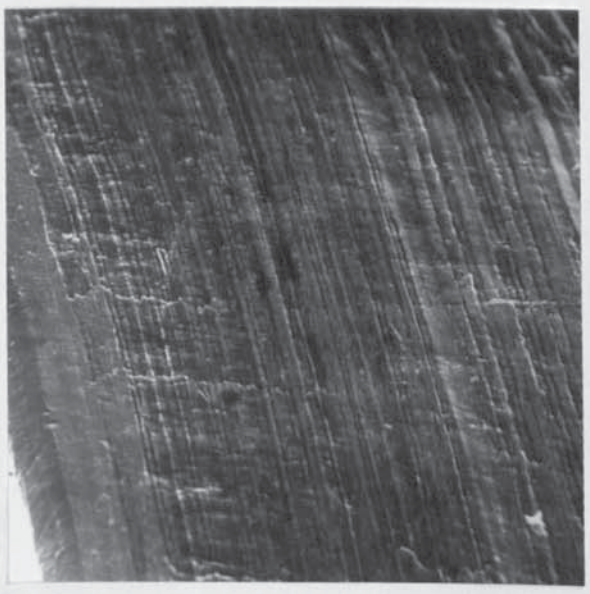

Fig. 7.2.11. BH260 Edge x 160

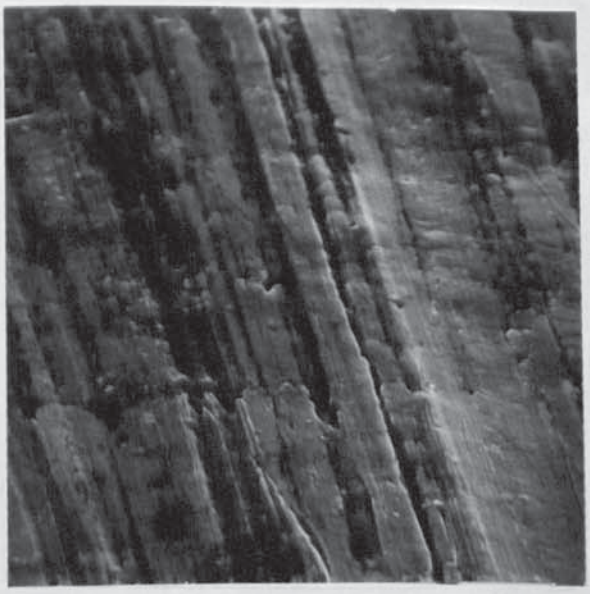

Fig. 7.2.12. BH260 Edge x 1.6k

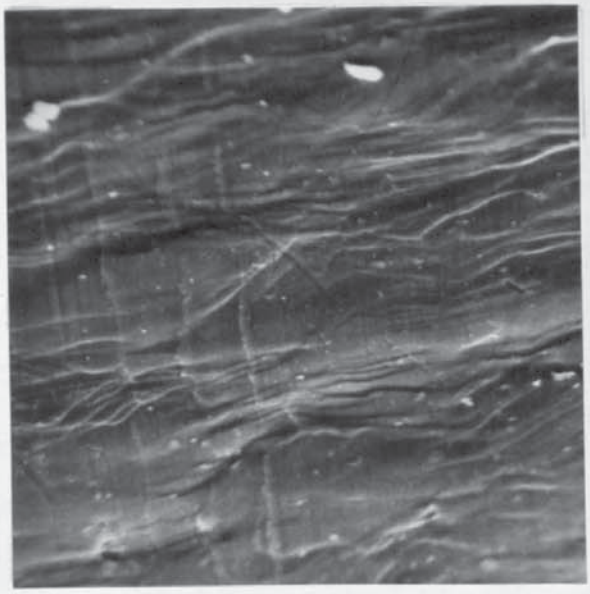

Fig. 7.2.13. BH260I Dull x 600

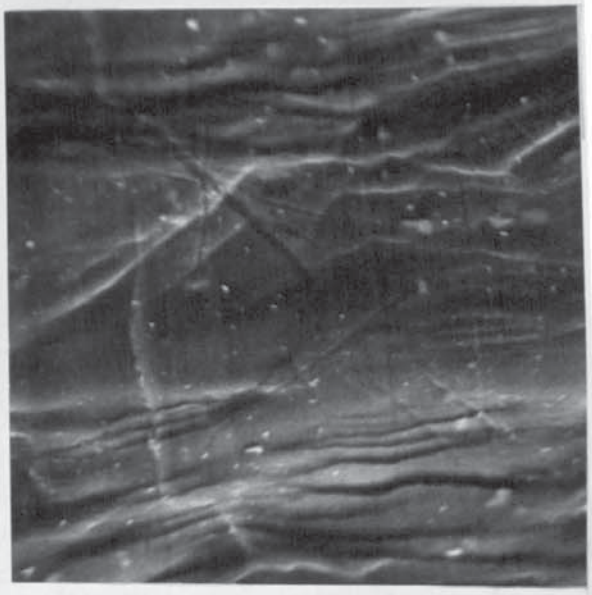

Fig. 7.2.14. BH260I Dull x 1.6k

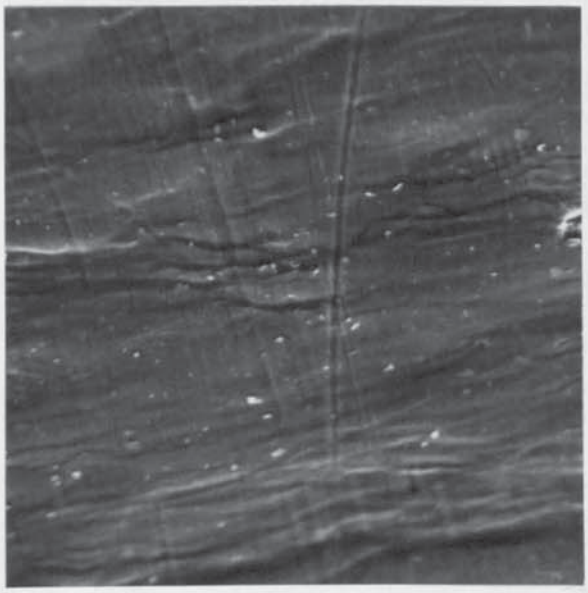

Fig. 7.2.15. BH260I Bright x 600

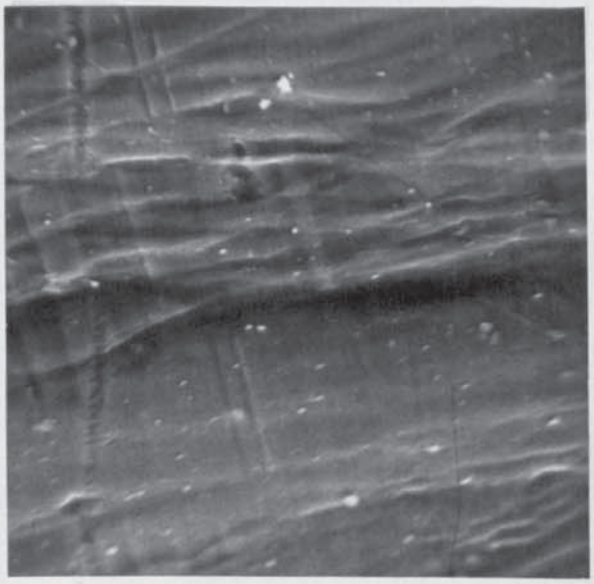

Fig. 7.2.16. BH260I Bright x 1.6

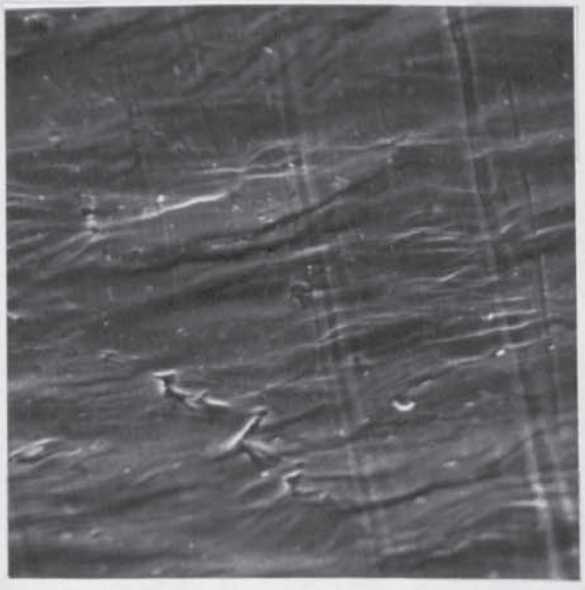

Fig. 7.2.17. BH260I Dull x 600

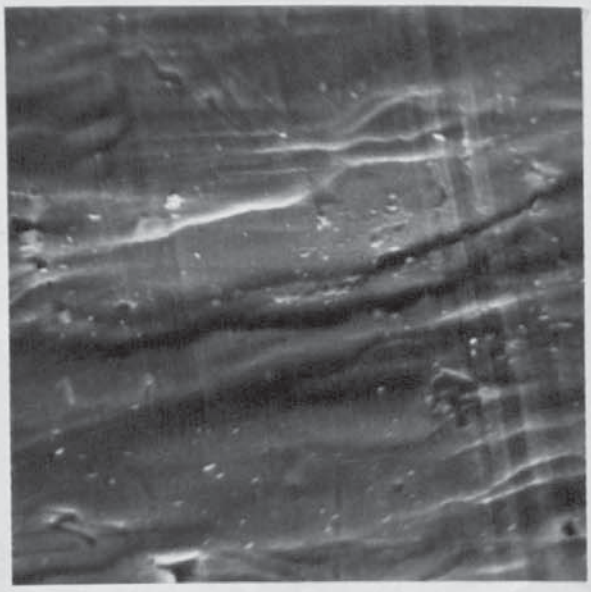

Fig. 7.2.18. BH260I Dull x 1.6k

Graph No. 7.3.1.

Blank-holder Friction Force v Draw Ironing Die Oscillatory Amplitude for various Draw-ratios

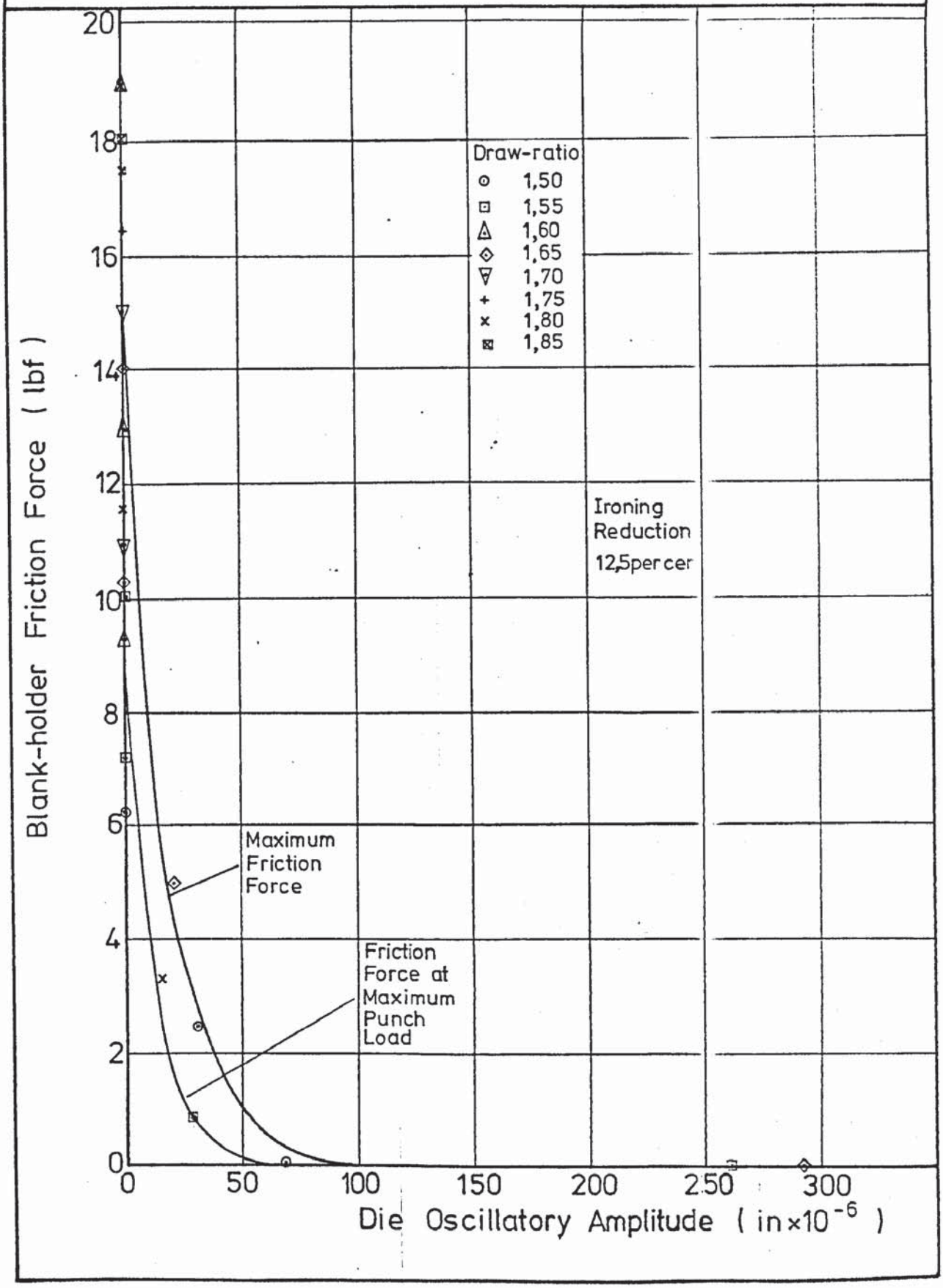

Graph No. 7.3.2.

Maximum Punch Load v Draw Ironing Die Oscillatory Amplitude for various Draw-ratios

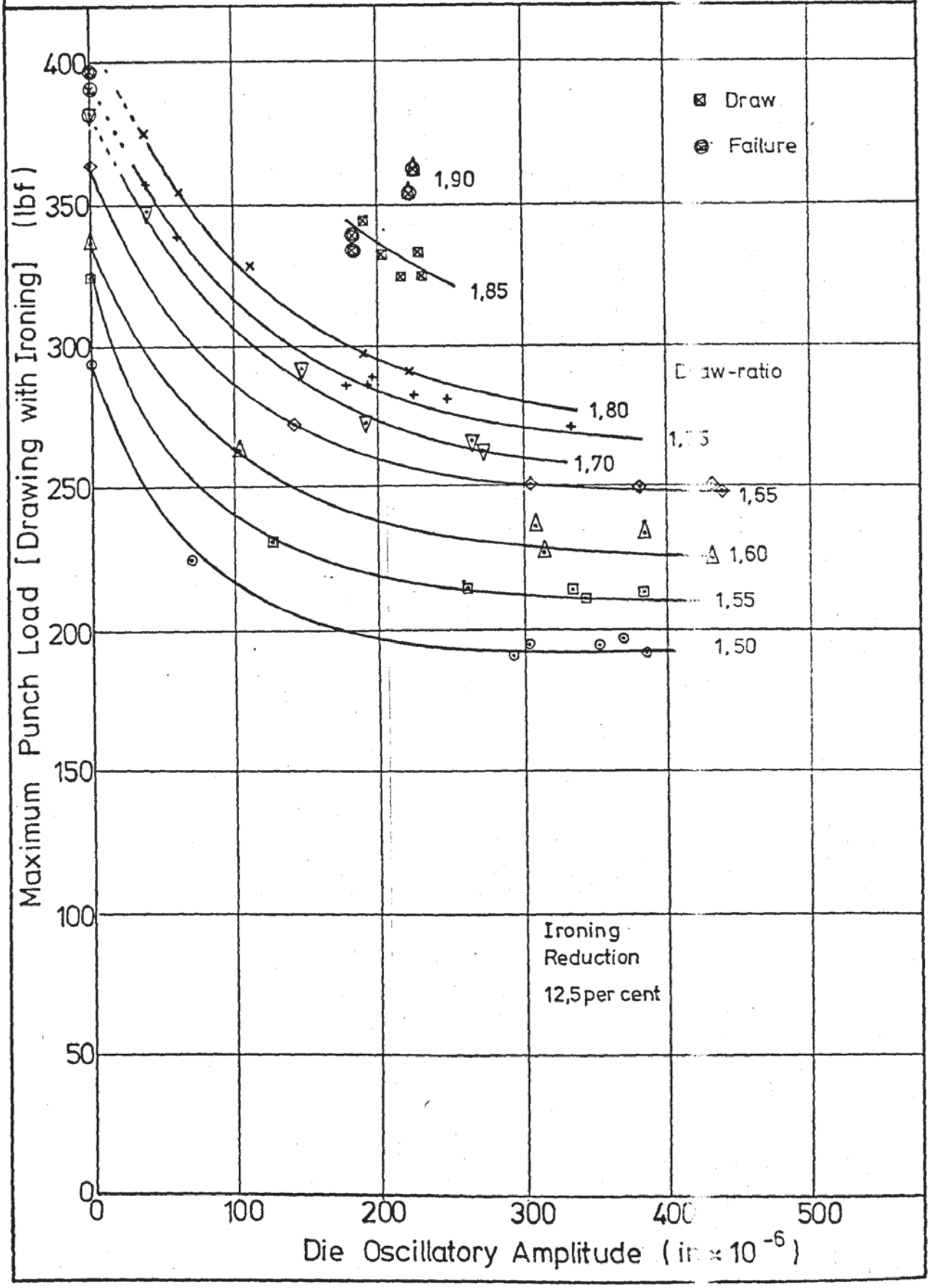

Graph No. 7.3.3.

Effect of Draw Ironing Die Velocity Ratio on the Limiting Draw-ratio

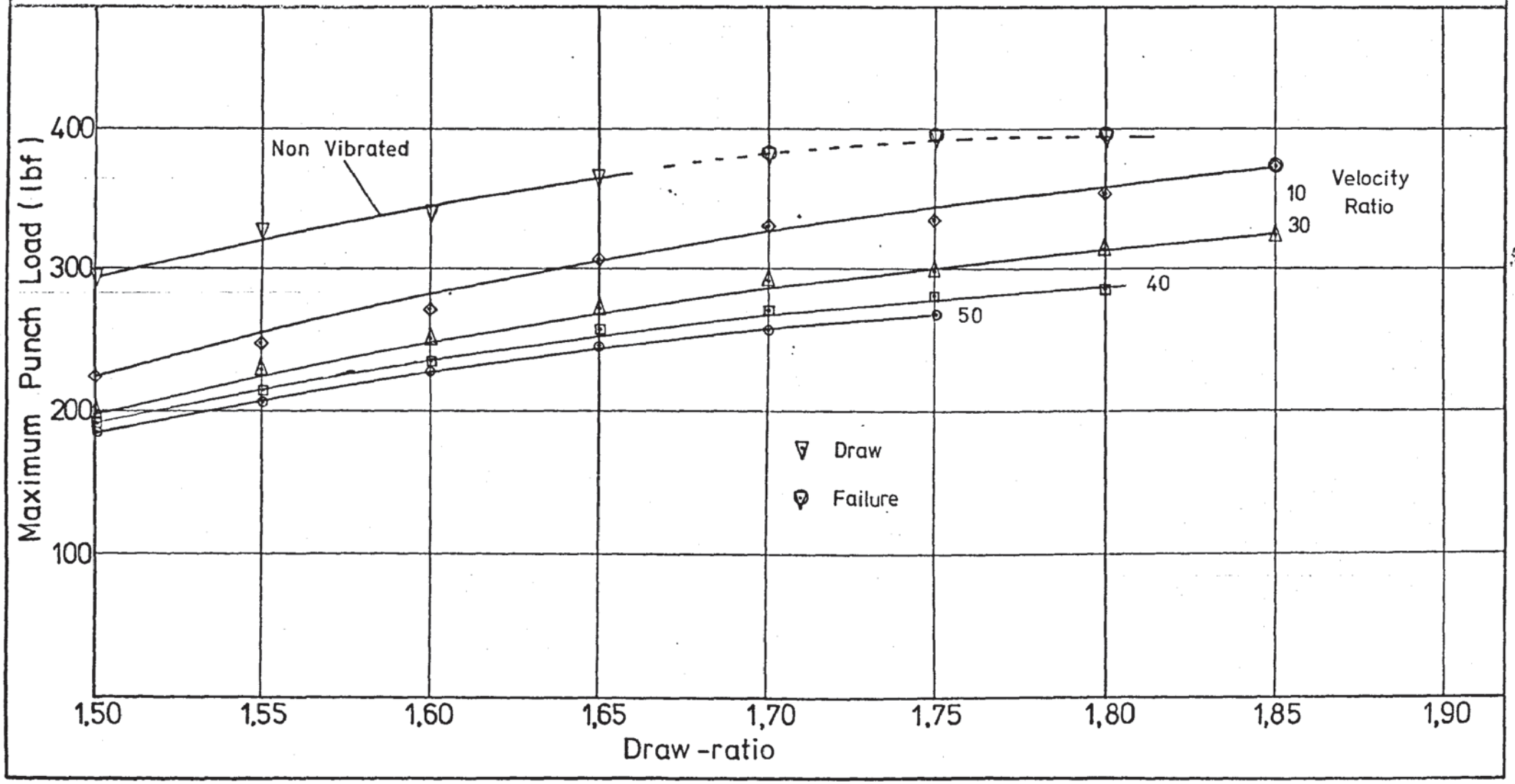

Graph No. 7. 3. 4.

Draw Ironing Die Separating Force v Draw Ironing Die Oscillatory Amplitude at the Maximum Punch Load (Ironing) for various Draw-ratios

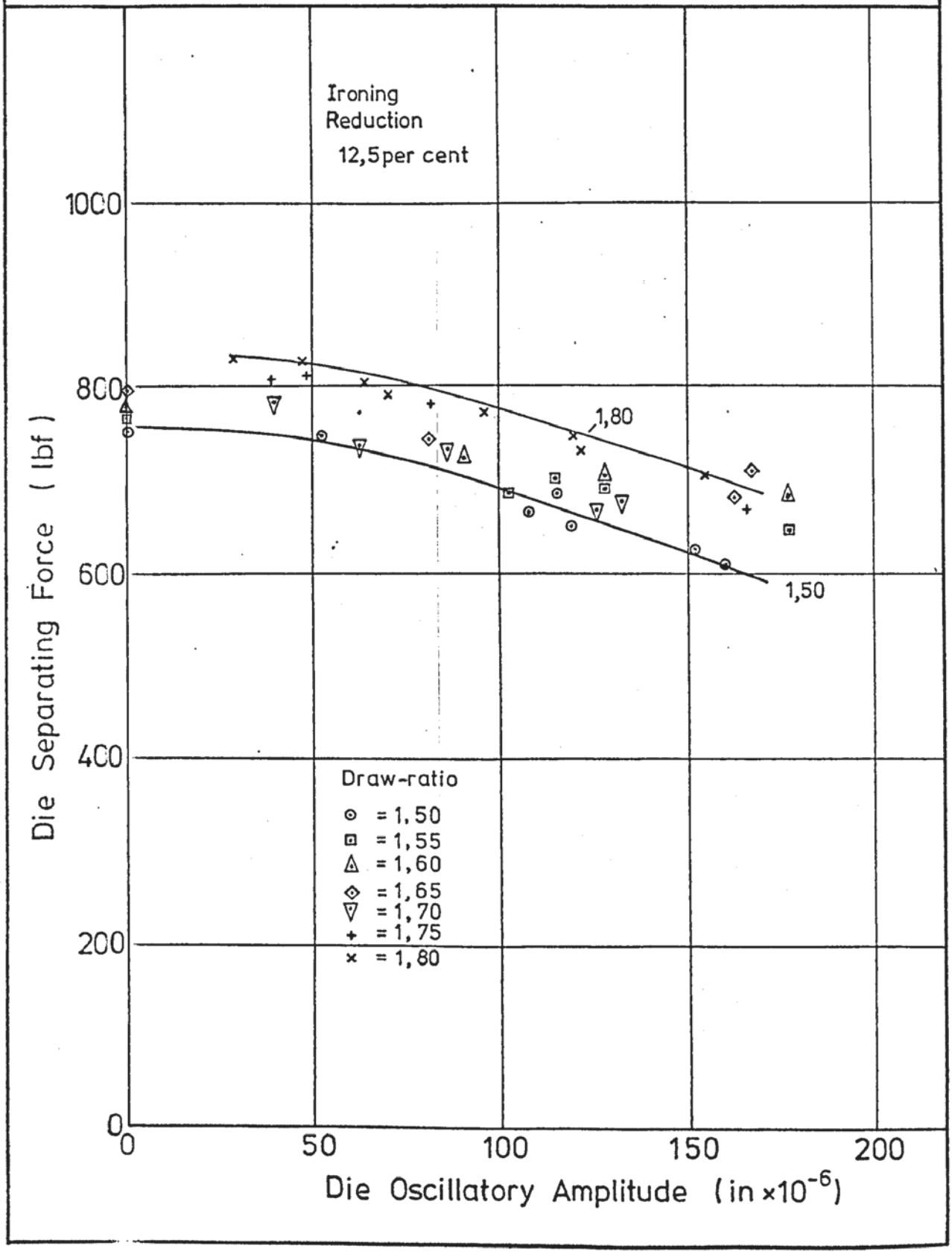

Graph No. 7.3.5.

Maximum Punch Load (Ironing) v Draw Ironing Die Oscillatory Amplitude for various Ironing Reductions

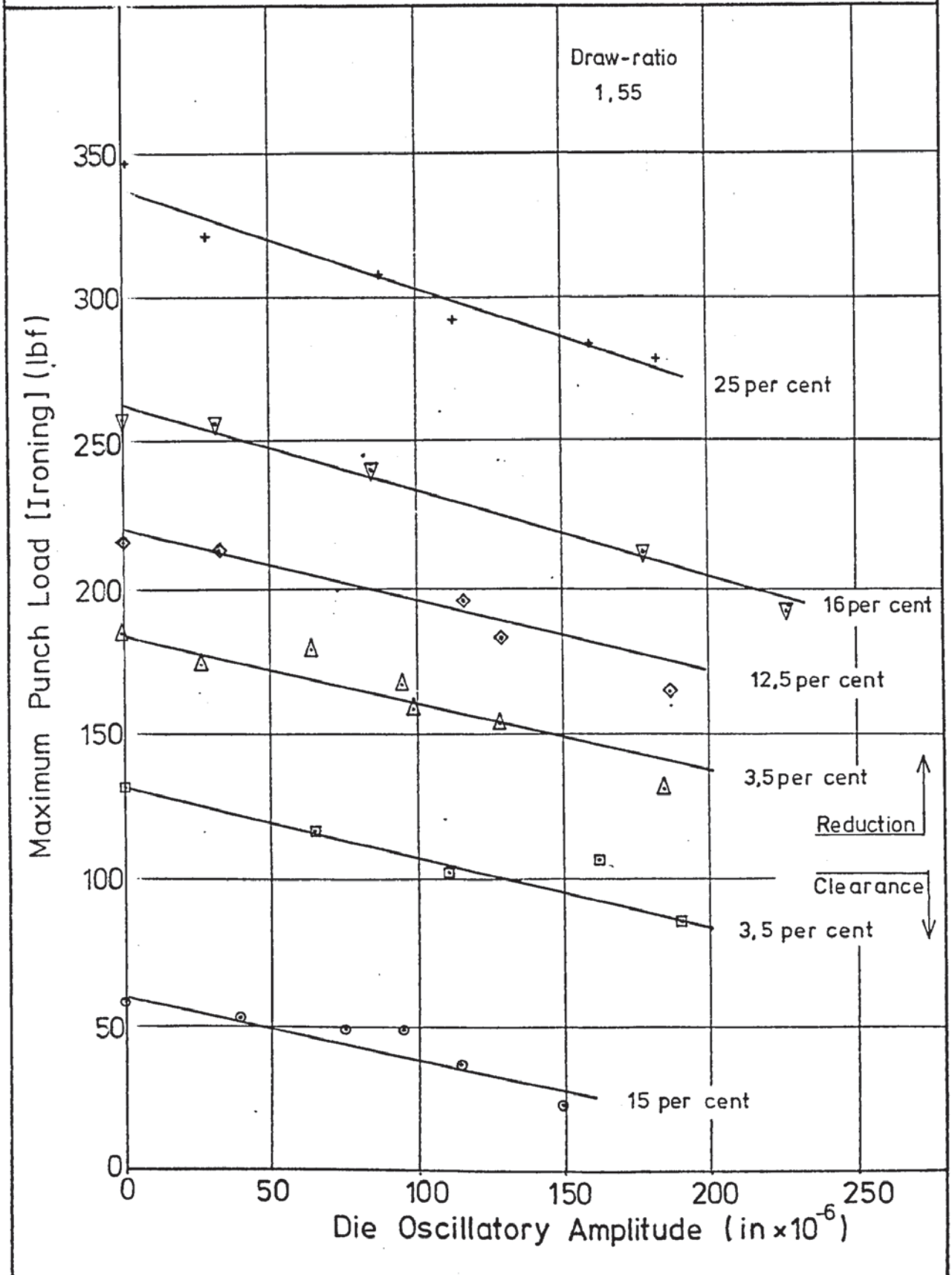

Graph No. 7.3.6.

Draw Ironing Die Separating Force v Draw Ironing Die Oscillatory Amplitude for various Ironing Reductions

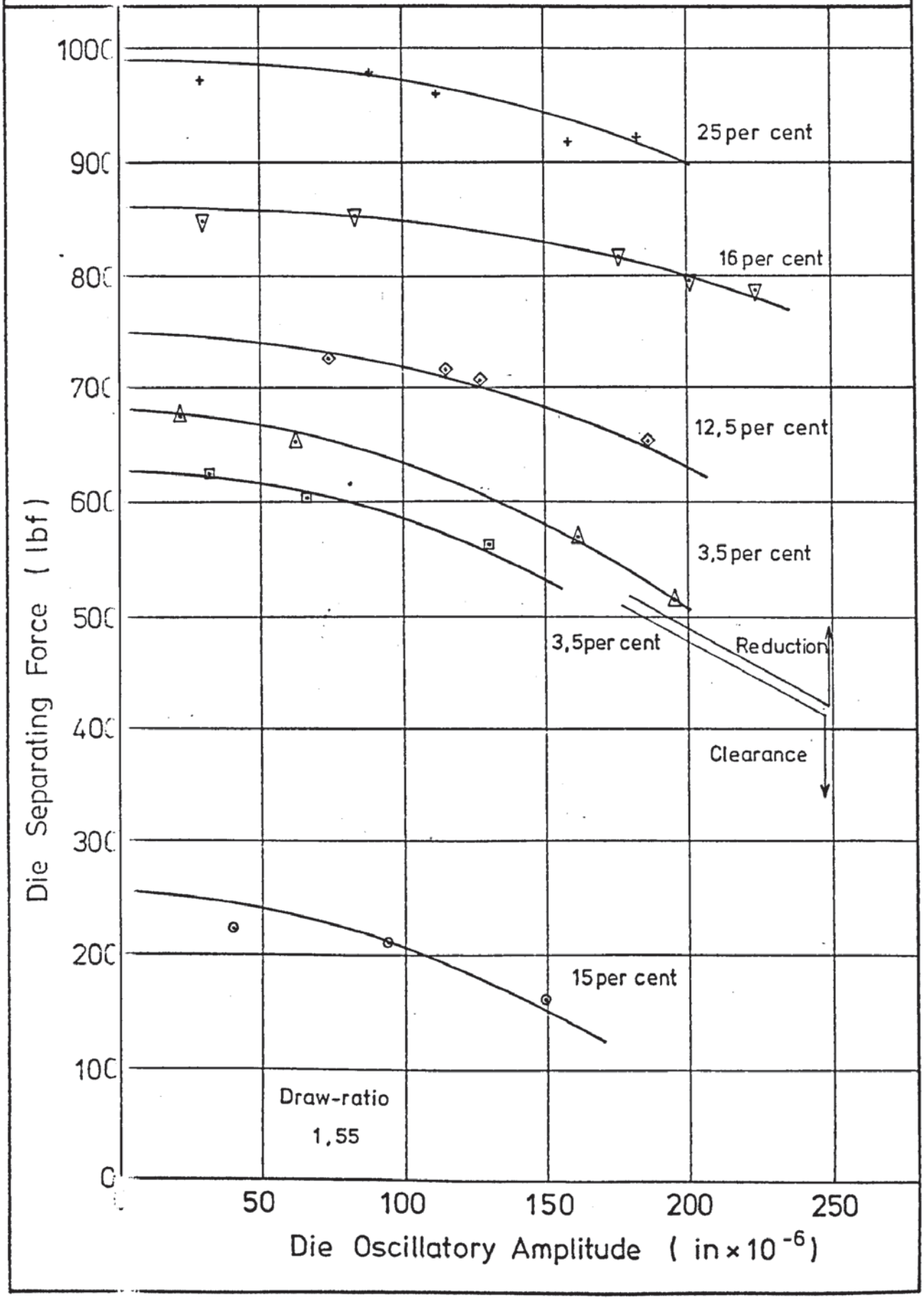

Graph No. 7.3.7.

Effect of Draw Ironing Die Oscillatory Amplitude on the Limiting Draw-ratio for various Ironing Reductions

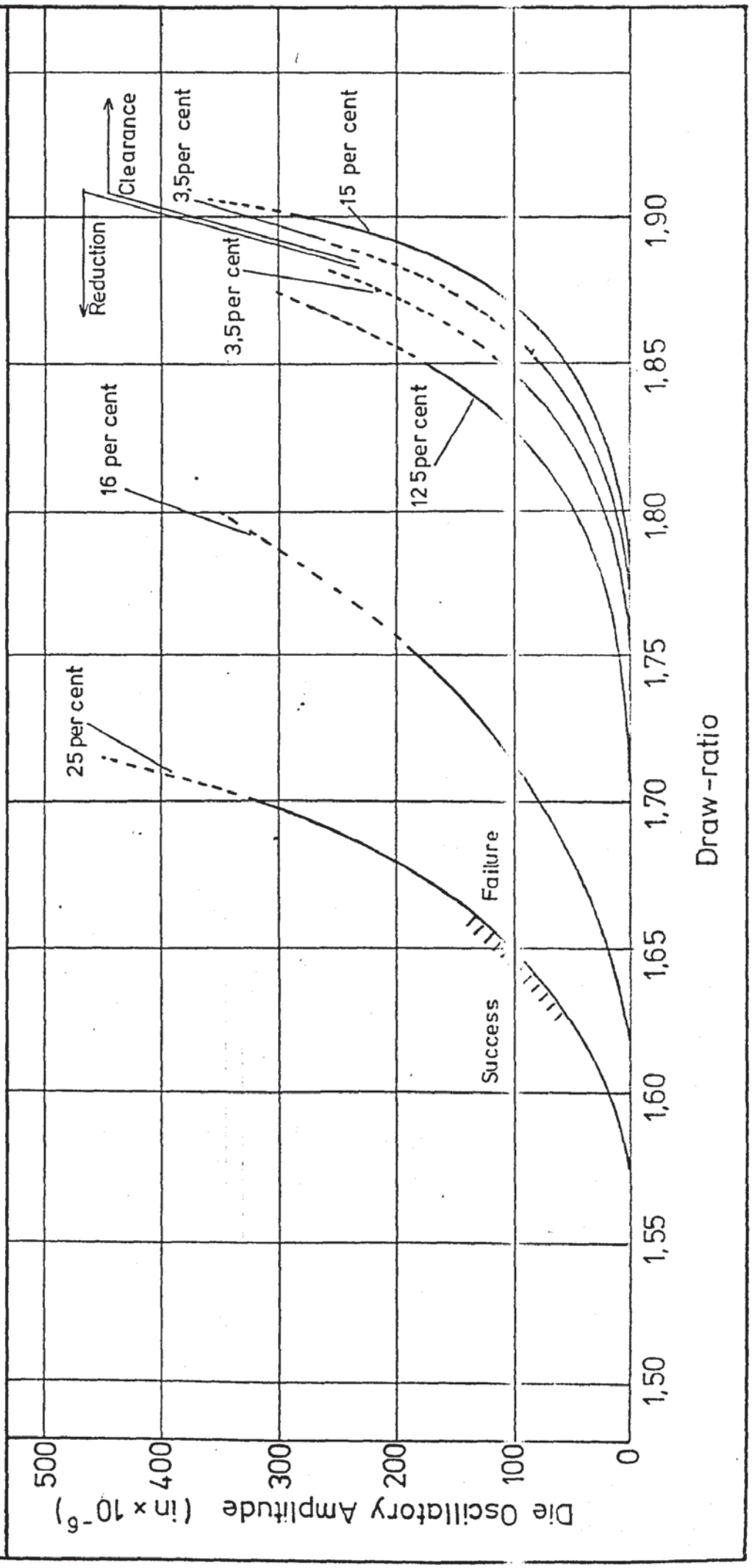

Low Velocity Tests.		Table No.7 5.1.
Test Number.	Maximum Punch Load	Velocity Ratio
40 DI-175-180 V7	294*	53
40 DI-175-260 V7	275*	90
40 DI-175- 60 V5	332*	17
40 DI-175-120 V5	310*	53
40 DI-175-140 V5	287*	58
40 DI-175-180 V5	310*	58
40 DI-175-200 V5	302*	75
40 DI-175-260 V5	283*	96
40 DI-175-140 V3	302*	230

Draw Ratio = 1.75

Ironing Reduction = 12.5 per cent.

* = Specimen Failed.

Tests Using Different Lubricants. Table No. 7.3.2.

Lubricant	Maximum Punch Load.	Velocity Ratio
1. Colloidial M.D.S. in Toluene	325* 344*	57.2 34.5
2. Lanoline	298* 302*	51.2 57.8
3. Colloidial Graphite in oil	313* 313*	54.1 55.9
4. Aludraw No.8	298* 344*	55.1 17.8
5. TD 45	343*	18.0
6. Cindolube	294*	52.7
7. P.T.F.E. Sheet top surface	298*	66.0

Draw Ratio = 1.75

Ironing Reduction = 12.5 per cent

* = Specimen Failed.

Lubricant Suppliers :

1,2 Acheson Colloids Company.

4, Allcard & Company.

5,6 Edgar Vaughan & Company.

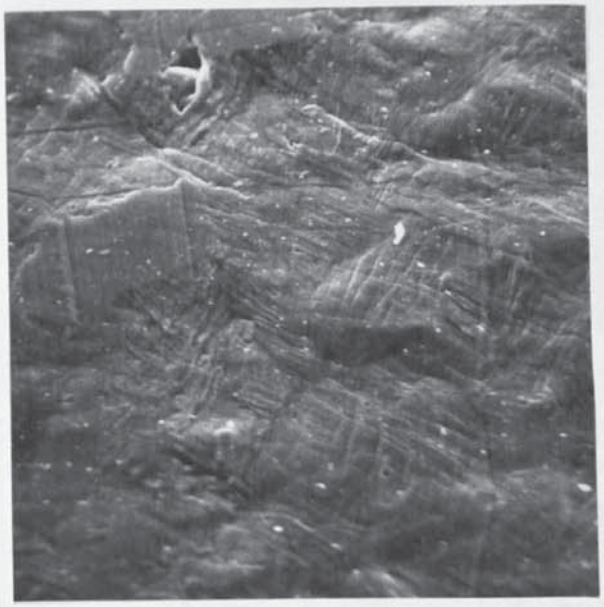

Fig. 7.3.1. DI260 Top x 600

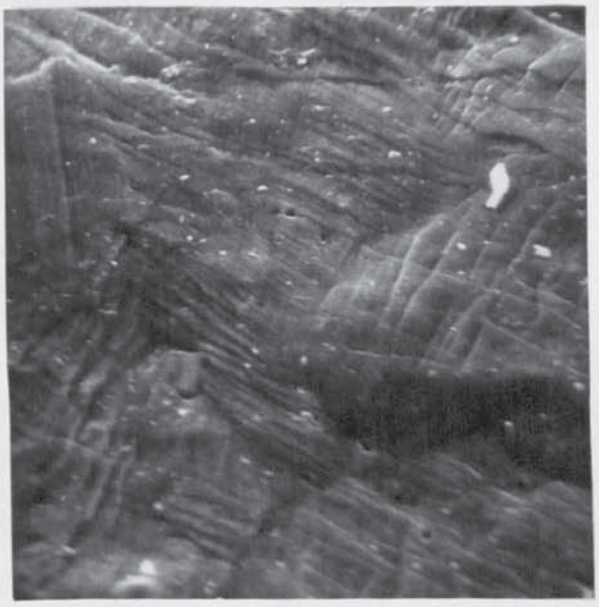

Fig. 7.3.2. DI260 Top x 1.6k

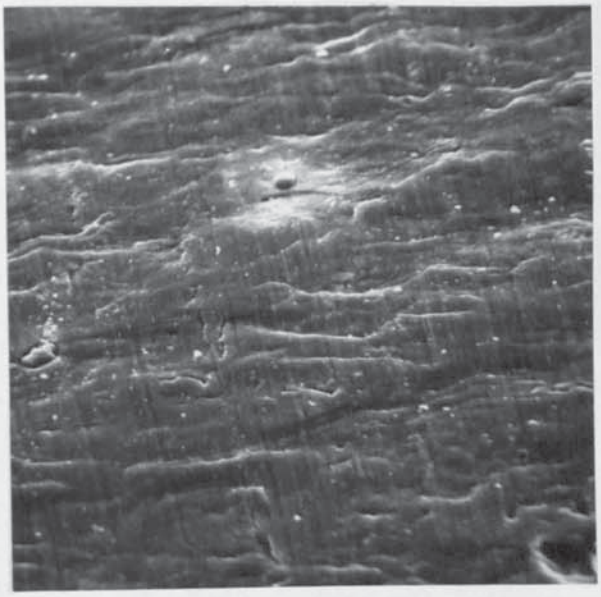

Fig. 7.3.3. DI260 Bottom x 600

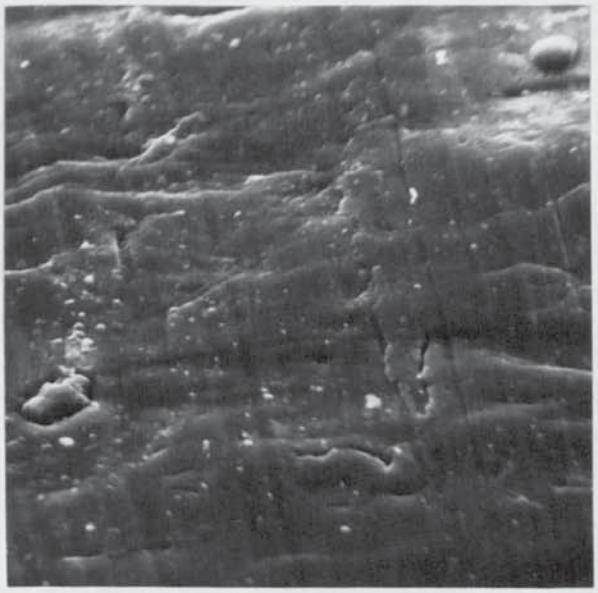

Fig. 7.3.4. DI260 Bottom x 1.6k

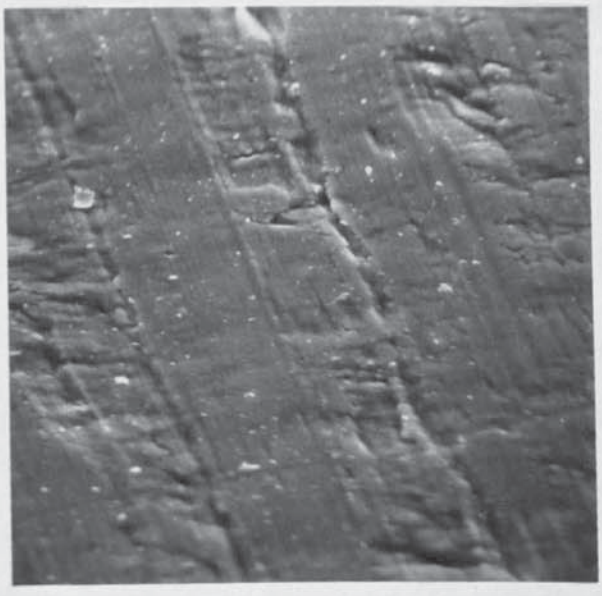

Fig. 7.3.5. DI260 Edge x 600

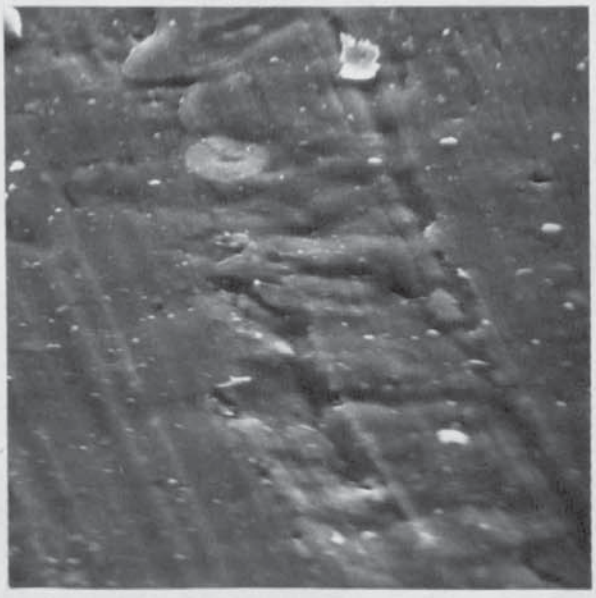

Fig. 7.3.6. DI260 Edge x 1.6k

Graph No. 7.4.1.

Maximum Punch Load v Blank-holder Oscillatory Load for various Draw-ratios

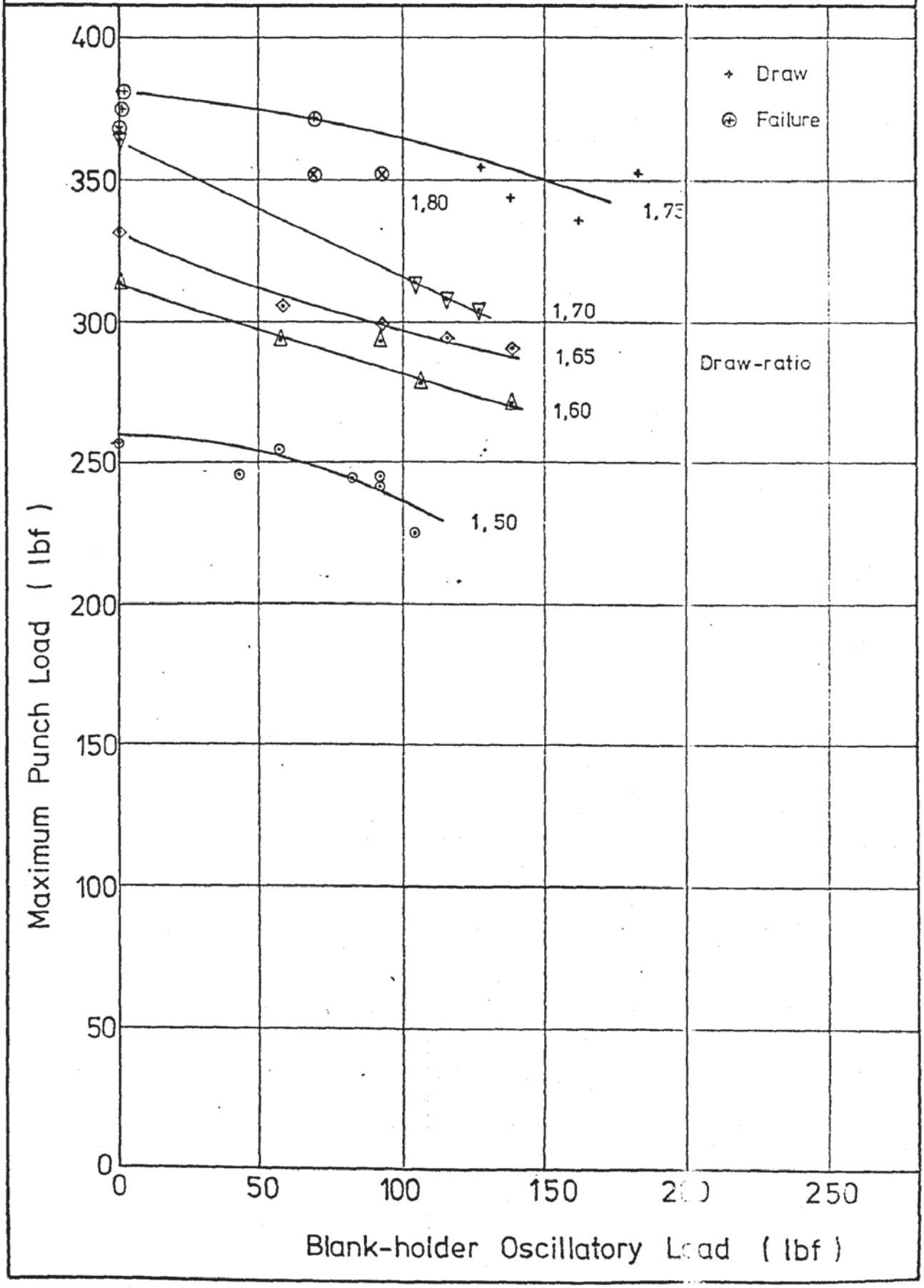

8. DISCUSSION OF RESULTS.

8.1. Punch Vibrations.

The effect of punch oscillatory amplitude upon the maximum punch load recorded during the drawing operation is shown in graph 7.1.1. For each particular draw-ratio as the oscillatory amplitude is increased the maximum punch load decreases in an almost linear manner, the reduction occurring more rapidly at the lower levels of excitation with a tendency to display a more linear relationship as the oscillatory amplitude is increased. The oscillatory amplitude is represented by the velocity ratio which is the ratio of maximum oscillatory punch velocity to the normal drawing velocity.

This trend is repeated for the whole range of draw-ratios tested up to the limiting draw-ratio, i.e., the maximum size of specimen that could be drawn successfully.

The influence of punch oscillatory amplitude upon the blank-holder friction force is demonstrated in graph 7.1.2. This series of curves is obtained at the minimum value of the blank-holder friction force. Comparing the minimum friction force obtained at the higher oscillatory amplitudes with that obtained in the non-vibrated case it can be seen that there is a marked reduction at the higher amplitudes. This reduction in the friction force is not reflected in an improvement in the limiting draw-ratio however because this minimum value of blank-holder friction force does not occur simultaneously with the peak punch load. The ultra-violet record reveals that the minimum friction force occurs early in the draw before the punch load has reached its peak value.

Graph 7.1.3. demonstrates the results of punch oscillations upon the die oscillatory amplitude since it was energy transferred from the oscillatory punch that caused the wedge dies to oscillate. Comparing the die amplitude with the punch amplitude of graph 7.1.2 the low level of energy transfer becomes apparent, the die oscillatory

amplitudes being less than one tenth of the punch amplitudes. At the lower levels of die excitation the blank-holder friction force remains constant at the non-oscillatory level but as the die amplitude rises beyond a certain level a reduction in blank-holder friction force is obtained, this reduction being more marked at the higher draw-ratios. This observation can be explained by considering the ratio of maximum die oscillatory velocity to drawing velocity which, for the particular drawing velocity used in this series of tests, has unity value at a die oscillatory amplitude of approximately 9×10^{-6} in. At values of die amplitude below this the blank-holder friction force remains constant whilst the few results which are at larger die amplitudes do indicate a reduction in the friction force, which agrees qualitatively with the theoretical model proposed to account for the effect of these punch vibrations. The larger reductions of blank-holder friction force obtained at the higher draw-ratios can be considered to be a consequence of the higher punch loading necessary for these draw-ratios. The larger blank-holder loads cause a greater frictional force which, on proportional reduction by the oscillating dies, will give greater friction force reductions at the higher draw-ratios. In addition, higher drawn strip tension will result in a better energy transfer to the wedge dies for a given punch amplitude.

The effect of punch and die vibrations on the blank-holder frictional force has been shown in graphs 7.1.2 and 7.1.3 but the usefulness of this system of applying oscillatory energy to the deep-drawing process must be judged by the effect of the vibrations upon the limiting draw-ratio. Graph 7.1.4 of the maximum punch load against draw-ratio shows, from the experimental data obtained, that an increase in the draw-ratio results in a linear increase in the draw load. As the amplitude of punch vibration is increased so the displacement of the curve to a lower range of maximum punch loads becomes more marked. This load was recorded by an ultra-violet galvanometer, as previously

described in the instrumentation section, and was therefore the mean load representing the mean state of stress in the partially drawn product and not the instantaneous stress within the specimen. An indication of the existence of an instantaneous stress can be deduced from a consideration of the limiting draw-ratio. Both the non-vibrated and punch vibrated specimens at a draw-ratio of 1.80 failed whilst the 1.75 draw-ratio specimens were successfully drawn in both cases. The limiting draw-ratio for these specimens therefore lies somewhere in this range and leads to the conclusion that the reduction in punch load recorded is largely caused by superposition of the alternating stress, due to tool vibration, on that which is steadily applied by the moving punch, the sum of these stresses being that required to draw the non-vibrated specimen. Some contribution to the reduction in the draw-load will be made by the reduction in blank-holder friction force but this is not sufficient to have a noticeable effect upon the limiting draw-ratio.

Graph 7.1.5 represents the reduction in maximum punch load against draw-ratio for various die oscillatory amplitudes, the oscillatory energy being applied to the dies directly. Comparing with graph 7.1.4 the apparent fall in the mean punch load can be observed but in this case there is also an increase in the draw-ratio from a value less than 1.80 to a value between 1.85 and 1.90. This increase in the draw-ratio is clearly beneficial and it also shows that the decrease in punch load is caused by something other than superposition. Comparing the die oscillatory amplitudes obtained with those from graph 7.1.3 the largest amplitude obtained with punch vibrations was below the lowest amplitude used when the wedge-dies were oscillated directly which serves to demonstrate further the reason for this oscillatory punch system being ineffective.

It was noticeable that the drawing oil used to lubricate the specimens which were drawn with ultrasonic vibrations was, on removal

from the wedge dies, discoloured. This discolouration arose from a suspension of metallic particles in the oil and was evidence of surface abrasion caused by the oscillatory motion of the partly drawn specimen. As a result of this appearance a limited number of drawn specimens were examined in more detail using a stereoscan electron microscope; these photographs are reproduced in the previous section as Fig. 7.1.1 to Fig. 7.1.6. The photographs of the surface only cover a fraction of the whole specimen but care was taken to ensure that the section of surface was representative of the whole, both in the preparation of the stereoscan electron microscope sample and in the selection of the particular area of the sample for examination.

Comparing the surfaces of the drawn specimen which were in contact with the blank-holder and die surfaces, the surface in contact with the blank-holder appears to have been subject to more surface agitation than the surface in contact with the die. The surface finish of both die and blank-holder was similar and therefore this surface condition is attributed to relative movement between specimen and blank-holder in excess of that occurring between specimen and die. This condition occurs when the specimen and die oscillate whilst the blank-holder remains stationary. This surface effect was most noticeable when using the higher punch oscillatory amplitudes.

During the testing at the higher draw-ratios it was observed that whilst the specimen drawn under non-oscillatory conditions drew successfully, specimens drawn under oscillatory conditions did occasionally fail at the punch profile radius. The drawing of the specimen through the wedge dies is caused by the tensile stress at the die throat which is provided by the punch and transmitted through the partly drawn specimen to the die throat. The material is bent under tension over the die profile radius between the die throat and the punch profile radius which results in a frictional constraint over

the die radius. The use of an oscillatory punch induces oscillatory stresses into the drawn material which are transmitted up towards the die throat. The peak oscillatory stress is damped out by both internal shear and external friction over the die radius so that the drawing stress at the die throat is less than that at the punch profile radius. Thus the peak oscillatory stresses can cause failure of the strip adjacent to the punch nose radius whilst the stress at the die throat is not greatly affected because of this damped superposition of stresses effect and therefore the drawing of the specimen does not respond to this peak oscillatory stress.

The observation of the signal outputs from the piezo-ceramic crystals on the wedge dies indicated that some ultrasonic power was being transferred from the punch to the wedge dies. This amplitude was much smaller than the punch amplitude, and so consideration was given to ways of increasing the effectiveness of the transfer of energy from the punch to the dies.

During the first series of tests it had emerged that the resonant frequency of the punch system was effectively kept constant by the active mounting system. The resonant frequency of the die system was seen to vary according to the drawn length of the partially deformed specimen despite the very small amplitudes being monitored.

This variation in the resonant condition of the specimen was seen to correspond to the length of the ultrasonic path. To take advantage of the resonant effects it was decided to re-tune the punch system to match the resonant frequency of the die system when an undeformed specimen was in position in the dies and the blank-holder pressure was applied. Under these conditions the resonant frequency was different from that of the unloaded dies due to the changed nature of the boundary conditions for the conical concentrators. Thus the new resonant frequency was determined and the punch system retuned, (the tuning process as described previously),

to match the resonant frequency of the loaded dies. Resonant conditions at the beginning of the draw were considered to be the best compromise since the frictional constraint between the specimen and the blank-holder was at its greatest value soon after the draw started. This observation was noted from the friction load traces of specimens drawn without the application of ultrasonic vibrations.

This new system was now tested in the same manner as the old system. The punch was vibrated at essentially the same range of amplitudes as before but now the resonant frequency was slightly different. The amplitude as transferred to the dies was observed on the oscilloscope as previously. The retuning of the system did give an improvement in the amplitude and the oscillatory amplitude levels were sufficient to give a noticeable effect upon the frictional force; however, this improvement was not reflected by any increase in the limiting draw-ratio.

Throughout all the work on the oscillatory punch, the mean punch load was observed to be reduced by an amount which was dependent upon oscillatory amplitude. This reduction in punch load was suspected of being caused by the stress-superposition effect in which the stress to cause drawing was reached cyclicly and thus if the peaks of this stress were at the drawing stress then obviously the mean stress was at a level somewhere below this drawing stress. Consequently, as a result of the ultra-violet recorder galvanometer being unable to respond to this rapid variation in stress only the mean stress was recorded.

The punch load cell strain-gauge bridge did respond to the ultrasonic frequency as observed on the oscilloscope. Attempts were not made to record this variation in punch loading because of the difficulty in interpreting the results. Instantaneous readings of stress at the load cell were likely to be of little use, i.e., the stress within the partly drawn specimen was required. The approach to this would have been to measure the stress directly with strain-gauges

bonded directly to the strip, but in this particular piece of apparatus it was not practicable because of the very limited space into which gauges could be bonded. In addition, the very short travel that was available for further drawing once the partly drawn specimen, complete with gauge, had been replaced in the wedge dies for drawing would not be sufficient to obtain any meaningful results.

Instead the less direct method of assessing peak stress levels, that is, the effect of the vibrations upon the limiting draw-ratio was selected as being the most reliable method of determining the effectiveness of the process. This method was based upon the concept that under oscillatory conditions the specimen responds to the instantaneous stress levels rather than the mean level. Thus a real effect upon the drawing process will be one which leads to a lower drawing stress, which in turn will mean that a larger draw-ratio can be used before the drawing stress becomes high enough to cause failure in the drawn region of the specimen.

From the results for the punch vibrations it can be seen, however, that over the range of conditions tested no increase in the limiting draw-ratio was detected, despite the slight reduction in the friction force between blank-holder and specimen. The cause of this was insufficient oscillatory amplitude of the wedge dies, a factor that was realised as being critical to the success of the operation. The results, in this respect, were disappointing since the work by Young detected, by means of a tuned punch system, a useful amount of power being transferred from the vibrated wedge dies up into the punch; it was a natural consequence to see if the converse was true.

The analysis of the conditions within the drawing zone during punch vibrations has shown the conditions necessary for friction force reduction to be present, albeit for a smaller proportion of each cycle than that obtained when using die vibrations but despite this the results only indicate the presence of a stress-superposition mechanism which indicates the effectiveness of inducing oscillatory stresses

into the work piece in the region of contact around the punch nose. The energy available for die vibration was unfortunately much below this level, as indicated by the very low level of die excitation with the corresponding lack of effect on the limiting draw-ratio. This problem of energy transfer was realised to be serious but despite this it was hoped that sufficient energy would be available to vibrate the dies with an amplitude sufficiently great to give a friction-vector effect, especially since the work of Young on die vibrations had indicated that the friction-vector effects were detectable at quite low levels of die excitation.

Punch vibrations were from the outset considered to have only a limited chance of success. The process depended upon the transfer of sufficient energy to the tuned die system through the small section of the drawn specimen. This system has as its basic weakness the use of a thin metal specimen, under conditions of plastic deformation, for energy transfer. Devices in which use is made of thin flanges are used extensively as systems which prevent the escape of ultrasonic energy, such as the flange portions of active mounts and nodal flanges, both types of system being used in the equipment for the drawing tests and by the same token it is an ineffective way of transmitting high powers from one large system to another.

8.2. Blank-holder Vibration.

The effect of 'radial' blank-holder vibrations on the deep-drawing process is summarised in Graph 7.2.1. which shows the influence of blank-holder oscillatory amplitude upon the maximum punch load for each draw-ratio under investigation. It can be seen that at the lower draw-ratios the maximum punch load is reduced from its non-oscillatory value as the blank-holder oscillatory amplitude increases, the reductions being less marked at the higher oscillatory amplitudes.

At the higher draw-ratios the specimens begin to fail under non-oscillatory conditions whilst under oscillatory conditions, providing there is sufficient oscillatory power, the maximum punch loads are reduced to a level which enables the draws to be successful. This trend continues with failures beginning to occur at the lower oscillatory amplitudes and finally failures occurring under all drawing conditions at the highest draw-ratios since frictional assistance alone cannot reduce the tensile drawing stress sufficiently to avoid failure. In Graph 7.2.2., maximum punch load against draw-ratio the effect of the vibrations in reducing the maximum punch load to below the non-oscillatory value and thus reducing the severity of the drawing operation can be clearly seen. From both of these graphs it can be seen that the greatest effects of the vibrations occur at the lower amplitudes, the maximum punch load showing little change with amplitude at the highest amplitudes tested.

The non-vibrated specimens fractured at a draw-ratio of 1.70 whereas when the blank-holders were oscillated the specimens at a draw-ratio of 1.90 could be drawn successfully provided the oscillatory amplitude was high enough.

At the draw-ratio of 1.95 all of the samples failed apart from some of those drawn at the highest oscillatory amplitude. Thus the limiting draw-ratio using ultrasonic vibrations was somewhere between 1.90 and 1.95, this being an increase of over 12 per cent. The maximum punch load varied with oscillatory amplitude and as the limiting

draw-ratio was approached reductions of up to 30 per cent were recorded. The reductions in punch load at the highest draw-ratios tested were quite small because of the premature failure of the specimen.

The effect of blank-holder oscillatory amplitude on the die separating force is shown in Graph 7.2.3. The maximum compressive force was reduced with increasing oscillatory amplitude because of the effective friction reduction on the top surface of the blank-holder. The results obtained from this load cell exhibited some scatter which is attributed to the fact that the load cell was not measuring the blank-holder friction in isolation but as a combination of forces including the force necessary to deform the material, which was larger than the friction force being monitored.

For the same 'Variac' setting on the ultrasonic generator, i.e. similar electrical energy input, lower oscillatory amplitudes were obtained when drawing the larger specimens. This observation was attributed to the greater initial loading on the blank-holders caused by both the higher blank-holder load necessary to maintain a constant initial pressure on the blank and the higher forces necessary to deform these larger specimens.

The influence of blank-holder oscillatory amplitude on the reductions in the die separation force obtained was reduced at the higher oscillatory amplitudes because of the large oscillatory velocity to drawing velocity ratio which existed at these amplitudes. Referring to Figs. 3.3.2 and 3.3.3 the influence of a drawing velocity several hundred times less than the peak oscillatory velocity can be seen to have little influence upon the proportion of the half-cycle during which friction reversal can occur. Thus the friction reduction obtained was virtually at its maximum value at the higher blank-holder amplitudes tested.

Further information on the maximum effect of the blank-holder vibrations was obtained from the limited number of low-velocity tests

undertaken. The results of low-velocity tests upon draw-ratios of 1.90 and 1.95 which had been found to be near the limiting drawing conditions under oscillatory blank-holder drawing at normal velocities are presented in Table 7.2.3.

The use of low velocities in these tests enabled greater oscillatory velocity to drawing velocity ratios to be examined. No improvements in the limiting draw-ratio or the die separation force reduction were obtained. This confirms the observation made at normal drawing speeds that the blank-holder vibrations have a rapid effect at the lower amplitudes which becomes almost constant at the higher amplitudes. At the lowest drawing velocity tested the specimens failed because of galling of the strip in contact with the blank-holder surface.

The die separation force load cell recorded the component of the drawn strip tension in the horizontal direction. Initially, as the punch contacted the undeformed wedge specimen the central portion of the specimen was displaced from its horizontal plane as it was formed over the punch nose and die radii. This process also rotated the direction of the strip tension force from horizontal to almost vertical, the vertical direction only being achieved in zero clearance tooling.

Initially, the die separation force load cell was subject to a compressive load which reached a maximum at about 0.25 in. of punch travel at which point the specimen was established over the punch nose. As the punch advanced further the specimen was drawn over the die radius and the strip tension increased as a result of the more severe bending and unbending operations. At the same time, the line of action of the strip tension moved towards the vertical plane. This resulted in the compressive horizontal force acting on the die separation force load cell being reduced because of the changing direction of the strip tension. In addition, the resultant force from the pressure of the drawn strip over the die radius had a tensile

component in the horizontal direction. The effect of this force on the die separation load cell was to reduce the initial compressive force and this continued as the force became tensile as the maximum punch load was reached.

Under oscillatory conditions changes in frictional conditions were indicated by variations in the die separating force. The effect of blank-holder vibrations was to reduce the effective friction force on the top surface of the blank which reduced the drawn strip tension and in so doing the initial compressive stress on the die separating force load cell was reduced. Further into the draw, when the strip tension was producing a tensile die separation force, the reduction in the strip tension caused by the vibrations lowered the tensile stress acting on the die separating force load cell.

The results of the intermittent tests carried out on the whole range of draw-ratios demonstrated the effects of the application of vibrations on each particular specimen, Table 7.2.1. The switching mechanism was arranged to apply the vibrations for periods of 0.1 sec. with equal periods without vibrations interposed between, the drawing process starting without vibrations.

The non-oscillatory punch loads recorded in the intermittent tests were greater than the corresponding loads recorded during a non-vibrated test, which was considered to be caused by the transition from sliding friction during oscillatory drawing to the static friction, which had to be overcome during the non-oscillatory period.

The intermittent tests could not be used to determine the effects of vibrations on the limiting draw-ratio because the specimens all failed when the vibrations were switched off once the non-oscillatory limiting draw-ratio was exceeded. Failure did occur with the intermittent tests at a lower draw-ratio than when drawing without vibrations. This was considered to be caused by the effect of the suddenly applied load, when the vibrations were switched off, giving rise to greater stresses in the drawn strip than those during

the normal non-oscillatory process.

Under these experimental conditions the draw-ratio was reduced from 1.70 for normal non-vibrated drawing to 1.65 for drawing with intermittent application of blank-holder vibrations.

The results of the tests using various lubricants are shown in Table 7.2.2. The draw-ratio chosen for the oscillatory tests was 1.80 so that the drawing operation would be quite severe. The use of different lubricants under oscillatory conditions did not have any marked effect upon the punch load, all the specimens were drawn successfully when the oscillatory amplitude was similar to that using the normal drawing oil. Under non-oscillatory conditions the specimens all failed with the exception of those drawn using a film of P.T.F.E. between the top surface of the blank and the blank-holder. This use of P.T.F.E. film was extended to determine the limiting draw-ratio under these conditions. It was found that using this method the improvement in the limiting draw-ratio was almost as great as that obtained with blank-holder vibrations.

From these tests it was concluded that using P.T.F.E. film gave a friction reduction effect on the top surface of the blank similar to that obtained when using blank-holder vibrations.

The effect of 'radial' die vibrations applied to the wedge dies has been reported by Young[65] to give increases in the depth of draw of approximately 20 per cent. This was attributed to a reduction in the frictional force on the top surface of the specimen and also the friction over the die radius was shown to be reduced by the die oscillations. The assumption made during this drawing process was that the specimen and die moved with the same oscillatory motion. When the dies were moving towards the punch the friction force acting on the top surface acted in the conventional direction whilst when the dies were moving away from the punch the friction force on the top surface was reversed. The reversal of the specimen motion was ensured by the wedge of the die which prevented relative movement of the specimen

in the die. This mechanism is unique to the wedge drawing process because in the cup drawing operation there is not the same positive constraint on the sample forcing it to move away from the punch during the half-cycle when the drawing takes place. Thus in the cup drawing operation the blank may not move away from the punch with the same amplitude of oscillation thus reducing the friction vector reversal effect on the top surface of the specimen.

The criticism that wedge drawing with 'radial' die vibrations could be a more effective process than the corresponding axi-symmetric operation because the different methods of causing the blank to oscillate does not apply to the application of 'radial' vibrations to the wedge blank-holders. This is because with blank-holder vibrations the blank-holder is free to oscillate over the surface of the specimen in both the wedge and axi-symmetric drawing processes.

The surfaces of the drawn specimens were examined using a Stereoscan Electron Microscope, in order that the proposed oscillatory mode could be further substantiated. Samples from the top, bottom and edge of drawn specimens were examined from both the vibrated and non-vibrated tests.

The non-vibrated samples showed similarities between the top and bottom surfaces after drawing, the bottom surface which was in contact with the die showing slightly more surface disruption because of the additional contact over the die radius. The surface at the edge of the specimen still retained the markings characteristic of the milling operation used in the production of the wedge specimens, despite the drawing through the wedge dies. These photographs are reproduced in Figs. 7.2.1 to 7.2.6 respectively.

Under oscillatory conditions the underside of the specimen in contact with the die retained the rolling marks present on the undeformed blank as in the non-vibrated case. The top surface had little original surface marking because of the oscillatory motion of the blank-holder which was in contact with this surface. The

condition of the edge of the specimen appeared unchanged, again retaining the machining marks from the specimen preparation. The photographs of these surfaces are reproduced in Figs. 7.2.7 to 7.2.12.

A difference between the drawing process with and without vibrations was demonstrated by the appearance of the samples drawn during the intermittent testing. The drawn samples had bright and dull bands across the top face corresponding to the periods with and without vibrations. The photographs of these bright and dull bands, however, do not reveal any noticeable difference in the surfaces at high magnification which demonstrates that during intermittent testing the surfaces are only slightly affected because of the short time interval for which the vibrations are applied. The Stereoscan photographs are reproduced in Figs. 7.2.13 to 7.2.18.

Hardness tests were performed on specimens drawn with and without the application of ultrasonic vibrations. The details of the testing procedure are contained in Appendix A.5.2 and the results of the tests on specimens drawn with blank-holder vibrations are shown in Tables A.5.2 to A.5.2.3 of this Appendix.

For a draw-ratio of 1.55 the complete range of samples which were drawn at various blank-holder oscillatory amplitude levels were hardness tested at intervals of 0.1 in. along the specimen. The hardness of all the samples increased with the distance up the 'wall' of the specimen which was due to the increasing amount of deformation which the material high up in the cup wall had undergone.

On comparing the hardness at the same point for samples drawn with different levels of ultrasonic excitation there was no noticeable difference between the specimens drawn either with vibrations or without vibrations.

These hardness tests were carried out immediately after deformation and they were repeated a few days later. This was to ascertain if any temporary changes were made to the material properties during

oscillatory drawing.

Hardness tests were performed on the 'bright' and 'dull' banded specimens obtained when drawing with vibrations applied intermittently. Once again no changes between the two sections were detected, only the increasing hardness as the height up the 'wall' of the specimen increased.

Thus, within the limitations of the hardness test as a measure of mechanical properties, all the tests performed indicated that the vibrations had not overheated the samples or affected their subsequent mechanical properties.

The processes of wedge drawing with both die vibrations and axial punch vibrations are discontinuous drawing processes. Drawing, with die vibrations, only took place during the half-cycle when the dies were moving apart the oscillatory velocity being greater than the drawing velocity for the majority of the other half-cycle when the dies were moving together. The blank-holder frictional force was, therefore, always assisting the drawing process since when it was acting in the conventional direction the specimen was not being drawn. The tensile stress in the drawn section of the specimen was, therefore, always below the normal drawing stress because of the frictional force assistance.

The drawing process with blank-holder vibrations is continuous since the velocity of the specimen within the wedge dies is not affected by the blank-holder oscillatory movements. Thus the drawing process is assisted by the friction force for up to one half of the oscillatory cycle, the friction acting in its normal direction for the other half-cycle. The drawing stresses are therefore acting conventionally for over one half of each oscillatory cycle. The increase in the limiting draw-ratio shows that blank-holder vibrations have a real effect on the process despite the period of peak stresses during each cycle. It is therefore as if the material responds to the mean drawing stress.

8.3. Draw Ironing Die Vibration.

The effect of 'radial' die vibrations upon the frictional force acting between the top surface of the specimen and the blank-holder is shown in Graph 7.3.1. Once the velocity ratio between the maximum oscillatory velocity and the drawing speed was increased beyond its unity value, corresponding approximately to an oscillatory amplitude of 9×10^{-6}in. at the normal (maximum) drawing speed, the friction-vector reversal mechanism commenced. With further increases in the oscillatory amplitude the effective frictional force was rapidly eliminated.

This rapid reduction of the frictional force with increasing oscillatory amplitude is reflected in the maximum punch load curves, Graph 7.3.2. For the ironing reduction selected of 12.5 per cent of nominal starting gauge, the maximum punch load recorded was that primarily associated with the drawing operation. A secondary peak resulting from the ironing operation also occurred, at a later stage of the draw. The levels of oscillatory amplitude achieved at the lower draw-ratios were sufficient to maximise the reduction in punch load that could be achieved by the 'radial' vibrations.

As the draw-ratio increased, the maximum amplitude that could be achieved with the higher loading on the dies was reduced and this prevented the maximum reduction in the punch load that was possible from being obtained.

As the specimen size and hence maximum punch load was increased the specimens began to fail, first under non-oscillatory conditions and, finally, at the highest draw-ratio, under all drawing conditions.

The effect of die oscillatory amplitude on the improvements in the limiting draw-ratio is more readily seen in Graph 7.3.3 which demonstrates the higher punch load necessary as the draw-ratio was increased.

The increase in the punch load as the draw-ratio was increased caused failure in the non-oscillatory case at a draw-ratio of 1.65.

As the velocity ratio was increased the assistance this gave to the process reduced the punch load thus enabling the limiting draw-ratio to be increased to bring the punch load back to its former level. At the highest velocity ratio tested the limiting draw-ratio was 1.85, an increase over the non-oscillatory case of 12 per cent.

In the ironing part of the process the die separating force increased towards the top of the specimen 'wall' as a consequence of the natural thickening due to 'radial' drawing within the wedge dies. The application of oscillatory amplitude had little effect upon the die separating force as shown in Graph 7.3.4. A reduction in the die separating force with increasing oscillatory amplitude is shown but this is considered to be an apparent reduction. This reduction resulted from stress-superposition effects within each oscillatory die system giving a mean load lower than the peak oscillatory load.

As the draw-ratio was increased the increases in the die separating force observed were due to the heavier ironing reduction undertaken. This increased reduction was necessary because the maximum specimen 'wall' thickness increased with the higher draw-ratios.

The values of die separating force obtained from these two load cells did exhibit some scatter. This was considered to be due, in part, to the characteristics of the load cells which, as explained in Section 5.3.6., were affected by hysteresis effects.

The effect of die oscillatory amplitude upon the maximum ironing punch load is shown in Graph 7.3.5. The family of curves were obtained with a draw-ratio of 1.55 which was chosen in order that a wide range of ironing reductions could be obtained without specimen failure. The reduction in the maximum ironing punch load has an almost linear relationship with the oscillatory amplitude although the relationship at low oscillatory amplitudes was not examined. There could be some non-linearity caused by the finite oscillatory

velocity necessary before the reversed flow mechanism described in Section 3.6.2. could occur. The maximum ironing punch load at the light reductions was much smaller and separate from the maximum punch load due to the drawing process. As the ironing reduction increased the maximum ironing punch load increased more than the drawing load, initially, because the ironing reduction at the maximum drawing load was reduced by the natural thinning which occurs during the drawing operation.

The corresponding family of curves which relate to the die separating force at this maximum ironing punch load are shown in Graph 7.3.6. These have the same form as Graph 7.3.4.

Assembling the data from all the various ironing reductions tested onto one graph, Graph 7.3.7., the dependence of the limiting draw-ratio upon both oscillatory amplitude and the ironing reduction can be seen.

The draw-ratio of 1.90 was only attained when the tooling was set to give a clearance of 15 per cent of the nominal starting gauge. At this clearance there was no ironing, initially, because of thinning due to bending and unbending over the die radius. Ironing began approximately three-quarters of the way up the 'wall' of the drawn sample. Comparing this result with those of the blank-holder vibrations, Graph 7.2.1., it can be seen that using blank-holder vibrations, a draw-ratio of 1.95 was accomplished. The effects of 'radial' die vibrations, therefore, appear inferior to blank-holder vibrations, but, a direct comparison between these results is not considered valid mainly because of the different wedge dies that were used in each case. Different batches of specimen material were used which, although of the same commercial specification, could differ sufficiently to affect the results in this way. 'Radial' die vibrations are considered to be more effective because of the friction reduction over the die radius, which was demonstrated by Young. In addition, when examining blank-holder vibrations it was shown to be

possible to eliminate the effect of friction by causing it to act both in the drawing direction and opposite to the drawing direction, for equal periods. Die vibrations, in wedge drawing, however, caused intermittent drawing with the majority of the drawing taking place when the frictional force was assisting the drawing operation.

The examination of the surfaces of a specimen leaving the wedge die using a Stereoscan Electron Microscope revealed marked differences between the top and bottom surfaces. The top surface, Figs. 7.3.1. and 7.3.2. can be seen to have been subjected to a greater degree of surface disruption than the bottom surface, Figs. 7.3.3. and 7.3.4. This is attributed to the motion of the specimen which under the action of die vibrations was forced to reciprocate over the blank-holder (top) surface. The bottom surface in contact with the die was only subject to the radial drawing in action and thus retains more of the original surface markings.

At the light ironing reductions examined it can be seen that because of the natural thinning in the drawing operation, increases in the ironing reduction only affect the ironing punch load maximum and, therefore, the limiting draw-ratio is not affected.

The maximum ironing reduction that was successfully undertaken was 25 per cent. At this reduction the use of 'radial' die vibrations increased the limiting draw-ratio from 1.55 to 1.70, an increase of 10 per cent. The height of the 'wall' of this ironed specimen was increased by over 33 per cent.

The highest ironing reduction examined was 55 per cent although no specimens were successfully drawn at the draw-ratio of 1.55, which was the only one tested. The application of die oscillations did, however, extend the period of drawing and ironing before failure occurred.

The results of the tests during which the oscillations were applied intermittently followed a similar pattern to the normal tests. When the vibrations were switched off the punch load rose

to a value equal to that obtained in a non-vibrated test. Once the specimen sizes were above the non-vibrated limiting draw-ratio the specimen failed during the intermittent tests when the vibrations were switched off, demonstrating the lack of any permanent effects upon the specimen. Under both non-vibrated and intermittent tests the limiting draw-ratio was the same. These observations differ slightly from those made during blank-holder vibrations when intermittent testing was found to lower the limiting draw-ratio occasionally. This difference could be due to the lower blank-holder frictional forces which acted in the draw ironing process as a result of the operation being limited to smaller specimen sizes.

A typical ultra-violet trace obtained during an intermittent test is reproduced in Fig. 6.3.1. The reduction of the punch load obtained on the application of the die vibrations can be seen to become much less effective as the die separation force was increased. In this ironing region the loading on the dies caused a considerable reduction in the oscillatory amplitude which could not be entirely compensated for by increasing the output from the ultrasonic generator.

In order to examine the effects of increasing the oscillatory work done on the system, a limited number of low drawing velocity tests were performed. The results of these tests are presented in Table 7.3.1. A combination of ironing reduction and draw-ratio that was critical was selected in order that improvements to the process would be reflected by an increase in the limiting draw-ratio. This increase in the velocity ratio was primarily intended to enlarge the proportion of oscillatory work in the ironing process, although the effectiveness of the drawing process also was increased. The increase in the velocity ratio was not sufficient to affect the limiting draw-ratio, however, although at the highest velocity ratio obtained the punch travel was increased before failure occurred.

Some tests were performed in which the oscillatory frequency was

altered manually during the drawing operation. On analysing these results it was found that the resonant frequency of the loaded die system varied throughout the drawing operation. An automatic frequency control unit for the ultrasonic generator was available and this unit was temporarily fitted in order to determine if the resonant conditions could be maintained. Tests performed with the oscillatory frequency automatically controlled by this unit were found to result in failure, however, whilst the same test performed using the resonant frequency set at the beginning of the draw was successful.

This deterioration in the limiting draw-ratio was considered to be caused by a number of factors, some of which were not the fault of the automatic control unit.

In use the fluctuation in the oscillatory amplitude was reduced in comparison with a normal test although it was evident that the overall level of oscillatory amplitude was reduced. The greatest fault, however, was that the two die systems had slightly different resonant frequencies. This difference was normally compensated for by driving the transducers at the frequency which was midway between the two systems, so that both dies were operating at a slightly off-resonant frequency. With the automatic frequency control, however, the feedback signal was taken from a piezo-ceramic crystal on one of the dies. Thus the resonant frequency of one of the dies was maintained but the other die, which did not control the system, was forced into a non-resonant condition and consequently the oscillatory amplitude was reduced considerably. This particular problem would not arise in the cup drawing operation since there would be only one oscillatory system. Another fault with the system was that it was sensitive to transient vibrations. When the dies were momentarily relieved of the blank-holder pressure as the periphery of the specimen disappeared over the die radius, the oscillatory amplitude rose rapidly. This rise could cause the

a.f.c. unit to operate at multiples of the resonant frequency with a resultant reduction in the oscillatory amplitude.

The use of this unit was therefore discontinued, mainly because of the problems outlined which were peculiar to this wedge drawing apparatus. Such a system if it was controlled correctly could provide useful assistance to the drawing operation.

The method of increasing the height of the ironed wall by increasing the blank size is limited by the maximum draw-ratio which can be used. This range of blank sizes is reduced with increases in the ironing reduction as shown in Graph 7.3.7. As the ironing reduction is increased from zero, light reductions can be undertaken without affecting the drawability of the material since the additional work is only required after the maximum punch load has passed. Once the ironing reduction exceeds the natural thinning which occurs at the bottom of the wall the maximum drawing load is increased. This affects the limiting draw-ratio because the ironed wall can no longer support the total tensile load required and failure therefore occurs.

The reversal of material flow over part of the ironing die proposed to account for the improvements to the ironing process can on consideration of Figs. 3.6.6. and 3.6.7. be seen to have the ability to decrease the work done by the drawing stress and instead introduce this work through the oscillatory dies. Under conventional conditions the force within the die resulting from the frictional constraint over the surface and the die pressure normal to the surface acts against the drawing load. If the direction of the friction force is reversed the component of the resultant force which acts in the upstream direction will be reduced. For low die angles and a high coefficient of friction this resultant, inclined at the angle of friction, would have a component acting in the downstream direction thus assisting the ironing process by forcing the material through the die. Thus, providing there is a reversal

of flow within the die there will be some assistance given to the ironing process. The section within the die over which flow reversal occurs is affected by the drawing velocity and the oscillatory amplitude since both of these parameters affect the rate of change of the volume of material in the die. For a large oscillatory die volume change and a low drawing velocity the flow reversal would occur over much of the die surface thus giving a large reduction in the drawing stress. This effect was considered to be limited only by the amount of work which could be introduced through the oscillatory dies. The limitation on the maximum reduction possible was therefore considered to arise in the drawing operation, therefore attempts were made to improve this part of the process.

The results of draw ironing tests using various lubricants are shown in Table 7.3.2. The same ironing reduction and draw-ratio as used in the low velocity tests was used in order that any real improvements in the limiting draw-ratio could be easily seen. The same range of lubricants as had been used in the blank-holder vibration tests was used. No improvements in the limiting draw-ratio were obtained however, demonstrating the similar effectiveness of all the lubricants under these conditions.

The use of P.T.F.E. sheet on the top surface of the specimen which had been of assistance in the blank-holder vibration process had not, however, resulted in any improvement to the draw ironing process. It was considered that this difference arose because the blank-holder vibrations effectively eliminated the frictional force whilst die vibrations used this frictional force to assist the drawing process. Therefore, the virtual elimination of the frictional force on the top surface was detrimental to the draw ironing process.

At the same draw-ratio and ironing reduction as the lubrication tests a sample was successfully drawn without vibrations when the top and bottom faces were lubricated with P.T.F.E. film. This

improvement was attributed to the reduction in the friction force acting between the blank and die and therefore further tests using various combinations of P.T.F.E. and lubricant were performed. The results are presented in Table 7.3.3.

These results all reflect changes in the frictional conditions acting on each of the specimen faces. The use of P.T.F.E. on the bottom and oil on the top surface of the specimen enabled the draw-ratio to be increased from 1.70 to 1.80 when frictional assistance was provided by the oscillating dies.

On extending the P.T.F.E. lubrication around the edge of the specimen the frictional conditions were further eased. This enabled a similar increase in the limiting draw-ratio to be achieved without the use of vibrations. This particular test demonstrated the important influence that edge friction has in the wedge drawing process which was demonstrated in section 3.2.1.

This final series of tests further illustrated the influence of the drawing operation within the draw ironing process and also the frictional constraints which still apply even when friction on the top surface of the blank has been eliminated by the die oscillations.

Hardness tests performed upon samples ironed with and without vibrations using both oil and P.T.F.E. lubrication are listed in Appendix A5 Table A.5.2.4.

The hardness increased up the 'wall' of the specimens because of the increased deformation but the comparison between the four specimens produced under different conditions did not reveal any major differences in hardness.

8.4. Blank-holder Swaging.

The effect of applying a low frequency oscillatory blank-holder pressure to the deep-drawing process is shown in Graph 7.4.1. This shows the effect the variations in the blank-holder load have upon the maximum punch load for various draw-ratios.

In use the static blank-holder pressure was set to some intermediate value and the oscillatory pressure increased until the peak pressure was equal to the static pressure normally applied. The effects of such oscillatory blank-holder pressures were to reduce the maximum punch load according to the pressure amplitude used. The pressure produced by the hydraulic jack did not reproduce the sinusoidial motion of the actuator piston rod, but was distorted to become a series of sharp pressure peaks, each peak corresponding to the compressive movement of the jack. During drawing the increase in the blank-holder pressure produced a corresponding rise in the punch load and friction load cell readings. The marginal improvement in the limiting draw-ratio which was increased from 1.75 to 1.80 was considered to result from changes in frictional forces within the wedge dies.

The oscillatory blank-holder pressure never exceeded the static pressure that was normally applied and therefore the friction force considered over a complete oscillatory cycle would be reduced both on the top and bottom surfaces of the specimen. When considered over the complete cycle the effective friction force would therefore be reduced from its non-oscillatory value. The yielding situation within the wedge dies would not be assisted by the oscillatory blank-holder pressure since this never rose above its non-oscillatory value. The effect of this pressure was to reduce the load on the deforming specimen within the wedge dies with similar results to those shown in Appendix A4, Graph A.4.1. The periodic re-application of the blank-holder pressure up to its non-oscillatory value was sufficient to resist the formation of wrinkles.

This system although effective was different to that described in section 3.6. In this section a blank-holder swaging mechanism was described which would enable the punch load to be reduced not only by the reduction in blank-holder pressure as previously described but also by maintaining the thickness of the deforming blank at its starting gauge whilst still in the wedge dies. The effectiveness of this system was limited by the amount of extrusion which could take place. This was dependent upon the thickening of the blank at any position in the draw, since if there was no thickening the vibrations would be ineffective. Such a system would not function with the hydraulically controlled blank-holder pressure because the rigidity necessary to deform the blank could not be achieved with the hydraulic system.

The low frequency pressure pulses used in this series of tests were not, therefore, considered to create a situation truly representative of oscillatory metal deformation. Their use was considered because only simple modifications to the wedge drawing apparatus were required to enable this system to be examined.

9. CONCLUSIONS.

9.1. Punch Vibration.

The application of axial punch vibrations to the deep-drawing process resulted in reductions of up to 30 per cent in the mean punch load being obtained. These reductions were attributed to stress super-position effects because such reductions in punch load were not reflected by any improvement in the limiting draw-ratio established under non-oscillatory conditions.

When the punch and dies had the same resonant frequency the application of oscillatory power to the punch did result in a transfer of power to the wedge dies but this was not sufficient to make any noticable improvements in the process.

9.2. Blank-holder Vibration.

The application of 'radial' blank-holder vibrations resulted in a friction reduction effect upon the top surface of the specimen in contact with the blank-holder. This friction reduction reduced the punch load and also enabled the limiting draw-ratio to be increased.

Over the range of draw-ratios and oscillatory amplitudes tested reductions in punch loads of up to 30 per cent were recorded whilst the limiting draw-ratio was raised from 1.75 to 1.95, an increase of 12 per cent.

9.3. Draw Ironing Die Vibration.

The use of 'radial' die vibrations in the draw ironing operation increased the reduction that could be achieved. At a gauge reduction of 25 per cent of the nominal starting gauge, which was the highest ironing reduction successfully attempted the limiting draw-ratio was raised from 1.55 to 1.70, an increase of 10 per cent. The corresponding increase in the depth of the drawn specimen was over 33 per cent.

The increase in the reduction attainable was shown to be caused by improvements in the frictional conditions over the top surface of the specimen when in the wedge dies. Improvements in the ironing process were considered to be caused by a reversal of friction within part of the ironing die. This effect was not quantified but the conditions under which the mechanism could operate were determined and the experimental tests were shown to operate within these limits.

9.4. Blank-holder Swaging.

The use of a low frequency oscillatory blank-holder pressure enabled the draw-ratio in the deep-drawing process to be increased from 1.70 to 1.75, an increase of 3 per cent.

Whilst blank-holder swaging vibrations are considered to be a useful and important mechanism, this low frequency system which has been examined is not thought to be a viable process.

10. RECOMMENDATIONS FOR FURTHER WORK.

The application of axial punch vibrations to the deep-drawing process has been shown to enable a slight friction reduction effect to occur at the interface of the specimen and blank-holder. Theoretical considerations predict that such a system can only, however, give a marginal improvement to the drawing process. In addition, for this effect to occur the drawing die must be radially resonant at the punch oscillatory frequency. The transfer of energy from the punch to the die system was only sufficient to achieve an extremely small die oscillatory amplitude and it was difficult to increase this because the energy transfer was dependent upon the drawn strip tension which varied throughout the draw. The necessity of having a tuned die system in addition to the resonant punch introduces an additional complication to a system which is limited in its ultimate effectiveness by the effectiveness of radial die vibrations which are produced as a consequence of the punch vibrations.

For these reasons the use of axial punch vibrations as a means of increasing the limiting draw-ratio are not considered to be worth investigating further although they could find a use in assisting the stripping of thin-walled ironed shells from the punch.

The 12 per cent increase in the limiting draw-ratio obtained with 'radial' blank-holder vibrations is considered to be a worthwhile improvement to the process. Therefore it is recommended that such a process could be applied to a cup drawing operation if a similar improvement in the drawability of a material is required.

The use of either blank-holder or die vibrations in the deep-drawing process result in a friction vector reversal mechanism on the top (blank-holder) surface of the specimen. Friction acting over a similar section of the bottom (die) surface of the blank cannot be reduced by this system of vibration, even if both components are vibrated simultaneously. Nevertheless, this frictional

constraint in the deep-drawing process is a sizeable proportion of the total drawing stress and therefore its elimination, even over one surface, gives these useful improvements in the limiting draw-ratio.

The assistance that radial blank-holder vibrations can give to the deep-drawing process is limited to the effective elimination of friction constraints on the top surface of the blank. The use of blank-holder swaging vibrations could however prove to be an effective means of further reducing the necessary drawing load by altering the yield situation within the radial drawing-in portion of the cupping operation.

The system obtained using low frequency vibrations was not considered to have reproduced the conditions necessary for the predicted effects to have occurred because of the lack of rigidity in the hydraulic system used to apply the blank-holder pressure. It is considered that an examination of the deep-drawing process with blank-holder swaging vibrations applied to a fixed-clearance system should give useful improvements to this process. This is because in addition to the friction reduction caused by surface separation the drawing load will be reduced by the extrusion of the specimen by the blank-holder causing flow reversal within a section of the die. The frictional force within this reversed flow region will thus assist the drawing process because of the zero die angle between blank-holder and die.

In the application of radial vibrations to the draw ironing process the effects on the two component parts of the system, namely deep-drawing and wall ironing, can be considered separately. The punch load due to the drawing operation can only be reduced by an amount corresponding to the elimination of friction on the top surface of the specimen. In the wall ironing process such a limit does not apply and providing the tensile strength of the drawn cup wall is sufficient, the only limitation under favourable conditions to the reduction in the punch load is that this reduction in the

work done by the tensile (drawing) stress has to be matched by an increase in the work done by the oscillatory die. There is a limit in the amount of energy that can be introduced into the system through the die due to fatigue problems which become apparent when undertaking heavy reductions. This was noticeable in the wedge drawing operation when during ironing, the system could not maintain the required oscillatory amplitude due to the power input being insufficient.

The drawing load acts as a back tension in the ironing operation which the ironed strip has to support. The maximum ironing reduction possible is therefore determined by the drawing load rather than the ironing load which thus limits the maximum reduction possible in the draw ironing process. In order to obtain the maximum reductions of area it is recommended that wall ironing should become a separate additional operation to the deep-drawing process in both the analogue and the axi-symmetric cases.

In the ironing process the frictional force acting within the die constrains the process and therefore increases the ironing load. The friction force acting between the punch and material assists the ironing process because the punch always moves with a greater velocity than the material within the die. The friction force resists the flow of material up the punch and thus helps to push the material through the die. The use of radial die vibrations to reduce the frictional force are therefore only effective at the die interface. The ironing process is thus improved to a lesser extent by radial vibrations than a process in which all the frictional forces oppose the drawing, such as tube drawing over a plug. Despite this the draw ironing process warrants further investigation due to its commercial importance.

At this stage in the development of oscillatory metalworking techniques the recommendations for further work involve studying the commercial implications of these processes. Broadly speaking

the reduction in the draw forces obtained when using oscillatory deformation enables the area reduction at each stage to be increased thus reducing the number of operations which saves time and possible interstage anneals. Alternatively processes which were not possible conventionally, or required expensive routes, can be attempted and the savings in the processing routes being used to offset the capital cost of the equipment.

It is recommended that when using vibrations in the swaging of the material much consideration is given to the losses within the oscillatory system. This is necessary in order to maximise the oscillatory amplitude because compared with friction vector reversal systems the tools are heavily loaded. This was demonstrated in the draw ironing process by the large reduction in the die oscillatory amplitude as the ironing process began. Poorly designed mounting systems have been found to be an important source of energy loss.

Finally the oscillatory systems must be designed to resist the effects of fatigue since any stress concentrations quickly lead to failure at the ultrasonic frequencies used.

ACKNOWLEDGMENTS.

The author would like to extend his thanks to The Departments of Mechanical and Production Engineering for permission to undertake this research programme and the Science Research Council in awarding a Studentship for this project.

He would also like to express his gratitude to his Supervisor, Professor D.H. Sansome, for his invaluable assistance and encouragement at all times.

Further, the author wishes to acknowledge the assistance of the late Mr. E. Denchfield and Mr. S. Twamley for arranging the construction of the apparatus, and Mr. G. Jones for his help with the instrumentation.

His appreciation is also conveyed to Ultrasonics Limited for the provision of ultrasonic transducers and generator spares, and to Edgar Vaughan Limited for supplying the drawing oil.

The help of his colleagues on numerous occasions and the assistance of Mrs. S.A. Smith and Mrs. M.G. Holdaway in the typing of this manuscript is also acknowledged.

BIBLIOGRAPHY.

(1) Blaha, F. and Langenecker, B. 'Elongation of zinc mono-crystals under ultrasonic action'. Die Naturwissenschaften, 1955. 42 (20), 556.

(2) Vang, A. 'Material forming and drawing with the aid of vibrations'. U.S. Patent No.2,393,131. January 1946.

(3) Rosenthal, A.H. 'Machine for mechanically working materials'. U.S. Patent No.2,452,211. October 1948.

(4) Nevill, G.E. and Brotzen, F.R. 'The effect of vibrations on the static yield strength of low-carbon steel'. Proc. Am. Soc. for testing materials 1957. 57,751.

(5) Fridman, H.D. and Levesque, P. 'Reduction of static friction by sonic vibration'. Jnl. Appl. Phys. October 30 1959. p.1572.

(6) Lee, D., Sata, T. and Bakofen, W.A. 'The reduction of compressive deformation resistance by cyclic loading'. Jnl. Inst. Metals 1964-1965. 23, 416.

(7) Mitskevich, A.M. 'Motion of a body over a vibrating surface'. Soviet Physics - Acoustics 1968. 13 (3) 348

(8) Pohlman, R. and Lehfeldt, E. 'Influence of ultrasonic vibration on metallic friction'. Ultrasonic Oct. 1966. p.178.

(9) Lenkiewicz, W. 'The sliding friction process - effect of external vibrations'. Wear 1969. 13, 99.

(10) Nosal, V.V. and Rymsha, O.M. 'Reducing the drawing forces by ultrasonic oscillations of the drawplate, and determination of the technological parameters of tube drawing'. Stal (in English). Feb.1966. 2, 135.

(11) Jones, J.B. 'Ultrasonic metal deformation processing'. International Conference Manufacturing Tech. 1967. p.983.

(12) Dawson, G.R., Winsper, C.E. and Sansome, D.H. 'Application of high and low-frequency oscillations to the plastic deformation of metals'. Metal Forming. August and September 1970.

(13) Severdenko, V.P. and Petrenko, V.V. 'On the role of heating and ultrasonic oscillation reducing the resistance to deformation in upsetting steels'. 21.5.1969. Physico Tech. Inst. Acad. Sci., White Russia.

(14) Severdenko, V.P. et al. 'Change of external friction by free upsetting of steel 20 in an ultrasonic field'. Doklady Akademii, Nauk, BSSR. 1970. 14, 6.

(15) Severdenko, V.P. et al. 'Effect of superimposed vibrations on force requirement in three-dimensional forming'. Kuzn-Shtamp Proizvodstvo. Nov.1970. pp.6-7

(16) Severdenko, V.P. and Petrenko, V.V. 'Effect of ultrasonic vibrations on the effectiveness of lubricant in closed upsetting of steel 20'. Physicotechnical Institute, Academy of Sciences of the Belorussian SSR., Minsk. Fiziko-Khimicheskaya Mekhania Materialov, Vol.6. No.6. pp. 7-9. Nov.-Dec.1970.

(17) Petukhov, V.I. et al. 'Extrusion of aluminium in an ultrasonic field'. Kuzn-Shtamp 1972. Mar.(3). 5-7.

(18) Petukhov, V.I. et al. 'On the extrusion of metals using ultrasonic radial oscillations'. Kuznecho-Shtampov. 1972. Nov.(11). 14-15.

(19) Vatrushin, L.S. 'Efficiency of drawing in an ultrasonic field'. Soviet Jnl. Nonferrous Metals. June 1967. 8 (6) pp. 91.95.

(20) Gebr Bohler & Co. 'Shaping of deformable metallic materials'. British Patent No.1344966.

(21) Severdenko, V.P. et al. 'Drawing titanium alloy wires with the super-position of ultrasound'. Doklady Akad. Nauk, Beloruss, SSR. Russia. 1973 April. pp.325-328.

(22) Severdenko, V.P. 'Wire drawing using transverse ultrasonic vibrations'. Doklady Akad., Nauk, Beloruss, SSR. Russia. June 1971. pp. 499-501.

(23) Sämann, K.H. 'Wire drawing with high frequency mechanical vibration'. wt-Z.ind Fertig. Vol.61. (1971) pp. 672-676.

(24) Winsper, C.E. and Sansome, D.H. 'A study of the mechanics of wire drawing with superimposed ultrasonic stress'. Proc. 10th Machine Tool Design and Research Conference, Manchester. Sept.1969. p.553.

(25) Winsper, C.E. and Sansome, D.H. 'Fundamentals of ultrasonic drawing'. Jnl. Inst. Metals 1969. 97, 274.

(26) Winsper, C.E. and Sansome, D.H. 'The superposition of longitudinal sonic oscillations on the wire drawing process'. Proc. Inst. Mech. Engrs. 1968-69. 183 (1).

(27) Pohlman, R. 'The reduction of friction and the forming of metals by generating high frequency bending stresses'. Ultrasonics 1971. Conference Proceedings.

(28) Langenecker, B. and Jones, V.O. 'Macrasonic wire drawing and tube bending'. Proc. 1st. Int. Symp. High-Power Ultrasonics. Graz, Austria. 17-19 September 1970.

(29) Severdenko, V.P. 'Drawing a section with the help of ultrasound'. Doklady Akad., Nauk, Beloruss, SSR. (Russia). May 1971. pp. 422-424.

(30) Severdenko, V.P., Stepanenko, A.V. and Kulag[illegible] N. 'Drawing strip with the aid of ultrasound'. Doklady [illegible]ad., Nauk, Beloruss, SSR. 1973 17 (8). 710-713.

(31) Biddell, D.C. Private communication.

(32) Severdenko, V.P. et al. 'Ultrasonic metal-drawing programs'. Izvest-Akad., Nauk, Beloruss, SSR. Fiz-Tekh. N[illegible]l. 1970.

(33) Severdenko, V.P. et al. 'Effect of ultrasound on the drawing of metals under conditions of hydrodynamic friction'. Izvest-Akad., Nauk, Beloruss, SSR. Fiz-Tekh. N[illegible].4. 1970. pp.92-93

(34) Severdenko, V.P. et al. 'Drawing tubes from aluminium alloys with ultrasonics'. Physicho Tech. Inst., Academy of Sciences. White Russia. 2.3.1972.

(35) Kolpashnikov, A.I. 'Investigation of tube drawing from aluminium alloys using ultrasonics'. Tsvet Metally (Russia). 1972 April. pp.60.62.

(36) Dragan, O. and Segal, E. 'Cold drawing of carbon steel tubes under the influence of ultrasonics'. Metalurgia 1970 Oct. pp.629-632.

(37) Dragan, O. 'Cold drawing of tubes on an ultrasonically activated plug'. Ultrasonics International 1973. Conference Proceedings. pp. 254-256.

(38) Winsper, C.E. and Sansome, D.H. 'Application of ultrasonic vibrations to the plug drawing tube'. Metal Forming, March 1971. 38 (3). pp. 71-75.

(39) Sugahara, T. et al. 'Application of ultrasonic vibration to metal tube drawing process'. Nippon Kokan Technical Report - Overseas. December 1970. pp.51-59.

(40) Waterhouse, W.J. Private communication.

(41) Dawson, G.R. 'Ultrasonic radial die oscillations in floating-plug tube drawing'. Ultrasonics International 1975. Conference Proceedings. pp. 206-209.

(42) Mikhenl'man, A.I. and Mashchinov, A.N. 'Effect of ultrasonic vibrations on friction between solids'. Russian Engineering Journal 1969. Volume XLIX. No.1. pp.41-42.

(43) Konovalov, G.G. et al. 'Reduction of the forces of sliding friction by introducing longitudinal ultrasonic vibrations'. Doklady Akad., Nauk, Beloruss. 1973 May 17 (5). pp.420-422.

(44) Severdenko, V.P. et al. 'Rolling and drawing with ultrasound'. Nauka i Tekhnika, Minsk (1970). p.239.

(45) Severdenko, V.P et al. 'Effect of ultrasonics on the process of plastic deformation'. Doklady Akad., Nauk, Beloruss. 1971 March 15 (3). pp. 217-218.

(46) Severdenko, V.P. and Petrenko, V.V. 'On softening of steels deformed with ultrasound'. Doklady Akad., Nauk, Beloruss. 1969 13 (13). pp. 1083-1085.

(47) Severdenko, V.P. and Petrenko, V.V. 'Residual stresses of the second kind in (carbon and alloy) steels worked in an ultrasonic field'. Metallovedeni i Term, Obrabotka Metallov Russ. 1971 3 (66-67).

(48) Severdenko, V.P. et al. 'Residual stresses in metal rolled with application of ultrasonic vibrations'. Metallovedenie i Termicheskaya Obrabotka Metallov No.1. pp. 68-69. January 1971.

(49) Mizuno, M. and Kuno, T. 'Basic studies of plastic working with vibration'. Bulletin of the JSME Vol.1 , No.91. Jan.1973.

(50) Kleesattel, C.M. Private communication.

(51) Severdenko, V.P. et al. 'Nature of surface of polycrystalline aluminium deformed by ultrasound'. Doklady Akad., Nauk, BSSR. 1971. 51, 4.

(52) Gindin, I.A. et al. 'The plastic strain of polycrystalline aluminium under the influence of ultrasonic pulses'. Fizika Tverdogo Tela Vol.11, No.11. pp. 323[illegible]-3241. November 1969.

(53) Puskar, A. 'Effect of ultrasound on mechanical properties of mild steel'. Hutnicke Listy, Vol.26, No. , 1971. pp.652-656.

(54) Dragan, O., Atanasiu, N. and Segal, E. 'Effect of ultrasonics on the properties of carbon steel'. Metalurgia 24. 1972. No.12.

(55) Langenecker, B., Jones,V.O., and Illiewich, . . 'Metal plasticity in macrosonic fields'. Proceedin[illegible] 1st. Int. Symp. High-Power Ultrasonics. Graz. September 19[illegible].

(56) Langenecker, B. 'Dislocation damping in macrosonic fields'. Proceedings 1st. Int. Symp. High-Power Ultrasonics. 1970.

(57) Langenecker, B. 'Basic concepts and industrial applications of macrosonic metal deformation'. Ultrasonics International Conference Proceedings 1971.

(58) Langenecker, B. and Vodep, O. 'Metal plasticity in macrosonic fields'. Ultrasonics International Conference Proceedings 1975. pp. 202-205.

(59) Bajons, P. et al. 'Ultrasonic fatigue testing method - its practical application'. Ultrasonics International Conference Proceedings 1975. pp. 95-101.

(60) McKaig, H.L. 'The application of ultrasonic energy in the deformation of metals'. Defense Metals Information Centre, Battell Memorial Institute, Columbus, Ohio.

(61) Peacock, J. 'Forming goes ultrasonic'. Am. Machinist/ Metalworking Manfng. Nov.1961. 105, 83.

(62) Langenecker, B., Fountain, C.V. and Jones, V.O. 'Ultrasonics: an aid to metal forming?'. Metal Progress, April 1964. 85, 97.

(63) Kristoffy, I. 'Metal forming with vibrating tools'. Trans. A.S.M.E. Jnl. Eng. Ind. Nov.1969. p.1168.

(64) Rothman, D. and Sansome, D.H. 'An investigation of rod-drawing with die rotation'. Int. Jnl. Mach. Tool Design and Research. Vol.10. pp. 179-192.

(65) Young, M.J.R. Ph.D. Thesis. University of Aston in Birmingham.

(66) Loxley,E.M.and Swift, H.W. 'The wedge drawing test'. Engineering 1945. Vol.159. pp. 38-40, 77-80, 136-138.

(67) Biddell, D. and Sansome, D.H. 'The deep-drawing of cans with ultrasonic radial oscillations applied to the die'. Ultrasonics International 1973. Conference Proceedings.

(68) Smith, A.W., Young, M.J.R. and Sansome, D.H. 'Preliminary results on the effect of ultrasonic vibratic on an analogue of the deep-drawing process'. Ultrasonics I ternational 1973. Conference Proceedings. pp. 250-253.

(69) Smith, A.W. and Sansome, D.H. 'An experimen l investigation of the effect of blank-holder vibrations on n analogue of the deep-drawing process'. Ultrasonics Inte ational 1975. Conference Proceedings. pp. 210-213.

(70) Eaves, A.E., Smith, A.W., Waterhouse, W.J. a l Sansome, D.H. 'Review of the application of ultrasonic vib tions to deforming metals'. Ultrasonics. July 1975. pp. 162-170.

(71) Chung, S.Y. and Swift, H.W. 'Cup drawing fr a flat blank'. Proc. Inst. Mech. Engrs. 1951. 165 pp. 19 .

(72) Hill, R. 'The mathematical theory of plasti ty'. Clarendon Press Oxford 1950.

(73) Sachs, G. Metallwirtschaft, Vol. 9 (1930) ,213.

APPENDIX A.

A.1. Design of the Oscillating Punch System.

A.1.1. Design of Conical Concentrator.

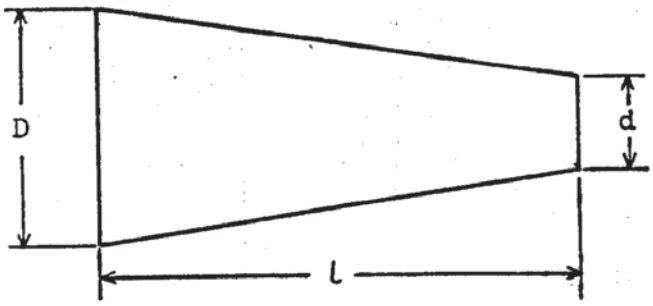

Assume plane wave propagation

At resonance for Conical Concentrator, $\tan kl = \dfrac{kl}{\dfrac{(kl)^2 N + 1}{(1-N)^2}}$

where $k^2 = \dfrac{\omega^2 \rho}{E} = \dfrac{\omega^2}{C_e^2}$

$\omega = 2\pi f$ is the angular frequency of the vibration.

C_e = longitudinal wave velocity in material.

$N = \dfrac{D}{d}$

Selecting : D = 4 in. d = 1 in. giving N = 4

f = 12.75 kHz

From graph No. A.1.1.

kl = 3.63

also kl = 0.404

thus giving l = 9 in.

The physical dimensions of the conical concentrator are therefore determined.

These dimensions can be substituted into the resonance equation for the loaded concentrator in order to determine the load impedance necessary :

$$\tan kl = \frac{k \dfrac{Xh}{\omega_0 l'} (\alpha l + 1) + \alpha^2 l}{\alpha \dfrac{Xh}{\omega_0 l'} + k (\alpha l + 1) + \dfrac{\alpha^2}{k}}$$

Graph No. A.1.1.

Conical Concentrator Resonant Conditions

Variation of kl and N against $\frac{N}{(1-N)^2}$

From $\tan kl = \frac{kl}{\frac{(kl)^2 N}{(1\ N)^2} + 1}$

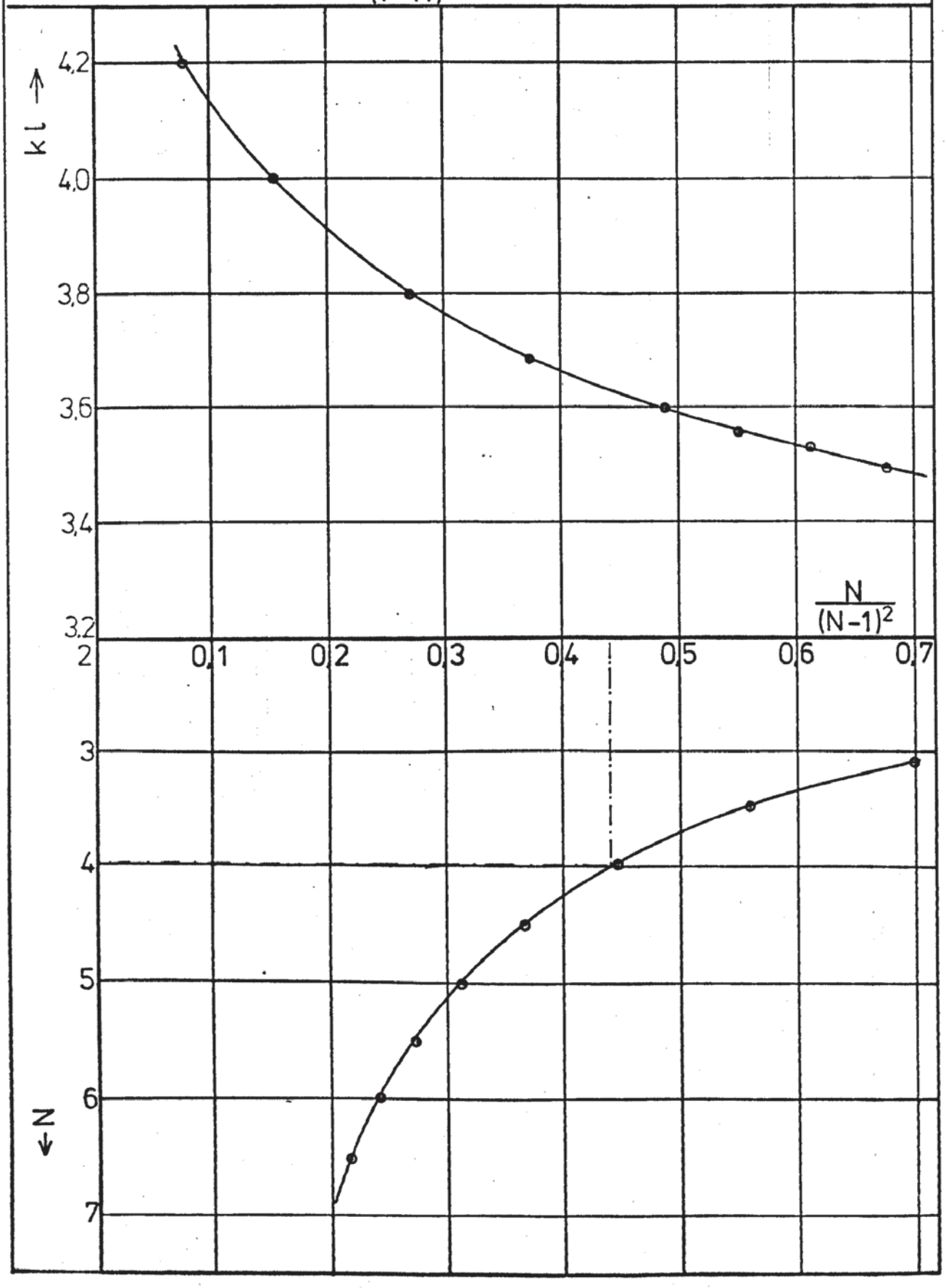

$\omega_o l'$ = Wave impedance at narrow end of conical concentrator.

Xh = Load impedance

$$\alpha = \frac{N-1}{l} = \frac{3}{9} = \frac{1}{3}$$

k = 0.404

l = 9 in.

$$\text{Tan } kl = 0.532 = \frac{0.404 \frac{Xh}{\omega_o l'} (4 + 1)}{\frac{1}{3} \frac{Xh}{\omega_o l'} + 0.404 (4) + \frac{1}{9 \times 0.404}}$$

$$\omega_o l' = S\sqrt{E\rho} = \frac{\pi}{4} \times 5.73 \times 10^4 \text{ lb. s}^{-1}$$

$$\omega_o l = 4.5 \times 10^4 \text{ lb. s}^{-1}$$

Substituting for $\omega_o l$

$$0.532 = \frac{\frac{0.404\ Xh}{4.5 \times 10^4} \times 4 + 1}{\frac{1}{3} \frac{Xh}{4.5 \times 10^4} + 0.404 (4) + \frac{1}{9 \times 0.404}}$$

$$0.532 = \frac{0.359\ Xh \times 10^{-4} + 1}{Xh\ 7.42 \times 10^{-6} + 1.891}$$

$$Xh = \frac{6 \times 10^{-3}}{31.96 \times 10^{-6}}$$

thus load impedance Xh = 187.5 lb s^{-1} for resonance.

A.1.2. Design of Punch.

The mechanical impedance of any vibrating system can be expressed as a complex function of the form

$Zh = Rh \pm iXh$ where Rh = Resistance, Xh = Inertia and elastic

Assume the rectangular punch constitutes an "ideal" rod system i.e. a system without resistive losses

For such a system

Oscillatory force $Fm = Fml \cos \alpha x + i \dot{\xi} ml \omega_o \sin \alpha x$

Oscillatory velocity $\dot{\xi}m = \dot{\xi}ml \cos \alpha x + i \frac{Fml}{\omega_o} \sin \alpha x$

α = phase shift constant $\frac{2\pi}{\lambda}$

Now for a free-end system, oscillatory force at end $Fml = 0$

So $Fm = i \dot{\xi} ml \omega_o \sin \alpha x$

$\dot{\xi}m = \dot{\xi}ml \cos \alpha x$

$$Zin = \frac{Fm}{\dot{\xi}m} = i\omega_o \tan \alpha l$$

$$= i\, Xin$$

where wave impedance $\omega_o = \sqrt{\frac{m_1}{c_1}}$ m_1 = mass / unit length, c_1 = flexibility / unit length

also $c_1 = \frac{1}{ES}$, $m_1 = S\rho$ S = cross sectional area, ρ = density, E = modulus of elasticity

Hence load impedance Zin of the punch can be expressed

$$Zin = i S\sqrt{\rho E} \tan \omega \sqrt{\frac{\rho}{E}}\, l \quad , \text{ since } \alpha = \frac{2\pi f}{\sqrt{\frac{E}{\rho}}}$$

Thus Zin of punch =

$$\frac{23}{32} \times \frac{45}{32}\ in^2 \sqrt{0.283 \frac{lb}{in^3} \times 30 \times 10^6 \frac{lbf}{in^2} \left[32.2 \frac{lb\ ft}{lbf\ s^2}\right]\left[\frac{12\ in}{ft}\right]}$$

$$\times \tan \left(2\pi \times 13 \times 10^3 \sqrt{\frac{0.283}{30 \times 10^6} \frac{lb\ in^2}{in^3\ lbf} \left[\frac{lbf\ s^2}{32.2\ lb\ ft}\right]\left[\frac{ft}{12\ in}\right]}\ l\right)$$

$Z_{in} = 5.789 \times 10^4 \frac{lb}{s} \tan 0.4035\, l$

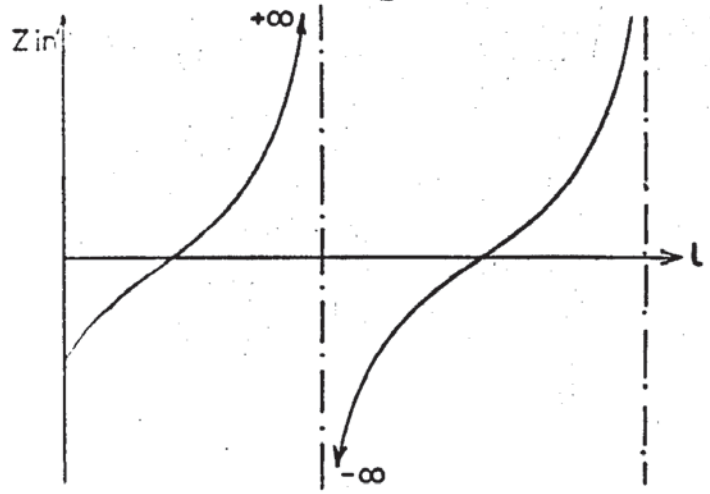

Thus since Zin is a tan function of length, l, any value of Zin can be obtained by choosing the appropriate length as can be seen from the graph.

The punch constitutes a reactive load only for an "ideal " system which becomes the load on the intermediate rod section.

For such a system

$$\frac{F_{ml}}{X_h} = \dot{\xi}_{ml}$$

$$\text{So } F_m = F_{ml}\left[\cos \alpha x + i\frac{\omega_o}{X_h}\sin \alpha x\right]$$

$$F_m = F_{ml}\ \frac{\cos \alpha x \cos\varphi + \sin \alpha x \sin\varphi}{\cos\varphi}$$

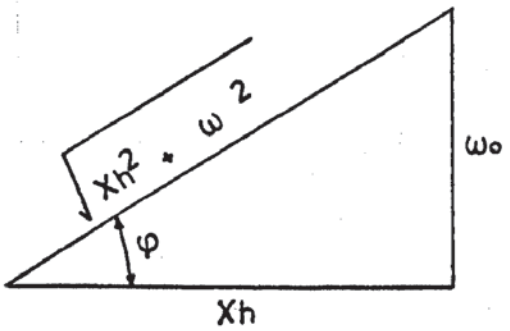

$$F_m = F_{ml}\ \frac{\cos(\alpha x - \varphi)}{\cos \varphi}$$

$$\text{Similarly } \dot{\xi}_m = i\frac{F_{ml}}{\omega_o}\ \frac{\sin(\alpha l - \varphi)}{\cos \varphi}$$

$$\text{hence } Z_{in} = -i\omega_o \cot(\alpha l - \varphi) \qquad \text{where } \varphi = \tan^{-1}\frac{\omega_o}{X_h}$$

Comparing with a fixed end system.

$$Z_{in} = -i\omega_o \cot \alpha l$$

A system with a reactive load can be made equivalent to a system

Graph No. A.1.2.

Variation of Zin with Punch Length

From $Z\,in = 5{,}79 \times 10^{4} \frac{lb}{s} \times \tan 0{,}402 \frac{1}{in} \, l$

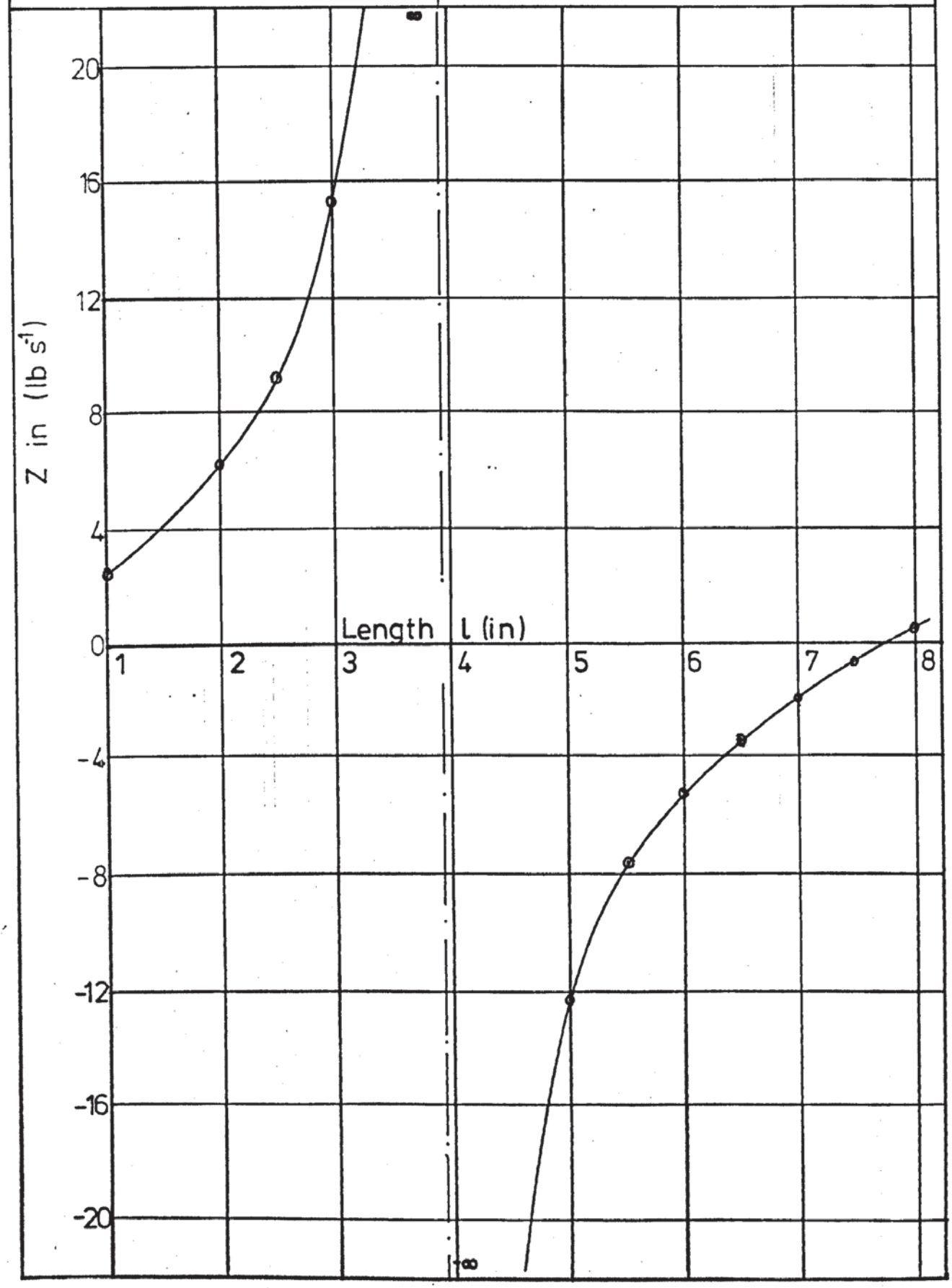

with a fixed end if its length is such that

$$\cot (\alpha l - \varphi) = \cot \alpha l_e$$

$$\alpha l - \varphi = \alpha l_e$$

$$l_e = l - \frac{\varphi}{\alpha} = l - \varphi\frac{\lambda}{2\pi}$$

$$l_e = l - \frac{\tan^{-1} \frac{\omega_o \lambda}{Xh}}{2\pi}$$

or difference between systems is $\dfrac{\tan^{-1} \frac{\omega_o \lambda}{Xh}}{2\pi}$

Zin of rod system for reactive load

$$= - i\omega_o \cot (\alpha l - \varphi) = Xin$$

where $\tan\varphi = \frac{\omega_o}{Xh}$ (Xh = load)

From Graph of Zin v l (A.1.2.)

select l = 7.88 in. in order that the load impedance on the next section Zin = 0. Thus the system corresponds to that of a free ended one.

Zin of rod system = $- i\omega \cot (\alpha l - \varphi)$

If l = 3.89 , Xin = ∞

so $\cot \alpha l = 0$

Thus for a fastened end system load impedance on next section is again = 0

Thus for rod system

$Zin = - i\omega_o \cot (\alpha l - \frac{\pi}{2})$ since Xh = 0

$$\tan\varphi = \frac{\omega_o}{Xh} = \infty$$

thus $\varphi = \frac{\pi}{2}$, $\frac{3\pi}{2}$ etc.,

Equating to Zh of conical horn

$$187.5 \frac{lb}{s} = \omega_o \cot (\alpha l - \frac{\pi}{2})$$

$$\frac{4.48 \times 10^4}{\tan (0.4035\ l - \frac{\pi}{2})}$$

So 239 = $\tan (0.4035\ l - \frac{\pi}{2})$, 0.40351 = 3.136

or l = 7.774 in. = length of parallel rod.

A.1.3. Tuning of the Punch System.

For a loaded conical concentrator

$$\tan kl = \frac{k \frac{Xh}{\omega_o l'} (\alpha l + 1) + \alpha^2 l}{\alpha \frac{Xh}{l'} + k (\alpha l + 1) + \frac{\alpha^2}{k}}$$

for the tuned conical concentrator

$l = 9.2$ in

$N = 4.046$

$kl = 3.636$

$k = 0.3952$

$$\alpha = \frac{N-1}{l} = \frac{3.046}{9.2}$$

$$\alpha = 0.3311$$

$$\text{Thus } \tan kl = \frac{0.53844 = 0.3952 \frac{Xh}{\omega_o l'} (4.046) + 1.008}{0.3311 \frac{Xh}{\omega_o l'} + 0.3952 \times (4.046) + \frac{0.3311^2}{0.3952}}$$

$$0.5384 = \frac{0.3952 \frac{Xh}{\omega_o l'} 4.046 + 1.008}{0.3311 \frac{Xh}{\omega_o l'} + 1.599 + 0.2774}$$

$$\omega_o l' = S\sqrt{E\rho} = \frac{\pi}{4} \times 5.73 \times 10^4 \frac{lb}{s}$$

$$\omega_o l' = 4.5 \times 10^4 \text{ lb.s}^{-1}$$

$$0.5384 = \frac{\frac{0.3952}{4.5 \times 10^4} Xh \frac{s}{lb} \times 4.046 + 1.008}{\frac{0.3311}{4.5 \times 10^4} Xh \frac{s}{lb} + 1.599 + 0.2774}$$

$$0.5384 (7.357 \times 10^{-6} Xh + 1.8734) = 0.3553 Xh \times 10^{-4} + 1.008$$

$$3.961 \times 10^{-6} Xh + 1.008 = 0.3553 Xh \times 10^{-4} + 1.008$$

$$\text{thus } Xh = 0$$

Thus the input impedance to the intermediate rod section is also = 0

For this system

$$Z_{in} - i\omega_o \cot(\alpha l - \varphi) = 0$$

$$\tan(\alpha l - \varphi) = \infty$$

$$\text{or } \alpha l - \varphi = \frac{\pi}{2}, \frac{3\pi}{2} \text{ etc.,}$$

thus $\alpha l = \pi$ since $\varphi = \tan^{-1}\frac{\omega_o}{X_h} = \tan^{-1}\infty$

$$= \frac{\pi}{2}$$

now $$\alpha = \frac{2\pi f}{\sqrt{\frac{E}{\rho}}}$$

so $$\frac{2\pi f}{\sqrt{\frac{E}{\rho}}} l = \pi$$

$$l = \frac{1}{2f}\sqrt{\frac{E}{\rho}}$$

$$l = \frac{1}{2 \times 12.75 \times 10^3} \text{ s} \sqrt{\frac{30 \times 10^6 \text{ lbf}}{0.283 \text{ lb}} \frac{\text{in}^3}{\text{in}^2} \left[\frac{32.2 \text{ lb ft}}{\text{lbf s}^2}\right]\left[\frac{12 \text{ in}}{\text{ft}}\right]}$$

$l = 7.9368$ in.

Length of intermediate rod = 7.937 in.

A.2. Preparation of Wedge Specimens.

A.2.1. Production of Blanks.

The specimen requirements for each particular series of tests were estimated and sufficient material was obtained. For any individual series of tests the specimens were all taken from one sheet, and in every case the longitudinal axis of each specimen was aligned with the rolling direction. These precautions were taken to ensure a supply of specimens with uniform drawing properties.

The specimens were produced by shearing the sheet material into rectangular oversize blanks with the longitudinal axis being aligned with the rolling direction. These blanks were sorted into packs containing approximately 20 blanks and assembled into a drilling jig, in order that a $\frac{3}{16}$ in. diameter hole could be drilled through the mid-point of each blank. The purpose of this hole was to locate the specimen for subsequent machining operations and also to position the specimen on the punch nose during the establishment of the specimen around the punch in the drawing operation.

After drilling the locating hole in each specimen the blanks were cleaned to remove any burrs produced by this operation.

A.2.2. Milling the Wedge Shape.

The production of the wedge shape was achieved by pack milling on a numerically-controlled milling machine. This machine was capable of position control to within 0.0002 in. and straight line motion between co-ordinate points. The simplest specimen shape consisted of two wedges connected by a strip of material of width equal to that of the die throat. This shape, however, was not satisfactory because of the stress-raiser caused by the central location hole. To prevent fracture at this point the width of the material in this region was increased. This modification to the geometry of the centre of the specimen was of no consequence to the drawing process because the region of stretch-forming over the punch nose was not being examined during any stage of these investigations.

Drawing No. A.2.1.

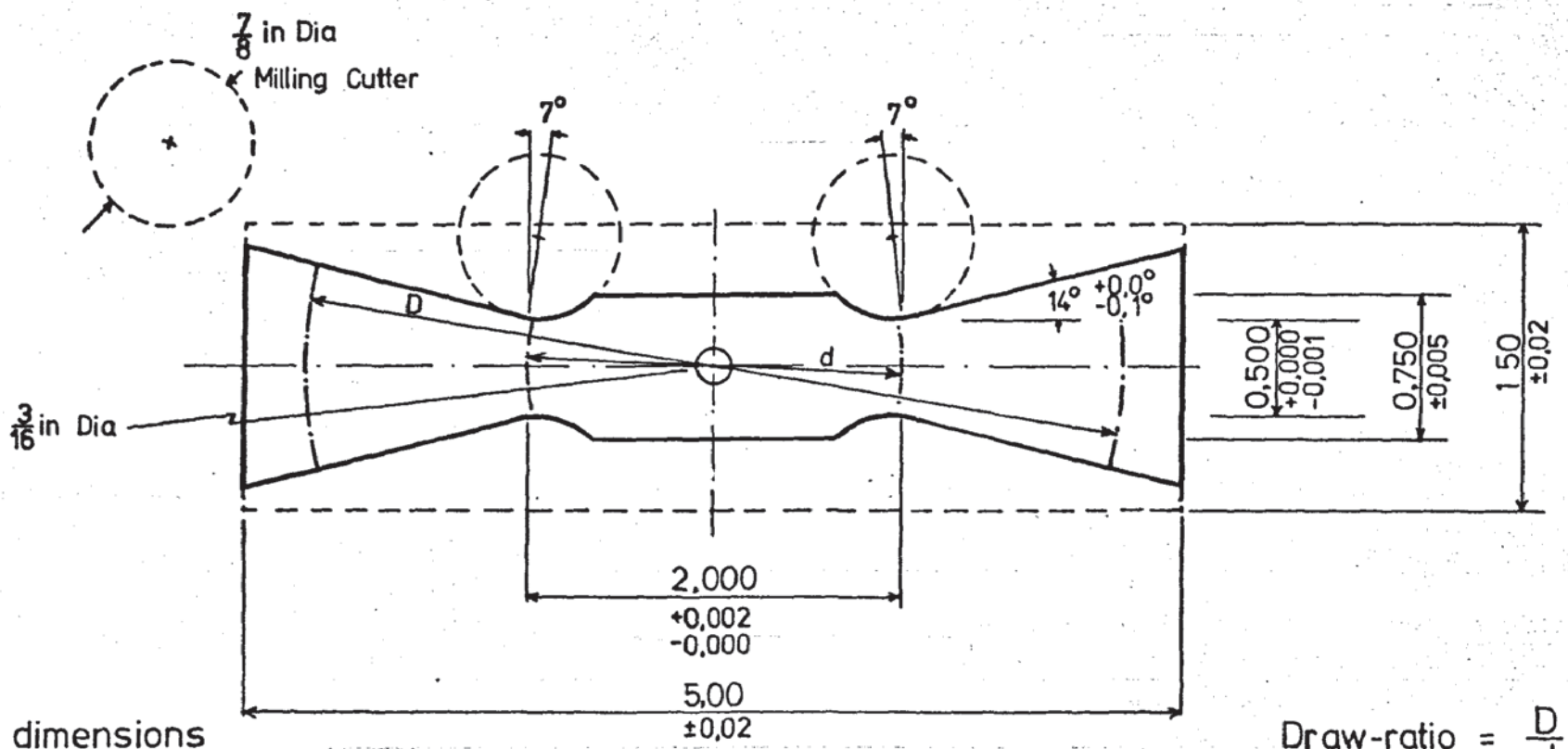

Note :- All dimensions in inches

Draw-ratio = $\frac{D}{d}$

Detail of Wedge Specimen

Drawing No A.2.2.

Wedge Specimen Milling Jig

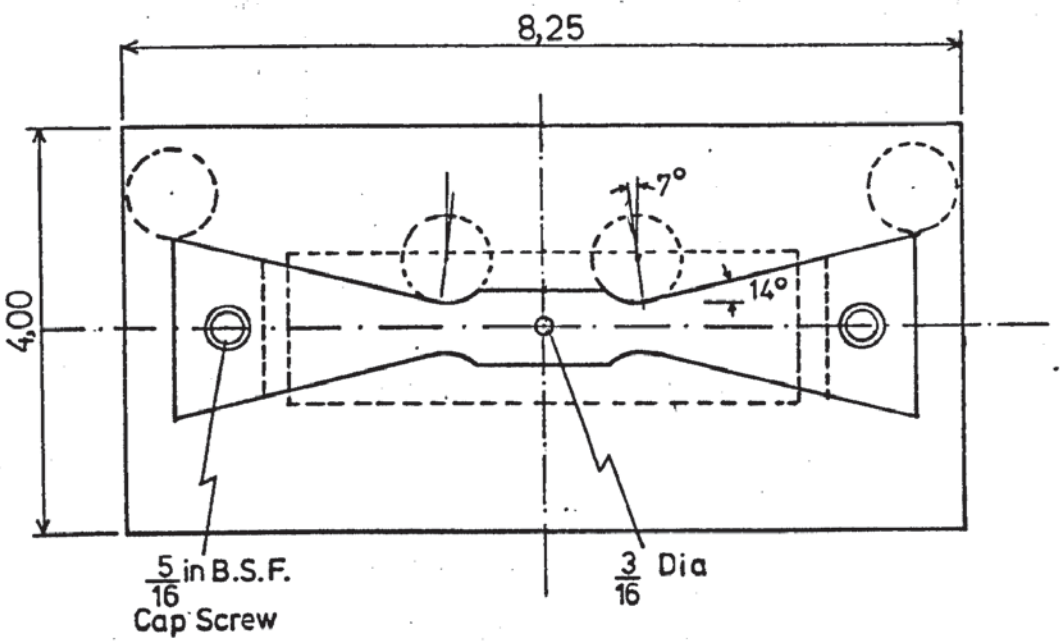

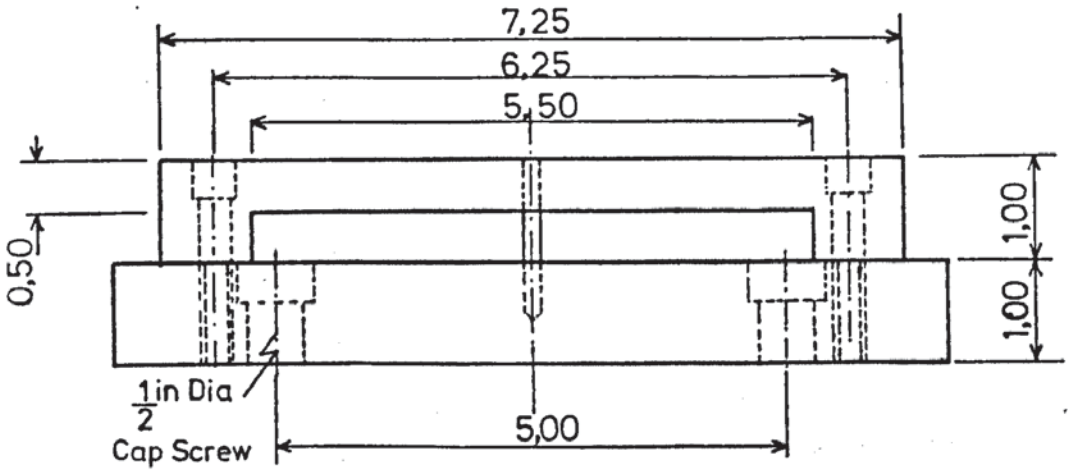

Scale :- Half Size

All dimensions in inches

All Tolerances ± 0,01

Machine Programme for Milling Wedge Specimens

N001	G54	X-0028981	Y0011784				M03
N002	G55			T001	R-0015000		M08
N003		X-0009466	Y0006892			F01000	
N004			Y0008142				
N005		X0009466					
N006			Y0006892				
N007		X0028981	Y0011784				
N008				T000	R0000000		
N009			Y-0011784				
N010				T001	R-0015000		
N011		X0009466	Y-0006892			F01000	
N012			Y-0008142				
N013		X-0009466					
N014			Y-0006892				
N015		X-0028981	Y-0011784				
N016				T000	R0000000		
N017	G54	X-0028981	Y0011734				
N018	G55			T001	R-0015000		
N019		X-0009466	Y0006842				
N020			Y0008092				
N021		X0009466					
N022			Y0006842				
N023		X0028981	Y0011734				
N024				T000	R0000000		
N025			Y-0011734				
N026				T001	R-0015000		
N027		X0009466	Y-0006842				
N028			Y-0008092				
N029		X-0009466					
N030			Y-0006842				
N031		X-0028981	Y-0011734				
N032				T000	R0000000		M05
N033		X0000000	Y0000000				M30

Note: Operations N001-N016 Roughing Cut

N017-N033 Finishing Cut

Co-ordinates in 0.0001 in. Units

Programme suitable for Aluminium Specimens.

$\frac{7}{8}$ in. Milling Cutters necessary.

A gradual transition in specimen width from the central to the wedge sections was necessary to avoid the effects of stress concentrations which could cause premature failure at the narrow section of the specimen. A large radius was desirable but the numerically-controlled milling machine was unable to reproduce curves other than by generation from a large number of flat surfaces. This difficulty was avoided by selecting a milling cutter with its radius equal to that required on the specimen. From the required shape of the specimen and the diameter of the milling cutter it was possible to lay out a series of co-ordinates for the machine controller and work out a suitable programme. This programme was punched onto the paper tape input which controlled the machine. Two cycles of the machine were used, the first was a roughing cut to produce an over-size specimen and, the second, a finishing cut brought the specimens down to the correct dimensions.

During the initial stages of production of these specimens many were rejected because of 'chatter' marks along the milled edges. The process of machining these specimens was studied in an attempt to alleviate these problems and three modifications to the process were made which proved very effective in eliminating this problem. A shorter spindle was fitted to the milling machine to give greater rigidity and a new milling cutter was obtained which was interchanged with the old one after the roughing cycle had been completed.

The inconvenience of the tool change mid-way through machining a batch was tolerated because of the necessity to have a sharp tool for the final cut and the fact that the geometry of the finished article was dependent upon the diameter of the milling cutter. Once a cutter was worn and reground it could only be used in the roughing operation because of its now smaller diameter.

The final modification was that of reversing the direction of cutter travel so that the tool was cutting against the direction of movement, rather than with it as had been the former practice.

A.2.3. Preparation of Specimens of Various Draw-Ratios.

The wedge shaped specimens thus produced by the numerically-controlled milling were all too long and a further machining operation was necessary before they were ready for use. The sheared ends of the specimens had to be reduced to an arc of radius equal to the requirement for the particular draw-ratio under test. The procedure was to shear off the majority of the excess and make up a pack of approximately 20 as before. This pack was located by the central hole and mounted into a simple clamping rig which was in turn attached to a circular table. The circular table was used on a vertical milling machine where an end mill was used to remove the final amount of material. The clamping plates used were of the same diameter as the specimen size required so that the pack had as much support as possible during the milling operation. The jig was rotated on the circular table during the milling which generated the circular arc required. On completion of one end the table was rotated through 180 degrees and the other end machined likewise.

In order to speed the production of these specimens and also to produce a better machined finish on the specimens another method was developed. The machining was carried out on a lathe which had the added advantage that the cutting tools used could easily be maintained in a sharp condition, which gave the best results. This jig was mounted on a spigot which was mounted in the lathe chuck. The specimens were located on another spigot concentric with the first. A cover plate of the required diameter fitted over this spigot and a clamping plate was tightened over this cover plate thus holding the pack of specimens firmly in place.

On completion of the manufacture of a batch of specimens, they were deburred if necessary and washed in a degreasing agent to remove the mixture of cutting oil and metal fines remaining from the machining operations.

A.3. The Ultrasonic Generator.

A.3.1. General Description.

The ultrasonic power unit, comprising the high frequency electrical supply and the magneto-strictive transducers used to convert the electrical signal into mechanical ultrasonic vibrations, was a RAPICLEAN 3000 unit supplied by Ultrasonics Ltd. This unit had originally been built for an ultrasonic cleaning bath but the robustness of the laminated nickel magneto-strictive transducers made such a unit ideal for oscillatory metal working. The transducers had a resonant frequency of the order of 13 kHz and the electrical components of the generator were designed to operate at this frequency.

The oscillatory frequency was determined by the resonant frequency of the R-C network which controlled the oscillator valve. The output from the oscillator circuit, after amplification, was connected to the grids of the two output valves, where it generated the high-frequency, high-voltage output. Output power was supplied by a 3 KV output, mains input transformer. The mains supply into this transformer was controlled by a Variac variable transformer which in turn regulated the high voltage applied to the output valve anodes. This high-frequency, high-power oscillating supply was linked to the magneto-strictive transducers by an output transformer which also reduced the voltage across the transducer coils. This circuit containing the transducer coils was another resonant circuit, resistors and capacitors within the generator being varied to make this circuit resonant.

The magneto-strictive effect is independent of polarity and therefore the mechanical oscillations would occur at twice the generator frequency if only the alternating supply was applied. This undesirable effect was prevented by applying a low voltage large bias current to the magneto-strictive coils thus preventing the reversal of the current flow associated with the oscillatory voltage.

A.3.2. Rebuilding of the Generator.

The generator had initially been used with the individual chassis wired up on a large bench. This arrangement eventually became unsatisfactory because of space requirements and an original manufacturer's cabinet was obtained to rehouse the unit.

After reconditioning this cabinet and whilst the generator was being rebuilt into it, the opportunity was taken to alter some of the circuitry. These alterations enabled controls used during the drawing operation to be located adjacent to the press and blank-holder controls. All these external controls were wired through an additional connector so that the generator could be removed quickly in the event of any fault developing, a situation not unlikely considering the age and service of the generator.

This new arrangement was more satisfactory because the energising of the high-voltage circuit was now dependent upon the doors of the cabinet and the thermal cut-outs being closed. These thermal cut-outs were used to protect the output valves and magneto-strictive transducers from excessive temperature rises.

The use of the metal cabinet had the further advantage of screening some of the electrical and electro-magnetic interference produced within the generator from the rest of the instrumentation. This produced an improvement in the quality of the signal traces obtained from the ultra-violet recorder.

A.3.3. Tuning of the Generator.

The oscillatory frequency of the generator was varied by changing the resistance within the oscillator circuit with the frequency control rheostat. This control was used to tune the oscillatory system during the metal working operations.

The output of the generator, whilst controlled by the Variac variable transformer, had to be tuned to obtain its maximum output. The output from the oscillatory circuit was maximised by driving the oscillator valves until the sinusoidal waveform was almost beginning to distort. The final tuning adjustment possible was that within the magneto-strictive transducer circuit. This circuit was tuned by varying the capacitance within the circuit until it was resonant and the maximum oscillatory output was obtained. This tuning operation was necessary whenever the transducer system in use was altered.

A.3.4. Specification of the 3kW RAPICLEAN Generator.

Typical Outputs.

E.H.T. Primary Current	12 a
E.H.T. D.C. Volts	5-6 kv
E.H.T. Secondary Current	350-450 ma
Magnetisation Current	9-13 a
Magnetisation Voltage	18-35 v
Drive H.T.	400 v
EF 91 Anode D.C. Volts	60-180 v
EF 91 Anode P. to P. Volts	150-200 v
EF 91 Screen Volts	280-350 v
EF 91 Cathode D.C. Volts	4 v
807 Anode P. to P. Volts	650-1100 v
807 Screen	220-250 v
807 Grid P. to P.	50 v
Output Valve Grid P. to P. Volts	250-300 v
Output Valve Grid Negative	-90 to -100 v
Output Valve Screen D.C.	450-550 v
R/F Current	2-4 a

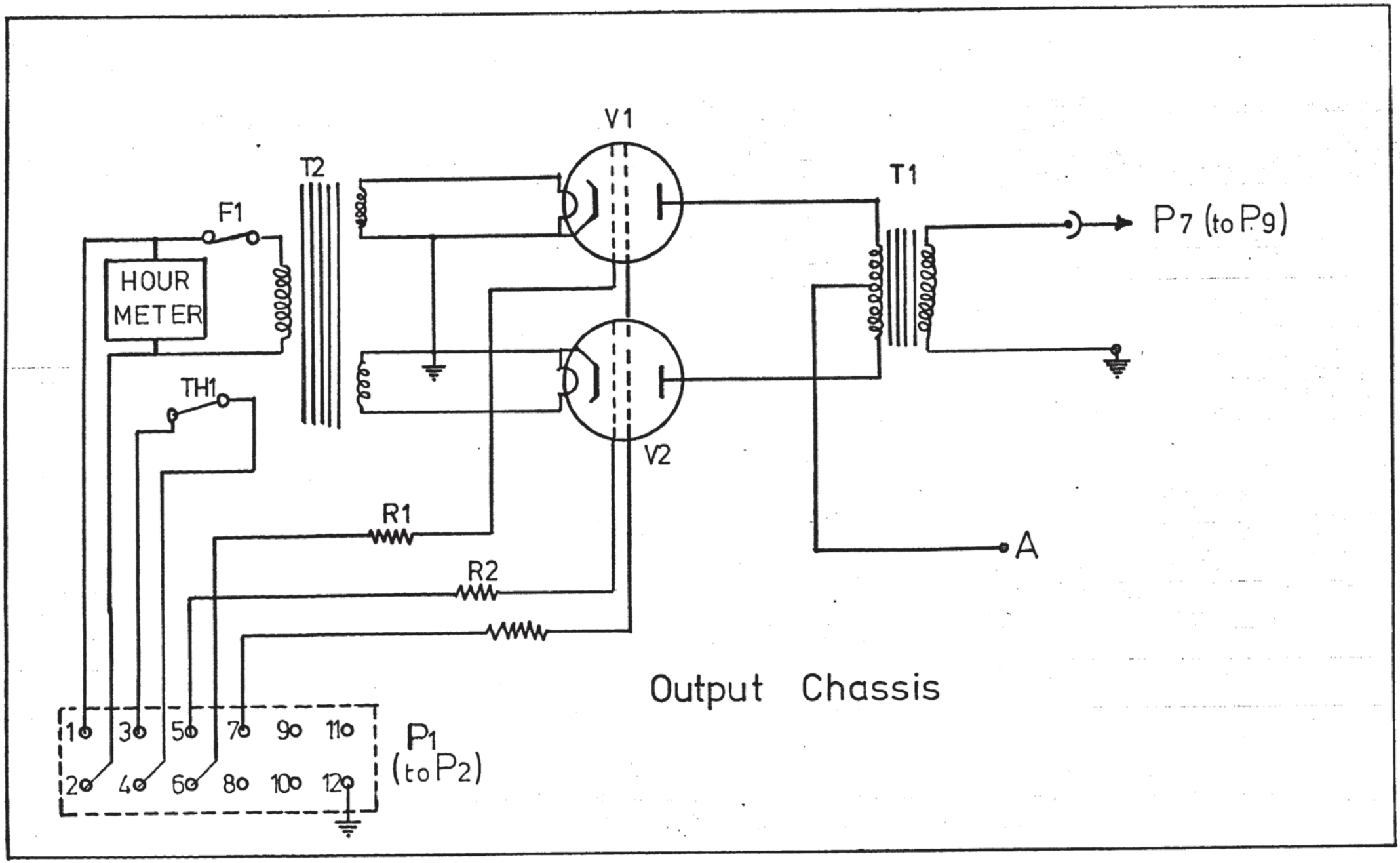
V1
T2
T1
F1
HOUR
METER
P7 (to P9)
TH1
V2
R1
R2
A
Output Chassis
1
3
5
7
9
11
2
4
6
8
10
12
P1
(to P2)

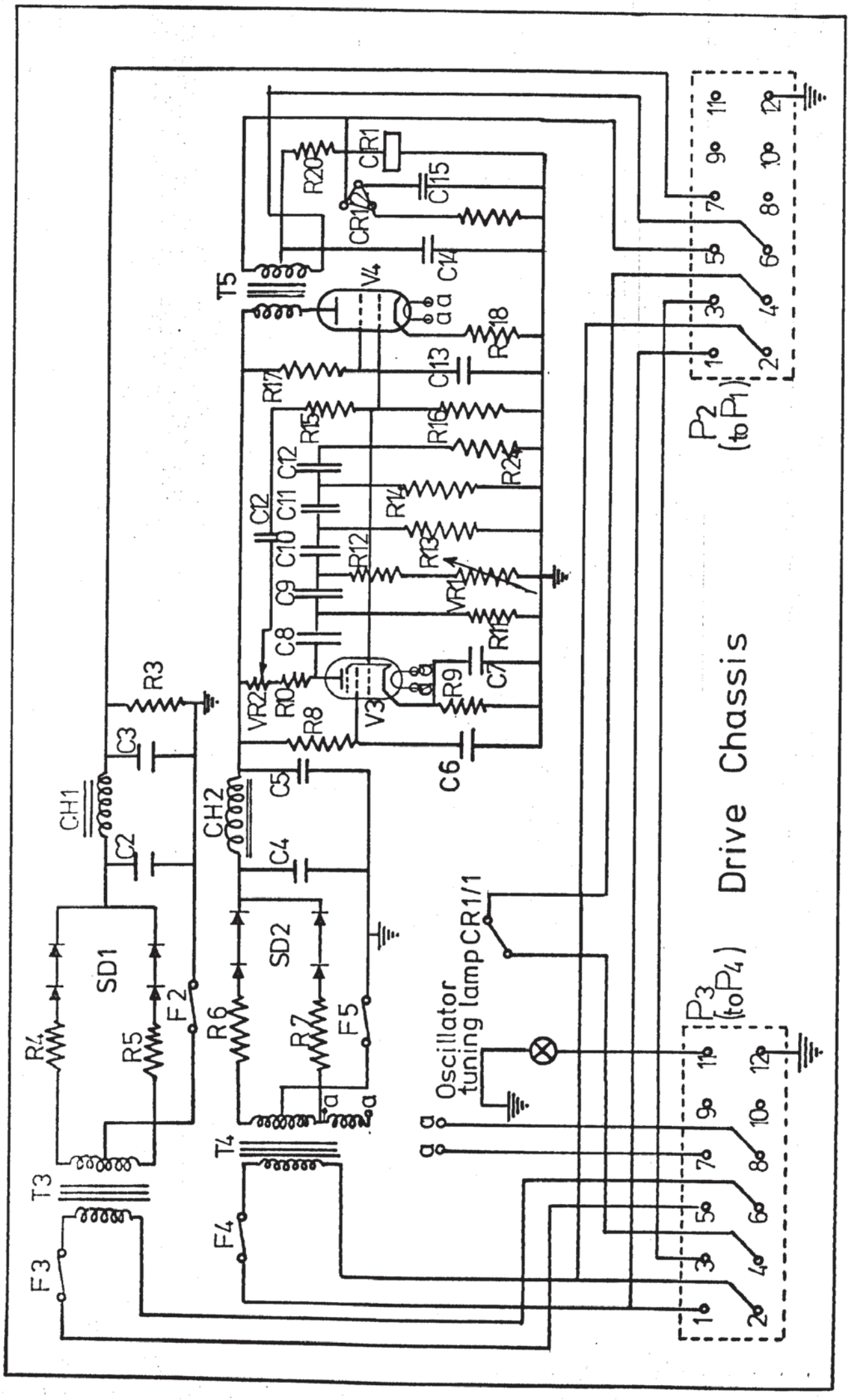
Drive Chassis
P2 (to P1)
P3 (to P4)
T3
T4
T5
V3
V4
SD1
SD2
CH1
CH2
CR1
CR1/1
F2
F3
F4
F5
R3
R4
R5
R6
R7
R8
R9
R10
R11
R12
R13
R14
R15
R16
R17
R18
R20
R24
VR1
VR2
C2
C3
C4
C5
C6
C7
C8
C9
C10
C11
C12
C13
C14
C15
Oscillator tuning lamp

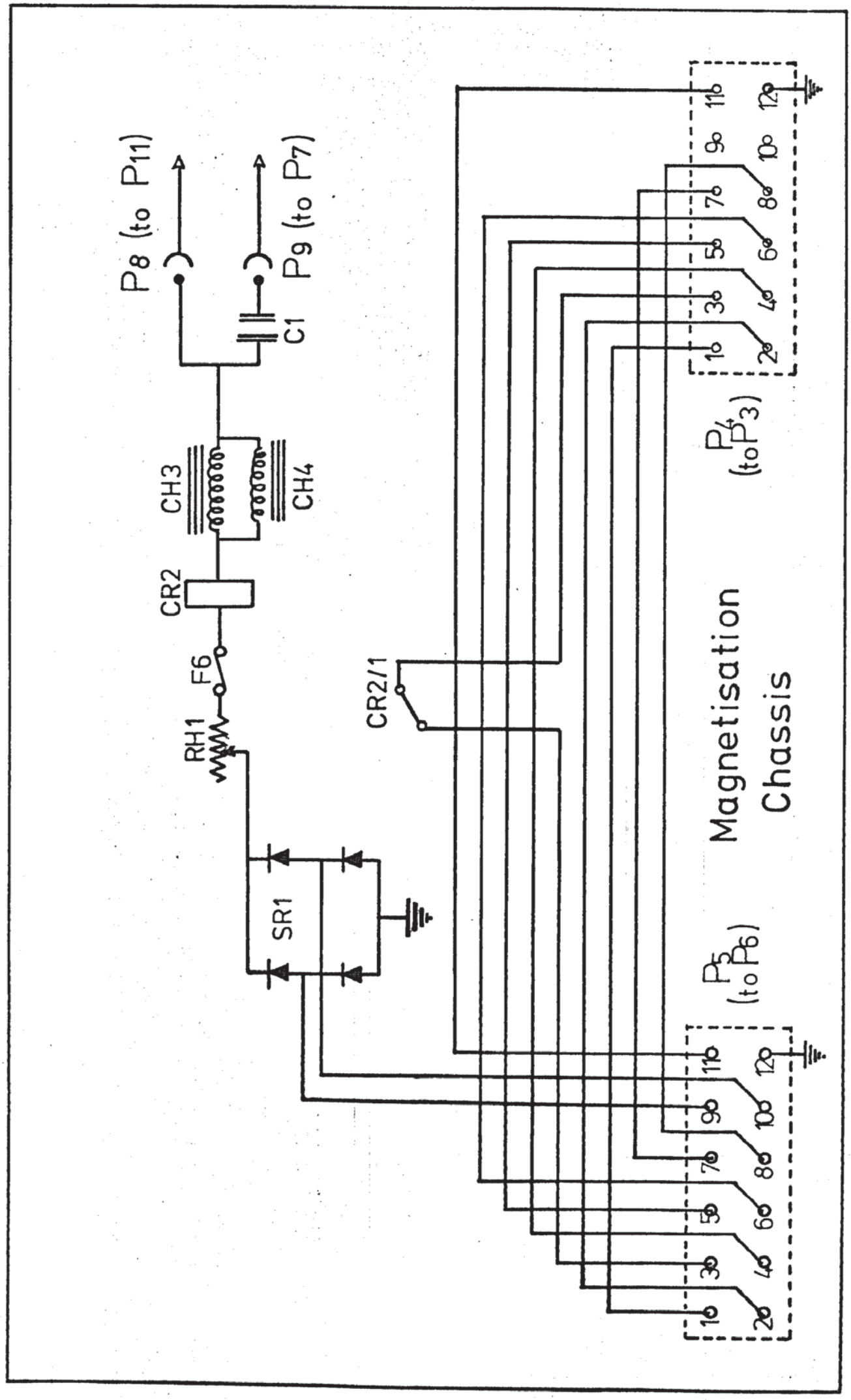
P8 (to P11)
P9 (to P7)
C1
CH3
CH4
CR2
F6
RH1
SR1
CR2/1
Magnetisation
Chassis
P4 (to P3)
P5 (to P6)
10
20
30
40
50
60
70
80
90
100
110
120

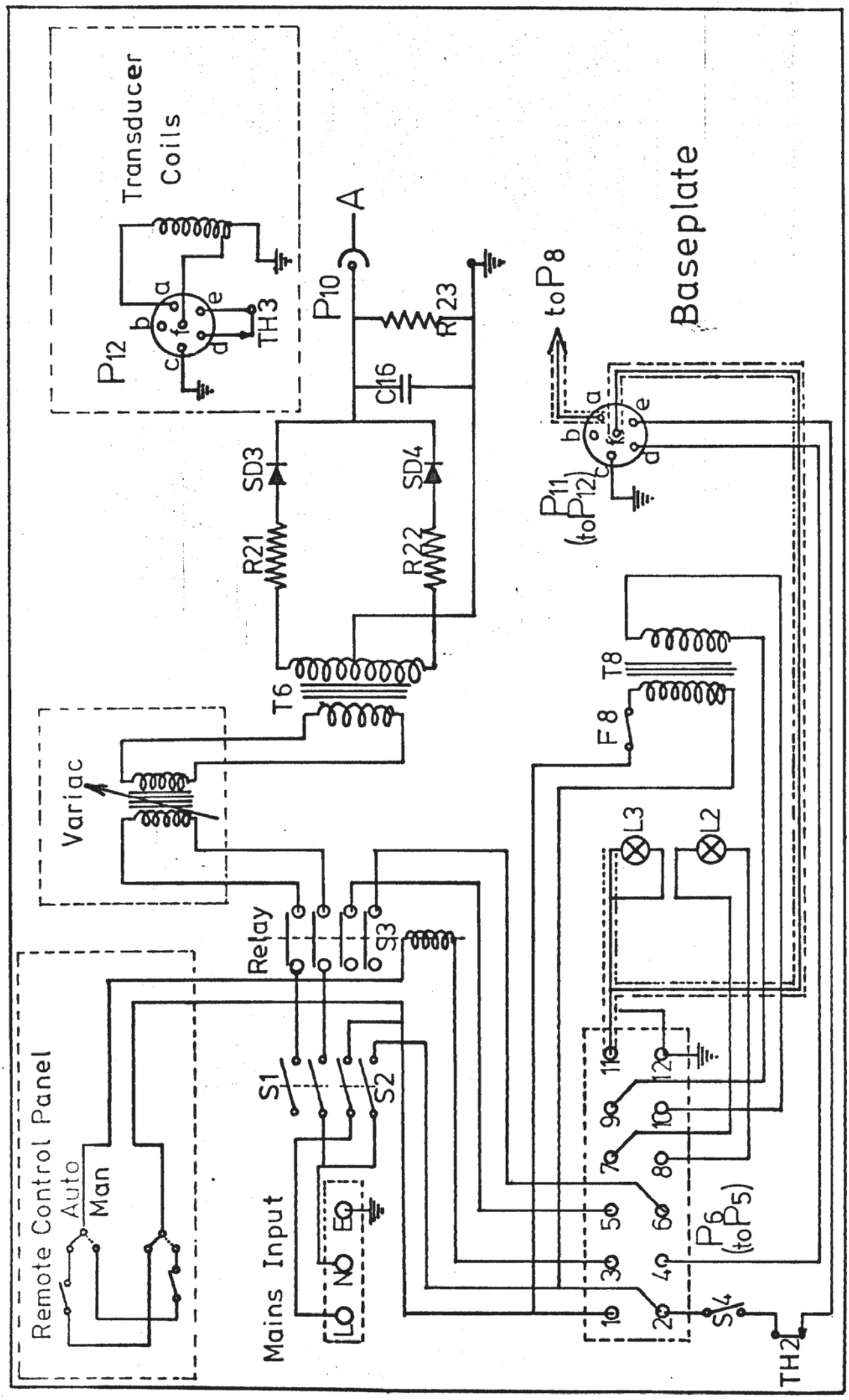
Transducer Coils
P12
TH3
P10
A
R23
C16
SD3
SD4
R21
R22
T6
Variac
Relay
S3
S1
S2
Mains Input
LO NO EQ
Remote Control Panel
Auto
Man
Baseplate
toP8
P11 (toP12)
T8
F8
L3
L2
P6 (toP5)
S4
TH2

External Connectors on Ultrasonic Generator

Output Plug 13 (Baseplate)

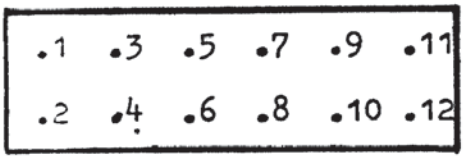

1 -
2 -
3 (Blue) to 3 Pin 6
4 (Blue) to Relay Coil
5 (Red) to Relay Contact 1
(Brown) to Anode Transformer
6 (Black) to Relay Contact 3
7 -
8 (Blue) to Anode Transformer
9 (Coaxial,Blue) to Frequency Counter Red Plug Pin 5
10 (Coaxial,Red/Black) to Frequency Control Red Plug Pin 4
11 (Coaxial,Red/Black).to Tuning Lamp Circuit
12 Earth

Red Plug (Drive Chassis)

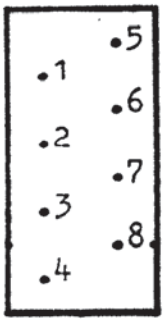

1 Amplitude Pot Windings (Brown)
2 Amplitude Pot Windings (Blue)
3 Amplitude Pot Slider (Green)
4 Frequency Control (Coaxial Red/Black)
5 Frequency Counter (Coaxial Blue)
6 -
7 -
8 -

A.4. Standardisation of Blank-holder Conditions.

A.4.1. General Introduction.

The purpose of a blank-holder during deep drawing is to control the movement of the material during the radial drawing-in process. The material in this region is subject to a biaxial stress system, i.e., a tensile radial stress and a compressive circumferential stress. This circumferential stress causes the partly deformed blank to be in a state of instability because buckling can occur more readily than normal compression. This instability reveals itself as wrinkling of the blank at the circumference before drawing over the die radius. For a given draw-ratio this problem is more severe in thin gauge materials; conversely, heavy gauge materials can often be drawn without the use of a blank-holder, especially if special forms of die profiles, i.e., tractrix, are used. This is because of the greater bending resistance of thicker material.

The blank-holder controls this problem of wrinkling by not allowing the material to form the corrugations. In doing so, by applying a third compressive stress to the normal plane of the material, it also introduces a frictional force which adds to the drawing load. If the blank-holder load is too high, excessive thinning, or even fracture, of the material will occur. There exists, therefore, the desirability of keeping the blank-holder load at a level just sufficient to prevent wrinkling. The interfacial frictional force is also dependent upon the lubrication between tool and blank and, additionally, the amount of lubricant applied to the blank can affect its susceptibility to wrinkling independently of the blank-holder load.

A.4.2. Standardisation of Lubrication and Blank-holder Pressure.

In order to determine the effect of ultrasonic vibration of the tooling upon blank-holder friction, it was desirable to eliminate the variables which could be introduced by lubrication and blank-holder load. Lubrication was standardised by dipping the specimens into the drawing oil and allowing the excess oil to drain away for a predetermined period of time. This time period was initially determined by recording the time taken for the mass of a lubricated sample to become constant, indicating that the draining away of the oil was complete.

The blank-holder load was to be set so that the initial pressure on the undeformed blank remained constant for each individual draw-ratio under test.

A.4.3. Selection of Standard Blank-holder Pressure.

The graph A.4.1 shows the effect of blank-holder load upon the punch load for what was determined to be a near critical draw-ratio for this test with standard lubrication conditions. At the very low specific pressures there was virtually no radial drawing in before the material folded badly. With increasing pressure the folding gradually became wrinkling and at a pressure of 400 lbf.in^{-2} it was virtually non-existent. At 500 lbf.in^{-2} the specimens were fracturing. The operating pressure was thus standardised at 450 lbf. in^{-2} at which wrinkle-free specimens were produced. This pressure was the one applied initially to the undeformed blank. Naturally, in the absence of an oil pressure controller linked to the current area of blank in contact with the blank-holder, the specific pressure increases during the draw. Draw-ratios greater than 1.70 which were above the limiting draw-ratio under these conditions could not be evaluated in this screening but they were considered unlikely to present any wrinkling problems because of the higher blank-holder loads. Conversely, the lowest ratios could be considered more likely to cause problems but on examination this problem did not arise.

Graph No. A.4.1

Selection of Blank-holder Pressure

Maximum Punch Load v Blank-holder Pressure

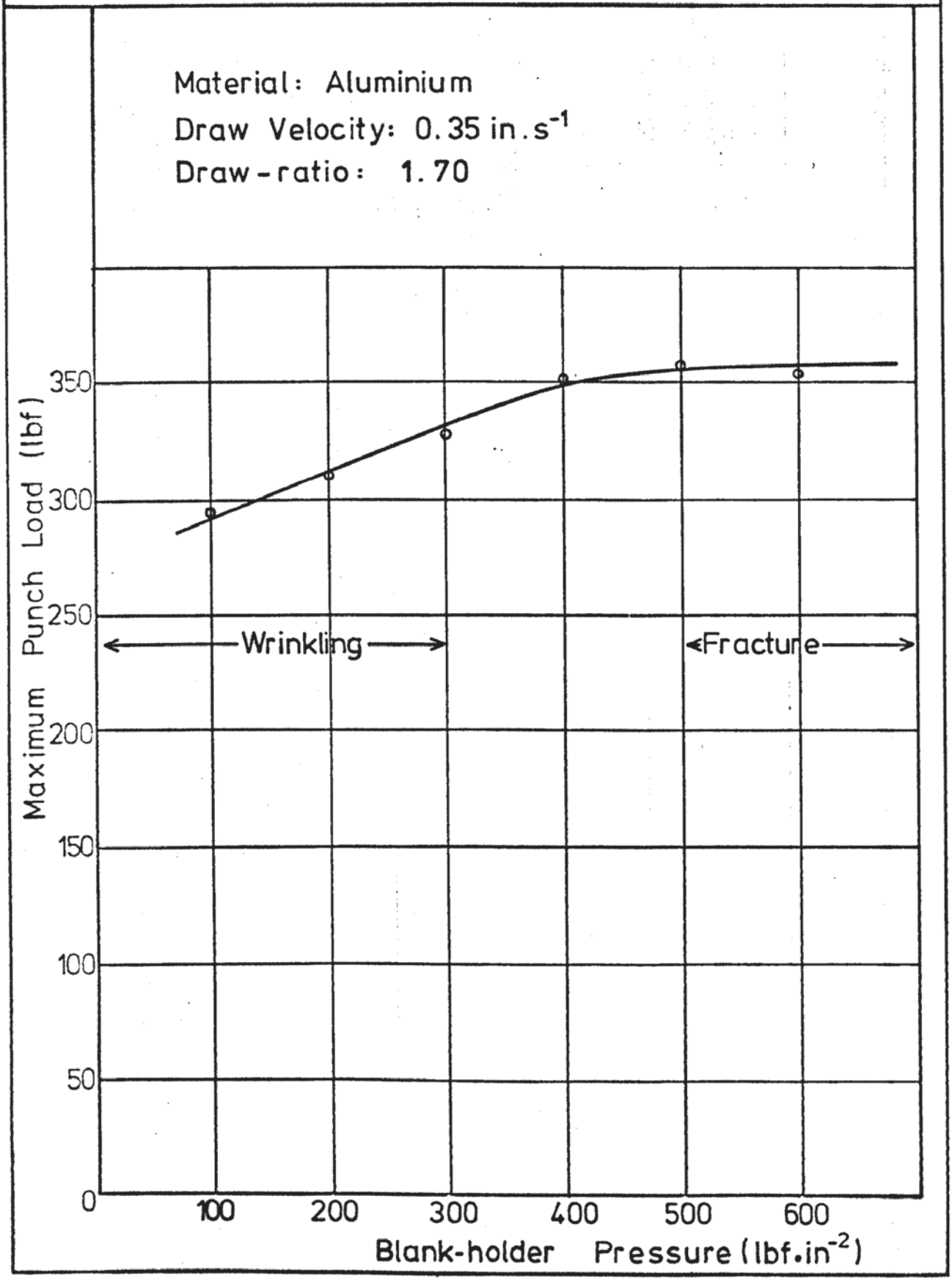

SELECTION OF STANDARD BLANK-HOLDER LOAD

Material: Aluminium	Draw-Ratio: 1.70	Punch Velocity: 0.35 $in.s^{-1}$	Table Number: A.4.1.

Test Number:		1.70-0-BH 100	1.70-0-BH 200	1.70-0-BH 300
Blank-Holder Load lbf	Right Hand	45	98	138
	Left Hand	46	92	138

Punch Travel in.	Punch Load P lbf	Die Sep. Force D lbf	Punch Load P lbf	Die Sep. Force D lbf	Punch Load P lbf	Die Sep. Force D lbf
Max.P	296	2c	309	0	328	6t
Max.D	128	70c	144	70c	147	57c
0.1	35	45c	35	39c	43	29c
0.2	96	68c	99	66c	112	53c
0.3	181	64c	192	66c	200	49c
0.4	251	33c	261	33c	280	21c
0.5	283	14c	299	12c	323	4c
0.6	296	20c	307	2c	328	6t
0.7	285	2t	304	2t	325	8t
0.8	259	8t	283	6t	299	12t
0.9	221	10t	245	10t	261	12t
1.0	173	10t	197	10t	221	14t
1.1	69	10t	123	10t	155	12t
1.2	19	19t	40	16t	40	12t

SELECTION OF STANDARD BLANK-HOLDER LOAD

Material: Aluminium	Draw-Ratio: 1.70	Punch Velocity: 0.35 $in.s^{-1}$	Table Number: A.4.1.

Test Number:		1.70-0-BH 400	1.70-0-BH 500	1.70-0-BH 600
Blank-Holder Load lbf	Right Hand	187	228	277
	Left Hand	184	230	276

Punch Travel in.	Punch Load P lbf	Die Sep. Force D lbf	Punch Load P lbf	Die Sep. Force D lbf	Punch Load P lbf	Die Sep. Force D lbf
Max.P	349	12t	357	16t	349	10t
Max.D	155	49c	133	43c	160	41c
0.1	53	25c	48	23c	43	16c
0.2	136	47c	125	41c	120	39c
0.3	229	37c	221	35c	216	35c
0.4	296	12c	301	14c	304	10c
0.5	336	4t	341	6t	*349	*10t
0.6	347	12t	355	14t	*Failed at 0.5 in travel	
0.7	347	16t	*357	*16t		
0.8	320	18t	*Failed at 0.65 in travel			
0.9	280	18t				
1.0	237	18t				
1.1	184	16t				
1.2	67	20t				

A.4.4. Standard Blank-holder Loads.

The blank-holder loads required at the standard initial pressure of 450 $lbf.in^{-2}$ were calculated from a consideration of the initial area of the undeformed blank.

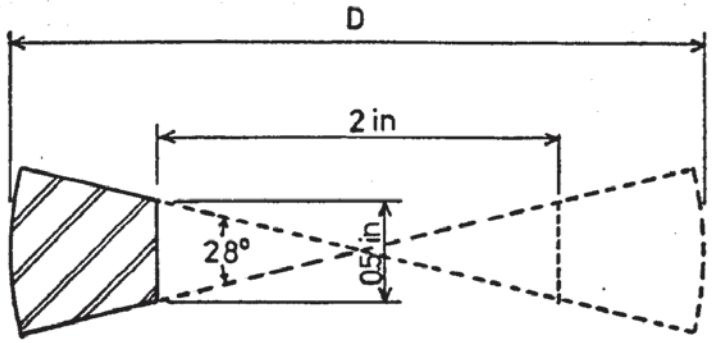

Area of 1 section = $\frac{\pi}{4} D^2 \times \frac{28}{360} - \frac{1}{4}$ in^2

D (in)	Area of One Section	Load at pressure of 450 $lbf.in^{-2}$
3.0	0.299	135
3.1	0.337	152
3.2	0.375	169
3.3	0.415	187
3.4	0.456	205
3.5	0.498	224
3.6	0.541	244
3.7	0.586	264
3.8	0.632	284
3.9	0.679	306
4.0	0.727	327

A.4.5. Determination of Linear Roller Bearing Friction.

The blank-holder and dies were separated from the blank-holder pressure plate and subpress base respectively by the use of linear roller bearings. The purpose of these bearings was to minimise the frictional constraint on these two components by any other part of the system, in order that frictional forces on the load cells would be essentially that at the tool-workpiece interface.

In order to determine the frictional force, due to the linear roller bearings, acting upon the blank-holder and die these two components were loaded between the roller bearings and the force to move the tools against friction was noted.

The load on each blank-holder to apply an initial blank-holder pressure of 450 lbf. $in.^{-2}$ to the specimen was determined and this load was applied through the roller bearings to the blank-holder and die assembly with an hydraulic jack and proving ring. The frictional force was measured by increasing the tension on a spring balance until the assembly began to move, the maximum force being noted.

This was repeated for a variety of loads corresponding to each draw-ratio and the frictional force as shown in the table.

Draw-ratio	Blank-holder load (lbf)	Proving ring deflection	Friction force (lbf)
1.50	134.9	38.42	0.8
1.55	151.6	43.18	0.8
1.60	169.0	48.14	0.9
1.65	186.8	53.21	0.9
1.70	205.3	58.48	0.9
1.75	224.2	63.86	0.9
1.80	243.7	69.42	0.9
1.85	263.8	75.14	0.9
1.90	284.4	81.01	0.9
1.95	305.6	87.05	0.9
2.00	327.3	93.23	0.9

A.5. Material Properties.

A.5.1. The Tensile Test.

Specimens suitable for the preparation of tensile test pieces were taken from the sheet material with their longitudinal axis orientated to the rolling direction. The test pieces were prepared in accordance with British Standard 18 and had a width of 0.5 in. and a gauge length of 2.5 in. Several samples from each sheet of material used in the drawing tests were prepared and the tensile tests were performed on an Instron Universal testing machine. The results of these tests are summarised in Table A.5.1.

Table A.5.1.

Material: Commercially-pure Aluminium
Deep-drawing quality

Strain rate 0.2 in.min^{-1}

Proof-stress taken at 0.2 per cent strain

Test No.	Gauge in.	Width in.	U.T.S. lbf/in^2	Elongation per cent	Proof-stress lbf/in^2
Sheet 1					
1	0.0281	0.494	11.74×10^3	42.4	4.68×10^3
2	0.0282	0.495	11.82×10^3	42.2	4.51×10^3
3	0.0281	0.494	11.88×10^3	-	4.39×10^3
Sheet 2					
4	0.0280	0.494	11.85×10^3	44.0	4.48×10^3
5	0.0280	0.494	11.77×10^3	41.9	4.69×10^3
6	0.0280	0.494	11.85×10^3	-	4.55×10^3

Graph No. A.5.1.

Tensile Tests

Tensile Load v Elongation

Material: C.P. Aluminium Sheet 1

Strain rate: 0,2 in.min^{-1}

Gauge length: 2,5 in.

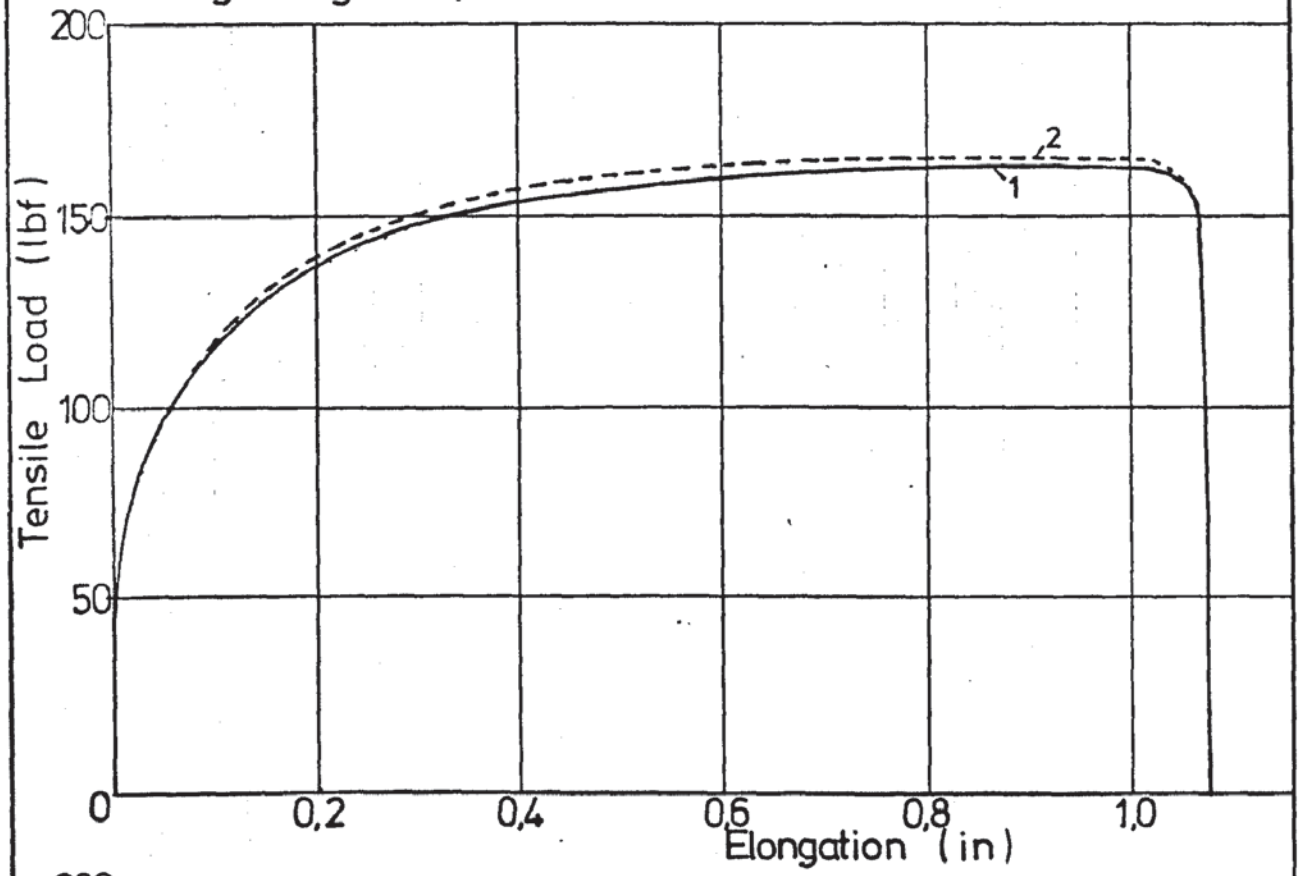

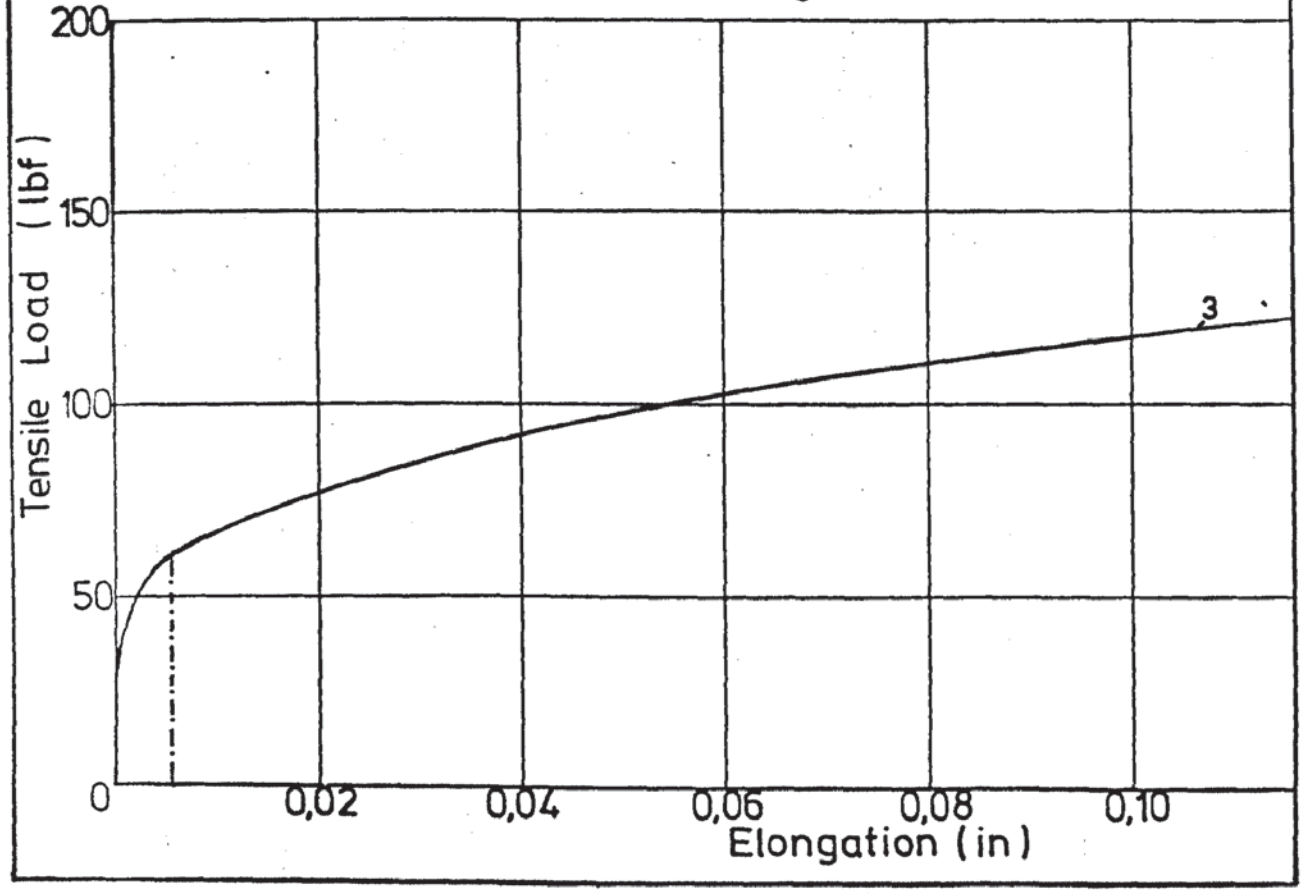

Graph No. A.5.2.

Tensile Tests

Tensile Load v Elongation

Material: C. P. Aluminium Sheet 2

Strain rate: 0,2 in min^{-1}

Gauge length: 2,5 in

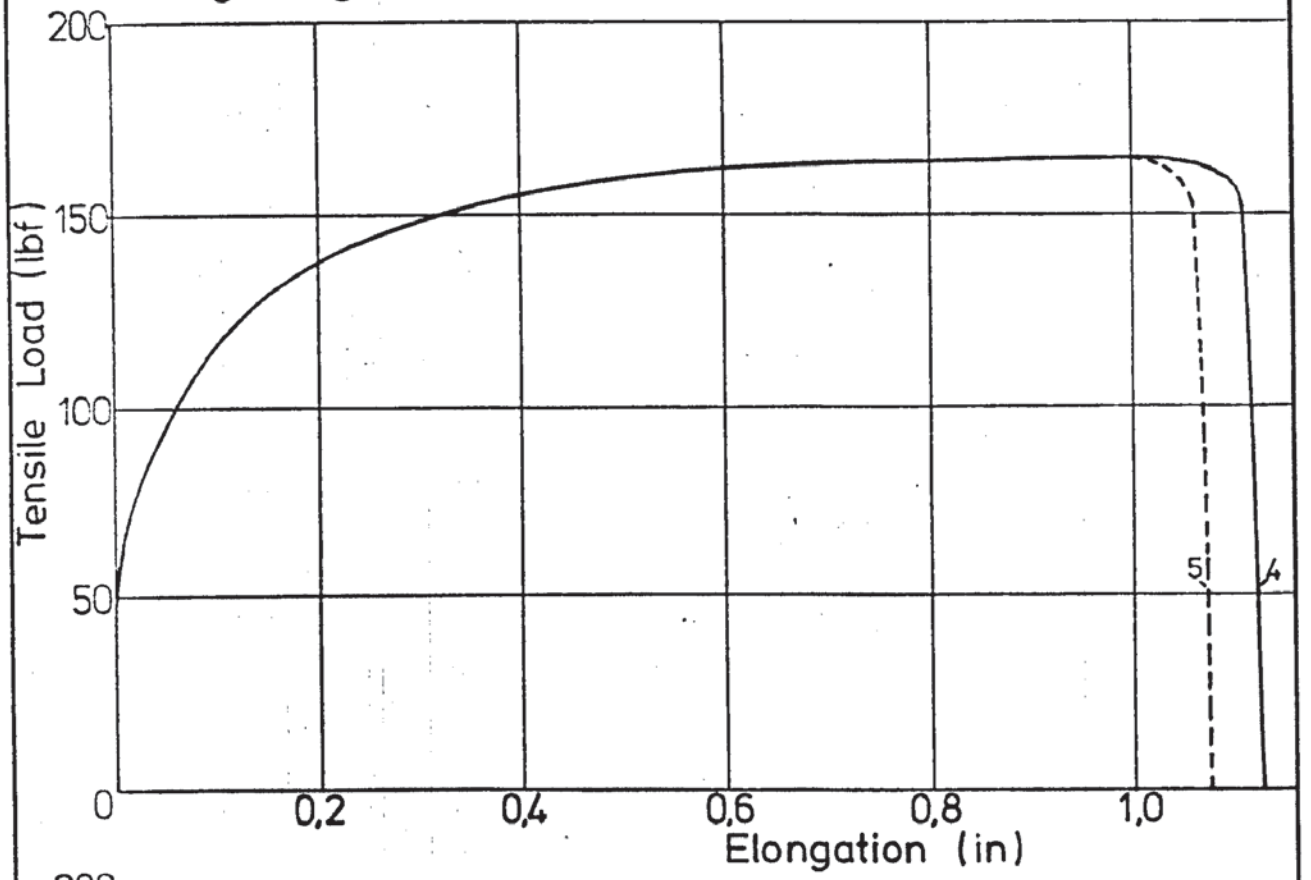

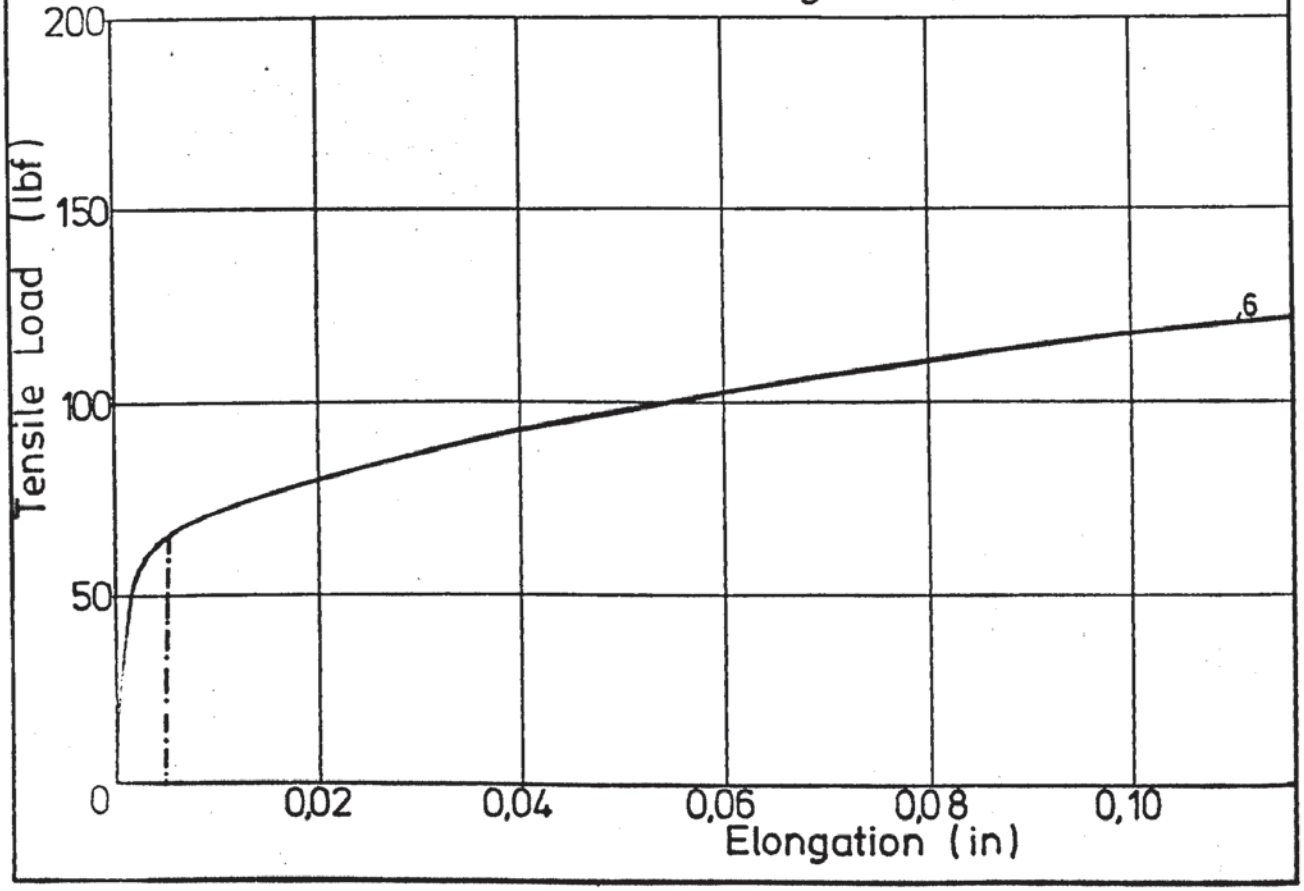

A.5.2. Hardness Tests.

Preliminary hardness testing was performed on samples of the sheet aluminium, which were likely to be of lower hardness than the drawn specimens, in order to determine a reliable method of hardness testing.

Two hardness testing machines were available, a Rockwell 30T ball indentor and a Vickers Pyramid Diamond indentor. The Rockwell was initially preferred because of the ease and rapidity of performing multiple hardness tests. Hardness tests were made on samples of the material, using both machines and the hardness numbers were compared.

The results using the Rockwell 30T were consistently higher than those using the Vickers Pyramid Diamond, and when comparing the indentations it could be seen that the Rockwell indentation had marked through to the reverse (anvil) side of the sample in some places, thus affecting the hardness number.

The indentation from the Vickers Pyramid Diamond testing showed much less penetration amd therefore this machine was used for all the subsequent hardness testing despite its slower operating procedure. When testing drawn samples the two drawn sides of the 'U' shape were separated from the centre of the sample to enable each part to be positioned under the indentor. Hardness tests were performed at intervals of 0.1 in., from the punch profile radius to the top of the specimen, the average of three indentations being taken at each position.

SURFACE HARDNESS TESTS

Table Number:	A.5.2.1.
Material:	Aluminium
Draw-Ratio:	1.55
Punch Velocity:	0.34 in.s^{-1}
Frequency:	12.55 kHz
Vickers Hardness Number Scale:	1.0 kg

Distance From Sample Base in.	Drawing Test Numbers: BH-155-0 to BH-155-260									
	-0	-20	-60	-100	-140	-180	-220	-260	Undeformed material.	
0.1	28.0	30.9	29.3	28.0	26.4	29.0	27.9	28.6	24.4	23.7
0.2	28.7	29.7	29.4	28.1	26.0	29.4	28.2	29.8	25.8	25.4
0.3	33.9	30.9	32.5	32.5	31.2	30.7	30.3	31.2		
0.4	33.9	34.2	34.8	32.2	32.9	31.3	32.8	32.4		
0.5	35.4	34.2	34.5	32.7	33.0	33.6	32.7	32.5		
0.6	36.6	33.6	34.8	32.7	33.6	34.3	34.0	35.1		
0.7	36.6	34.2	36.3	33.9	34.0	35.7	35.7	32.5		
0.8	35.1	34.5	35.7	35.7	34.2	35.8	36.3	34.8		
0.9	38.3	33.9	35.1	37.0	35.1	36.2	32.2	35.4		

NOTE: Tests completed within 4 hours of drawing.

SURFACE HARDNESS TESTS

Table Number:	A.5.2.2.
Material:	Aluminium
Draw-Ratio:	1.55
Punch Velocity:	0.34 $in.s^{-1}$
Frequency:	12.55 kHz
Vickers Hardness Number Scale:	1.0 kg

Distance from Sample Base in.	Drawing Test Numbers: BH-155-0 to BH-155-260									
	-0	-20	-60	-100	-140	-180	-220	-260	Undeformed material.	
0.1	28.0	30.9	29.2	27.8	26.5	28.7	27.8	28.7	24.4	23.7
0.2	28.7	29.7	29.4	28.1	26.0	29.4	28.2	29.8	25.8	25.4
0.3	33.9	30.9	32.5	32.5	31.2	30.7	30.3	31.2		
0.4	33.9	34.2	34.8	32.2	32.9	31.3	32.8	32.4		
0.5	35.4	34.2	34.5	32.7	32.2	33.6	32.7	32.5		
0.6	36.6	33.6	34.8	32.7	33.6	34.3	34.0	35.1		
0.7	36.6	34.2	36.3	33.9	34.0	35.7	35.7	32.5		
0.8	35.1	34.5	35.7	35.1	34.2	35.8	36.3	34.8		
0.9	38.3	33.9	35.1	37.0	35.1	36.1	37.2	35.4		

SURFACE HARDNESS TESTS

Table Number:	A.5.2.3.
Material:	Aluminium
Draw-Ratio:	1.65
Punch Velocity:	0.35 $in.s^{-1}$
Frequency:	12.63 kHz
Vickers Hardness Number Scale:	1.0 kg & 2.5 kg

Distance From Sample Base in.	Drawing Test Number: BH-165-260I									
	1.0 kg scale					Mean value	2.5 kg scale			Mean value
0.1 B	35.2	35.1	35.0	35.2	35.0	35.1	35.0	35.2	34.3	34.9
0.2 D	36.0	35.9	34.2	35.9	35.5	35.5	34.2	33.5	34.2	34.0
0.3 B	37.0	35.7	36.0	36.3	36.3	36.3	34.2	33.3	34.2	34.0
0.4 D	36.6	37.0	35.4	36.0	34.5	35.9	35.8	35.8	37.2	36.2
0.5 B	35.4	35.1	35.3	36.0	37.6	36.0				
0.6 B	36.0	38.0	38.0	36.0	37.0	36.8				
0.7 B	37.4	37.6	35.1	34.8	36.6	36.1				
0.8 B	37.3	37.3	36.6	38.0	38.0	37.7				

Note. B = Bright surface

D = Dull surface

SURFACE HARDNESS TESTS

Table Number:	A.5.2.4.
Material:	Aluminium
Draw-Ratio:	1.60
Punch Velocity:	0.33 in.s^{-1}
Frequency:	12.84 kHz
Vickers Hardness Number Scale:	1.0 kg

Distance From Sample Base in.	Drawing Test Numbers: 40DI-160-0 to 40DI-160-180									
	-0			-180				-180V4		
0.2	39.7	40.5	40.1	39.7	39.0	37.3	38.0	40.5	41.7	40.1
0.4	39.7	40.5	39.7	41.3	40.9	40.5	40.1	42.5	42.5	42.1
0.6	38.7	39.4	40.5	40.1	39.0	40.1	39.5	40.5	40.9	41.3
0.8	39.7	40.5	39.4	39.4	39.4	39.7	39.6	42.1	39.7	40.5
1.0	40.8	41.6	40.5	40.1	39.4	42.1	39.0	41.3	39.4	40.9
	-0P-1 P.T.F.E. Lubrication. -260P-1									
0.2	42.1	43.3	40.1	41.3		36.6	31.9	36.1	35.0	
0.4	40.5	40.2	40.1	40.2		40.5	41.7	41.7	40.9	
0.6	39.0	39.7	40.5	40.3		42.1	40.5	41.3	41.3	
0.8	40.1	42.5	43.3	45.9		40.1	40.5	41.3	41.0	
1.0	40.1	39.4	43.7	42.1		41.7	40.9	39.7	40.1	

A.6. The Hydraulic Oscillator.

A.6.1. General Description.

The unit was operable over a frequency range of 0 to 500 Hz with a thrust of 4,500 lbf. and stroke of 0.25 in.

The oscillator was controlled by a single-channel servo system, the position of the piston being indicated by means of a rotary transducer.

The transducer was an a.c. pick-up, the feed-back signal from this being demodulated prior to amplification in the d.c. amplifier. The output from the transducer was proportional to the actual displacement. Negative feed-back was employed to maintain stability in the system.

A.6.2. The Actuator.

The actuator was a double-acting jack with a rod extension at each end. Hydraulic fluid under pressure was delivered from the powerpack via servo valves to the actuator. The total movement of the jack was 0.25 in. and its cross-sectional area was 1.5 in^2. When supplied with oil at the maximum flow rate of 6 $gal.min^{-1}$ at a pressure of 3,000 $lbf.in^{-2}$, the maximum dynamic thrust was 3,000 lbf. with a velocity of 18.5 $in.s.^{-1}$. Under static conditions a thrust of 4,500 lbf. was available.

A.6.3. Hydraulic Power Supply.

The unit comprised a pressure-compensated variable-delivery pump driven by an electric motor. The pressurised fluid was delivered to the actuator via an accumulator and a filter. The return flow passed through a fan driven oil-cooler back to the reservoir.

A.6.4. Control Unit.

Servo Unit - The Servo Unit controlled the actuator and power was supplied from an oscillator. 'Gain' was in switched increments with a 'fine' control spanning the set increments.

A balance control enabled the jack to be located at any position

prior to vibration being superimposed.

Carrier Generator Unit - This unit supplied a 24 volt R.M.S. at 2.4 kHz to the feed-back transducer and demodulator.

Power Supply Unit - This provided a stabilised 12 volt supply for operating the servo unit.

A.6.5. Specification.

Actuator.

Bearing type	Drained Gland
Frequency Range	d.c. to 500 Hz.
Stroke	± 0.125 in.
Effective Ram Area	1.5 in^2.
Maximum Thrust	4,500 lbf.
Thrust at Maximum Velocity	3,000 lbf.
Maximum Velocity	18.5 $in.s^{-1}$
Mounting	Flange at end drilled with 7 holes 17/32 in.dia on a 7 in P.C.D.
Piston Rod	1 7/8 in.BSF. thread by 13/16 in. deep with a 1 in. dia hole drilled through the piston centre along its axis.

Hydraulic Power Supply Unit.

Fluid Type	Shell Tellus 27
Fluid Capacity	15 gallon
Filter	5 micron
Pump Delivery	6 $gal.min.^{-1}$
System Pressure	3,000 $lbf.in^{-2}$
Electronic Motor (Pump)	15 hp.
Electric Motor (Cooler)	0.5 hp.
Accumulator	Charged at 1500 $lbf.in^{-2}$

Electronic Control Unit.

Internal Oscillator Range.	0.01 to 1000 Hz.
External Signal Input.	5 volt peak
Input Impedence	20 x 10^3 ohms.

APPENDIX B.

Punch Amplitude Calibration

Distec Output v

Crystal Galvanometer Deflection

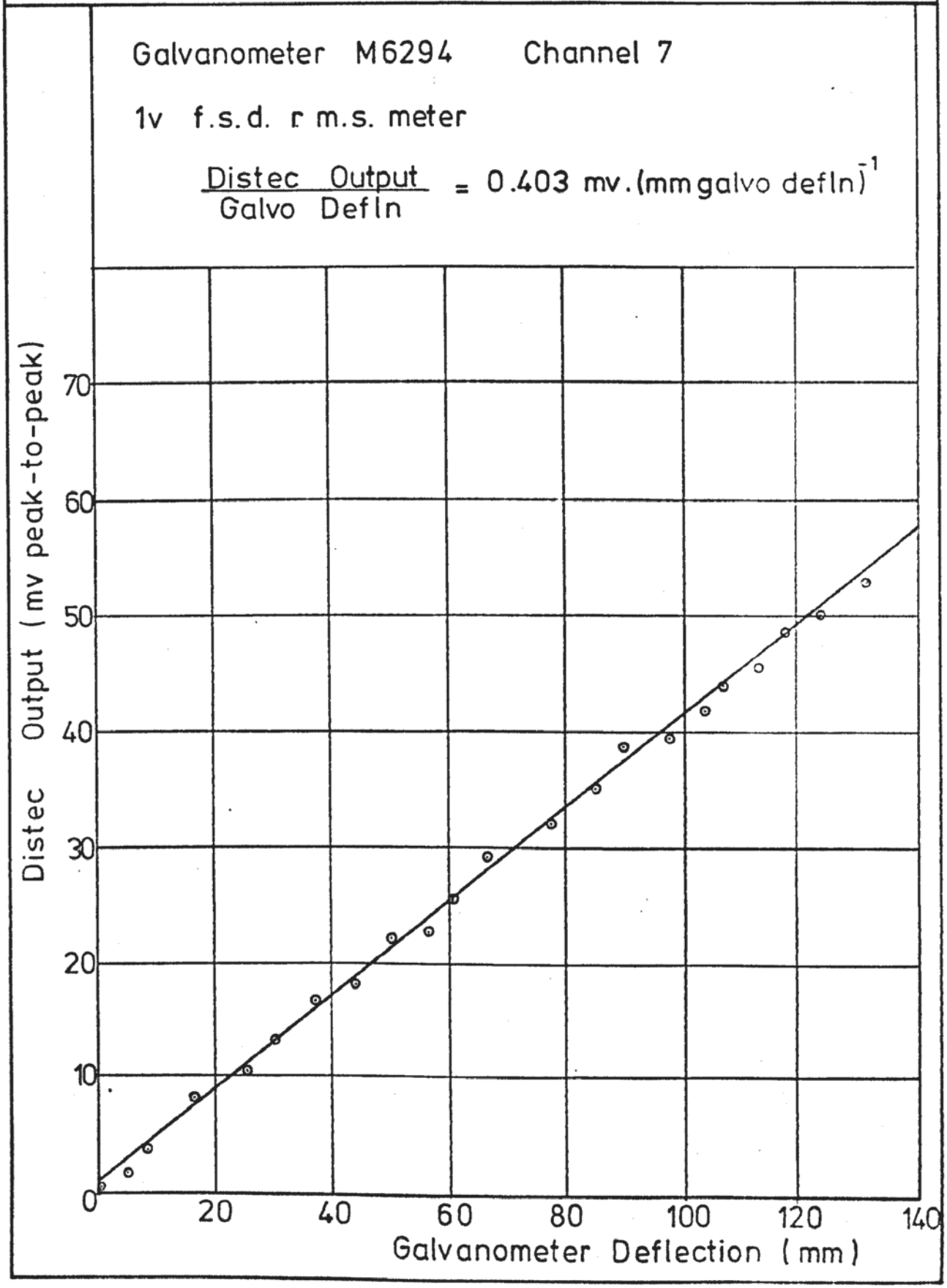

Die Amplitude Calibration

Distec Output v

Die Crystal Galvanometer Deflection

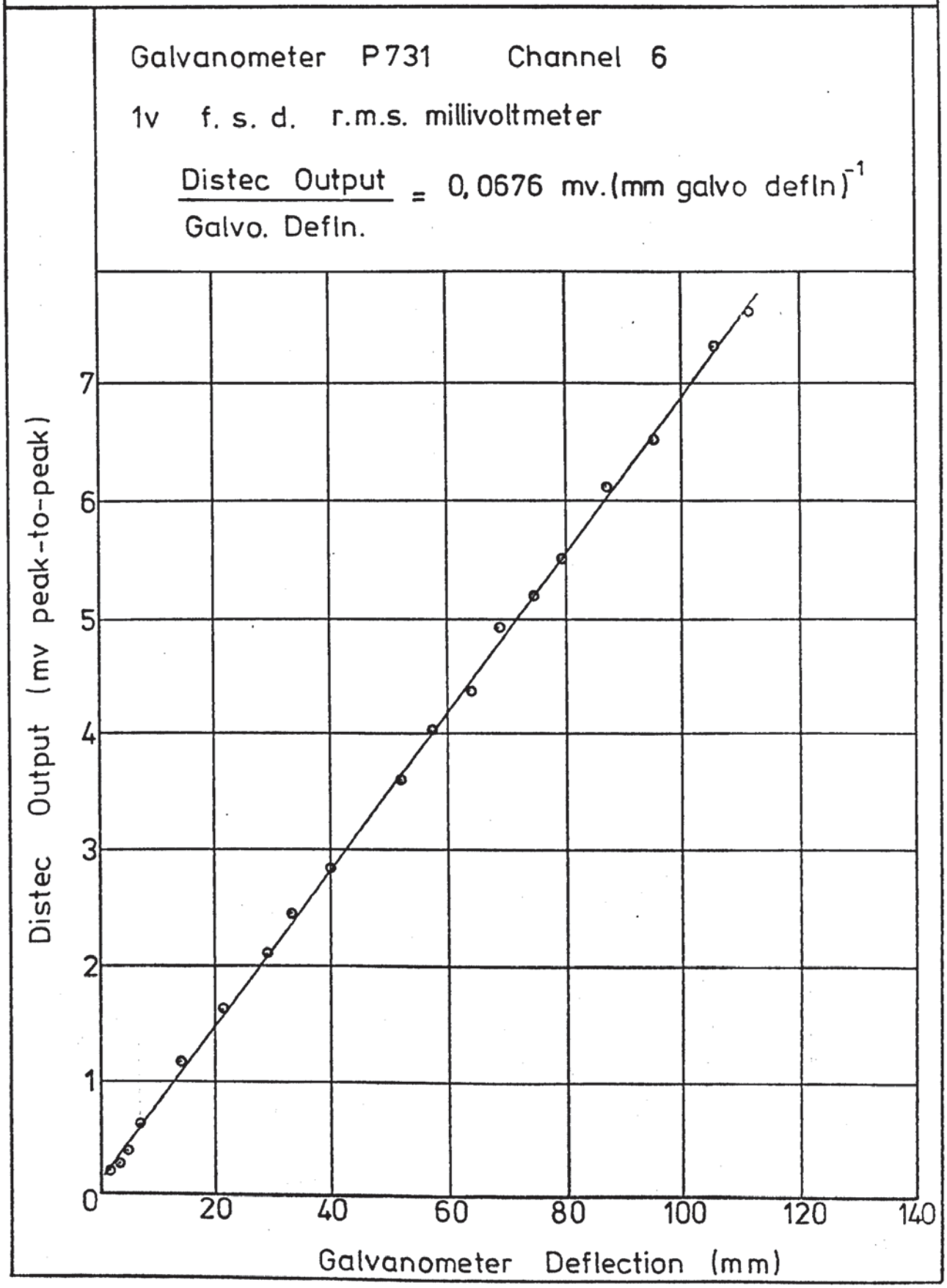

Punch Load Calibration

Punch Load v Galvanometer Deflection

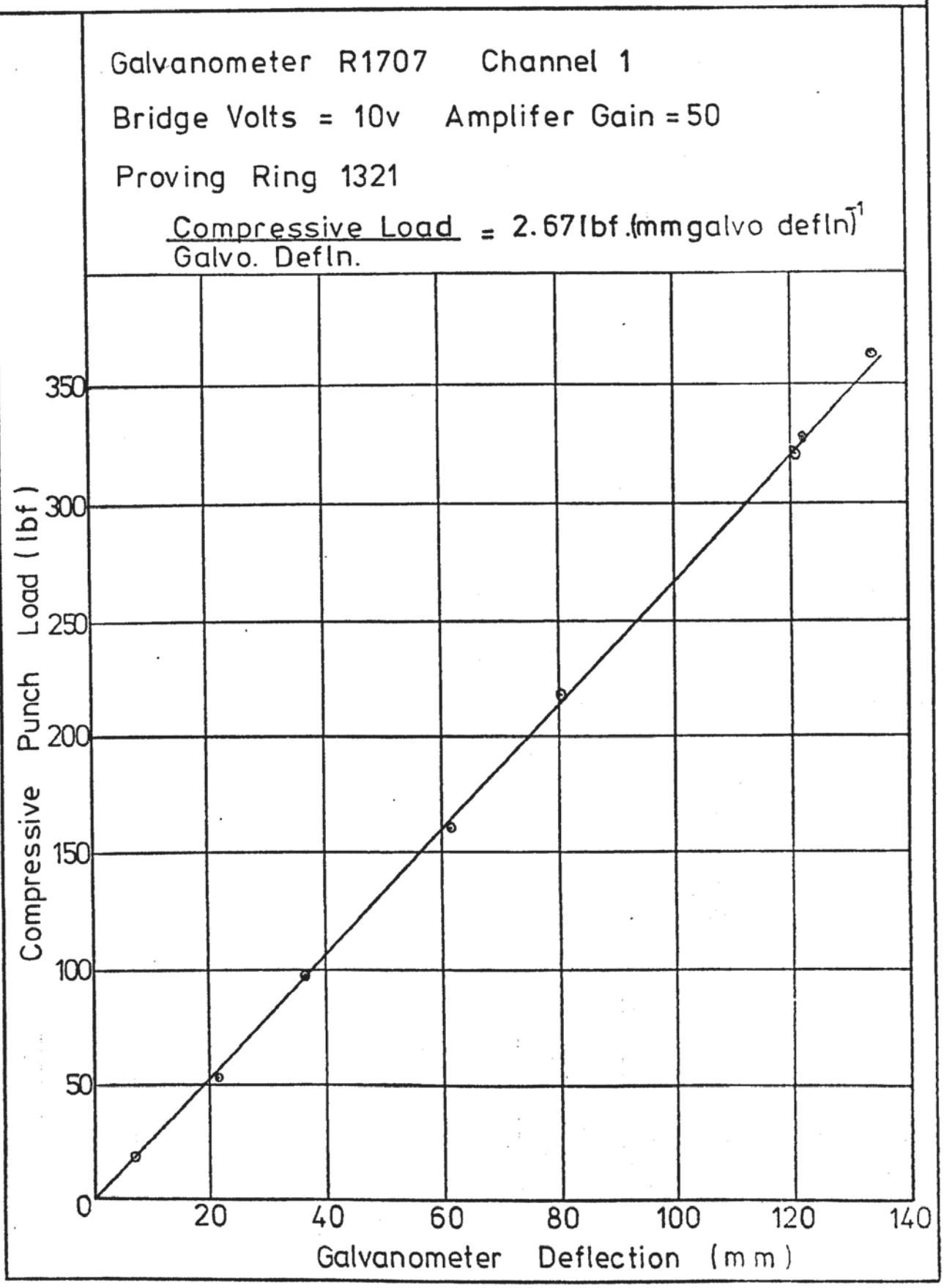

Friction Load Cell Calibration
Compressive Load v
Load Cell Galvanometer Deflection

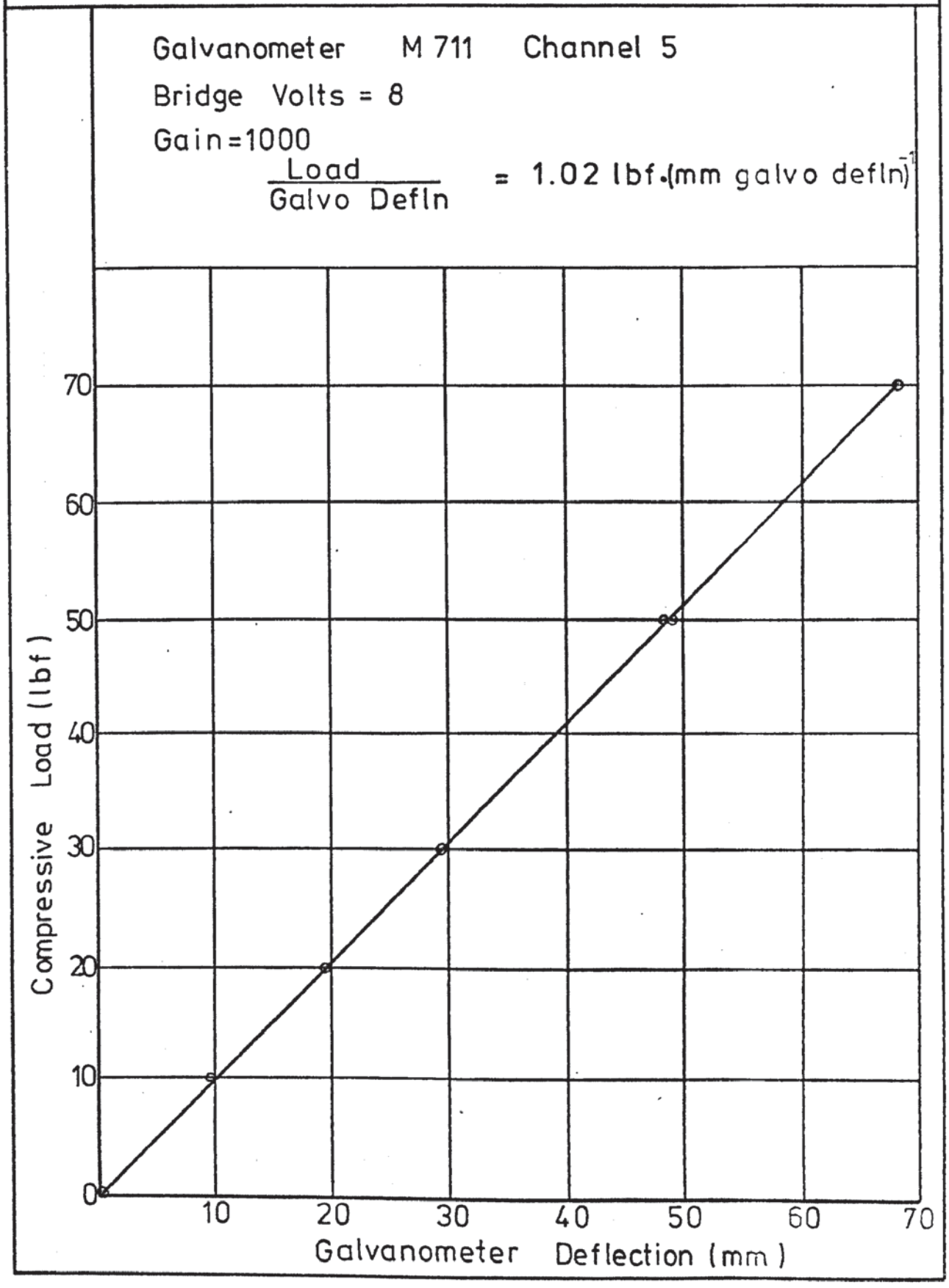

Friction Load Cell Calibration

Compressive Load v

Load Cell Galvanometer Deflection

Galvanometer M 711 Channel 5

Bridge Volts = 8v

Gain = 2000

$$\frac{\text{Load}}{\text{Galvo Defln}} = 0{,}476 \text{ lbf.(mm galvo defln)}^{-1}$$

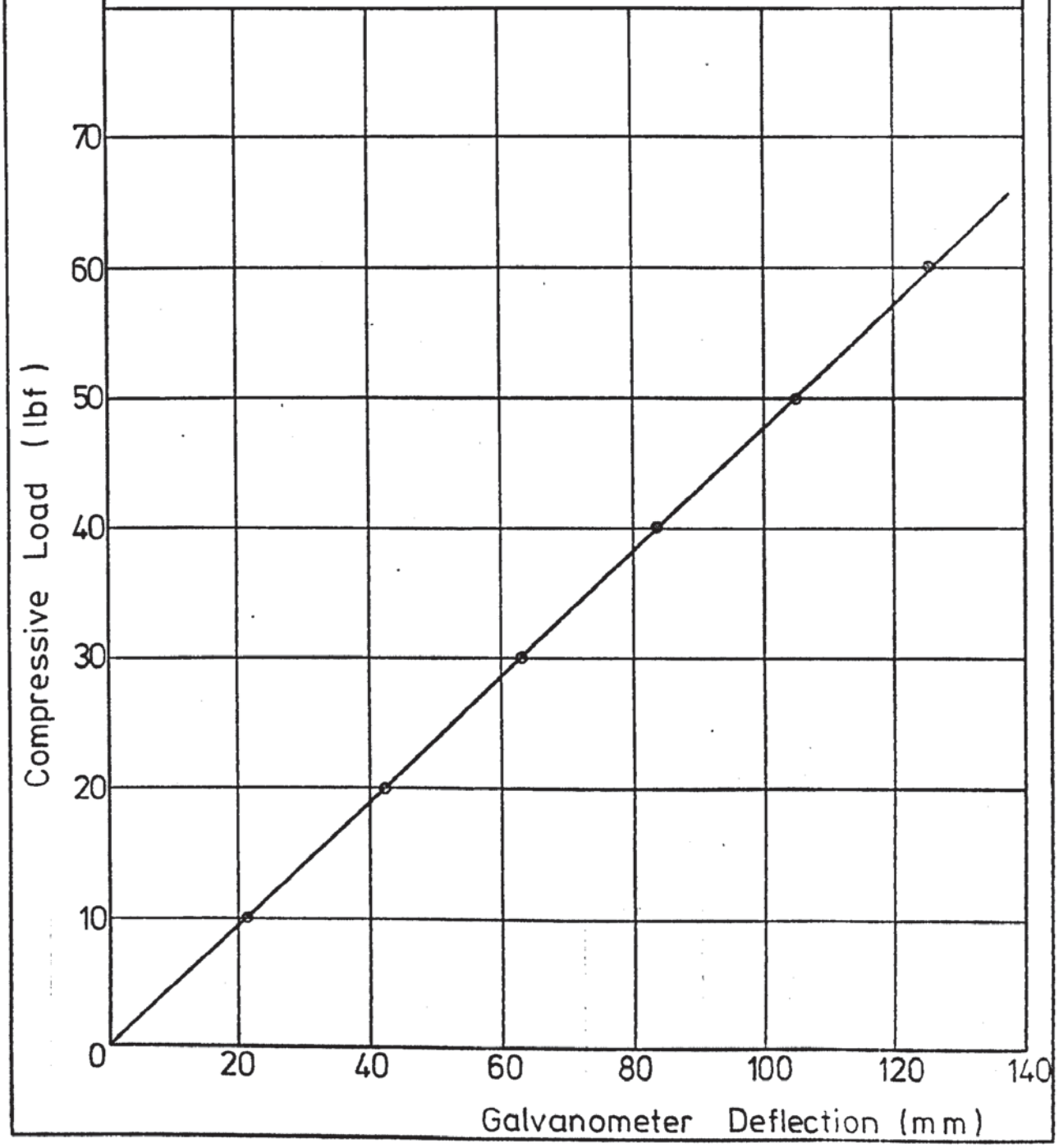

Punch Displacement Calibration

Punch Displacement v Galvanometer Deflection

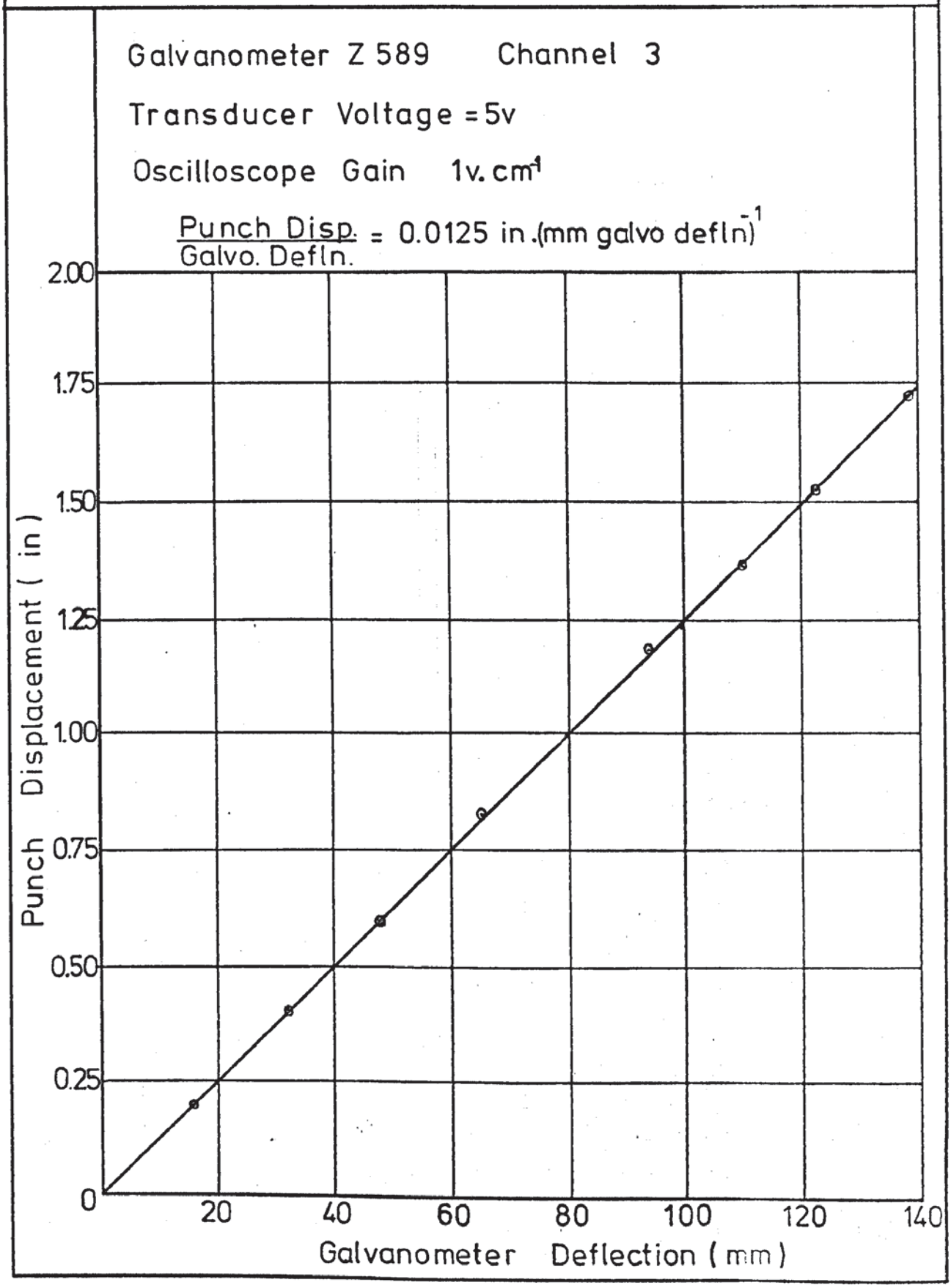

L.H. Blank-holder Load Cell Calibration
Compressive Load v
Load Cell Galvanometer Deflection

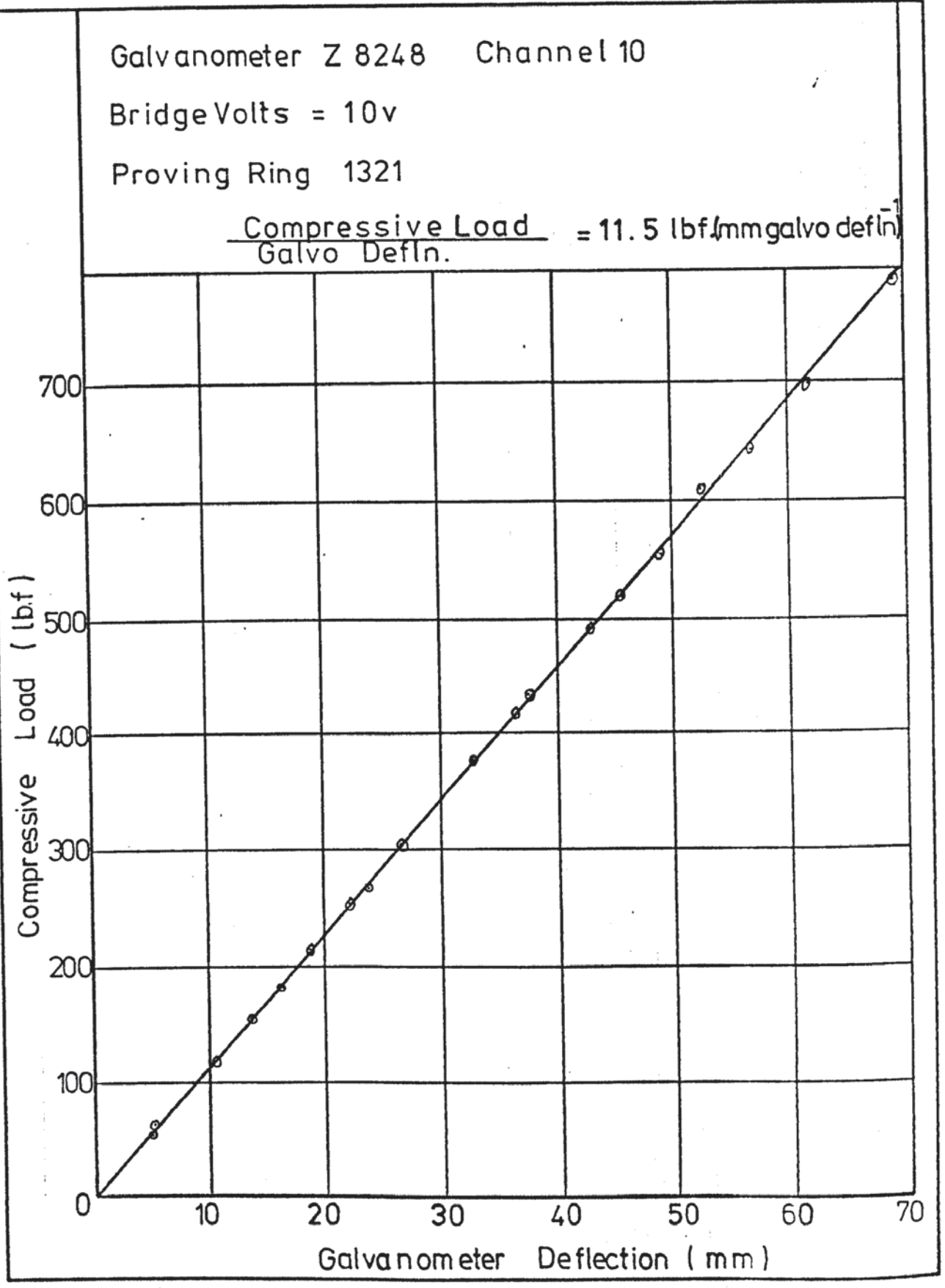

R.H. Blank-holder Load Cell Calibration

Compressive Load v Load Cell Galvanometer Deflection

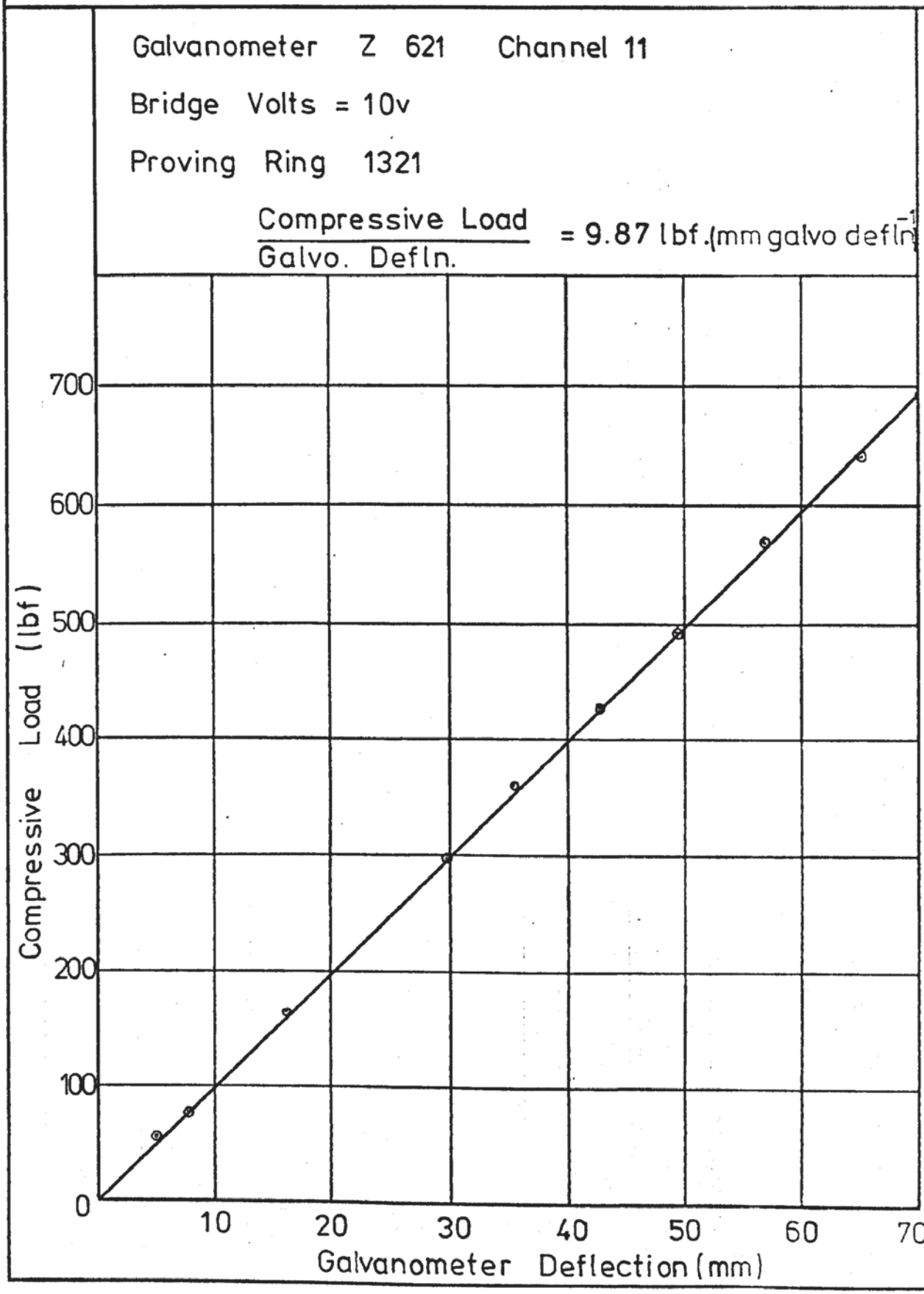

L.H. Blank-holder Amplitude Calibration

Distec Output v Crystal Galvanometer Deflection

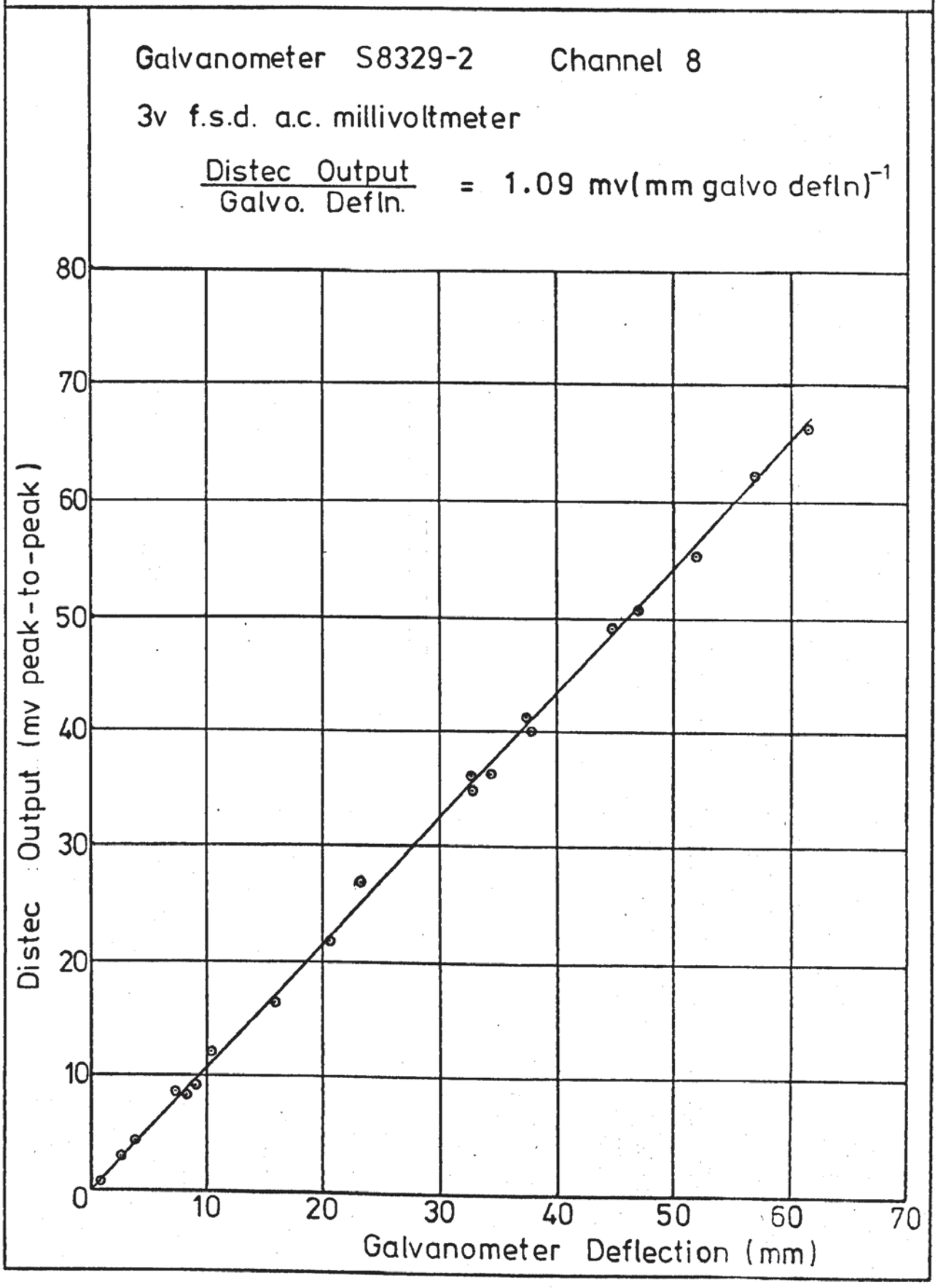

R.H. Blank-holder Amplitude Calibration
Distec Output v
Crystal Galvanometer Deflection

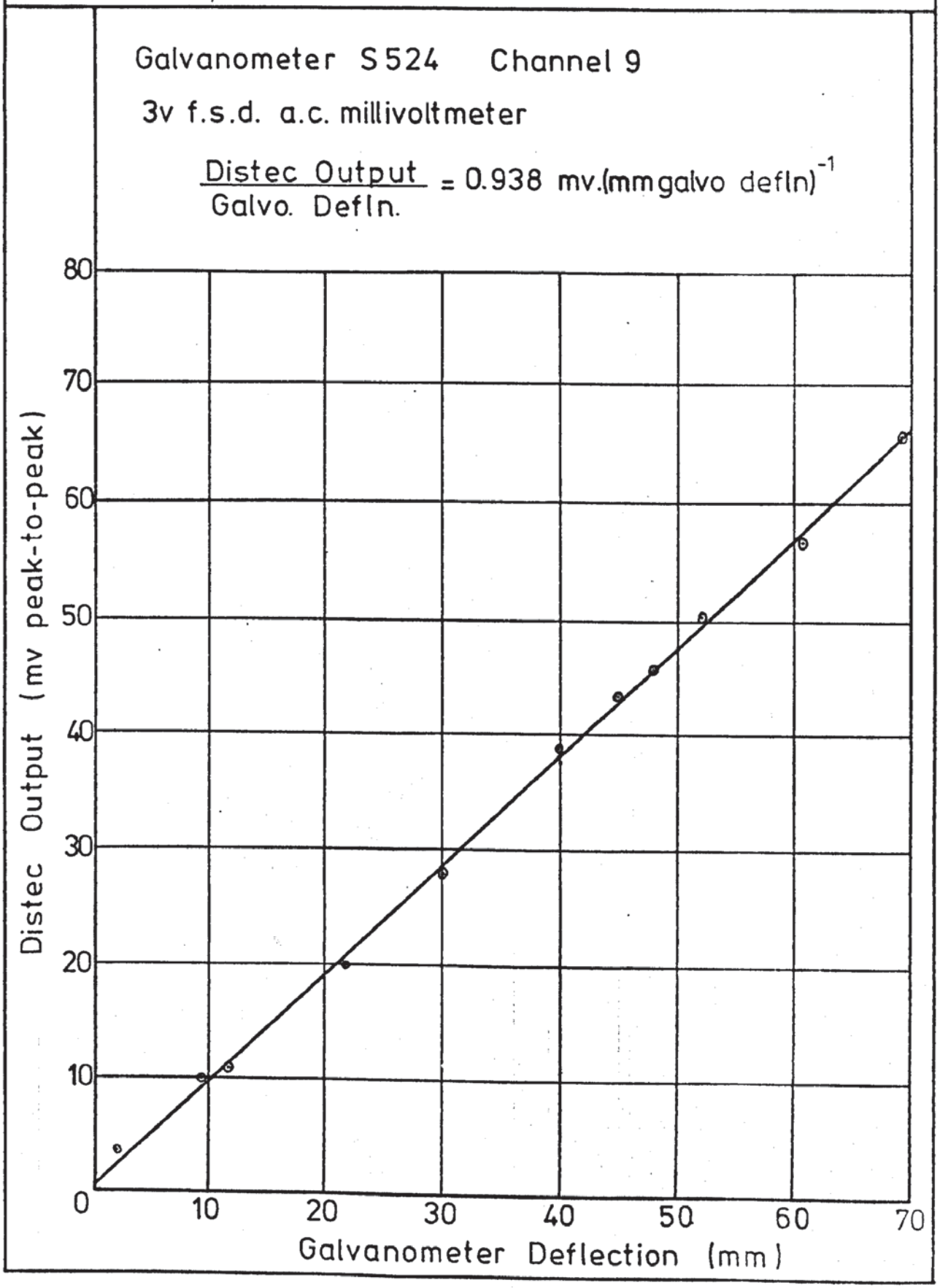

Distec Displacement Sensor Calibration

Output of Probe v

Distance from Material

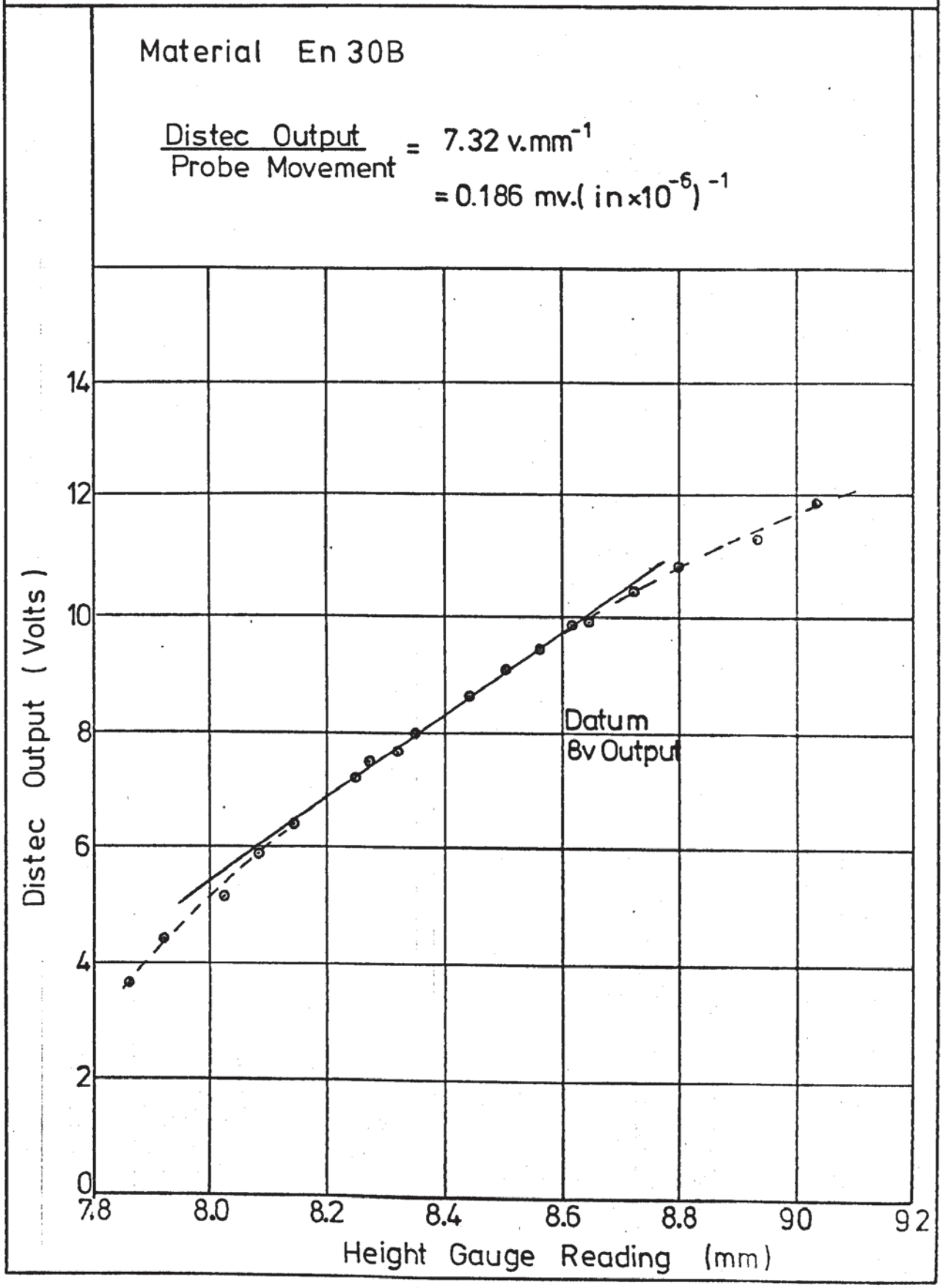

Die Separation Force Load Cell Calibration

Tensile Force v

Galvanometer Deflection

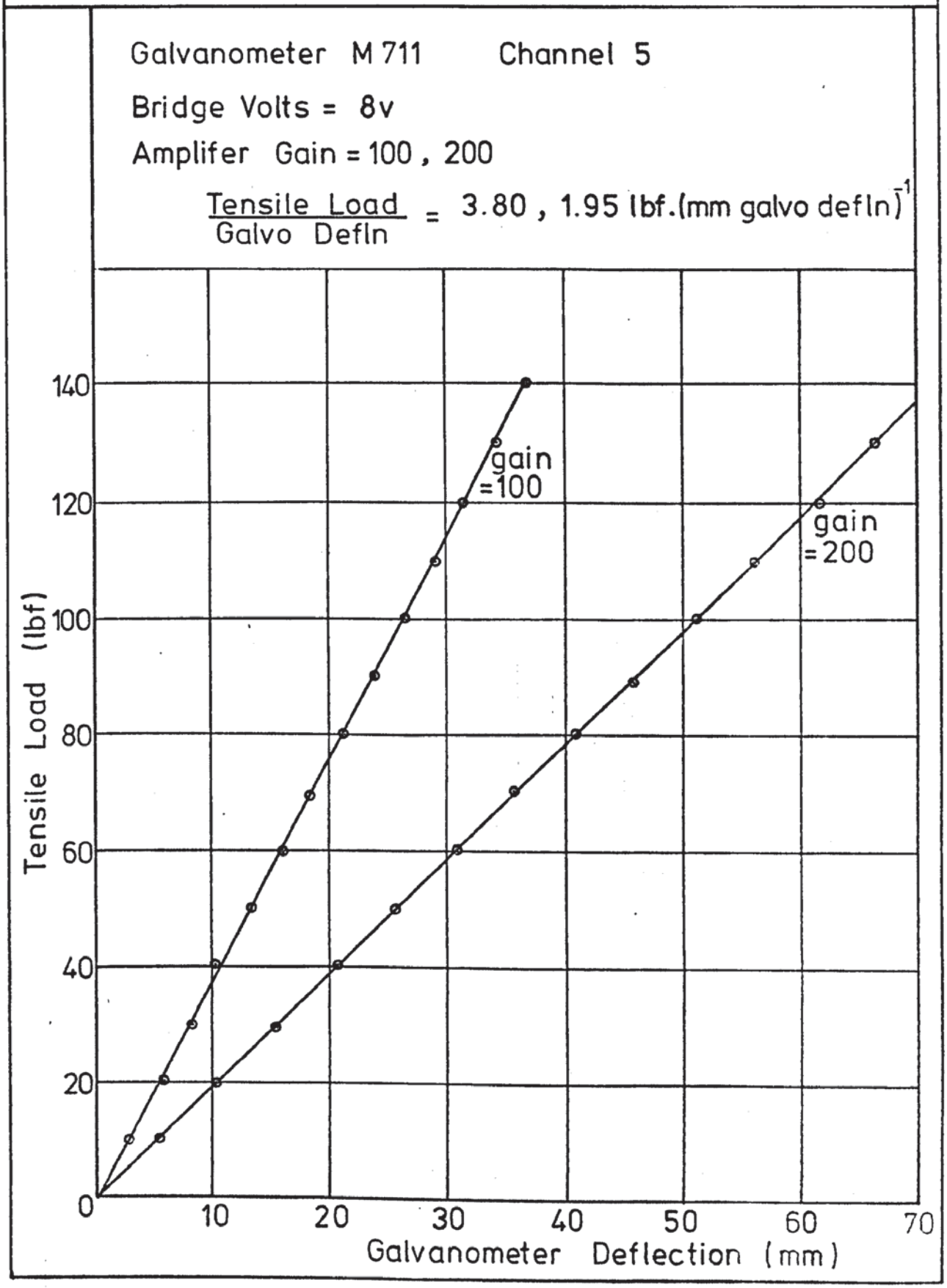

Punch Velocity Calibration

Punch Velocity v Galvanometer Deflection

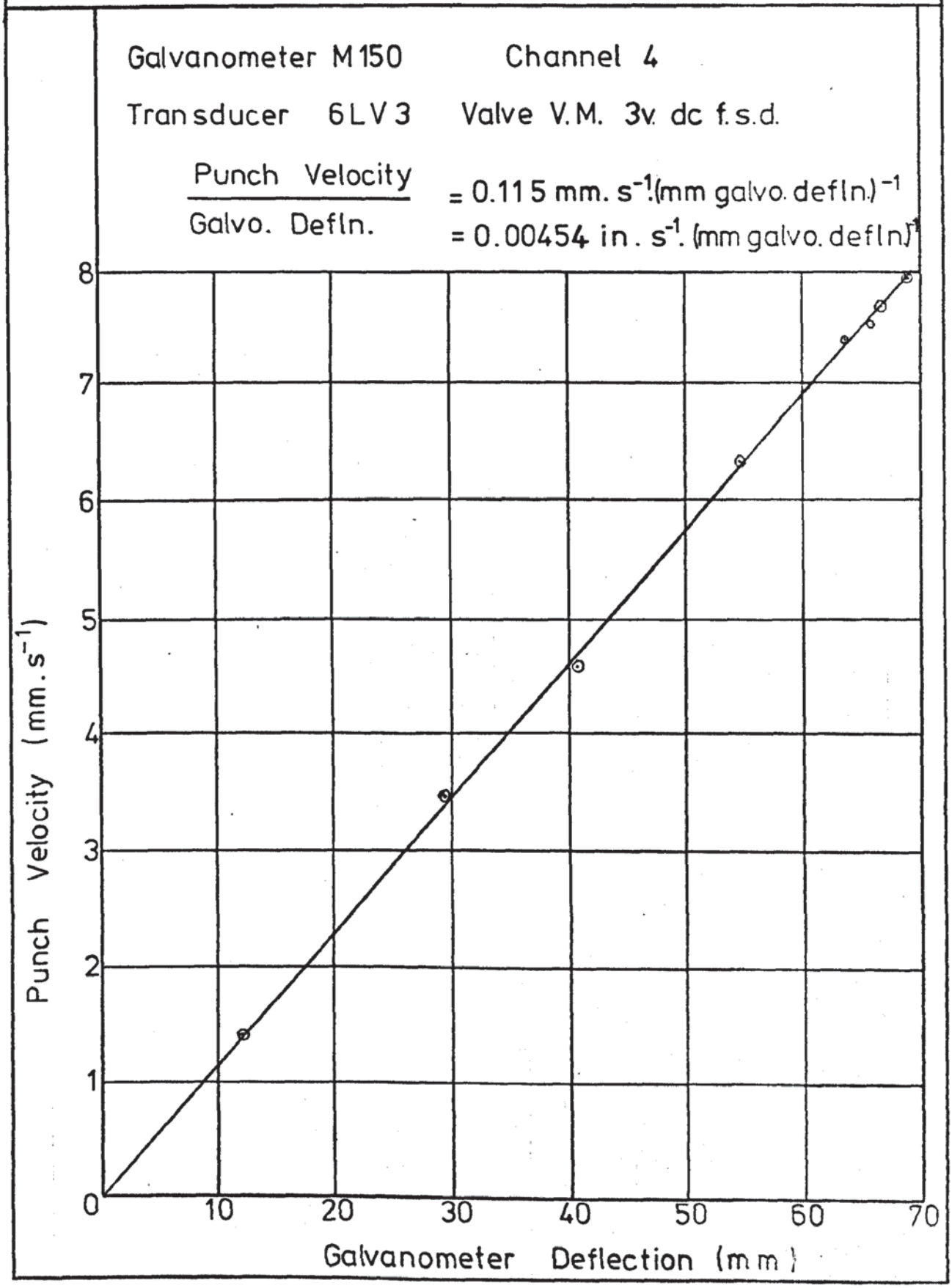

L.H. Ironing Die Amplitude Calibration

Distec Output v Crystal Galvanometer Deflection

Galvanometer S 8329-2 Channel 8

3v f.s.d. a.c. millivoltmeter

$$\frac{\text{Distec Output}}{\text{Galvo. Defln.}} = 3.46 \text{ mv.(mm galvo defln)}^{-1}$$

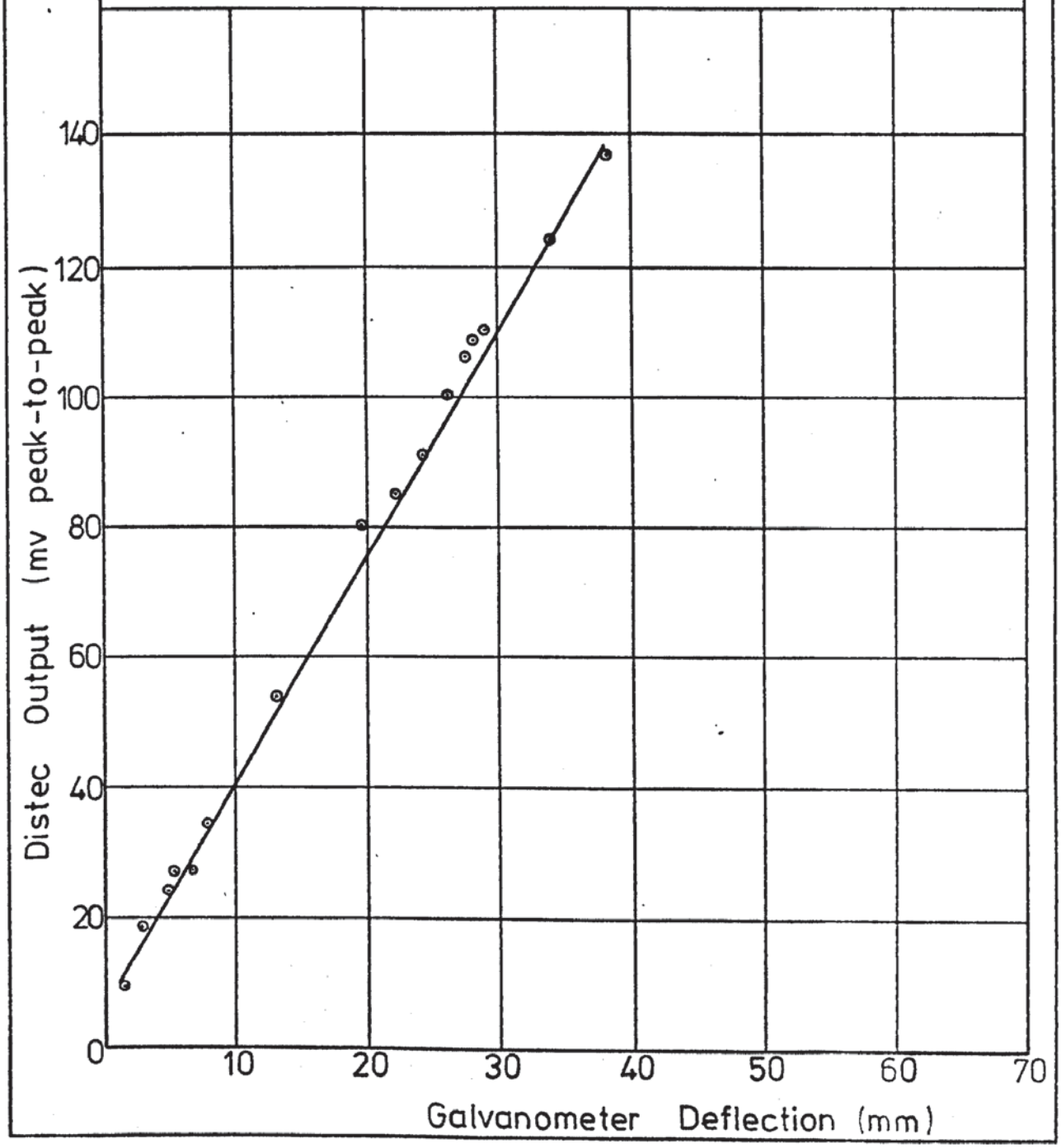

R.H. Ironing Die Amplitude Calibration

Distec Output v Crystal Galvanometer Deflection

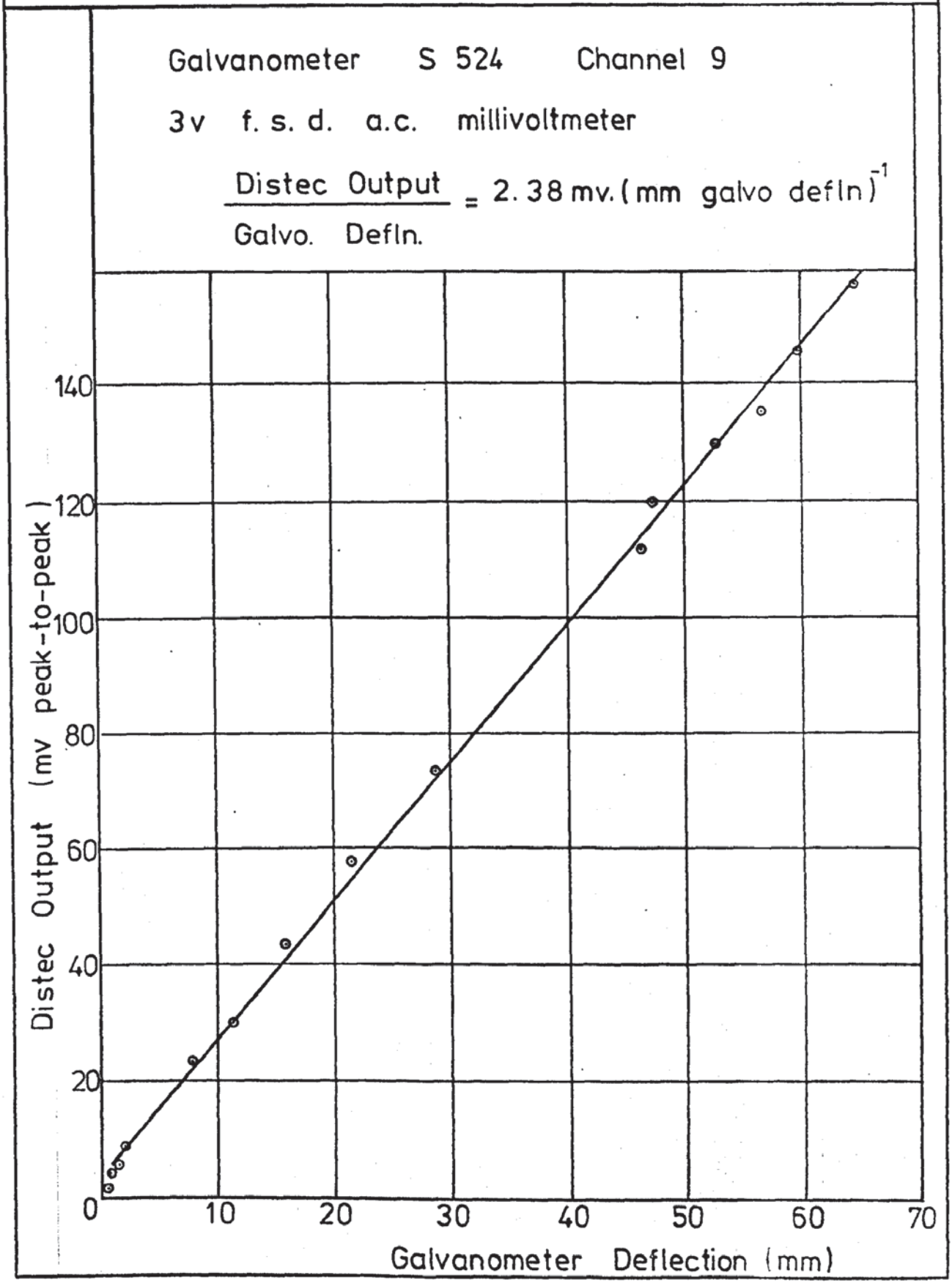

Ironing Punch Load Cell Calibration
Proving Ring Deflection v Galvanometer Deflection

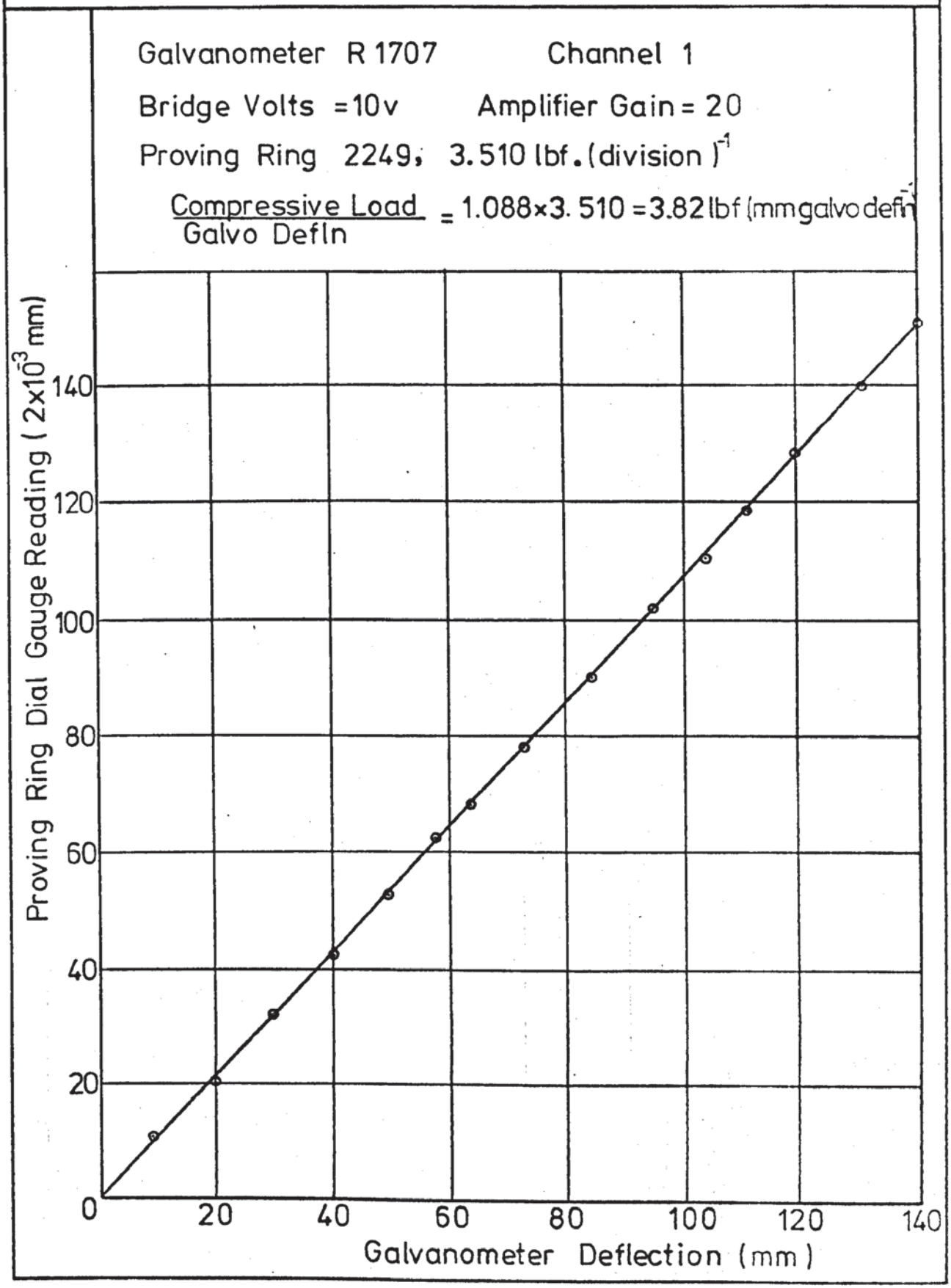

L.H. Die Diaphragm Load Cell Calibration

Proving Ring Deflection v Galvanometer Deflection

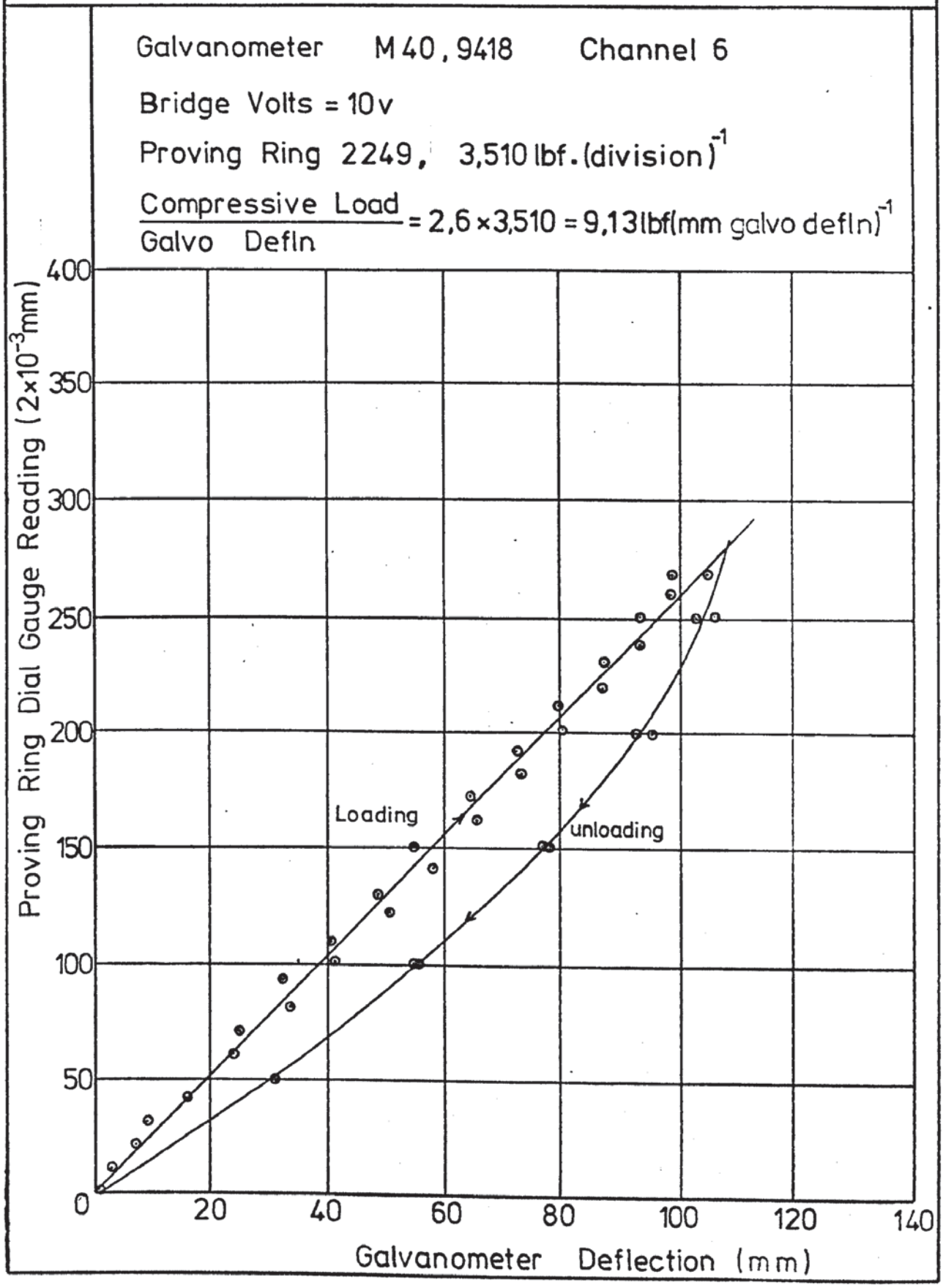

R.H. Die Diaphragm Load Cell Calibration

Proving Ring Deflection v Galvanometer Deflection

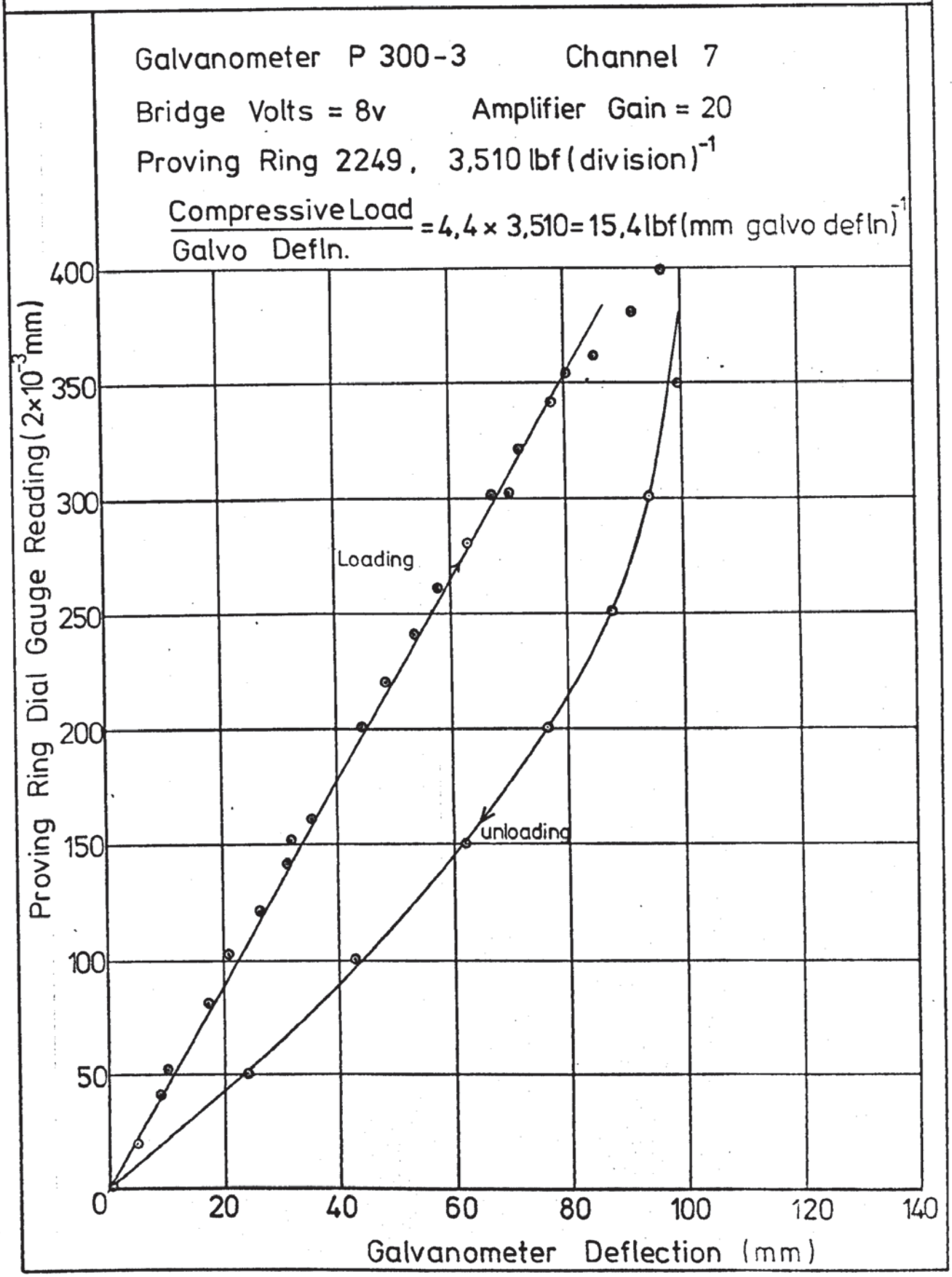

Proving Ring Calibration
Compressive Load v
Proving Ring Deflection

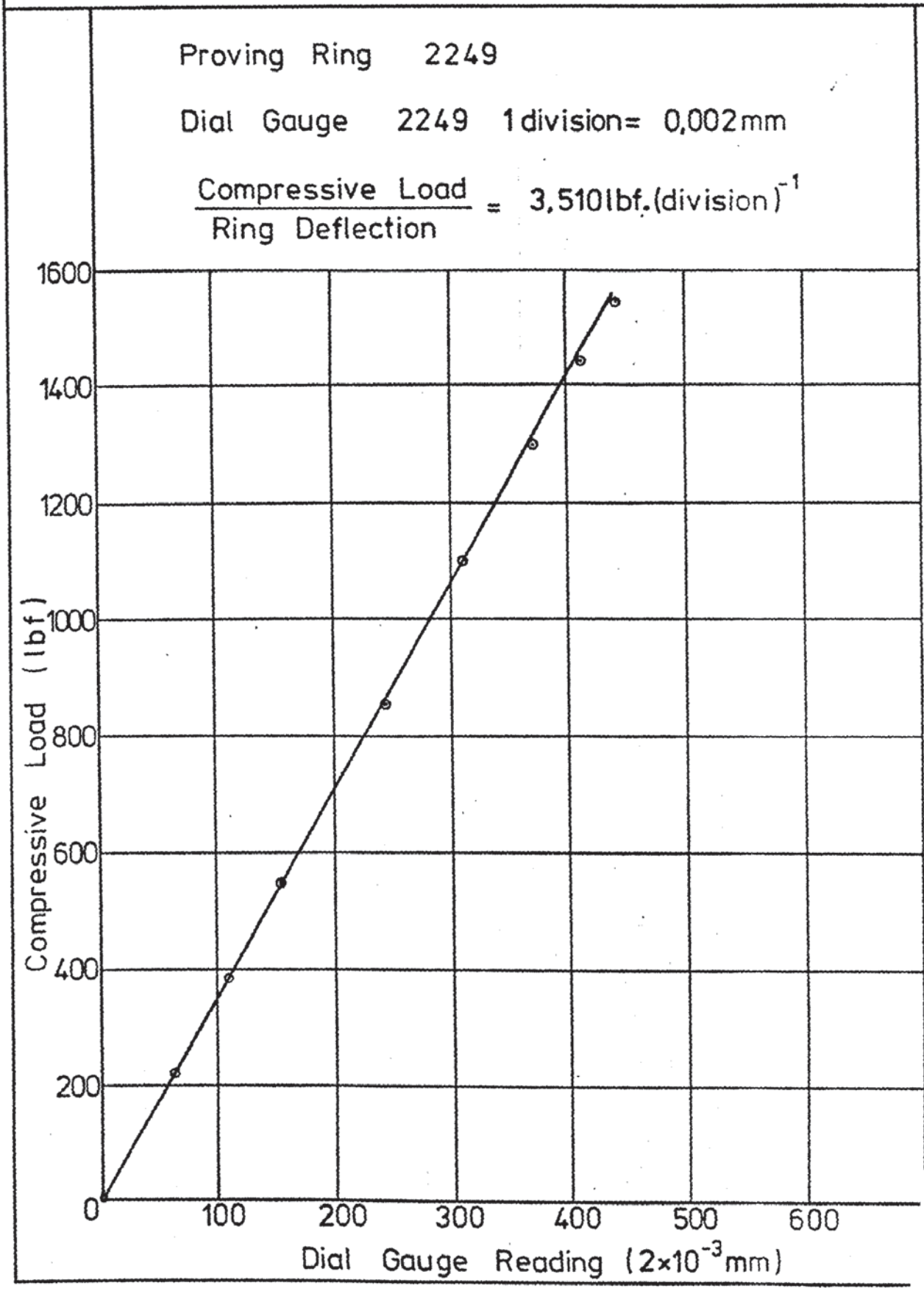

APPENDIX C.

Test Number: P-150-0,1	Material: Aluminium	Draw-Ratio: 1.50	Table Number: P.1

Punch Velocity:	Blank-Holder Force lbf.		Frequency:
0.35 $in.s^{-1}$	Left Hand	Right Hand	- kHz
	130	154	

Punch Travel in.	Punch Load P. lbf			B-H Friction Force F. lbf.			Oscillatory Amplitdue in.x 10^{-6}		Velocity Ratio	
	Osc.	Non Osc.	Osc. Comp.	Osc.	Non Osc.	Osc. Comp.	Punch	Die	Punch	Die
P.max 1.2		267			7.1					
F.max 0.3		61			18.4					
F.min 1.05		251			6.1					

Test Number: P-150-0,2	Material: Aluminium	Draw-Ratio: 1.50	Table Number P.2

Punch Velocity:	Blank-Holder Force lbf.		Frequency:
0.35 $in.s^{-1}$	Left Hand	Right Hand	- kHz
	140	130	

Punch Travel in.	Punch Load P. lbf.			B-H Friction Force F. lbf.			Oscillatory Amplitude, in.x 10 $^{-6}$		Velocity Ratio	
	Osc.	Non Osc.	Osc. Comp.	Osc.	Non Osc.	Osc. Comp	Punch	Die	Punch	Die
P.max 1.35		245			10.2					
F.max 0.25		29			18.4					
F.min 1.05		221			7.01					

Test Number:	Material:	Draw-Ratio:	Table Number:
P-150-100	Aluminium	1.50	P.3

Punch Velocity:	Blank-Holder Force lbf.		Frequency:
	Left Hand	Right Hand	
0.35 in.s^{-1}	130	135	12.75 kHz

Punch Travel in.	Punch Load P. lbf			B-H Friction Force F. lbf.			Oscillatory Amplitdue in.x 10^{-6}		Velocity Ratio	
	Osc.	Non Osc.	Osc. Comp.	Osc.	Non Osc.	Osc. Comp.	Punch	Die	Punch	Die
P.max 1.3	227	256	29	9.2	8.7	0.5	91	0	10.5	0
F.max 0.25	37	45	8	22.4	18.4	-4.0	74	0	8.5	0
F.min 0.95	184	236	52	2.6	6.6	4.0	119	0	13.6	0
P.A.max 0.7.	131			4.1			132	0	15.1	0

Test Number:	Material:	Draw-Ratio:	Table Number
P-150-160	Aluminium	1.50	P.4

Punch Velocity:	Blank-Holder Force lbf.		Frequency:
	Left Hand	Right Hand	
0.35 in.s^{-1}	130	150	12.81 kHz

Punch Travel in.	Punch Load P. lbf.			B-H Friction Force F. lbf.			Oscillatory Amplitude $_{6}$ in.x 10 -		Velocity Ratio	
	Osc.	Non Osc.	Osc. Comp.	Osc.	Non Osc.	Osc. Comp	Punch	Die	Punch	Die
P.max 1.4	224	256	32	9.2	8.7	-0.5	173	8.3	19.8	1.0
F.max 0.3	51	45	- 6	21.4	18.4	-3.0	126	1.3	14.5	0.2
F.min 1.0	181	236	55	1.6	6.6	5.0	217	6.9	24.9	0.8
P.A.max 0.8	147			2.0			225	5.5	25.9	0.6

Test Number: P-150-220	Material: Aluminium	Draw-Ratio: 1.50	Table Number: P.5.

Punch Velocity: 0.35 $in.s^{-1}$	Blank-Holder Force lbf.		Frequency: 12.75 kHz
	Left Hand 141	Right Hand 135	

Punch Travel in.	Punch Load P. lbf.			B-H Friction Force F. lbf.			Oscillatory Amplitude in.x 10^{-6}		Velocity Ratio	
	Osc.	Non Osc.	Osc. Comp.	Osc.	Non Osc.	Osc. Comp.	Punch	Die	Punch	Die
P.max 1.35	200	256	56	9.2	8.7	0.5	247	13.5	28.4	1.6
F.max 0.25	29	45	16	20.4	18.4	-2.0	167	1.3	19.2	2.0
F.min 1.05	179	236	57	3.1	6.6	3.5	290	12.4	33.3	1.4
P.A.mx 0.85	147			4.1			294	8.7	33.8	1.0

Test Number: P-150-270,1	Material: Aluminium	Draw-Ratio: 1.50	Table Number: P.6

Punch Velocity: 0.35 $in.s^{-1}$	Blank-Holder Force lbf.		Frequency: 12.77 kHz
	Left Hand 130	Right Hand 185	

Punch Travel in.	Punch Load P. lbf.			B-H Friction Force F. lbf.			Oscillatory Amplitude in.x 10^{-6}		Velocity Ratio	
	Osc.	Non Osc.	Osc. Comp.	Osc.	Non Osc.	Osc. Comp.	Punch	Die	Punch	Die
P.max 1.35	200	256	56	7.1	8.7	1.6	264	18.9	30.3	2.2
F.max 0.2	37	45	8	16.3	18.4	2.1	180	4.0	20.7	0.5
F.min 1.0	168	236	68	2.0	6.6	4.6	293	14.9	33.6	1.7

Test Number: P-150-270,2	Material: Aluminium	Draw-Ratio: 1.50	Table Number: P.7
Punch Velocity: 0.35 $in.s^{-1}$	Blank-Holder Force lbf. Left Hand 132	Right Hand 183	Frequency: 12.76 kHz

Punch Travel in.	Punch Load P. lbf.			B-H Friction Force F. lbf.			Oscillatory Amplitude in.x 10^{-6}		Velocity Ratio	
	Osc.	Non Osc.	Osc. Comp.	Osc.	Non Osc.	Osc. Comp.	Punch	Die	Punch	Die
P.max 1.35	203	256	53	9.2	8.7	-0.5	245	20.4	28.2	2.3
F.max 0.2	32	45	13	13.3	18.4	5.1	223	3.5	25.6	0.4
F.min 1.05	165	236	71	2.0	6.6	4.6	293	18.2	33.6	2.1

Test Number: P-155-0	Material: Aluminium	Draw-Ratio: 1.55	Table Number: P.3
Punch Velocity: 0.35 $in.s^{-1}$	Blank-Holder Force lbf. Left Hand 151	Right Hand 155	Frequency: - kHz

Punch Travel in.	Punch Load P. lbf.			B-H Friction Force F. lbf.			Oscillatory Amplitude in.x 10^{-6}		Velocity Ratio	
	Osc.	Non Osc.	Osc. Comp.	Osc.	Non Osc.	Osc. Comp.	Punch	Die	Punch	Die
P.max 1.4		280			13.3					
F.max 0.35		53			20.4					
F.min 0.85		200			9.2					

Test Number: P-155-100	Material: Aluminium	Draw-Ratio: 1.55	Table Number: P.9

Punch Velocity: 0.35 $in.s^{-1}$	Blank-Holder Force lbf.		Frequency: 12.80 kHz
	Left Hand 164	Right Hand 146	

Punch Travel in.	Punch Load P. lbf.			B-H Friction Force F. lbf.			Oscillatory Amplitude in.x 10^{-6}		Velocity Ratio	
	Osc.	Non Osc.	Osc. Comp.	Osc.	Non Osc.	Osc. Comp.	Punch	Die	Punch	Die
P.max 1.4	251	280	29	12.2	13.3	1.1	100	5.8	11.4	0.7
F.max 0.2	27	53	26	18.4	20.4	2.0	106	0	12.2	0
F.min 0.75	155	200	45	1.0	9.2	8.2	154	5.5	17.7	0.6
P.A.mx 0.65	133			2.0			156	4.7	17.9	0.5

Test Number: P-155-160	Material: Aluminium	Draw-Ratio: 1.55	Table Number: P.10

Punch Velocity 0.35 $in.s^{-1}$	Blank-Holder Force lbf.		Frequency: 12.75 kHz
	Left Hand 160	Right Hand 165	

Punch Travel in.	Punch Load P. lbf.			B-H Friction Force F. lbf.			Oscillatory Amplitude in.x 10^{-6}		Velocity Ratio	
	Osc.	Non Osc.	Osc. Comp.	Osc.	Non Osc	Osc. Comp.	Punch	Die	Punch	Die
P.max 1.35	240	280	40	12.2	13.3	1.1	139	7.3	16.0	0.8
F.max 0.2	29	53	24	13.3	20.4	7.1	169	1.1	19.4	0.1
F.min 0.75	139	200	61	0	9.2	9.2	238	8.0	27.3	0.9
P.A.mx 0.65	125			0			241	6.9	27.7	0.8

Test Number: P-155-220	Material: Aluminium	Draw-Ratio: 1.55	Table Number: P.11

Punch Velocity: 0.35 $in.s^{-1}$	Blank-Holder Force lbf.		Frequency: 12.83 kHz
	Left Hand 146	Right Hand 176	

Punch Travel in.	Punch Load P. lbf.			B-H Friction Force F. lbf.			Oscillatory Amplitude in.x 10^{-6}		Velocity Ratio	
	Osc.	Non Osc.	Osc. Comp.	Osc.	Non Osc.	Osc. Comp.	Punch	Die	Punch	Die
P.max 1.35	237	280	43	13.3	13.3	0	202	13.1	23.2	1.5
F.max 0.2	35	53	18	16.3	20.4	4.1	210	3.0	24.1	0.3
F.min 0.75	152	200	48	0	9.2	9.2	308	14.5	35.4	1.7

Test Number: P-155-270	Material: Aluminium	Draw-Ratio: 1.55	Table Number: P.12

Punch Velocity 0.35 $in.s^{-1}$	Blank-Holder Force lbf.		Frequency: 12.73 kHz
	Left Hand 150	Right Hand 170	

Punch Travel in.	Punch Load P. lbf.			B-H Friction Force F. lbf.			Oscillatory Amplitude in.x 10^{-6}		Velocity Ratio	
	Osc.	Non Osc.	Osc. Comp.	Osc.	Non Osc.	Osc. Comp.	Punch	Die	Punch	Die
P.max 1.35	216	280	64	11.2	13.3	2.1	247	15.6	28.4	1.8
F.max 0.2	21	53	32	12.2	20.4	8.2	245	3.5	28.2	0.4
F.min 0.7	128	200	72	0	9.2	9.2	325	13.1	37.3	1.5

Test Number: P-160-0	Material: Aluminium	Draw-Ratio: 1.60	Table Number: P.13
Punch Velocity: 0.35 $in.s^{-1}$	Blank-Holder Force lbf. Left Hand 184	Right Hand 175	Frequency: - kHz

Punch Travel in.	Punch Load P. lbf.			B-H Friction Force F. lbf.			Oscillatory Amplitude in.x 10^{-6}		Velocity Ratio	
	Osc.	Non Osc.	Osc. Comp.	Osc.	Non Osc.	Osc. Comp.	Punch	Die	Punch	Die
P.max 1.5		296			12.2					
F.max 0.25		32			21.4					
F.min 1.0		237			9.2					

Test Number: P-160-100	Material: Aluminium	Draw-Ratio: 1.60	Table Number: P.14
Punch Velocity 0.35 $in.s^{-1}$	Blank-Holder Force lbf. Left Hand 175	Right Hand 165	Frequency: 12.91 kHz

Punch Travel in.	Punch Load P. lbf.			B-H Friction Force F. lbf.			Oscillatory Amplitude in.x 10^{-6}		Velocity Ratio	
	Osc.	Non Osc.	Osc. Comp.	Osc.	Non Osc	Osc. Comp.	Punch	Die	Punch	Die
P.max 1.5	264	296	32	9.2	12.2	3.0	117	6.9	13.4	0.8
F.max 0.25	35	32	- 3	14.3	21.4	7.1	59	0	6.7	0
F.min 1.05	221	237	16	4.1	9.2	5.1	150	5.5	17.2	0.6
P.A.mx 0.85	176			5.1			156	4.0	17.9	0.5

Test Number: P-160-160	Material: Aluminium	Draw-Ratio: 1.60	Table Number: P.15
Punch Velocity: 0.35 $in.s^{-1}$	Blank-Holder Force lbf. Left Hand 185	Right Hand 170	Frequency: 12.73 kHz

Punch Travel in.	Punch Load P. lbf.			B-H Friction Force F. lbf.			Oscillatory Amplitude in.x 10^{-6}		Velocity Ratio	
	Osc.	Non Osc.	Osc. Comp.	Osc.	Non Osc.	Osc. Comp.	Punch	Die	Punch	Die
P.max 1.6	264	296	32	12.2	12.2	0	165	9.1	19.0	1.1
F.max 0.3	51	32	-19	18.4	21.4	3.0	83	0	9.5	0
F.min 1.02	216	237	21	3.1	9.2	6.1	204	7.6	23.4	0.9
P.A.mx 0.9	194			4.1			208	6.9	23.9	0.8

Test Number: P-160-220	Material: Aluminium	Draw-Ratio: 1.60	Table Number: P.16.
Punch Velocity 0.35 $in.s^{-1}$	Blank-Holder Force lbf. Left Hand 170	Right Hand 180	Frequency: 12.83 kHz

Punch Travel in.	Punch Load P. lbf.			B-H Friction Force F. lbf.			Oscillatory Amplitude in.x 10^{-6}		Velocity Ratio	
	Osc.	Non Osc.	Osc. Comp.	Osc.	Non Osc.	Osc. Comp.	Punch	Die	Punch	Die
P.max 1.5	256	296	40	22.4	12.2	-10.2	241	12.4	27.7	1.4
F.max 0.25	32	32	0	15.3	21.4	6.1	113	1.3	13.0	0.2
F.min 0.95	200	237	37	1.6	9.2	7.6	262	8.7	30.1	1.0
P.A.mx 0.85	165			2.0			273	8.0	31.4	0.9

Test Number: P-160-270	Material: Aluminium	Draw-Ratio: 1.60	Table Number: P.17

Punch Velocity: 0.35 $in.s^{-1}$	Blank-Holder Force lbf.		Frequency: 12.78 kHz
	Left Hand 180	Right Hand 175	

Punch Travel in.	Punch Load P. lbf.			B-H Friction Force F. lbf.			Oscillatory Amplitude in.x 10^{-6}		Velocity Ratio	
	Osc.	Non Osc.	Osc. Comp.	Osc.	Non Osc.	Osc. Comp.	Punch	Die	Punch	Die
P.max 1.7	227	296	69	7.1	12.2	5.1	293	20.0	33.7	2.3
F.max 0.2	29	32	3	16.3	21.4	5.1	182	1.3	20.9	0.2
F.min 1.15	192	237	45	0	9.2	9.2	293	15.6	33.7	1.8

Test Number: P-165-0,1	Material: Aluminium	Draw-Ratio: 1.65	Table Number: P.18

Punch Velocity 0.35 $in.s^{-1}$	Blank-Holder Force lbf.		Frequency: - kHz
	Left Hand 176	Right Hand 184	

Punch Travel in.	Punch Load P. lbf.			B-H Friction Force F. lbf.			Oscillatory Amplitude in.x 10^{-6}		Velocity Ratio	
	Osc.	Non Osc.	Osc. Comp.	Osc.	Non Osc.	Osc. Comp.	Punch	Die	Punch	Die
P.max 1.65		328			18.4					
F.max 0.3		69			31.6					
F.min 1.0		275			16.8					

Test Number: P-165-0,2	Material: Aluminium	Draw-Ratio: 1.65	Table Number: P.19
Punch Velocity: 0.35 $in.s^{-1}$	Blank-Holder Force lbf. Left Hand 176	Right Hand 190	Frequency: - kHz

Punch Travel in.	Punch Load P. lbf.			B-H Friction Force F. lbf.			Oscillatory Amplitude in.x 10^{-6}		Velocity Ratio	
	Osc.	Non Osc.	Osc. Comp.	Osc.	Non Osc.	Osc. Comp.	Punch	Die	Punch	Die
P.max 1.4		317			18.4					
F.max 0.4		75			26.5					
F.min 1.0		251			15.3					
		Speciman Failed								

Test Number: P-165-100	Material: Aluminium	Draw-Ratio: 1.65	Table Number: P.20
Punch Velocity 0.35 $in.s^{-1}$	Blank-Holder Force lbf. Left Hand 190	Right Hand 200	Frequency: 12.83 kHz

Punch Travel in.	Punch Load P. lbf.			B-H Friction Force F. lbf.			Oscillatory Amplitude in.x 10^{-6}		Velocity Ratio	
	Osc.	Non Osc.	Osc. Comp.	Osc.	Non Osc.	Osc. Comp.	Punch	Die	Punch	Die
P.max 1.75	288	328	40	17.3	18.4	1.1	76	5.5	8.7	0.6
F.max 0.25	37	69	32	25.5	31.6	6.1	85	0	9.8	0
F.min 0.9	208	275	67	5.1	16.8	11.7	128	4.0	14.7	0.5
P.A.mx 0.65	163			10.2			143	3.3	16.4	0.4
D.A.mx								6.6		0.8

Test Number: P-165-160	Material: Aluminium	Draw-Ratio: 1.65	Table Number: P.21

Punch Velocity: 0.35 $in.s^{-1}$	Blank-Holder Force lbf.		Frequency: 12.73 kHz
	Left Hand 190	Right Hand 200	

Punch Travel in.	Punch Load P. lbf.			B-H Friction Force F. lbf.			Oscillatory Amplitude in.x 10^{-6}		Velocity Ratio	
	Osc.	Non Osc.	Osc. Comp.	Osc.	Non Osc.	Osc. Comp.	Punch	Die	Punch	Die
P.max 1.7	280	328	48	19.4	18.4	- 1.0	87	5.5	10.0	0.6
F.max 0.25	51	69	18	23.5	31.6	8.1	137	0.7	15.7	0.1
F.min 0.9	208	275	67	6.1	16.8	10.7	141	4.7	16.2	0.5
P.A.mx 0.6	141			17.3			160	2.1	18.4	0.2
D.A.								6.9		0.8

Test Number: P-165-220,1	Material: Aluminium	Draw-Ratio: 1.65	Table Number: P.22

Punch Velocity 0.35 $in.s^{-1}$	Blank-Holder Force lbf.		Frequency: 12.83 kHz
	Left Hand 195	Right Hand 190	

Punch Travel in.	Punch Load P. lbf.			B-H Friction Force F. lbf.			Oscillatory Amplitude in.x 10^{-6}		Velocity Ratio	
	Osc.	Non Osc.	Osc. Comp.	Osc.	Non Osc.	Osc. Comp.	Punch	Die	Punch	Die
P.max 1.45	240	328	88	7.1	18.4	11.3	245	10.9	28.2	1.3
F.max 0.25	40	69	29	20.4	31.6	11.2	180	2.1	20.7	0.2
F.min 1.0	184	275	91	0	16.8	16.8	293	9.8	33.7	1.1
P.A.mx 0.8	157			1.0			310	7.3	35.6	0.8
		Speciman failed								

Test Number: P-165-220,2	Material: Aluminium	Draw-Ratio: 1.65	Table Number: P.23

Punch Velocity: 0.35 $in.s^{-1}$	Blank-Holder Force lbf.		Frequency: 12.89 kHz
	Left Hand 193	Right Hand 198	

Punch Travel in.	Punch Load P. lbf.			B-H Friction Force F. lbf.			Oscillatory Amplitude in.x 10^{-6}		Velocity Ratio	
	Osc.	Non Osc.	Osc. Comp.	Osc.	Non Osc.	Osc. Comp.	Punch	Die	Punch	Die
P.max 1.4	251	328	77	11.2	18.4	7.2	262	10.2	30.1	1.2
F.max 0.2	37	69	32	21.4	31.6	10.2	158	1.3	18.2	0.2
F.min 0.9	187	275	88	3.1	16.8	13.7	288	7.6	33.1	0.9
P.A.mx 0.8	168			4.1			295	6.6	33.9	0.8

Test Number: P-165-270	Material: Aluminium	Draw-Ratio: 1.65	Table Number: P.24

Punch Velocity: 0.35 $in.s^{-1}$	Blank-Holder Force lbf.		Frequency: 12.75 kHz
	Left Hand 189	Right Hand 195	

Punch Travel in.	Punch Load P. lbf.			B-H Friction Force F. lbf.			Oscillatory Amplitude in.x 10^{-6}		Velocity Ratio	
	Osc.	Non Osc.	Osc. Comp.	Osc.	Non Osc.	Osc. Comp.	Punch	Die	Punch	Die
P.max 1.4	235	328	93	10.2	18.4	8.2	295	9.5	35.9	1.1
F.max 0.2	32	69	37	16.3	31.6	15.3	245	3.0	28.2	0.3
F.min 0.75	147	275	128	0	16.8	16.8	329	10.2	37.8	1.2
	Specimen failed									

Test Number: P-170-0,1	Material: Aluminium	Draw-Ratio: 1.70	Table Number: P.25

Punch Velocity: 0.35 $in.s^{-1}$	Blank-Holder Force lbf.		Frequency: - kHz
	Left Hand 210	Right Hand 220	

Punch Travel in.	Punch Load P. lbf.			B-H Friction Force F. lbf.			Oscillatory Amplitude in.x 10^{-6}		Velocity Ratio	
	Osc.	Non Osc.	Osc. Comp.	Osc.	Non Osc.	Osc. Comp.	Punch	Die	Punch	Die
P.max 1.65		.347			22.4					
F.max 0.4		80			39.8					
F.min 1.15		304			18.4					

Test Number: P-170-0,2	Material: Aluminium	Draw-Ratio: 1.70	Table Number: P.26

Punch Velocity 0.35 $in.s^{-1}$	Blank-Holder Force lbf.		Frequency: - kHz
	Left Hand 210	Right Hand 220	

Punch Travel in.	Punch Load P. lbf.			B-H Friction Force F. lbf.			Oscillatory Amplitude in.x 10^{-6}		Velocity Ratio	
	Osc.	Non Osc.	Osc. Comp.	Osc.	Non Osc.	Osc. Comp.	Punch	Die	Punch	Die
P.max 1.70		344			20.4					
F.max 0.5		108			32.6					
F.min 1.20		304			14.3					

Test Number: P-170-100,1	Material: Aluminium	Draw-Ratio: 1.70	Table Number: P.27
Punch Velocity: 0.35 $in.s^{-1}$	Blank-Holder Force lbf. Left Hand 215	Right Hand 220	Frequency: 12.79 kHz

Punch Travel in.	Punch Load P. lbf			B-H Friction Force F. lbf.			Oscillatory Amplitdue in.x 10^{-6}		Velocity Ratio	
	Osc.	Non Osc.	Osc. Comp.	Osc.	Non Osc.	Osc. Comp.	Punch	Die	Punch	Die
P.max 1.65	341	346	5	21.4	21.4	0	22	1.3	2.5	0.1
F.max 0.45	72	94	22	35.7	36.2	0.5	22	0	2.5	0
F.min 1.15	304	304	0	17.3	16.4	-1.0	26	1.3	3.0	0.1
P.A.max 0.9	253			20.4			28	0	3.2	0
		Specimen failed								

Test Number: P-170-100,2	Material: Aluminium	Draw-Ratio: 1.70	Table Number P.28
Punch Velocity: 0.35 $in.s^{-1}$	Blank-Holder Force lbf. Left Hand 210	Right Hand 215	Frequency: 12.83 kHz

Punch Travel in.	Punch Load P. lbf.			B-H Friction Force F. lbf.			Oscillatory Amplitude in.x 10^{-6}		Velocity Ratio	
	Osc.	Non Osc.	Osc. Comp.	Osc.	Non Osc.	Osc. Comp	Punch	Die	Punch	Die
P.max 1.70	341	346	5	19.4	21.3	2.0	20	1.3	2.3	0.1
F.max 0.40	85	94	9	29.7	36.2	6.5	20	0	2.3	0
F.min 1.0	277	304	27	13.3	16.4	3.1	28	1.3	3.2	0.1
P.A.max 0.9	253			14.3			30	0	3.5	0

Test Number: P-170-160,1.	Material: Aluminium	Draw-Ratio: 1.70	Table Number: P.29
Punch Velocity: 0.35 $in.s^{-1}$	Blank-Holder Force lbf. Left Hand 210	Right Hand 215	Frequency: 12.85 kHz

Punch Travel in.	Punch Load P. lbf.			B-H Friction Force F. lbf.			Oscillatory Amplitude in.x 10^{-6}		Velocity Ratio	
	Osc.	Non Osc.	Osc. Comp.	Osc.	Non Osc.	Osc. Comp.	Punch	Die	Punch	Die
P.max 1.45	264	346	82	15.3	21.4	6.1	113	5.5	13.0	0.6
F.max 0.4	75	94	19	23.4	36.2	12.8	195	3.0	22.4	0.3
F.min 1.0	235	304	69	8.2	16.4	8.2	160	6.2	18.4	0.7
P.A.mx 0.65	152			14.3			234	4.7	26.9	0.5
		Specimen failed								

Test Number: P-170-160,2	Material: Aluminium	Draw-Ratio: 1.70	Table Number: P.30
Punch Velocity 0.35 $in.s^{-1}$	Blank-Holder Force lbf. Left Hand 212	Right Hand 218	Frequency: 12.79 kHz

Punch Travel in.	Punch Load P. lbf.			B-H Friction Force F. lbf.			Oscillatory Amplitude in.x 10^{-6}		Velocity Ratio	
	Osc.	Non Osc.	Osc. Comp.	Osc.	Non Osc	Osc. Comp.	Punch	Die	Punch	Die
P.max 1.45	284	346	62	15.3	21.4	6.1	156	6.9	17.9	0.8
F.max 0.3	53	94	41	27.5	36.2	8.7	141	3.0	16.2	0.3
F.min 0.95	211	304	93	6.1	16.4	10.3	212	6.9	24.4	0.8
P.A.mx 0.75	160			10.2			249	5.5	28.6	0.6
		Specimen failed								

Test Number: P-170-220	Material: Aluminium	Draw Ratio: 1.70	Table Number: P.31
Punch Velocity: 0.35 in.s^{-1}	Blank-Holder Force lbf. Left Hand 215	Right Hand 215	Frequency: 12.83 kHz

Punch Travel in.	Punch Load P. lbf.			B-H Friction Force F. lbf.			Oscillatory Amplitude in.x 10^{-6}		Velocity Ratio	
	Osc.	Non Osc.	Osc. Comp.	Osc.	Non Osc.	Osc. Comp.	Punch	Die	Punch	Die
P.max 1.3	269	346	77	10.2	21.4	11.2	212	8.4	24.4	1.0
F.max 0.3	59	94	35	23.4	36.2	12.8	204	2.1	23.4	0.2
F.min 0.95	197	304	107	4.1	16.4	12.3	299	8.0	34.4	0.9
P.A.max 0.8	163			6.1			299	6.6	34.4	0.8

Test Number: P-170-270	Material: Aluminium	Draw-Ratio:	Table Number: P.32
Punch Velocity: 0.35 in.s^{-1}	Blank-Holder Force lbf. Left Hand 210	Right Hand 215	Frequency: 12.80 kHz

Punch Travel in.	Punch Load P. lbf.			B-H Friction Force F. lbf.			Oscillatory Amplitude in.x 10^{-6}		Velocity Ratio	
	Osc.	Non Osc.	Osc. Comp.	Osc.	Non Osc.	Osc. Comp.	Punch	Die	Punch	Die
P.max 1.25	237	346	109	5.1	21.4	16.3	295	10.9	33.9	1.3
F.max 0.3	53	94	41	24.5	36.2	11.7	199	1.3	22.9	0.2
F.min 1.0	200	304	104	3.1	16.4	13.3	295	10.2	33.9	1.2
		Specimen failed								

Test Number: P-175-0,1	Material: Aluminium	Draw Ratio: 1.75	Table Number: P.33
Punch Velocity: 0.35 in.s^{-1}	Blank-Holder Force lbf.		Frequency:
	Left Hand 230	Right Hand 235	12.79 kHz

Punch Travel in.	Punch Load P. lbf.			B-H Friction Force F. lbf.			Oscillatory Amplitude in.x 10^{-6}		Velocity Ratio	
	Osc.	Non Osc.	Osc. Comp.	Osc.	Non Osc.	Osc. Comp.	Punch	Die	Punch	Die
P.max 1.35		349			22.4					
F.max 0.55		149			41.8					
F.min 1.35		349			22.4					
		Specimen failed								

Test Number: P-175-0,2	Material: Aluminium	Draw-Ratio: 1.75	Table Number: P.34
Punch Velocity: 0.35 in.s^{-1}	Blank-Holder Force lbf.		Frequency:
	Left Hand 225	Right Hand 234	12.83 kHz

Punch Travel in.	Punch Load P. lbf.			B-H Friction Force F. lbf.			Oscillatory Amplitude in.x 10^{-6}		Velocity Ratio	
	Osc.	Non Osc.	Osc. Comp.	Osc.	Non Osc.	Osc. Comp.	Punch	Die	Punch	Die
P.max 1.35		360			22.4					
F.max 0.5.		149			37.7					
F.min 1.35		360			22.4					
		Specimen failed								

Test Number: P-175-100,1	Material: Aluminium	Draw Ratio: 1.75	Table Number: P.35
Punch Velocity: 0.35 in.s^{-1}	Blank-Holder Force lbf. Left Hand 220	Right Hand 223	Frequency: 12.79 kHz

Punch Travel in.	Punch Load P. lbf.			B-H Friction Force F. lbf.			Oscillatory Amplitude in.x 10^{-6}		Velocity Ratio	
	Osc.	Non Osc.	Osc. Comp.	Osc.	Non Osc.	Osc. Comp.	Punch	Die	Punch	Die
P.max 1.35	331	355	24	19.4	22.4	3.0	67	3.0	7.7	0.3
F.max 0.45	99	149	50	33.6	40	6.4	85	0.7	9.8	0.1
F.min 1.15	309	355	46	18.4	22.4	4.0	78	2.1	9.0	0.2
P.A.max 0.65	176			30.6			111	1.3	12.8	0.2

Test Number: P-175-100,2	Material: Aluminium	Draw-Ratio: 1.75	Table Number: P.36
Punch Velocity: 0.35 in.s^{-1}	Blank-Holder Force lbf. Left Hand 210	Right Hand 215	Frequency: kHz

Punch Travel in.	Punch Load P. lbf.			B-H Friction Force F. lbf.			Oscillatory Amplitude in.x 10^{-6}		Velocity Ratio	
	Osc.	Non Osc.	Osc. Comp.	Osc.	Non Osc.	Osc. Comp.	Punch	Die	Punch	Die
P.max 1.25	320	355	35	20.4	22.4	2.0	74	3.0	8.5	0.3
F.max 0.35	75	149	74	31.6	40	8.4	72	0.7	8.3	0
F.min 1.05	293	355	62	19.4	22.4	3.0	87	3.0	10.0	0.3
P.A.max 0.75	211			26.5			106	1.3	12.2	0.2

Test Number: P-180-0,1	Material: Aluminium	Draw Ratio: 1.80	Table Number: P.37
Punch Velocity: 0.35 $in.s^{-1}$	Blank-Holder Force lbf.		Frequency:
	Left Hand 248	Right Hand 254	12.78 kHz

Punch Travel in.	Punch Load P. lbf.			B-H Friction Force F. lbf.			Oscillatory Amplitude in.x 10^{-6}		Velocity Ratio	
	Osc.	Non Osc.	Osc. Comp.	Osc.	Non Osc.	Osc. Comp.	Punch	Die	Punch	Die
P.max 1.05		341			30.6					
F.max 0.45		101			45.9					
F.min 1.05		341			30.6					
		Specimen failed								

Test Number: P-180-0,2	Material: Aluminium	Draw-Ratio: 1.80	Table Number: P.38
Punch Velocity: 0.35 $in.s^{-1}$	Blank-Holder Force lbf.		Frequency:
	Left Hand 250	Right Hand 253	12.81 kHz

Punch Travel in.	Punch Load P. lbf.			B-H Friction Force F. lbf.			Oscillatory Amplitude in.x 10^{-6}		Velocity Ratio	
	Osc.	Non Osc.	Osc. Comp.	Osc.	Non Osc.	Osc. Comp.	Punch	Die	Punch	Die
P.max 1.2		344			26.5					
F.max 0.55		160			41.8					
F.min 1.2		344			26.5					
		Specimen failed								

Test Number: P-180-100,1	Material: Aluminium	Draw-Ratio: 1.80	Table Number: P.39
Punch Velocity: 0.35 $in.s^{-1}$	Blank-Holder Force lbf.		Frequency: 12.79 kHz
	Left Hand 250	Right Hand 260	

Punch Travel in.	Punch Load P. lbf			B-H Friction Force F. lbf.			Oscillatory Amplitdue in.x 10^{-6}		Velocity Ratio	
	Osc.	Non Osc.	Osc. Comp.	Osc.	Non Osc.	Osc. Comp.	Punch	Die	Punch	Die
P.max 1.05	291	343	52	23.4	28.5	5.1	154	3.3	17.7	0.4
F.max 0.35	69	131	62	35.7	43.8	8.1	80	0	9.2	0
F.min 1.05	291	343	52	23.4	28.5	5.1	154	3.3	17.7	0.4
P.A.max 0.80	237			26.5			176	3.2	20.2	0.4
		Specimen failed								

Test Number: P-180-100,2	Material: Aluminium	Draw-Ratio: 1.80	Table Number P.40
Punch Velocity: 0.35 $in.s^{-1}$	Blank-Holder Force lbf.		Frequency: 12.81 kHz
	Left Hand 248	Right Hand 255	

Punch Travel in.	Punch Load P. lbf.			B-H Friction Force F. lbf.			Oscillatory Amplitude in.x 10^{-6}		Velocity Ratio	
	Osc.	Non Osc.	Osc. Comp.	Osc.	Non Osc.	Osc. Comp	Punch	Die	Punch	Die
P.max 1.10	293	343	50	24.4	28.5	4.1	145	3.7	16.7	0.4
F.max 0.4.	112	131	19	31.6	43.8	12.2	74	0.7	8.5	0.1
F.min 1.10	110	343	233	24.4	28.5	4.1	145	3.7	16.7	0.4
P.A.max 0.85	229			26.5			167	3.5	19.2	0.4
		Specimen failed								

Test Number: BH-150-0-1	Material: Aluminium	Draw Ratio: 1.50	Table Number: BH 1

Drawing Speed:	Blank-holder Force:		Frequency:
	Left Hand	Right Hand	
0.31 $in.s^{-1}$	133 lbf	148 lbf	- kHz

Punch Travel in	Punch Load P lbf			Die Separating Force D lbf			Blank-holder Amp. in $\times 10^{-6}$			Vel. Ratio
	Osc.	Non-osc.	Osc. comp	Osc.	Non. osc.	Osc. comp	L.H.	R.H.	Mean	
$\hat{D}$0.22	-	117	-	-	48.8	-	-	-	-	-
$\hat{P}$0.46		228			3.9t					
0.10		40			31.3					
0.20		105			48.8					
0.30		183			39.0					
0.40		220			7.8					
0.50		224			11.7t					
0.60		198			21.5t					
0.70		157			24.4t					
0.80		87			21.5t					
0.90										
1.00										
1.10										

Test Number: BH-150-20	Material: Aluminium	Draw Ratio: 1.50	Table Number: BH 2

Drawing Speed:	Blank-holder Force:		Frequency:
	Left Hand	Right Hand	
0.31 $in.s^{-1}$	132 lbf	148 lbf	12.62 kHz

Punch Travel in	Punch Load P lbf			Die Separating Force D lbf			Blank-holder Amp. in $\times 10^{-6}$			Vel. Ratio
	Osc.	Non-osc.	Osc. comp	Osc.	Non-osc.	Osc. comp	L.H.	R.H.	Mean	
$\hat{D}$0.21	107	117	10	52.7	48.8	3.4	23	8	16	2.0
$\hat{P}$0.44	200	228	28	7.8	3.9t	11.7	29	8	19	2.4
0.10	37	40	3	35.2	31.3	3.9	23	8	16	2.0
0.20	99	105	6	50.8	48.8	2.0	18	5	12	1.5
0.30	160	183	23	41.0	39.0	2.0	41	5	23	2.9
0.40	197	220	23	15.6	7.8	7.8	35	5	20	2.5
0.50	192	224	32	3.0	11.7t	12.7	29	8	19	2.3
0.60	163	198	35	11.7t	21.5t	9.8	29	8	19	2.3
0.70	125	157	32	15.6t	24.4t	8.8	23	8	16	2.0
0.80	48	87	39	10.7t	21.5t	10.8	29	8	19	2.3
0.90										
1.00										
1.10										

Test Number: BH-150-60	Material: Aluminium	Draw Ratio: 1.50	Table Number: BH 3

Drawing Speed:	Blank-holder Force:		Frequency:
	Left Hand	Right Hand	
0.31 in.s^{-1}	127 lbf	138 lbf	12.61 kHz

Punch Travel in	Punch Load P lbf			Die Separating Force D lbf			Blank-holder Amp. in x 10^{-6}			Vel. Ratio
	Osc.	Non-osc.	Osc. comp	Osc.	Non. osc.	Osc. comp	L.H.	R.H.	Mean	
$\hat{D}$0.21	99	117	118	44.9	48.8	3.9	64	28	46	5.8
$\hat{P}$0.43	195	228	33	9.8	3.9t	13.7	82	30	56	7.1
0.10	32	40	8	27.3	31.3	4.0	47	25	36	4.5
0.20	91	105	14	43.0	48.8	5.8	64	28	46	5.8
0.30	152	183	31	35.2	39.0	3.8	64	33	49	6.2
0.40	189	220	31	15.6	7.8	7.8	82	30	56	7.1
0.50	181	224	43	2.0t	11.7t	9.7	88	33	61	7.7
0.60	141	198	57	9.8t	21.5t	11.7	100	43	70	8.9
0.70	99	157	58	13.7t	24.4t	10.7	117	81	99	12.5
0.80	27	87	50	15.6t	21.5t	5.9	117	131	124	15.6
0.90										
1.00										
1.10										

Test Number: BH-150-100	Material: Aluminium	Draw Ratio: 1.50	Table Number: BH 4

Drawing Speed:	Blank-holder Force:		Frequency:
	Left Hand	Right Hand	
0.31 in.s^{-1}	138 lbf	138 lbf	12.63 kHz

Punch Travel in	Punch Load P lbf			Die Separating Force D lbf			Blank-holder Amp. in x 10^{-6}			Vel. Ratio
	Osc.	Non-osc.	Osc. comp	Osc.	Non-osc.	Osc. comp	L.H.	R.H.	Mean	
$\hat{D}$0.25	99	117	18	40.0	48.8	8.8	217	121	169	21.7
$\hat{P}$0.45	175	228	53	11.7	3.9t	15.6	229	131	180	23.1
0.10	27	40	13	17.6	31.3	13.7	176	116	146	18.7
0.20	72	105	33	37.1	48.8	11.7	205	121	163	20.9
0.30	128	183	55	35.2	39.0	3.8	223	121	172	22.1
0.40	168	220	52	19.5	7.8	10.7	229	126	178	22.8
0.50	165	224	59	3.9	11.7t	15.6	234	136	185	23.7
0.60	131	198	67	5.9t	21.5t	15.6	229	176	203	26.1
0.70	99	157	58	11.7t	24.4t	12.7	229	297	263	33.8
0.80	37	87	50	13.7t	21.5t	7.8	229	227	228	29.3
0.90										
1.00										
1.10										

Test Number: BH-150-140	Material: Aluminium	Draw Ratio: 1.50	Table Number: BH 5

Drawing Speed:	Blank-holder Force:		Frequency:
	Left Hand	Right Hand	
0.31 in.s^{-1}	132 lbf	148 lbf	12.62 kHz

Punch Travel in	Punch Load P lbf			Die Separating Force D lbf			Blank-holder Amp. in x 10^{-6}			Vel. Ratio
	Osc.	Non-osc.	Osc. comp	Osc.	Non. osc.	Osc. comp	L.H.	R.H.	Mean	
$\hat{D}$0.25	99	117	18	36.1	48.8	12.7	246	262	254	32.1
$\hat{P}$0.42	157	228	71	7.8	3.9t	11.7	334	307	321	40.6
0.10	24	40	16	19.5	31.3	11.8	176	323	250	31.6
0.20	69	105	36	35.2	48.8	13.6	217	302	260	32.9
0.30	123	183	60	31.3	39.0	7.7	299	222	261	33.0
0.40	155	220	65	9.8	7.8	2.0	328	302	315	39.8
0.50	144	224	80	2.0t	11.7t	9.7	340	338	339	42.9
0.60	120	198	78	9.8t	21.5t	11.7	328	363	346	43.7
0.70	91	157	66	13.7t	24.5t	10.8	322	383	353	44.6
0.80	27	87	60	15.6t	21.5t	5.9	281	252	267	33.7
0.90										
1.00										
1.10										

Test Number: BH-150-180	Material: Aluminium	Draw Ratio: 1.50	Table Number: BH 6

Drawing Speed:	Blank-holder Force:		Frequency:
	Left Hand	Right Hand	
0.32 in.s^{-1}	121 lbf	148 lbf	12.62 kHz

Punch Travel in	Punch Load P lbf			Die Separating Force D lbf			Blank-holder Amp. in x 10^{-6}			Vel. Ratio
	Osc.	Non-osc.	Osc. comp	Osc.	Non-osc.	Osc. comp	L.H.	R.H.	Mean	
$\hat{D}$0.22	88	117	29	36.1	48.8	12.7	322	358	340	42.4
$\hat{P}$0.40	163	228	65	5.9	3.9t	9.8	445	398	422	52.6
0.10	32	40	8	21.5	31.3	9.8	281	358	320	39.9
0.20	83	105	22	35.2	48.8	13.6	316	358	337	42.0
0.30	136	183	47	25.4	39.0	13.6	410	388	399	49.7
0.40	163	220	57	5.9	7.8	1.9	445	398	422	52.6
0.50	144	224	80	5.9t	11.7t	5.8	451	398	425	53.0
0.60	112	198	86	13.7t	21.5t	7.8	428	403	416	51.9
0.70	75	157	82	15.6t	24.4t	8.8	387	368	378	47.1
0.80										
0.90										
1.00										
1.10										

Test Number: BH-150-220	Material: Aluminium	Draw Ratio: 1.50	Table Number: BH 7

Drawing Speed:	Blank-holder Force:		Frequency:
	Left Hand	Right Hand	
0.30 in.s^{-1}	138 lbf	128 lbf	12.62 kHz

Punch Travel in	Punch Load P lbf			Die Separating Force D lbf			Blank-holder Amp. in x 10^{-6}			Vel. Ratio
	Osc.	Non-osc.	Osc. comp	Osc.	Non. osc.	Osc. comp	L.H.	R.H.	Mean	
$\hat{D}$ 0.23	88	117	29	39.1	48.8	9.7	428	383	406	52.9
$\hat{P}$ 0.44	167	228	61	7.8	3.9t	11.7	498	413	456	59.4
0.10	27	40	13	19.5	31.3	11.8	334	368	351	45.7
0.20	72	105	33	37.1	48.8	11.7	410	378	394	51.3
0.30	131	183	52	33.2	39.0	6.8	481	403	442	57.6
0.40	165	220	55	11.7	7.8	3.9	492	413	453	59.1
0.50	155	224	69	2.0t	11.7t	9.7	510	413	462	60.2
0.60	123	198	75	11.7t	21.5t	9.8	486	413	450	58.6
0.70	93	157	64	17.6t	24.4t	6.8	475	417	446	58.0
0.80	29	87	58	13.7t	21.5t	7.8	504	368	436	56.8
0.90										
1.00										
1.10										

Test Number: BH-150-260	Material: Aluminium	Draw Ratio: 1.50	Table Number: BH 8

Drawing Speed:	Blank-holder Force:		Frequency:
	Left Hand	Right Hand	
0.31 in.s^{-1}	150 lbf	138 lbf	12.62 kHz

Punch Travel in	Punch Load P lbf			Die Separating Force D lbf			Blank-holder Amp. in x 10^{-6}			Vel. Ratio
	Osc.	Non-osc.	Osc. comp	Osc.	Non-osc.	Osc. comp	L.H.	R.H.	Mean	
$\hat{D}$ 0.23	93	117	24	39.1	48.8	9.7	444	393	419	53.8
$\hat{P}$ 0.42	171	228	57	7.8	3.9t	11.7	850	418	634	81.4
0.10	26	40	14	19.5	31.3	11.8	369	383	376	48.3
0.20	75	105	30	37.1	48.8	11.7	363	393	378	48.6
0.30	133	183	50	33.2	39.0	6.8	346	408	377	48.4
0.40	169	220	51	11.7	7.8	3.9	334	418	376	48.2
0.50	160	224	64	3.9t	11.7t	7.8	328	423	378	48.6
0.60	123	198	75	12.7t	21.5t	8.8	334	416	375	48.1
0.70	99	157	58	18.6t	24.4t	5.8	328	418	373	47.9
0.80	32	87	55	19.5t	21.5t	2.0	346	403	375	48.1
0.90										
1.00										
1.10										

Test Number: BH-155-0	Material: Aluminium	Draw Ratio: 1.55	Table Number: BH 9
Drawing Speed: 0.33 in.s^{-1}	Blank-holder Force: Left Hand 149 lbf	Right Hand 158 lbf	Frequency: - kHz

Punch Travel in	Punch Load P lbf			Die Separating Force D lbf			Blank-holder Amp. in x 10^{-6}			Vel. Ratio
	Osc.	Non-osc.	Osc. comp	Osc.	Non. osc.	Osc. comp	L.H.	R.H.	Mean	
$\hat{D}$ 0.21	-	131	-	-	43.9	-	-	-	-	-
$\hat{P}$ 0.44		251			3.9					
0.10		48			29.3					
0.20		123			43.0					
0.30		203			31.3					
0.40		245			9.8					
0.50		245			3.9t					
0.60		219			7.8t					
0.70		181			7.8t					
0.80		125			19.5t					
0.90		40			31.3t					
1.00										
1.10										

Test Number: BH-155-20	Material: Aluminium	Draw Ratio: 1.55	Table Number: BH 10
Drawing Speed: 0.33 in.s^{-1}	Blank-holder Force: Left Hand 150 lbf	Right Hand 168 lbf	Frequency: 12.55 kHz

Punch Travel in	Punch Load P lbf			Die Separating Force D lbf			Blank-holder Amp. in x 10^{-6}			Vel. Ratio
	Osc.	Non-osc.	Osc. comp	Osc.	Non-osc.	Osc. comp	L.H.	R.H.	Mean	
$\hat{D}$ 0.22	123	131	8	54.6	43.9	10.7	6	5	6	0.7
$\hat{P}$ 0.46	251	251	0	13.7	3.9	9.8	21	5	13	1.5
0.10	43	48	5	37.1	29.3	7.8	6	5	6	0.7
0.20	117	123	6	54.7	43.0	11.7	6	5	6	0.7
0.30	200	203	3	44.9	31.3	13.6	9	5	7	0.8
0.40	245	245	0	21.5	9.8	11.7	18	5	12	1.4
0.50	245	245	0	7.8	3.9t	11.7	21	5	13	1.5
0.60	219	219	0	3.0	7.8t	10.8	23	5	14	1.7
0.70	181	181	0	0	7.8t	7.8	23	5	14	1.7
0.80	125	125	0	13.7t	19.5t	5.8	23	5	14	1.7
0.90	37	40	3	27.3t	31.3t	4.0	23	5	14	1.7
1.00										
1.10										

Test Number: BH-155-60	Material: Aluminium	Draw Ratio: 1.55	Table Number: BH 11

Drawing Speed:	Blank-holder Force:		Frequency:
	Left Hand	Right Hand	
0.34 in.s^{-1}	132 lbf	148 lbf	12.55 kHz

Punch Travel in	Punch Load P lbf			Die Separating Force D lbf			Blank-holder Amp. in x 10^{-6}			Vel. ratio
	Osc.	Non-osc.	Osc. comp	Osc.	Non. osc.	Osc. comp	L.H.	R.H.	Mean	
$\hat{D}$0.24	128	131	3	54.7	43.9	10.8	64	28	46	5.3
$\hat{P}$0.43	211	251	40	23.4	3.9	19.5	70	35	53	6.2
0.10	35	48	13	27.3	29.3	2.0	70	28	49	5.7
0.20	101	123	22	52.7	43.0	9.7	64	28	46	5.3
0.30	171	203	32	48.8	31.3	17.5	59	30	45	5.2
0.40	208	245	37	27.3	9.8	17.5	64	33	49	5.7
0.50	203	245	42	13.7	3.9t	17.6	64	38	51	5.9
0.60	173	219	46	9.8	7.8t	17.6	76	40	58	6.8
0.70	131	181	50	5.9	7.8t	13.7	76	53	60	7.7
0.80	64	125	61	9.8t	19.5t	9.7	82	181	132	15.4
0.90										
1.00										
1.10										

Test Number: BH-155-100	Material: Aluminium	Draw Ratio: 1.55	Table Number: BH 12

Drawing Speed:	Blank-holder Force:		Frequency:
	Left Hand	Right Hand	
0.34 in.s^{-1}	150 lbf	148 lbf	12.56 kHz

Punch Travel in	Punch Load P lbf			Die Separating Force D lbf			Blank-holder Amp. in x 10^{-6}			Vel. ratio
	Osc.	Non-osc.	Osc. comp	Osc.	Non-osc.	Osc. comp	L.H.	R.H.	Mean	
$\hat{D}$0.23	117	131	14	53.7	43.9	9.8	170	247	209	24.2
$\hat{P}$0.41	193	251	58	27.3	3.9	23.4	252	277	263	30.7
0.10	37	48	11	33.2	29.3	3.9	141	247	194	22.4
0.20	99	123	24	52.7	43.0	9.7	164	249	206	23.8
0.30	165	203	38	46.9	31.3	15.6	199	242	221	25.6
0.40	192	245	53	29.3	9.8	19.5	246	277	262	30.3
0.50	179	245	66	17.6	3.9t	21.5	252	292	272	31.5
0.60	149	219	70	17.6	7.8t	25.4	246	317	282	32.6
0.70	112	181	69	13.7	7.8t	21.5	234	328	281	32.5
0.80	48	125	77	9.8t	19.5t	9.7	199	312	256	29.6
0.90										
1.00										
1.10										

Test Number: BH-155-140	Material: Aluminium	Draw Ratio: 1.55	Table Number: BH 13
Drawing Speed: 0.34 in.s^{-1}	Blank-holder Force: Left Hand 150 lbf / Right Hand 168 lbf		Frequency: 12.53 kHz

Punch Travel in	Punch Load P lbf			Die Separating Force D lbf			Blank-holder Amp. in x 10^{-6}			Vel. Ratio
	Osc.	Non-osc.	Osc. comp	Osc.	Non. osc.	Osc. comp	L.H.	R.H.	Mean	
$\hat{D}$0.24	128	131	3	68.4	43.9	24.5	193	292	243	28.4
$\hat{P}$0.43	200	251	51	43.0	3.9	39.1	252	333	293	34.3
0.10	35	48	13	37.1	29.3	7.8	147	338	243	28.4
0.20	91	123	32	66.5	43.0	23.5	188	302	245	28.7
0.30	160	203	43	66.5	31.3	35.2	205	282	244	28.5
0.40	195	245	50	46.9	9.8	37.1	234	328	281	32.9
0.50	189	245	56	33.2	3.9t	37.1	252	312	282	33.0
0.60	157	219	62	25.4	7.8t	33.2	258	338	298	34.9
0.70	128	181	53	11.7	7.8t	19.5	252	383	318	37.2
0.80	69	125	56	9.8t	19.5t	9.7	422	328	375	43.9
0.90										
1.00										
1.10										

Test Number: BH-155-180	Material: Aluminium	Draw Ratio: 1.55	Table Number: BH 14
Drawing Speed: 0.34 in.s^{-1}	Blank-holder Force: Left Hand 150 lbf / Right Hand 168 lbf		Frequency: 12.54 kHz

Punch Travel in	Punch Load P lbf			Die Separating Force D lbf			Blank-holder Amp. in x 10^{-6}			Vel. Ratio
	Osc.	Non-osc.	Osc. comp	Osc.	Non-osc.	Osc. comp	L.H.	R.H.	Mean	
$\hat{D}$0.21	107	131	24	41.0	43.9	2.9	258	408	333	38.5
$\hat{P}$0.40	189	251	62	3.9	3.9	0	381	444	413	47.7
0.10	35	48	13	23.4	29.3	5.9	205	388	297	34.3
0.20	99	123	24	41.0	43.0	2.0	252	408	330	38.1
0.30	165	203	38	23.4	31.3	7.9	328	428	378	43.7
0.40	189	245	56	3.9	9.8	5.9	381	444	413	47.7
0.50	168	245	77	13.7t	3.9t	9.8	363	428	396	45.8
0.60	125	219	94	19.5t	7.8t	11.7	340	423	382	44.2
0.70	93	181	88	21.5t	7.8t	13.7	311	444	378	43.7
0.80	24	125	101	19.5t	19.5t	0	258	343	301	34.8
0.90										
1.00										
1.10										

Test Number: BH-155-220	Material: Aluminium	Draw Ratio: 1.55	Table Number: BH 15

Drawing Speed:	Blank-holder Force:		Frequency:
	Left Hand	Right Hand	
0.35 $in.s^{-1}$	150 lbf	161 lbf	12.55 kHz

Punch Travel in	Punch Load P lbf			Die Separating Force D lbf			Blank-holder Amp. in $\times 10^{-6}$			Vel. Ratio
	Osc.	Non-osc.	Osc. comp	Osc.	Non. osc.	Osc. comp	L.H.	R.H.	Mean	
$\hat{D}$0.20	104	131	27	43.0	43.9	0.9	305	413	359	39.9
$\hat{P}$0.40	189	251	62	5.9	3.9	2.0	387	444	416	46.3
0.10	37	48	11	27.3	29.3	2.0	252	413	333	37.1
0.20	104	123	19	43.0	43.0	0	305	413	359	39.9
0.30	163	203	40	25.4	31.3	5.9	363	428	396	44.1
0.40	189	245	56	5.9	9.8	3.9	387	444	416	46.3
0.50	165	245	80	6.8t	3.9t	2.9	398	444	421	46.8
0.60	125	219	94	16.6t	7.8t	8.8	393	454	424	47.2
0.70	88	181	93	15.6t	19.5t	3.9	340	433	387	43.1
0.80										
0.90										
1.00										
1.10										

Test Number: BH-155-260	Material: Aluminium	Draw Ratio:	Table Number: BH 16

Drawing Speed:	Blank-holder Force:		Frequency:
	Left Hand	Right Hand	
0.35 $in.s^{-1}$	150 lbf	168 lbf	12.55 kHz

Punch Travel in	Punch Load P lbf			Die Separating Force D lbf			Blank-holder Amp. in $\times 10^{-6}$			Vel. Ratio
	Osc.	Non-osc.	Osc. comp	Osc.	Non-osc.	Osc. comp	L.H.	R.H.	Mean	
$\hat{D}$0.20	101	131	30	41.0	43.9	2.9	428	464	446	50.9
$\hat{P}$0.40	187	251	64	2.0	3.9	1.9	539	509	524	59.8
0.10	37	48	11	23.4	29.3	5.9	369	469	419	47.8
0.20	101	123	22	41.0	43.0	2.0	428	464	446	50.9
0.30	165	203	38	23.4	31.3	7.9	481	494	488	55.7
0.40	187	245	58	2.0	9.8	7.8	539	509	524	59.8
0.50	168	245	77	13.7t	3.9t	9.8	516	494	505	57.7
0.60	128	219	91	19.5t	7.8t	11.7	486	499	493	56.3
0.70	101	181	80	21.5t	7.8t	13.7	428	499	464	53.0
0.80	21	125	104	23.4t	19.5t	3.9	381	413	397	45.3
0.90										
1.00										
1.10										

Test Number: BH-160-0	Material: Aluminium	Draw Ratio: 1.60	Table Number: BH 17
Drawing Speed: 0.35 in.s^{-1}	Blank-holder Force: Left Hand 161 lbf / Right Hand 188 lbf		Frequency: - kHz

Punch Travel in	Punch Load P lbf			Die Separating Force D lbf			Blank-holder Amp. in x 10^{-6}			Vel. Ratio
	Osc.	Non-osc.	Osc. comp	Osc.	Non. osc.	Osc. comp	L.H.	R.H.	Mean	
$\hat{D}$0.21	-	147	-	-	56.6	-	-	-	-	-
$\hat{P}$0.47		288			5.9					
0.10		59			37.9					
0.20		144			56.6					
0.30		235			43.0					
0.40		283			15.6					
0.50		286			5.9					
0.60		267			0					
0.70		224			15.6t					
0.80		165			15.6t					
0.90		51			23.4t					
1.00										
1.10										

Test Number: BH-160-160	Material: Aluminium	Draw Ratio: 1.60	Table Number: BH 18
Drawing Speed: 0.35 in.s^{-1}	Blank-holder Force: Left Hand 173 lbf / Right Hand 198 lbf		Frequency: 12.61 kHz

Punch Travel in	Punch Load P lbf			Die Separating Force D lbf			Blank-holder Amp. in x 10^{-6}			Vel. Ratio
	Osc.	Non-osc.	Osc. comp	Osc.	Non-osc.	Osc. comp	L.H.	R.H.	Mean	
$\hat{D}$0.22	123	147	24	50.8	56.6	5.8	387	307	347	38.8
$\hat{P}$0.43	211	288	77	18.0	5.9	12.1	527	343	435	48.6
0.10	43	59	16	29.3	37.1	7.8	357	318	338	37.8
0.20	112	144	32	48.8	56.6	7.8	381	307	344	38.4
0.30	184	235	51	39.1	43.0	3.9	416	307	362	40.5
0.40	208	283	75	21.5	15.6	5.9	504	333	419	46.8
0.50	208	286	78	15.6	5.9	9.7	533	353	443	49.5
0.60	173	267	94	15.6	0	15.6	574	363	469	52.4
0.70	136	224	88	0	15.6t	15.6	574	368	471	52.6
0.80	51	165	114	11.7t	15.6t	3.9	586	353	470	52.5
0.90										
1.00										
1.10										

Test Number: BH-160-200	Material: Aluminium	Draw Ratio: 1.60	Table Number: BH 19
Drawing Speed: 0.35 in.s^{-1}	Blank-holder Force: Left Hand 173 lbf	Right Hand 188 lbf	Frequency: 12.60 kHz

Punch Travel in	Punch Load P lbf			Die Separating Force D lbf			Blank-holder Amp. in x 10^{-6}			Vel. Ratio
	Osc.	Non-osc.	Osc. comp	Osc.	Non. osc.	Osc. comp	L.H.	R.H.	Mean	
$\hat{D}$0.22	120	147	27	56.6	56.6	0	375	373	374	41.8
$\hat{P}$0.43	208	288	80	27.3	5.9	21.4	481	408	445	49.7
0.10	40	59	19	33.2	37.1	4.9	340	378	359	40.1
0.20	109	144	35	56.6	56.6	0	375	373	374	41.8
0.30	179	235	56	46.9	43.0	3.9	410	388	399	44.6
0.40	208	283	75	31.3	15.6	15.7	457	403	430	48.1
0.50	205	286	81	23.4	5.9	17.5	539	413	476	53.2
0.60	173	267	94	17.6	0	17.6	533	428	481	53.7
0.70	139	224	85	0	15.6t	15.6	516	428	472	52.7
0.80	80	165	85	7.8t	15.6t	7.8	451	378	415	46.3
0.90										
1.00										
1.10										

Test Number: BH-160-260	Material: Aluminium	Draw Ratio: 1.60	Table Number: BH 20
Drawing Speed: 0.35 in.s^{-1}	Blank-holder Force: Left Hand 173 lbf	Right Hand 188 lbf	Frequency: 12.58 kHz

Punch Travel in	Punch Load P lbf			Die Separating Force D lbf			Blank-holder Amp. in x 10^{-6}			Vel. Ratio
	Osc.	Non-osc.	Osc. comp	Osc.	Non-osc.	Osc. comp	L.H.	R.H.	Mean	
$\hat{D}$0.21	123	147	24	62.5	56.6	5.9	440	403	422	47.7
$\hat{P}$0.43	200	288	88	38.1	5.9	32.2	498	438	468	52.9
0.10	40	59	19	44.9	37.1	6.8	410	408	409	46.2
0.20	117	144	27	60.5	56.6	3.9	440	423	432	48.8
0.30	176	235	59	58.6	43.0	15.6	469	433	451	50.9
0.40	200	283	83	41.0	15.6	25.4	486	444	465	52.5
0.50	197	286	89	31.3	5.9	25.4	527	454	491	55.5
0.60	168	267	99	27.3	0	27.3	557	454	506	57.2
0.70	136	224	88	7.8	15.6t	23.4	545	398	472	53.3
0.80										
0.90										
1.00										
1.10										

Test Number: BH-165-0	Material: Aluminium	Draw Ratio: 1.65	Table Number: BH 21
Drawing Speed: 0.34 in.s^{-1}	Blank-holder Force: Left Hand 184 lbf / Right Hand 188 lbf		Frequency: - kHz

Punch Travel in	Punch Load P lbf			Die Separating Force D lbf			Blank-holder Amp. in x 10^{-6}			Vel. Ratio
	Osc.	Non-osc.	Osc. comp	Osc.	Non. osc.	Osc. comp	L.H.	R.H.	Mean	
$\hat{D}$0.23	-	181	-	-	52.7	-	-	-	-	-
$\hat{P}$0.52		326			2.0t					
0.10		53			29.3					
0.20		147			50.8					
0.30		251			43.0					
0.40		310			13.7					
0.50		323			0					
0.60		318			2.0t					
0.70		280			7.8t					
0.80		243			21.5t					
0.90		187			25.4t					
1.00		80								
1.10										

Test Number: BH-165-160	Material: Aluminium	Draw Ratio: 1.65	Table Number: BH 22
Drawing Speed: 0.35 in.s^{-1}	Blank-holder Force: Left Hand 184 lbf / Right Hand 188 lbf		Frequency: 12.58 kHz

Punch Travel in	Punch Load P lbf			Die Separating Force D lbf			Blank-holder Amp. in x 10^{-6}			Vel. Ratio
	Osc.	Non-osc.	Osc. comp	Osc.	Non-osc.	Osc. comp	L.H.	R.H.	Mean	
$\hat{D}$0.21	125	181	56	44.9	52.7	7.8	258	272	265	29.9
$\hat{P}$0.47	213	326	113	15.1	2.0t	17.1	240	242	241	27.2
0.10	43	53	10	29.3	29.3	0	240	302	271	30.6
0.20	115	147	32	44.9	50.8	5.9	252	277	265	29.9
0.30	184	251	67	35.2	43.0	7.8	264	277	271	30.6
0.40	211	310	99	19.5	13.7	5.8	234	237	236	26.6
0.50	211	323	112	13.7	0	13.7	264	237	251	28.3
0.60	195	318	123	9.8	2.0t	11.8	311	227	269	30.4
0.70	155	280	125	3.9t	7.8t	3.9	328	262	295	33.3
0.80	120	243	123	7.8t	21.5t	13.7	369	398	384	43.4
0.90	40	187	147							
1.00										
1.10										

Test Number: BH-165-200	Material: Aluminium	Draw Ratio: 1.65	Table Number: BH 23
Drawing Speed: 0.35 in.s^{-1}	Blank-holder Force: Left Hand 184 lbf / Right Hand 198 lbf		Frequency: 12.58 kHz

Punch Travel in	Punch Load P lbf			Die Separating Force D lbf			Blank-holder Amp. in x 10^{-6}			Vel. Ratio
	Osc.	Non-osc.	Osc. comp	Osc.	Non. osc.	Osc. comp	L.H.	R.H.	Mean	
$\hat{D}$0.22	133	181	48	56.6	52.7	3.9	410	454	432	48.8
$\hat{P}$0.45	227	326	99	25.4	2.0t	23.4	352	418	385	43.5
0.10	48	53	5	37.1	29.3	7.8	375	474	425	48.1
0.20	120	147	27	54.7	50.8	3.9	398	464	431	48.7
0.30	189	251	62	46.8	43.0	3.8	410	423	417	47.1
0.40	221	310	89	29.3	13.7	15.6	363	423	393	44.4
0.50	221	323	102	25.4	0	25.4	346	418	382	43.1
0.60	205	318	113	15.6	2.0t	17.6	334	373	354	40.0
0.70	165	280	115	0	7.8t	7.8	322	348	335	37.8
0.80	131	243	112	2.0t	21.5t	19.5	311	318	315	35.6
0.90	48	187	139	21.5t	25.4t	3.9	340	408	374	42.2
1.00	21	80	59							
1.10										

Test Number: BH-165-260	Material: Aluminium	Draw Ratio: 1.65	Table Number: BH 24
Drawing Speed: 0.35 in.s^{-1}	Blank-holder Force: Left Hand 184 lbf / Right Hand 178 lbf		Frequency: 12.60 kHz

Punch Travel in	Punch Load P lbf			Die Separating Force D lbf			Blank-holder Amp. in x 10^{-6}			Vel. Ratio
	Osc.	Non-osc.	Osc. comp	Osc.	Non-osc.	Osc. comp	L.H.	R.H.	Mean	
$\hat{D}$0.20	104	147	43	46.9	52.7	5.8	404	383	394	44.6
$\hat{P}$0.48	216	326	110	9.8	2.0t	11.8	510	433	472	53.4
0.10	35	53	18	33.2	29.3	3.9	381	393	387	43.8
0.20	104	147	43	35.2	50.8	15.6	404	383	394	44.6
0.30	176	251	75	19.5	43.0	23.5	393	383	388	43.9
0.40	208	310	102	13.7	13.7	0	434	418	426	48.2
0.50	216	323	107	9.8	0	9.8	557	433	495	56.1
0.60	203	318	115	5.9t	2.0t	3.9	680	449	565	63.9
0.70	160	280	120	9.8t	7.8t	2.0	604	449	527	59.6
0.80	125	243	118	17.6t	21.5t	4.9	563	454	509	57.6
0.90	40	187	147	29.4t	25.4t	4.0	451	444	448	50.7
1.00										
1.10										

Test Number: BH-170-0	Material: Aluminium	Draw Ratio: 1.70	Table Number: BH 25

Drawing Speed:	Blank-holder Force:		Frequency:
	Left Hand	Right Hand	
0.35 in.s^{-1}	207 lbf	217 lbf	- kHz

Punch Travel in	Punch Load P lbf			Die Separating Force D lbf			Blank-holder Amp. in x 10^{-6}			Vel. Ratio
	Osc.	Non-osc.	Osc. comp	Osc.	Non. osc.	Osc. comp	L.H.	R.H.	Mean	
$\hat{D}$0.20	-	61	-	-	56.6	-	-	-	-	-
$\hat{P}$0.53		350			10.0					
0.10		61			39.1					
0.20		155			56.6					
0.30		256			41.0					
0.40		320			17.6					
0.50		347			9.8					
0.60		344			5.9					
0.70		323			0					
0.80		280			9.8t					
0.90		232			9.8t					
1.00		147			2.0t					
1.10		32			3.9t					

Test Number: BH-170-160	Material: Aluminium	Draw Ratio: 1.70	Table Number: BH 26

Drawing Speed:	Blank-holder Force:		Frequency:
	Left Hand	Right Hand	
0.35 in.s^{-1}	207 lbf	210 lbf	12.61 kHz

Punch Travel in	Punch Load P lbf			Die Separating Force D lbf			Blank-holder Amp. in x 10^{-6}			Vel. Ratio
	Osc.	Non-osc.	Osc. comp	Osc.	Non-osc.	Osc. comp	L.H.	R.H.	Mean	
$\hat{D}$0.22	141	61	80	50.8	56.6	5.8	264	287	276	31.2
$\hat{P}$0.52	259	350	91	17.6	10.0	7.6	299	343	321	36.3
0.10	40	61	21	29.3	39.1	9.8	252	302	277	31.3
0.20	117	155	38	48.8	56.6	7.8	264	287	276	31.2
0.30	200	256	56	41.0	41.0	0	270	287	279	31.6
0.40	243	320	77	23.4	17.6	5.8	258	287	273	30.9
0.50	256	347	91	15.6	9.8	5.8	293	338	316	35.8
0.60	251	344	93	13.7	5.9	7.8	340	353	347	39.3
0.70	213	323	110	9.8t	0	9.8	375	363	369	41.8
0.80	173	280	107	2.0t	9.8t	7.8	387	363	375	42.5
0.90	133	232	99	5.9t	9.8t	3.9	393	358	376	42.6
1.00	43	147	104	7.8t	2.0t	5.8	340	403	372	42.1
1.10										

Test Number: BH-170-200	Material: Aluminium	Draw Ratio: 1.70	Table Number: BH 27

Drawing Speed:	Blank-holder Force:		Frequency:
0.35 in.s^{-1}	Left Hand 196 lbf	Right Hand 202 lbf	12.62 kHz

Punch Travel in	Punch Load P lbf			Die Separating Force D lbf			Blank-holder Amp. in x 10^{-6}			Vel. Ratio
	Osc.	Non-osc.	Osc. comp	Osc.	Non. osc.	Osc. comp	L.H.	R.H.	Mean	
$\hat{D}$0.22	141	61	-80	54.7	56.6	1.9	316	328	322	36.5
$\hat{P}$0.50	264	350	86	23.4	10.0	13.4	375	363	369	41.8
0.10	43	61	18	29.3	39.1	9.8	305	328	317	35.9
0.20	117	155	38	52.7	56.6	3.9	311	323	317	35.9
0.30	208	256	48	46.9	41.0	5.9	322	333	328	37.2
0.40	251	320	69	29.3	17.6	11.7	311	333	322	36.5
0.50	264	347	83	23.4	9.8	13.6	375	363	369	41.8
0.60	248	344	96	15.6	5.9	9.7	440	387	412	46.7
0.70	211	323	112	7.8	0	7.8	451	393	422	47.8
0.80	171	280	109	3.9t	9.8t	5.9	451	413	432	49.0
0.90	128	232	104	23.4t	9.8t	13.6	410	423	417	47.2
1.00	40	147	107							
1.10										

Test Number: BH-170-260	Material: Aluminium	Draw Ratio: 1.70	Table Number: BH 28

Drawing Speed:	Blank-holder Force:		Frequency:
0.35 in.s^{-1}	Left Hand 196 lbf	Right Hand 200 lbf	12.61 kHz

Punch Travel in	Punch Load P lbf			Die Separating Force D lbf			Blank-holder Amp. in x 10^{-6}			Vel. Ratio
	Osc.	Non-osc.	Osc. comp	Osc.	Non-osc.	Osc. comp	L.H.	R.H.	Mean	
$\hat{D}$0.23	141	61	-80	44.9	56.6	11.7	363	363	363	41.1
$\hat{P}$0.50	245	350	105	19.5	10.0	9.5	422	413	418	47.3
0.10	37	61	24	31.3	39.1	7.8	346	378	362	41.0
0.20	109	155	46	43.0	56.6	13.6	357	368	363	41.1
0.30	192	256	64	46.9	41.0	5.9	363	363	363	41.1
0.40	235	320	85	27.3	17.6	9.7	375	388	382	43.2
0.50	245	347	102	19.5	9.8	9.7	422	413	418	47.3
0.60	235	344	109	17.6	5.9	11.7	463	418	441	49.9
0.70	200	323	123	11.7	0	11.7	486	423	455	51.5
0.80	165	280	115	0	9.8t	9.8	504	438	471	53.3
0.90	131	232	101	7.8t	9.8	2.0	516	449	483	54.7
1.00										
1.10										

Test Number: BH-175-0	Material: Aluminium	Draw Ratio: 1.75	Table Number: BH 29

Drawing Speed:	Blank-holder Force:		Frequency:
	Left Hand	Right Hand	
0.34 in.s^{-1}	219 lbf	227 lbf	- kHz

Punch Travel in	Punch Load P lbf			Die Separating Force D lbf			Blank-holder Amp. in x 10^{-6}			Vel. Ratio
	Osc.	Non-osc.	Osc. comp	Osc.	Non. osc.	Osc. comp	L.H.	R.H.	Mean	
$\hat{D}$0.22	-	176	-	-	48.8	-	-	-	-	-
$\hat{P}$0.49		363			0					
0.10		51			29.3					
0.20		149			46.9					
0.30		259			37.1					
0.40		334			11.7					
0.50		363			0					
0.60			Specimen Failed.							
0.70										
0.80										
0.90										
1.00										
1.10										

Test Number: BH-175-160	Material: Aluminium	Draw Ratio: 1.75	Table Number: BH 30

Drawing Speed:	Blank-holder Force:		Frequency:
	Left Hand	Right Hand	
0.35 in.s^{-1}	230 lbf	237 lbf	12.58 kHz

Punch Travel in	Punch Load P lbf			Die Separating Force D lbf			Blank-holder Amp. in x 10^{-6}			Vel. Ratio
	Osc.	Non-osc.	Osc. comp	Osc.	Non-osc.	Osc. comp	L.H.	R.H.	Mean	
$\hat{D}$0.22	152	176	24	56.6	48.8	7.8	205	212	209	25.9
$\hat{P}$0.53	286	363	77	21.5	0	21.5	211	318	265	30.3
0.10	48	51	3	33.2	29.3	3.9	193	292	243	27.8
0.20	136	149	13	54.7	46.9	7.8	205	217	211	24.1
0.30	219	259	40	44.9	37.1	7.8	211	222	217	24.8
0.40	261	334	73	25.4	11.7	13.7	199	217	208	23.8
0.50	280	363	83	19.5	0	19.5	188	267	228	26.1
0.60	280			19.5			234	348	291	33.3
0.70	261			7.8			270	348	309	35.3
0.80	224			3.9			305	358	332	38.0
0.90	181			2.0t			293	408	351	40.2
1.00	123			3.9t			334	398	366	41.9
1.10	27									

Test Number: BH-175-200	Material: Aluminium	Draw Ratio: 1.75	Table Number: BH 31

Drawing Speed:	Blank-holder Force:		Frequency:
	Left Hand	Right Hand	
0.35 in.s^{-1}	219 lbf	237 lbf	12.58 kHz

Punch Travel in	Punch Load P lbf			Die Separating Force D lbf			Blank-holder Amp. in x 10^{-6}			Vel. Ratio
	Osc.	Non-osc.	Osc. comp	Osc.	Non. osc.	Osc. comp	L.H.	R.H.	Mean	
$\hat{D}$0.23	152	176	24	58.6	48.8	9.8	270	312	291	35.3
$\hat{P}$0.55	278	363	85	29.3	0	29.3	217	348	283	32.4
0.10	40	51	11	35.2	29.3	5.9	258	343	301	34.4
0.20	117	149	32	56.6	46.9	9.7	270	318	294	33.6
0.30	208	259	51	52.7	37.1	15.6	275	307	291	33.3
0.40	259	334	75	33.2	11.7	13.5	270	292	281	32.1
0.50	272	363	91	25.4	0	25.4	223	287	255	29.2
0.60	272			27.3			223	368	296	33.9
0.70	253			21.5			264	393	329	37.6
0.80	219			11.7			328	408	368	42.1
0.90	176			5.9			346	428	387	44.3
1.00	117			9.8			398	438	418	47.8
1.10	27			2.0						

Test Number: BH-175-260-1	Material: Aluminium	Draw Ratio: 1.75	Table Number: BH 32

Drawing Speed:	Blank-holder Force:		Frequency:
	Left Hand	Right Hand	
0.36 in.s^{-1}	230 lbf	247 lbf	12.60 kHz

Punch Travel in	Punch Load P lbf			Die Separating Force D lbf			Blank-holder Amp. in x 10^{-6}			Vel. Ratio
	Osc.	Non-osc.	Osc. comp	Osc.	Non-osc.	Osc. comp	L.H.	R.H.	Mean	
$\hat{D}$0.24	147	176	29	56.6	48.8	7.8	850	343	596	65.6
$\hat{P}$0.56	264	363	99	21.5	0	21.5	850	403	627	69.2
0.10	40	51	11	35.2	29.3	5.9	850	353	602	66.4
0.20	115	149	34	54.7	46.9	7.8	850	343	597	65.8
0.30	195	259	64	48.8	37.1	11.7	850	338	594	65.5
0.40	240	334	94	29.3	11.7	17.6	850	333	592	65.3
0.50	261	363	102	21.5	0	21.5	850	373	612	67.5
0.60	261			21.5			850	408	629	69.4
0.70	248			15.6			850	423	637	70.3
0.80	227			2.0			850	433	642	70.8
0.90	184			0			850	438	644	71.1
1.00	136			2.0			850	438	644	71.1
1.10	48			3.9			850	368	609	67.2

Test Number: BH-175-260-2	Material: Aluminium	Draw Ratio: 1.75	Table Number: BH 33

Drawing Speed:	Blank-holder Force:		Frequency:
	Left Hand	Right Hand	
0.36 in.s^{-1}	219 lbf	237 lbf	12.58 kHz

Punch Travel in	Punch Load P lbf			Die Separating Force D lbf			Blank-holder Amp. in x 10^{-6}			Vel. Ratio
	Osc.	Non-osc.	Osc. comp	Osc.	Non. osc.	Osc. comp	L.H.	R.H.	Mean	
$\hat{D}$0.24	152	176	24	48.8	48.8	0	316	358	337	36.0
$\hat{P}$0.56	278	363	85	25.4	0	25.4	340	423	382	43.7
0.10	37	51	14	27.3	29.3	2.0	340	378	359	41.1
0.20	109	149	40	46.9	46.9	0	334	363	349	39.9
0.30	197	259	62	46.9	37.1	9.8	322	358	340	38.9
0.40	256	334	78	29.3	11.7	17.6	340	368	354	40.5
0.50	275	363	88	21.5	0	21.5	334	413	374	42.8
0.60	272			23.4			352	438	395	45.2
0.70	253			19.5			381	449	415	47.5
0.80	224			9.8			451	459	455	52.1
0.90	181			3.9			475	464	470	53.8
1.00	131			5.9			457	459	458	52.4
1.10	37									

Test Number: BH-180-0	Material: Aluminium	Draw Ratio: 1.80	Table Number: BH 34

Drawing Speed:	Blank-holder Force:		Frequency:
	Left Hand	Right Hand	
0.34 in.s^{-1}	219 lbf	247 lbf	- kHz

Punch Travel in	Punch Load P lbf			Die Separating Force D lbf			Blank-holder Amp. in x 10^{-6}			Vel. Ratio
	Osc.	Non-osc.	Osc. comp	Osc.	Non-osc.	Osc. comp	L.H.	R.H.	Mean	
$\hat{D}$0.25	-	197	-	-	74.2	-	-	-	-	-
$\hat{P}$0.45		355			29.3					
0.10		48			37.1					
0.20		141			68.3					
0.30		256			68.3					
0.40		334			43.0					
0.50		355			29.3					
0.60			Specimen failed							
0.70										
0.80										
0.90										
1.00										
1.10										

Test Number: BH-180-160	Material: Aluminium	Draw Ratio: 1.80	Table Number: BH 35

Drawing Speed:	Blank-holder Force:		Frequency:
	Left Hand	Right Hand	
0.35 in.s^{-1}	242 lbf	257 lbf	12.58 kHz

Punch Travel (in)	Punch Load P lbf			Die Separating Force D lbf			Blank-holder Amp. in x10^{-6}			Vel Ratio
	Osc.	Non-osc.	Osc. comp	Osc.	Non-osc.	Osc. comp	L.H.	R.H.	Mean	
$\hat{D}$0.95	173	197	24	70.3	74.2	3.9	170	131	151	17.3
$\hat{P}$0.58	299	355	56	33.2	29.3	3.9	158	11[illegible]	137	15.6
0.10	29	48	19	35.2	37.1	1.9	152	222	187	21.4
0.20	125	141	16	66.4	68.3	3.9	164	136	150	17.1
0.30	219	256	37	66.4	68.3	3.9	170	131	151	17.2
0.40	270	334	64	43.0	43.0	0	164	126	145	16.6
0.50	294	355	61	33.2	29.3	3.9	123	111	117	13.4
0.60	296			33.2			182	126	154	17.6
0.70	286			31.3			287	15[illegible]	222	25.4
0.80	264			25.4			334	13[illegible]	235	26.9
0.90	235			15.6			287	131	209	23.9
1.00	176			19.5			299	141	220	25.2
1.10	101			21.5			252	328	290	33.2

Test Number: BH-180-200	Material: Aluminium	Draw Ratio: 1.80	Table Number: BH 36

Drawing Speed:	Blank-holder Force:		Frequency:
	Left Hand	Right Hand	
0.34 in.s^{-1}	242 lbf	257 lbf	12.58 kHz

Punch Travel (in)	Punch Load P lbf			Die Separating Force D lbf			Blank-holder Amp. in x10^{-6}			Vel Ratio
	Osc.	Non-osc.	Osc. comp	Osc.	Non-osc.	Osc. comp	L.H.	R.H.	Mean	
$\hat{S}$0.24	163	197	34	54.7	74.2	19.5	217	192	205	23.7
$\hat{P}$0.56	294	355	61		29.3		188	161	175	20.3
0.10	45	48	3	29.3	37.1	7.8	211	328	270	31.3
0.20	128	141	13	52.7	68.3	15.6	217	197	207	24.0
0.30	213	256	43	48.8	68.3	19.5	217	197	207	24.0
0.40	267	334	67	31.3	43.0	11.7	211	171	191	22.1
0.50	288	355	67	23.4	29.3	5.9	176	156	166	19.2
0.60	291			19.5			211	176	194	22.5
0.70	283			17.6			322	186	254	29.4
0.80	261			9.8			352	166	259	30.1
0.90	232			5.9			346	166	256	29.7
1.00	168			11.7			357	207	282	32.7
1.10	104			11.7			316	479	398	46.2

Test Number: BH-180-260	Material: Aluminium	Draw Ratio: 1.80	Table Number: BH.37

Drawing Speed:	Blank-holder Force:		Frequency:
	Left Hand	Right Hand	
0.34 in.s^{-1}	242 lbf	257 lbf	12.60 kHz

Punch Travel in	Punch Load P lbf			Die Separating Force D lbf			Blank-holder Amp. in x 10^{-6}			Vel. Ratio
	Osc.	Non-osc.	Osc. comp	Osc.	Non. osc.	Osc. comp	L.H.	R.H.	Mean	
$\hat{D}$0.24	149	197	48	60.5	74.2	13.7	322	354	338	39.8
$\hat{P}$0.62	280	355	75	27.3	29.3	2.0	352	398	375	44.1
0.10	40	48	8	31.3	37.1	5.8	340	393	367	43.2
0.20	109	141	32	56.6	68.3	11.7	334	358	346	40.7
0.30	197	256	59	54.7	68.3	13.6	311	353	332	39.1
0.40	251	334	83	35.2	43.0	6.8	293	348	321	37.8
0.50	278	355	77	25.4	29.3	3.9	275	338	307	36.1
0.60	280			27.3			328	393	361	42.5
0.70	278			25.4			445	444	445	52.4
0.80	261			13.7			533	459	496	58.4
0.90	232			11.7			604	464	534	62.9
1.00	181			11.7			574	469	522	61.5
1.10	128			19.5			527	474	501	59.0

Test Number: BH-185-0	Material: Aluminium	Draw Ratio: 1.85	Table Number: BH 38

Drawing Speed:	Blank-holder Force:		Frequency:
	Left Hand	Right Hand	
0.35 in.s^{-1}	265 lbf	300 lbf	- kHz

Punch Travel in	Punch Load P lbf			Die Separating Force D lbf			Blank-holder Amp. in x 10^{-6}			Vel. Ratio
	Osc.	Non-osc.	Osc. comp	Osc.	Non-osc.	Osc. comp	L.H.	R.H.	Mean	
$\hat{D}$0.22	-	192	-	-	56.6	-	-	-	-	-
$\hat{P}$0.39		352			19.5					
0.10		64			31.3					
0.20		165			54.7					
0.30		283			44.9					
0.40		352			19.5					
0.50			Specimen failed							
0.60										
0.70										
0.80										
0.90										
1.00										
1.10										

Test Number: BH-185-160	Material: Aluminium	Draw Ratio: 1.85	Table Number: BH 39

Drawing Speed:	Blank-holder Force:		Frequency:
	Left Hand	Right Hand	
0.34 $in.s^{-1}$	265 lbf	286 lbf	12.59 kHz

Punch Travel (in)	Punch Load P lbf			Die Separating Force D lbf			Blank-holder Amp. in $x10^{-6}$			Vel Ratio
	Osc.	Non-osc.	Osc. comp	Osc.	Non-osc.	Osc. comp	L.H.	R.H.	Mean	
$\hat{D}$0.24	165	192	27	62.5	56.6	5.9	188	121	155	18.0
$\hat{P}$0.60	326	352	26		19.5		141	86	114	13.2
0.10	51	64	13	39.1	31.3	7.8	182	131	157	18.2
0.20	133	165	32	60.5	54.7	5.8	188	121	155	18.0
0.30	224	283	59	58.6	44.9	13.7	188	116	152	17.6
0.40	286	352	66	39.1	19.5	19.6	188	101	145	16.8
0.50	312			29.3			176	86	131	15.2
0.60	326			27.3			141	86	114	13.2
0.70	320			25.4			275	86	181	21.0
0.80	307			25.4			346	106	226	26.2
0.90	288			17.6			352	111	232	26.9
1.00	237			23.4			363	116	240	27.8
1.10	189			23.4			369	131	250	29.0
1.20	101			19.5			264	186	225	26.1
1.30	19			0						
1.40										
1.50										
1.60										

Test Number: BH-185-200	Material: Aluminium	Draw Ratio: 1.85	Table Number: BH 40

Drawing Speed: 0.35 in.s^{-1}	Blank-holder Force: Left Hand 265 lbf	Blank-holder Force: Right Hand 286 lbf	Frequency: 12.60 kHz

Punch Travel (in)	Punch Load P lbf			Die Separating Force D lbf			Blank-holder Amp. in x10^{-6}			Vel Ratio
	Osc.	Non-osc.	Osc. comp	Osc.	Non-osc.	Osc. comp	L.H.	R.H.	Mean	
$\hat{D}$0.24	160	192	32	56.6	56.6	0	246	136	191	21.9
$\hat{P}$0.60	301	352	45	52.7	19.5	33.2	246	141	194	22.2
0.10	37	64	27	27.3	31.3	4.0	234	302	268	30.7
0.20	117	165	48	52.7	54.7	2.0	246	141	194	22.2
0.30	219	283	64	52.7	44.9	7.8	246	141	194	22.2
0.40	272	352	80	35.2	19.5	15.7	240	131	186	21.3
0.50	296			23.4			211	126	169	19.3
0.60	307			21.5			158	121	140	16.1
0.70	296			19.5			293	141	217	24.8
0.80	283			19.5			410	192	301	34.5
0.90	259			13.7			486	176	331	37.9
1.00	216			13.7			416	166	291	33.3
1.10	163			17.6			434	469	452	51.8
1.20	88			15.6						
1.30	19			3.9t						
1.40										
1.50										
1.60										

Test Number: BH-185-260	Material: Aluminium	Draw Ratio: 1.85	Table Number: BH 41

Drawing Speed:	Blank-holder Force:		Frequency:
	Left Hand	Right Hand	
0.34 in.s^{-1}	253 lbf	286 lbf	12.58 kHz

Punch Travel (in)	Punch Load P lbf			Die Separating Force D lbf			Blank-holder Amp. in x10^{-6}			Vel Ratio
	Osc.	Non-osc.	Osc. comp	Osc.	Non-osc.	Osc. comp	L.H.	R.H.	Mean	
$\hat{D}$0.24	176	192	16	60.5	56.6	3.9	240	197	219	25.4
$\hat{P}$0.60	320	352	32	54.7	19.5	35.2	246	192	219	25.4
0.10	51	64	13	31.3	31.3	0	240	403	322	37.3
0.20	136	165	29	58.6	54.7	3.9	240	202	221	25.6
0.30	235	283	48	54.6	44.9	9.7	246	192	219	25.4
0.40	291	352	61	33.2	19.5	13.7	252	166	209	24.2
0.50	315			25.4			252	156	204	23.6
0.60	320			23.4			234	156	195	22.6
0.70	315			21.5			305	192	249	28.9
0.80	302			19.5			410	217	314	36.4
0.90	280			15.6			451	202	327	37.9
1.00	229			19.5			381	202	292	33.8
1.10	176			21.5			434	272	353	40.9
1.20	104			17.6			334	388	361	41.9
1.30	21			5.9t						
1.40										
1.50										
1.60										

Test Number: BH-190-0	Material: Aluminium	Draw Ratio: 1.90	Table Number: BH 42

Drawing Speed:	Blank-holder Force:		Frequency:
	Left Hand	Right Hand	
0.34 in.s^{-1}	242 lbf	247 lbf	- kHz

Punch Travel in	Punch Load P lbf			Die Separating Force D lbf			Blank-holder Amp. in x 10^{-6}			Vel. Ratio
	Osc.	Non-osc.	Osc. comp	Osc.	Non. osc.	Osc. comp	L.H.	R.H.	Mean	
$\hat{D}$0.24	-	213	-	-	58.6	-	-	-	-	-
$\hat{P}$0.37		331			35.2					
0.10		61			25.4					
0.20		160			54.7					
0.30		280			54.7					
0.40		331			35.2					
0.50			Specimen failed.							
0.60										
0.70										
0.80										
0.90										
1.00										
1.10										

Test Number: BH-190-160	Material: Aluminium	Draw Ratio: 1.90	Table Number: BH 43

Drawing Speed:	Blank-holder Force:		Frequency:
	Left Hand	Right Hand	
0.34 in.s^{-1}	242 lbf	245 lbf	12.60 kHz

Punch Travel in	Punch Load P lbf			Die Separating Force D lbf			Blank-holder Amp. in x 10^{-6}			Vel. Ratio
	Osc.	Non-osc.	Osc. comp	Osc.	Non-osc.	Osc. comp	L.H.	R.H.	Mean	
$\hat{D}$0.23	189	213	24	72.3	58.6	13.7	193	91	142	16.5
$\hat{P}$0.63	347	331	-16	31.3	35.2	3.9	152	66	109	12.6
0.10	56	61	5	41.0	25.4	15.6	170	91	131	15.2
0.20	147	160	13	68.4	54.7	13.7	188	91	140	16.2
0.30	245	280	35	66.6	54.7	11.9	193	91	142	16.5
0.40	307	331	24	41.0	35.2	5.8	188	86	137	15.9
0.50	334			33.2			182	76	129	14.9
0.60	347			35.2			164	72	118	13.7
0.70			Specimen failed.							
0.80										
0.90										
1.00										
1.10										

Test Number: BH-190-200	Material: Aluminium	Draw Ratio: 1.90	Table Number: BH 44

Drawing Speed:	Blank-holder Force:		Frequency:
	Left Hand	Right Hand	
0.34 $in.s^{-1}$	288 lbf	296 lbf	12.60 kHz

Punch Travel (in)	Punch Load P lbf			Die Separating Force D lbf			Blank-holder Amp. in $x10^{-6}$			Vel Ratio
	Osc.	Non-osc.	Csc. comp	Osc.	Non-osc.	Osc. comp	L.H.	R.H.	Mean	
$\hat{D}$0.24	176	213	37	58.6	58.6	0	223	141	182	21.1
$\hat{P}$0.64	350	331	-19	15.6	35.2	19.6	152	101	127	14.7
0.10	48	61	13	31.3	25.4	5.9	217	146	182	21.1
0.20	136	160	24	54.7	54.7	0	223	141	182	21.1
0.30	235	280	45	50.8	54.7	3.9	217	146	182	21.1
0.40	302	331	29	29.3	35.2	5.9	205	141	172	20.1
0.50	331			23.4			188	121	155	18.0
0.60	347			19.5			147	106	127	14.7
0.70	344			13.7			170	96	133	15.4
0.80	328			17.6			422	91	257	29.8
0.90	315			13.7			533	116	325	37.7
1.00	288			21.5			445	126	286	33.2
1.10	237			21.5			363	121	242	28.1
1.20	184			17.6			416	126	271	31.5
1.30	128			15.6						
1.40										
1.50										
1.60										

Test Number: BH-190-260	Material: Aluminium	Draw Ratio: 1.90	Table Number: BH 45

Drawing Speed:	Blank-holder Force:		Frequency:
	Left Hand	Right Hand	
0.35 in.s^{-1}	288 lbf	310 lbf	12.60 kHz

Punch Travel (in)	Punch Load P lbf			Die Separating Force D lbf			Blank-holder Amp. in x10^{-6}			Vel Ratio
	Osc.	Non-osc.	Osc. comp	Osc.	Non-osc.	Osc. comp	L.H.	R.H.	Mean	
↓0.25	187	213	26	66.5	58.6	7.9	299	151	225	25.8
↑0.63	334	331	3	23.4	35.2	11.8	240	136	188	21.5
0.10	48	61	13	31.3	25.4	5.9	275	227	251	28.7
0.20	136	160	24	60.6	54.7	5.9	299	146	223	25.5
0.30	237	280	43	58.6	54.7	3.9	299	156	228	26.1
0.40	296	331	35	35.2	35.2	0	275	146	211	24.2
0.50	320			25.4			270	141	206	23.6
0.60	334			23.4			240	136	188	21.5
0.70	326			23.4			299	136	218	25.0
0.80	315			25.4			498	161	330	37.8
0.90	307			19.5			592	192	392	44.9
1.00	275			27.3			598	212	405	46.4
1.10	219			25.4			568	222	395	45.3
1.20	165			23.4			533	252	393	45.1
1.30	104			7.8						
1.40										
1.50										
1.60										

Test Number: BH-195-0	Material: Aluminium	Draw Ratio: 1.95	Table Number: BH 46

Drawing Speed:	Blank-holder Force:		Frequency:
	Left Hand	Right Hand	
0.34 in.s^{-1}	292 lbf	300 lbf	- kHz

Punch Travel in	Punch Load P lbf			Die Separating Force D lbf			Blank-holder Amp. in x 10^{-6}			Vel. Ratio
	Osc.	Non-osc.	Osc. comp	Osc.	Non. osc.	Osc. comp	L.H.	R.H.	Mean	
$\hat{D}$0.24	-	248	-	-	68.35	-	-	-	-	-
$\hat{P}$0.37		382			37.1					
0.10		67			27.3					
0.20		187			66.5					
0.30		326			60.5					
0.40		382			37.1					
0.50			Specimen Failed.							
0.60										
0.70										
0.80										
0.90										
1.00										
1.10										

Test Number: BH-195-160	Material: Aluminium	Draw Ratio: 1.95	Table Number: BH 47

Drawing Speed:	Blank-holder Force:		Frequency:
	Left Hand	Right Hand	
0.34 in.s^{-1}	299 lbf	300 lbf	12.57 kHz

Punch Travel in	Punch Load P lbf			Die Separating Force D lbf			Blank-holder Amp. in x 10^{-6}			Vel. Ratio
	Osc.	Non-osc.	Osc. comp	Osc.	Non-osc.	Osc. comp	L.H.	R.H.	Mean	
$\hat{D}$0.25	221	248	27	80.1	68.5	11.7	182	91	137	16.1
$\hat{P}$0.47	382	382	0	41.0	37.1	3.9	170	60	115	13.5
0.10	61	67	6	43.0	27.3	15.7	152	106	129	15.1
0.20	157	187	30	76.2	66.5	9.7	182	86	134	15.7
0.30	275	326	51	76.2	60.5	15.7	188	96	142	16.6
0.40	360	382	22	52.7	37.1	15.6	176	86	131	15.4
0.50	382			41.0			170	60	115	13.5
0.60			Specimen Failed							
0.70										
0.80										
0.90										
1.00										
1.10										

Test Number: BH-195-220	Material: Aluminium	Draw Ratio: 1.95	Table Number: BH 48

Drawing Speed:	Blank-holder Force:		Frequency:
	Left Hand	Right Hand	
0.35 in.s^{-1}	299 lbf	301 lbf	12.58 kHz

Punch Travel in	Punch Load P lbf			Die Separating Force D lbf			Blank-holder Amp. in x 10^{-6}			Vel. Ratio
	Osc.	Non-osc.	Osc. comp	Osc.	Non. osc.	Osc. comp	L.H.	R.H.	Mean	
$\hat{D}$0.24	205	248	43	72.3	68.4	3.9	205	126	166	19.0
$\hat{P}$0.57	382	382	0	27.3	37.1	9.8	164	96	130	14.8
0.10	51	67	16	35.2	27.3	7.9	188	252	220	25.2
0.20	149	187	38	68.4	66.5	1.9	205	126	166	19.0
0.30	264	326	62	66.5	60.5	6.0	199	131	165	18.9
0.40	339	382	43	41.0	37.1	3.9	176	131	154	17.6
0.50	374			27.3			170	126	148	16.9
0.60	382			27.3			164	96	130	14.8
0.70			Specimen failed.							
0.80										
0.90										
1.00										
1.10										

Test Number: BH-195-260-1	Material: Aluminium	Draw Ratio: 1.95	Table Number: BH 49

Drawing Speed:	Blank-holder Force:		Frequency:
	Left Hand	Right Hand	
0.34 in.s^{-1}	299 lbf	302 lbf	12.58 kHz

Punch Travel in	Punch Load P lbf			Die Separating Force D lbf			Blank-holder Amp. in x 10^{-6}			Vel. Ratio
	Osc.	Non-osc.	Osc. comp	Osc.	Non-osc.	Osc. comp	L.H.	R.H.	Mean	
$\hat{D}$0.23	200	248	48	74.2	68.4	5.8	229	111	170	19.7
$\hat{P}$0.60	384	382	2	25.4	37.1	8.3	217	86	152	17.6
0.10	56	67	11	39.1	27.0	12.1	211	141	176	20.4
0.20	155	187	32	72.3	66.5	5.8	229	116	173	20.1
0.30	272	326	146	66.4	60.5	5.9	229	111	170	19.7
0.40	347	382	35	39.1	37.1	2.0	223	111	167	19.3
0.50	374			31.3			223	106	165	19.1
0.60	384			25.4			217	86	152	17.6
0.70			Specimen Failed.							
0.80										
0.90										
1.00										
1.10										

Test Number: BH-195-260-2	Material: Aluminium	Draw Ratio: 1.95	Table Number: BH 50

Drawing Speed:	Blank-holder Force:		Frequency:
	Left Hand	Right Hand	
0.35 $in.s^{-1}$	288 lbf	293 lbf	12.58 kHz

Punch Travel (in)	Punch Load P lbf			Die Separating Force D lbf			Blank-holder Amp. in $x10^{-6}$			Vel Ratio
	Osc.	Non-osc.	Osc. comp	Osc.	Non-osc.	Osc. comp	L.H.	R.H.	Mean	
$\hat{D}$0.24	208	248	40	86.0	68.4	17.6	270	217	244	27.9
$\hat{P}$0.69	384	382	2	29.3	37.1	7.8	152	116	134	15.3
0.10	56	67	11	41.0	27.3	6.3	217	353	285	32.6
0.20	160	187	27	82.0	66.5	15.5	229	197	213	24.4
0.30	278			58.6	60.5	21.5	234	186	210	24.1
0.40	347			50.8	37.1	21.5	229	131	180	20.6
0.50	374			41.0			223	111	167	19.1
0.60	382			29.3			193	116	155	17.8
0.70	384			27.3			152	116	134	15.4
0.80	382			29.3			164	116	140	16.0
0.90	376			29.3			334	151	243	27.8
1.00	352			41.0			316	181	249	28.5
1.10	315			43.0			340	192	266	30.5
1.20	253			41.0			363	176	270	30.9
1.30	197			14.0			387	192	290	33.2
1.40	117			5.9						
1.50	53			7.8t						
1.60										

Test Number: BH-195-260-3	Material: Aluminium	Draw Ratio: 1.95	Table Number: BH 51

Drawing Speed:	Blank-holder Force:		Frequency:
	Left Hand	Right Hand	
0.34 in.s^{-1}	288 lbf	290 lbf	12.58 kHz

Punch Travel (in)	Punch Load P lbf			Die Separating Force D lbf			Blank-holder Amp. in x10^{-6}			Vel Ratio
	Osc.	Non-osc.	Csc. comp	Osc.	Non-osc.	Osc. comp	L.H.	R.H.	Mean	
$\hat{D}$0.25	205	248	43	76.2	68.4	7.8	240	156	198	22.9
$\hat{P}$0.68	387	382	5	25.4	37.1	11.7	193	121	157	18.2
0.10	48	67	19	37.1	27.3	9.8	211	358	285	33.1
0.20	147	187	40	70.4	66.5	3.9	234	161	198	22.9
0.30	267	326	59	70.4	60.5	9.9	229	161	195	22.6
0.40	336	382	46	44.9	37.0	7.9	223	146	185	21.4
0.50	371			33.2			223	146	185	21.4
0.60	384			29.3			223	137	180	20.9
0.70	384			25.4			193	126	160	18.6
0.80	382			27.3			205	141	173	20.1
0.90	371			21.5			387	227	307	35.6
1.00	347			31.3			428	199	313	36.3
1.10	318			41.0			410	171	291	33.7
1.20	267			39.1			451	186	319	37.0
1.30	205			35.2			451	212	332	38.5
1.40	136			7.8						
1.50	67			5.9t						
1.60										

Test Number: BH-200-0	Material: Aluminium	Draw Ratio: 2.00	Table Number: BH 52

Drawing Speed:	Blank-holder Force:		Frequency:
	Left Hand	Right Hand	
0.35 in.s^{-1}	322 lbf	330 lbf	- kHz

Punch Travel in	Punch Load P lbf			Die Separating Force D lbf			Blank-holder Amp. in x 10^{-6}			Vel. Ratio
	Osc.	Non-osc.	Osc. comp	Osc.	Non. osc.	Osc. comp	L.H.	R.H.	Mean	
$\hat{D}$0.24	-	245	-	-	54.7	-	-	-	-	-
$\hat{P}$0.37		376			29.3					
0.10		64			21.5					
0.20		176			48.8					
0.30		320			48.8					
0.40		376			29.3					
0.50			Specimen Failed							
0.60										
0.70										
0.80										
0.90										
1.00										
1.10										

Test Number: BH-200-160	Material: Aluminium	Draw Ratio: 2.00	Table Number: BH 53

Drawing Speed:	Blank-holder Force:		Frequency:
	Left Hand	Right Hand	
0.34 in.s^{-1}	311 lbf	365 lbf	12.58 kHz

Punch Travel in	Punch Load P lbf			Die Separating Force D lbf			Blank-holder Amp. in x 10^{-6}			Vel. Ratio
	Osc.	Non-osc.	Osc. comp	Osc.	Non-osc.	Osc. comp	L.H.	R.H.	Mean	
$\hat{D}$0.25	229	245	16	76.2	54.7	21.5	170	101	136	15.8
$\hat{P}$0.45	392	376	16	37.1	29.3	7.8	158	76	117	13.6
0.10	61	64	3	35.2	21.5	13.7	152	111	132	15.3
0.20	163	176	13	68.4	48.8	19.6	158	101	130	15.1
0.30	296	320	24	70.3	48.8	21.5	176	101	139	16.1
0.40	376	376	0	46.9	29.3	17.6	164	91	128	14.9
0.50	392			37.1			158	76	117	13.6
0.60			Specimen Failed							
0.70										
0.80										
0.90										
1.00										
1.10										

Test Number: BH-200-200	Material: Aluminium	Draw Ratio: 2.00	Table Number: BH 54
Drawing Speed: 0.34 in.s^{-1}	Blank-holder Force: Left Hand 334 lbf	Right Hand 340 lbf	Frequency: 12.58 kHz

Punch Travel in	Punch Load P lbf			Die Separating Force D lbf			Blank-holder Amp. in x 10^{-6}			Vel. Ratio
	Osc.	Non-osc.	Osc. comp	Osc.	Non. osc.	Osc. comp	L.H.	R.H.	Mean	
$\hat{D}$0.26	229	245	16	74.2	54.7	19.5	193	111	152	17.6
$\hat{P}$0.50	398	376	22	33.2	29.3	3.9	164	76	120	13.9
0.10	53	64	11	35.2	21.5	13.7	170	136	153	17.7
0.20	160	176	16	68.4	48.8	19.6	188	106	147	17.1
0.30	283	320	37	68.4	48.8	19.6	188	116	152	17.6
0.40	360	376	16	43.0	29.3	13.7	182	101	142	16.5
0.50	398			33.2			164	76	120	13.9
0.60			Specimen Failed							
0.70										
0.80										
0.90										
1.00										
1.10										

Test Number: BH-200-260-1	Material: Aluminium	Draw Ratio: 2.00	Table Number: BH 55
Drawing Speed: 0.34 in.s^{-1}	Blank-holder Force: Left Hand 299 lbf	Right Hand 315 lbf	Frequency: 12.58 kHz

Punch Travel in	Punch Load P lbf			Die Separating Force D lbf			Blank-holder Amp. in x 10^{-6}			Vel. Ratio
	Osc.	Non-osc.	Osc. comp	Osc.	Non-osc.	Osc. comp	L.H.	R.E.	Mean	
$\hat{D}$0.25	222	245	23	82.0	54.7	27.3	234	116	175	20.3
$\hat{P}$0.50	390	376	74	37.0	29.3	7.7	205	106	156	18.1
0.10	53	64	11	37.0	21.5	15.5	205	197	201	23.3
0.20	155	176	21	74.2	48.8	25.4	229	121	175	20.3
0.30	275	320	165	76.2	48.8	27.4	234	121	178	20.7
0.40	358	376	18	48.8	29.3	19.5	223	116	170	19.7
0.50	390			37.1			205	106	156	18.1
0.60			Specimen Failed							
0.70										
0.80										
0.90										
1.00										
1.10										

Test Number: BH-200-260-2	Material: Aluminium	Draw Ratio: 2.00	Table Number: BH 56
Drawing Speed: 0.34 in.s^{-1}	Blank-holder Force: Left Hand 334 lbf / Right Hand 330 lbf		Frequency: 12.58 kHz

Punch Travel in	Punch Load P lbf			Die Separating Force D lbf			Blank-holder Amp. in x 10^{-6}			Vel. Ratio
	Osc.	Non-osc.	Osc. comp	Osc.	Non. osc.	Osc. comp	L.H.	R.H.	Mean	
$\hat{D}$ 0.25	205	245	40	78.1	54.7	23.4	246	162	204	24.0
$\hat{P}$ 0.57	395	376	79	37.1	29.3	7.8	193	131	162	19.1
0.10	48	64	16	33.2	21.5	11.7	240	413	327	38.5
0.20	144	176	32	70.3	48.8	21.5	246	378	312	36.7
0.30	256	320	36	72.3	48.8	23.5	240	156	198	23.3
0.40	334	376	42	52.7	29.3	23.4	217	187	202	23.8
0.50	379			39.1			205	151	178	20.9
0.60	395			37.2			193	131	162	19.1
0.70			Specimen Failed							
0.80										
0.90										
1.00										
1.10										

Punch Travel in	Punch Load P lbf	Die Separating Force Q lbf		Frict Force F lbf	Die Amplitude in x 10-5			Vel Ratio
		L.H.	R.H.		L.H.	R.H.	Mean	
Test Number: 30DI-150-0		Material: Aluminium		Draw Ratio: 1.50		Table Number: DI 1		
Drawing Speed: 0.32 in.s^{-1}		Blank-holder Force: Left Hand 115 lbf	Right Hand 123 lbf		Frequency: - kHz			
.D max 1.34	160	767	862	0	-	-	-	-
Pd max 0.40	294	137	246	6.19				
Pi max 1.20	206	694	801	0				
Test Number: 30DI-150-60		Material: Aluminium		Draw Ratio: 1.50		Table Number: DI 2		
Drawing Speed: 0.33 in.s^{-1}		Blank-holder Force: Left Hand 121 lbf	Right Hand 119 lbf		Frequency: 12.84 kHz			
.D max 1.36	115	785	839	0	56	51	54	6.6
Pd max 0.50	225	201	293	0	74	64	69	8.5
Pi max 1.20	210	712	785	0	56	45	51	6.3
Test Number: 30DI-150-120-1		Material: Aluminium		Draw Ratio: 1.50		Table Number: DI 3		
Drawing Speed: 0.33 in.s^{-1}		Blank-holder Force: Left Hand 115 lbf	Right Hand 114 lbf		Frequency: 12.84 kHz			
.D max 1.35	130	730	785	0	149	128	139	18.9
Pd max 0.40	195	32	92	0	298	307	303	36.9
Pi max 1.20	183	648	724	0	121	109	115	14.0
Test Number: 30DI-150-120-2		Material: Aluminium		Draw Ratio: 1.50		Table Number: DI 4		
Drawing Speed: 0.32 in.s^{-1}		Blank-holder Force: Left Hand 127 lbf	Right Hand 119 lbf		Frequency: 12.84 kHz			
.D max 1.34	130	703	739	0	140	128	134	16.8
Pd max 0.40	191	18	77	0	279	307	293	36.7
Pi max 1.20	183	630	708	0	112	102	107	13.4
Test Number: 30DI-150-180		Material: Aluminium		Draw Ratio: 1.50		Table Number: DI 5		
Drawing Speed: 0.32 in.s^{-1}		Blank-holder Force: Left Hand 121 lbf	Right Hand 123 lbf		Frequency: 12.84 kHz			
.D max 1.36	130	703	739	0	186	154	170	21.4
Pd max 0.40	195	27	92	0	372	333	353	44.5
Pi max 1.10	180	530	631	0	121	115	118	14.9

Punch Travel in	Punch Load P lbf	Die Separating Force D lbf		Frict Force F lbf	Die Amplitude in x 10^{-3}			Vel Ratio
		L.H.	R.H.		L.H.	R.H.	Mean	
Test Number: 30DI-150-220		Material: Aluminium		Draw Ratio: 1.50		Table Number: DI 6		
Drawing Speed: 0.32 in.s^{-1}		Blank-holder Force: Left Hand 115 lbf	Right Hand 119 lbf		Frequency: 12.84 kHz			
.D max 1.35	134	776	708	0	186	192	189	23.8
Pd max 0.40	199	128	92	0	409	333	371	46.8
Pi max 1.20	176	685	647	0	158	154	156	19.7
Test Number: 30DI-150-260		Material: Aluminium		Draw Ratio: 1.50		Table Number: DI 7		
Drawing Speed: 0.33 in.s^{-1}		Blank-holder Force: Left Hand 121 lbf	Right Hand 123 lbf		Frequency: 12.84 kHz			
.D max 1.34	126	666	693	0	205	166	186	22.5
Pd max 0.40	191	27	77	0	428	345	387	46.7
Pi max 1.20	176	593	662	0	149	154	152	18.4
Test Number: 30DI-155-0		Material: Aluminium		Draw Ratio: 1.55		Table Number: DI 8		
Drawing Speed: 0.33 in.s^{-1}		Blank-holder Force: Left Hand 150 lbf	Right Hand 188 lbf		Frequency: - kHz			
.D max 1.42	164	730	788	0	-	-	-	-
Pd max 0.50	325	657	262	7.14				
Pi max 1.28	218	173	739	0				
Test Number: 30DI-155-120		Material: Aluminium		Draw Ratio: 1.55		Table Number: DI 9		
Drawing Speed: 0.32 in.s^{-1}		Blank-holder Force: Left Hand 161 lbf	Right Hand 188 lbf		Frequency: 12.85 kHz			
.D max 1.42	126	730	739	0	130	115	123	15.2
Pd max 0.40	214	27	77	0	279	243	261	32.2
Pi max 1.30	176	676	724	0	121	109	115	14.2
Test Number: 30DI-155-180		Material: Aluminium		Draw Ratio: 1.55		Table Number: DI 10		
Drawing Speed: 0.32 in.s^{-1}		Blank-holder Force: Left Hand 161 lbf	Right Hand 188 lbf		Frequency: 12.84 kHz			
.D max 1.43	138	730	770	0	149	141	145	18.2
Pd max 0.40	214	27	77	0	391	282	337	42.2
Pi max 1.30	183	657	739	0	130	128	129	16.2

Punch Travel in	Punch Load P lbf	Die Separating Force D lbf		Frict Force F lbf	Die Amplitude in x 10^{-6}			Tel Ratio
		L.H.	R.H.		L.H.	R.H.	Mean	
Test Number: 30-DI-160-220		Material: Aluminium		Draw Ratio: 1.60			Table Number: DI 16	
Drawing Speed: 0.32 in.s^{-1}		Blank-holder Force: Left Hand 167 lbf	Right Hand 227 lbf				Frequency: 12.84 kHz	
.D max 1.52	126	717	739	0	195	179	187	23.4
Pd max 0.42	225	55	108	0	502	358	430	53.9
Pi max 1.40	176	666	724	0	186	166	176	22.1
Test Number: 30DI-160-260		Material: Aluminium		Draw Ratio: 1.60			Table Number: DI 17	
Drawing Speed: 0.32 in.s^{-1}		Blank-holder Force: Left Hand 167 lbf	Right Hand 217 lbf				Frequency: 12.84 kHz	
.D max 1.60	122	694	739	0	112	96	104	13.0
Pd max 0.46	225	27	77	0	335	294	315	39.5
Pi max 1.46	203	603	678	0	130	102	116	14.5
Test Number: 30DI-165-0		Material: Aluminium		Draw Ratio: 1.65			Table Number: DI 18	
Drawing Speed: 0.33 in.s^{-1}		Blank-holder Force: Left Hand 184 lbf	Right Hand 237 lbf				Frequency: - kHz	
.D max 1.65	172	803	847	0	-	-	-	-
Pd max 0.57	367	164	231	10.23				
Pi max 1.53	229	758	816	0				
Test Number: 30DI-165-120		Material: Aluminium		Draw Ratio: 1.65			Table Number: DI 19	
Drawing Speed: 0.32 in.s^{-1}		Blank-holder Force: Left Hand 173 lbf	Right Hand 237 lbf				Frequency: 12.83 kHz	
.D max 1.64	149	785	832	0	130	128	129	16.3
Pd max 0.54	252	73	139	0	298	282	290	36.6
Pi max 1.42	218	676	739	0	93	64	79	10.0
Test Number: 30DI-165-180		Material: Aluminium		Draw Ratio: 1.65			Table Number: DI 20	
Drawing Speed: 0.33 in.s^{-1}		Blank-holder Force: Left Hand 184 lbf	Right Hand 237 lbf				Frequency: 12.83 kHz	
.D max 1.64	141	776	801	0	149	154	152	18.6
Pd max 0.53	252	73	139	0	558	320	439	55.8
Pi max 1.50	199	730	770	0	167	154	161	19.7

Punch Travel in	Punch Load P lbf	Die Separating Force Q lbf		Frict Force F lbf	Die Amplitude in x 10^{-6}			Vel Ratio
		L.H.	R.H.		L.H.	R.H.	Mean	
Test Number: 30DI-165-220		Material: Aluminium		Draw Ratio: 1.65			Table Number: DI 21	
Drawing Speed: 0.34 in.s^{-1}		Blank-holder Force: Left Hand 184 lbf		Right Hand 247 lbf			Frequency: 12.83 kHz	
.D max 1.64	141	785	816	0	167	166	167	20.0
Pd max 0.57	248	73	123	0	614	282	448	53.7
Pi max 1.50	218	721	785	0	112	90	101	12.1
Test Number: 30DI-165-260		Material: Aluminium		Draw Ratio: 1.65			Table Number: DI 22	
Drawing Speed: 0.33 in.s^{-1}		Blank-holder Force: Left Hand 190 lbf		Right Hand 237 lbf			Frequency: 12.83 kHz	
.D max 1.72	118	758	770	0	130	154	142	17.3
Pd max 0.46	248	27	77	0	372	333	353	43.0
Pi max 1.57	195	694	739	0	167	166	167	20.3
Test Number: 30DI-170-0		Material: Aluminium		Draw Ratio: 1.70			Table Number: DI 23	
Drawing Speed: 0.31 in.s^{-1}		Blank-holder Force: Left Hand 196 lbf		Right Hand 326 lbf			Frequency: - kHz	
.D max								
Pd max 0.48	378	100	123	10.95	-	-	-	-
Pi max			Specimen	Failed				
Test Number: 30DI-170-60		Material: Aluminium		Draw Ratio: 1.70			Table Number: DI 24	
Drawing Speed: 0.31 in.s^{-1}		Blank-holder Force: Left Hand 196 lbf		Right Hand 346 lbf			Frequency: 12.85 kHz	
.D max 1.72	149	831	909	0	47	26	37	19.6
Pd max 0.78	348	137	216	0	47	32	40	21.2
Pi max 1.44	225	676	739	0	47	26	37	19.6
Test Number: 30DI-170-120		Material: Aluminium		Draw Ratio: 1.70			Table Number: DI 25	
Drawing Speed: 0.31 in.s^{-1}		Blank-holder Force: Left Hand 207 lbf		Right Hand 341 lbf			Frequency: 12.85 kHz	
.D max 1.73	145	813	862	0	112	102	107	13.8
Pd max 0.58	306	82	139	0	149	192	171	22.1
Pi max 1.48	218	685	739	0	74	51	63	8.1

Punch Travel in	Punch Load P lbf	Die Separating Force Q lbf		Frict Force F lbf	Die Amplitude in x 10^{-5}			Vel Ratio
		L.H.	R.H.		L.H.	R.H.	Mean	
Test Number: 30DI-170-180		Material: Aluminium		Draw Ratio: 1.70			Table Number: DI 26	
Drawing Speed: 0.32 in.s^{-1}		Blank-holder Force: Left Hand 213 lbf	Right Hand 336 lbf				Frequency: 12.85 kHz	
.D max 1.76	88	785	801	0	112	128	120	15.1
Pd max 0.50	267	46	77	0	335	192	264	33.3
Pi max 1.44	199	603	662	0	149	102	126	15.9
Test Number: 30DI-170-220		Material: Aluminium		Draw Ratio: 1.70			Table Number: DI 27	
Drawing Speed: 0.32 in.s^{-1}		Blank-holder Force: Left Hand 219 lbf	Right Hand 336 lbf				Frequency: 12.85 kHz	
.D max 1.77	130	776	816	0	130	141	136	17.2
Pd max 0.53	271	37	62	0	279	269	274	34.6
Pi max 1.60	210	703	755	0	93	77	85	10.7
Test Number: 30DI-170-260		Material: Aluminium		Draw Ratio: 1.70			Table Number: DI 28	
Drawing Speed: 0.31 in.s^{-1}		Blank-holder Force: Left Hand 230 lbf	Right Hand 336 lbf				Frequency: 12.85 kHz	
.D max 1.78	126	758	785	0	149	154	152	20.1
Pd max 0.50	260	37	77	0	279	256	268	35.4
Pi max 1.50	199	612	678	0	149	115	132	17.4
Test Number: 30DI-175-0		Material: Aluminium		Draw Ratio: 1.75			Table Number: DI 29	
Drawing Speed: 0.30 in.s^{-1}		Blank-holder Force: Left Hand 219 lbf	Right Hand 306 lbf				Frequency: - kHz	
.D max								
Pd max 0.40	424	27	46	10.95	-	-	-	-
Pi max			Specimen	Failed				
Test Number: 30DI-175-60		Material: Aluminium		Draw Ratio: 1.75			Table Number: DI 30	
Drawing Speed: 0.31 in.s^{-1}		Blank-holder Force: Left Hand 219 lbf	Right Hand 336 lbf				Frequency: 12.85 kHz	
.D max 1.82	183	831	893	0	47	26	37	4.9
Pd max 0.57	355	100	154	0	47	38	43	5.7
Pi max 1.60	248	785	832	0	47	26	37	4.9

Punch Travel in	Punch Load P lbf	Die Separating Force Q lbf		Frict Force F lbf	Die Amplitude in x 10^{-5}			Vel Ratio
		L.H.	R.H.		L.H.	R.H.	Mean	
Test Number: 30DI-175-120-1		Material: Aluminium		Draw Ratio: 1.75		Table Number: DI 31		
Drawing Speed: 0.31 in.s^{-1}		Blank-holder Force: Left Hand 219 lbf	Right Hand 336 lbf			Frequency: 12.85 kHz		
.D max 1.80	145	794	832	0	93	90	92	11.9
Pd max 0.56	287	68	108	0	149	205	177	22.8
Pi max 1.50	210	639	693	0	93	77	85	11.0
Test Number: 30DI-175-120-2		Material: Aluminium		Draw Ratio: 1.75		Table Number: DI 32		
Drawing Speed: 0.32 in.s^{-1}		Blank-holder Force: Left Hand 230 lbf	Right Hand 326 lbf			Frequency: 12.62 kHz		
.D max 1.80	191	840	893	0	56	38	47	5.8
Pd max 0.55	340	110	177	0	65	51	58	7.1
Pi max 1.68	195	785	847	0	56	38	47	5.8
Test Number: 30DI-175-180-1		Material: Aluminium		Draw Ratio: 1.75		Table Number: DI 33		
Drawing Speed: 0.31 in.s^{-1}		Blank-holder Force: Left Hand 224 lbf	Right Hand 336 lbf			Frequency: 13.00 kHz		
.D max 1.84	160	749	785	0	74	51	63	8.2
Pd max 0.60	290	73	123	0	223	166	195	25.4
Pi max 1.70	206	685	724	0	93	64	79	10.3
Test Number: 30DI-175-180-2		Material: Aluminium		Draw Ratio: 1.75		Table Number: DI 34		
Drawing Speed: 0.31 in.s^{-1}		Blank-holder Force: Left Hand 224 lbf	Right Hand 336 lbf			Frequency: 13.00 kHz		
.D max 1.85	160	785	832	0	112	115	114	14.9
Pd max 0.63	283	27	77	0	242	205	224	29.2
Pi max 1.73	233	749	816	0	93	64	79	10.3
Test Number: 30DI-175-180-3		Material: Aluminium		Draw Ratio: 1.75		Table Number: DI 35		
Drawing Speed: 0.31 in.s^{-1}		Blank-holder Force: Left Hand 265 lbf	Right Hand 356 lbf			Frequency: 12.88 kHz		
.D max 1.88	187	803	862	0	74	64	69	8.9
Pd max 0.64	287	64	123	3.81	391	192	292	37.8
Pi max 1.75	248	749	816	0	74	64	69	8.9

Punch Travel in	Punch Load P lbf	Die Separating Force Q lbf		Friction Force F lbf	Die Amplitude in x 10^{-3}			Wear Ratio
		L.H.	R.H.		L.H.	R.H.	Main	
Test Number: 30DI-175-220		Material: Aluminium		Draw Ratio: 1.75		Table Number: DI 36		
Drawing Speed: 0.32 in.s^{-1}		Blank-holder Force: Left Hand 219 lbf	Right Hand 306 lbf		Frequency: 12.85 kHz			
.D max 1.92	103	703	678	0	112	141	127	16.0
Pd max 0.60	271	27	62	0	242	230	236	29.8
Pi max 1.77	191	612	631	0	149	179	164	20.7
Test Number: 30-DI-175-260		Material: Aluminium		Draw Ratio: 1.75		Table Number: DI 37		
Drawing Speed: 0.32 in.s^{-1}		Blank-holder Force: Left Hand 219 lbf	Right Hand 306 lbf		Frequency: 12.85 kHz			
.D max 1.92	115	721	708	0	130	154	142	18.0
Pd max 0.59	283	18	62	0	260	230	245	31.1
Pi max 1.78	180	666	678	0	167	166	167	21.2
Test Number: 30DI-180-0		Material: Aluminium		Draw Ratio: 1.80		Table Number: DI 38		
Drawing Speed: 0.31 in.s^{-1}		Blank-holder Force: Left Hand 242 lbf	Right Hand 306 lbf		Frequency: - kHz			
.D max								
Pd max 0.38	386	27	62	11.42	-	-	-	-
Pi max			Specimen	Failed				
Test Number: 30DI-180-20		Material: Aluminium		Draw Ratio: 1.80		Table Number: DI 39		
Drawing Speed: 0.32 in.s^{-1}		Blank-holder Force: Left Hand 242 lbf	Right Hand 311 lbf		Frequency: 12.85 kHz			
.D max								
Pd max 0.45	390	73	123	3.33	19	13	16	2.0
Pi max			Specimen	Failed				
Test Number: 30DI-180-40		Material: Aluminium		Draw Ratio: 1.80		Table Number: DI 40		
Drawing Speed: 0.31 in.s^{-1}		Blank-holder Force: Left Hand 247 lbf	Right Hand 321 lbf		Frequency: 12.85 kHz			
.D max								
Pd max 0.52	359	91	54	0	28	26	27	3.5
Pi max			Specimen	Failed				

Punch Travel in	Punch Load P lbf	Die Separating Force D lbf		Frict Force F lbf	Die Amplitude in x 10⁻³			Tel Ratio
		L.H.	R.H.		L.H.	R.H.	Mean	
Test Number: 30DI-180-60		Material: Aluminium		Draw Ratio: 1.80		Table Number: DI 41		
Drawing Speed: 0.32 in.s^{-1}		Blank-holder Force: Left Hand 224 lbf	Right Hand 336 lbf		Frequency: 12.85 kHz			
.D max 1.92	199	840	924	0	37	19	28	3.6
Pd max 0.96	374	128	200	0	37	38	38	4.8
Pi max 1.78	252	785	878	0	37	19	28	3.6
Test Number: 30DI-180-80		Material: Aluminium		Draw Ratio: 1.80		Table Number: DI 42		
Drawing Speed: 0.31 in.s^{-1}		Blank-holder Force: Left Hand 242 lbf	Right Hand 346 lbf		Frequency: 12.84 kHz			
.D max 1.95	183	876	924	0	56	51	54	7.0
Pd max 0.96	359	164	231	0	74	51	63	8.1
Pd max 1.80	260	821	878	0	56	38	47	6.1
Test Number: 30DI-180-100		Material: Aluminium		Draw Ratio: 1.80		Table Number: DI 43		
Drawing Speed: 0.32 in.s^{-1}		Blank-holder Force: Left Hand 253 lbf	Right Hand 346 lbf		Frequency: 12.84 kHz			
.D max 1.92	187	840	909	0	56	38	47	5.9
Pd max 1.01	329	173	246	0	130	96	113	14.2
Pi max 1.80	260	794	878	0	56	38	47	5.9
Test Number: 30DI-180-120		Material: Aluminium		Draw Ratio: 1.80		Table Number: DI 44		
Drawing Speed: 0.33 in.s^{-1}		Blank-holder Force: Left Hand 265 lbf	Right Hand 316 lbf		Frequency: 12.84 kHz			
.D max 1.90	145	831	878	0	74	83	79	9.8
Pd max 0.63	298	23	46	0	205	179	192	23.8
Pi max 1.77	225	767	832	0	65	58	62	7.7.
Test Number: 30DI-180-140		Material: Aluminium		Draw Ratio: 1.80		Table Number: DI 45		
Drawing Speed: 0.32 in.s^{-1}		Blank-holder Force: Left Hand 247 lbf	Right Hand 296 lbf		Frequency: 12.84 kHz			
.D max 1.90	149	831	878	0	65	90	78	9.8
Pd max 0.63	290	32	68	0	233	205	219	27.4
Pi max 1.74	225	749	816	0	56	64	60	7.5

Punch Travel in	Punch Load P lbf	Die Separating Force D lbf		Frict Force F lbf	Die Amplitude in x 10^{-5}			Vel Ratio
		L.H.	R.H.		L.H.	R.H.	Mean	
Test Number: 30DI-180-180		Material: Aluminium		Draw Ratio: 1.80		Table Number: DI 46		
Drawing Speed: 0.32 in.s^{-1}		Blank-holder Force: Left Hand 247 lbf	Right Hand 296 lbf		Frequency: 12.84 kHz			
.D max 2.04	105	821	847	0	84	102	93	11.8
Pd max 0.67	302	18	54	0	242	230	236	29.9
Pi max 1.18	229	712	770	0	65	77	71	9.0
Test Number: 30DI-180-220		Material: Aluminium		Draw Ratio: 1.80		Table Number: DI 47		
Drawing Speed: 0.32 in.s^{-1}		Blank-holder Force: Left Hand 253 lbf	Right Hand 296 lbf		Frequency: 12.84 kHz			
.D max 2.00	157	803	847	0	93	115	104	13.2
Pd max 0.68	306	18	62	0	279	256	268	34.0
Pi max 1.80	218	712	785	0	112	128	120	15.2
Test Number: 30DI-180-60A		Material: Aluminium		Draw Ratio: 1.80		Table Number: DI 48		
Drawing Speed: 0.33 in.s^{-1}		Blank-holder Force: Left Hand 242 lbf	Right Hand 296 lbf		Frequency: a.f.c.kHz			
.D max								
Pd max 0.62	363	27	62	3.33	65	77	71	8.9
Pi max			Specimen	Failed				
Test Number: 30DI-180-120A		Material: Aluminium		Draw Ratio: 1.80		Table Number: DI 49		
Drawing Speed: 0.32 in.s^{-1}		Blank-holder Force: Left Hand 242 lbf	Right Hand 291 lbf		Frequency: a.f.c.kHz			
.D max								
Pd max 0.62	352	128	77	3.33	121	154	138	17.5
Pi max			Specimen	Failed				
Test Number: 30DI-180-180A-1		Material: Aluminium		Draw Ratio: 1.80		Table Number: DI 50		
Drawing Speed: 0.31 in.s^{-1}		Blank-holder Force: Left Hand 242 lbf	Right Hand 296 lbf		Frequency: a.f.c.kHz			
.D max								
Pd max 0.67	302	18	62	0	260	256	258	33.7
Pi max			Specimen	Failed				

Punch Travel in	Punch Load P lbf	Die Separating Force D lbf		Frict Force F lbf	Die Amplitude in x 10^{-3}			Vel Ratio
		L.H.	R.H.		L.H.	R.H.	Mean	
Test Number: 30DI-180-180A-2		Material: Aluminium		Draw Ratio: 1.80		Table Number: DI 51		
Drawing Speed: 0.33 in.s^{-1}		Blank-holder Force: Left Hand 230 lbf	Right Hand 296 lbf			Frequency: a.f.c. kHz		
.D max								
Pd max 0.64	336	18	62	0	205	192	199	24.7
Pi max			Specimen	Failed				
Test Number: 30DI-185-0		Material: Aluminium		Draw Ratio: 1.85		Table Number: DI 52		
Drawing Speed: 0.32 in.s^{-1}		Blank-holder Force: Left Hand 265 lbf	Right Hand 316 lbf			Frequency: - kHz		
.D max								
Pd max 0.42	397	27	62	0	-	-	-	-
Pi max			Specimen	Failed				
Test Number: 30DI-185-60		Material: Aluminium		Draw Ratio: 1.85		Table Number: DI 53		
Drawing Speed: 0.33 in.s^{-1}		Blank-holder Force: Left Hand 265 lbf	Right Hand 316 lbf			Frequency: 12.83 kHz		
.D max								
Pd max 0.50	363	64	108	0	56	90	73	8.9
Pi max			Specimen	Failed				
Test Number: 30DI-185-120		Material: Aluminium		Draw Ratio: 1.85		Table Number: DI 54		
Drawing Speed: 0.33 in.s^{-1}		Blank-holder Force: Left Hand 288 lbf	Right Hand 316 lbf			Frequency: 12.83 kHz		
.D max								
Pd max 0.73	340	23	54	0	186	179	183	22.3
Pi max			Specimen	Failed				
Test Number: 30DI-185-140		Material: Aluminium		Draw Ratio: 1.85		Table Number: DI 55		
Drawing Speed: 0.32 in.s^{-1}		Blank-holder Force: Left Hand 299 lbf	Right Hand 360 lbf			Frequency: 12.83 kHz		
.D max								
Pd max 0.80	336	18	54	0	186	179	183	22.9
Pi max			Specimen	Failed				

Punch Travel in	Punch Load P lbf	Die Separating Force D lbf		Frict Force F lbf	Die Amplitude in x 10^{-5}			Vel Ratio
		L.H.	R.H.		L.H.	R.H.	Mean	
Test Number: 30DI-185-160		Material: Aluminium		Draw Ratio: 1.85		Table Number: DI 56		
Drawing Speed: 0.33 in.s^{-1}		Blank-holder Force: Left Hand 299 lbf	Right Hand 326 lbf		Frequency: 12.83 kHz			
.D max 2.10	99	840	862	0	93	77	85	10.4
Pd max 0.70	344	27	77	0	205	179	192	23.5
Pi max 1.90	233	758	816	0	74	64	69	8.5
Test Number: 30DI-185-180-1		Material: Aluminium		Draw Ratio: 1.85		Table Number: DI 57		
Drawing Speed: 0.33 in.s^{-1}		Blank-holder Force: Left Hand 288 lbf	Right Hand 321 lbf		Frequency: 12.83 kHz			
.D max 2.10	153	840	893	0	74	83	79	9.7
Pd max 0.70	325	27	69	0	233	205	219	26.8
Pi max 1.90	237	740	816	0	74	64	69	8.5
Test Number: 30DI-185-180-2		Material: Aluminium		Draw Ratio: 1.85		Table Number: DI 58		
Drawing Speed: 0.33 in.s^{-1}		Blank-holder Force: Left Hand 299 lbf	Right Hand 321 lbf		Frequency: 12.83 kHz			
.D max 2.00	203	776	816	0	65	77	71	8.7
Pd max 0.70	332	14	39	0	214	192	203	24.9
Pi max 1.90	245	730	770	0	65	77	71	8.7
Test Number: 30DI-185-200		Material: Aluminium		Draw Ratio: 1.85		Table Number: DI 59		
Drawing Speed: 0.33 in.s^{-1}		Blank-holder Force: Left Hand 299 lbf	Right Hand 326 lbf		Frequency: 12.83 kHz			
.D max 2.00	172	794	816	0	93	96	95	11.6
Pd max 0.80	325	27	62	0	233	218	226	27.5
Pi max 1.90	299	740	801	0	93	102	98	11.9
Test Number: 30DI-185-240		Material: Aluminium		Draw Ratio: 1.85		Table Number: DI 60		
Drawing Speed: 0.32 in.s^{-1}		Blank-holder Force: Left Hand 299 lbf	Right Hand 326 lbf		Frequency: 12.85 kHz			
.D max 2.10	183	794	862	0	74	77	76	9.5
Pd max 0.77	334	18	62	0	233	218	226	28.3
Pi max 2.00	237	740	816	0	74	90	82	10.3

Punch Travel in	Punch Load P lbf	Die Separating Force D lbf		Frict Force F lbf	Die Amplitude in x 10^{-3}			Vel Ratio
		L.H.	R.H.		L.H.	R.H.	Mean	
Test Number: 30DI-190-0		Material: Aluminium		Draw Ratio: 1.90		Table Number: DI 61		
Drawing Speed: 0.32 in.s^{-1}		Blank-holder Force: Left Hand 259 lbf	Right Hand 276 lbf		Frequency: - kHz			
.D max								
Pd max 0.37	394	27	77	9.52	-	-	-	-
Pi max			Specimen Failed					
Test Number: 30DI-190-260-1		Material: Aluminium		Draw Ratio: 1.90		Table Number: DI 62		
Drawing Speed: 0.33 in.s^{-1}		Blank-holder Force: Left Hand 265 lbf	Right Hand 286 lbf		Frequency: 12.85 kHz			
.D max								
Pd max 0.62	355	14	54	0	242	205	224	27.3
Pi max			Specimen Failed					
Test Number: 30DI-190-260-2		Material: Aluminium		Draw Ratio: 1.90		Table Number: DI 63		
Drawing Speed: 0.32 in.s^{-1}		Blank-holder Force: Left Hand 265 lbf	Right Hand 286 lbf		Frequency: 12.85 kHz			
.D max								
Pd max 0.62	363	23	62	0	242	205	224	28.4
Pi max			Specimen Failed					
Test Number:		Material: Aluminium		Draw Ratio:		Table Number:		
Drawing Speed: in.s^{-1}		Blank-holder Force: Left Hand lbf	Right Hand lbf		Frequency: kHz			
.D max								
Pd max								
Pi max								
Test Number:		Material: Aluminium		Draw Ratio:		Table Number:		
Drawing Speed: in.s^{-1}		Blank-holder Force: Left Hand lbf	Right Hand lbf		Frequency: kHz			
.D max								
Pd max								
Pi max								

Blank-holder Swaging.		
Test Number	Max. Punch Load lbf.	Blank-holder Oscillatory Force lbf.
S-150-N	256	-
S-150-4	241	92
S-150-6	256	58
S-150-2	225	104
S-150-8	248	46
S-150-N	252	-
S-150-NV3	267	-
S-150-4V7	245	81
S-150-4V5	245	92
S-150-4V3	245	92
S-160-4	277	127
S-160-8	294	92
S-160-12	294	58
S-160-2	271	138
S-160-N	336	-
S-165-N	313	-
S-165-12	306	58
S-165-8	298	92
S-165-4	294	115
S-165-2	290	138
S-165-6	294	115
S-165-N	332	-
S-170-4	302	127
S-170-6	306	115
S-170-2	313	104
S-170-N	363	-
S-175-N	382	-
S-175-4	352	184
S-175-10	355	127
S-175-N	374	-
S-175-N	371	-
S-175-12	344	138
S-175-11	336	161